TOTAL SYNTHESIS OF (+)-18-*EPI*-LATRUNCULOL A

Brett Daniel Williams

A DISSERTATION

in

Chemistry

Presented to the Faculties of the University of Pennsylvania

in

Partial Fulfillment of the Requirements for the

Degree of Doctor of Philosophy

2013

Supervisor of Dissertation

_____

Professor Amos B. Smith, III

Rhodes-Thompson Professor of Chemistry

Graduate Group Chairperson

_____

Professor Gary A. Molander

Hirschmann-Makineni Professor of Chemistry

Dissertation Committee

Professor Marisa C. Kozlowski, Professor of Chemistry (Chair)

Professor Jeffrey D. Winkler, Merriam Professor of Chemistry

Professor Virgil Percec, P. Roy Vagelos Professor of Chemistry

TOTAL SYNTHESIS OF (+)-18-*EPI*-LATRUNCULOL A

ACKNOWLEDGMENTS

I would like to thank Professor Amos B. Smith, III, for choosing the synthetic target, (+)-18-*epi*-latrunculol A, and financially supporting me throughout my research. I also want to thank him for his mentorship (I have extracted some precious gems of advice from Professor Smith over the course of my graduate education) and for allowing me the freedom to be creative and explore new transformations–it has been a rewarding process. I would also like to thank my committee members for their helpful monitoring throughout my graduate career, specifically Professor Marisa Kozlowski for her exceptional advice on research, postdoctoral training, and grant writing. Professor Dailey has also been a tremendous asset and has provided helpful guidance in regards to computational calculations and five years of questions concerning physical organic chemistry.

I have to thank my fellow members of the Smith group for creating such a wonderfully open atmosphere in which to work and discuss chemistry as well as other topics.

I would like to thank Dr. George Furst and for his help in ascertaining high resolution spectral data and for his helpful discussions and Dr. Patrick Carroll for performing X-ray analyses of crystalline intermediates.

ABSTRACT

TOTAL SYNTHESIS OF (+)-18-*EPI*-LATRUNCULOL A

Brett D. Williams

Professor Amos B. Smith, III

The total synthesis of (+)-18-*epi*-latrunculol A was undertaken to provide synthetic access to a sufficient amount of the scarce, sponge-derived macrolide to facilitate further biological evaluation. Preliminary bioassays revealed (+)-18-*epi*-latrunculol A to exhibit a selective, solid tumor cytotoxicity, while being devoid of the actin depolymerization activity customary to the latrunculin family of natural products, making the epimeric natural product a compound of interest for chemotherapeutics. An enantioselective total synthesis of (+)-18-*epi*-latrunculol A was accomplished; key features of the synthesis include a functional group compatible cross metathesis reaction, an acid-mediated cyclization/equilibration, a Carreira alkynylation, and a late-stage Mitsunobu macrolactonization. Finally, a novel method was also discovered to achieve the cyclization of δ-hydroxy-*E*-enones under mild, photochemical conditions.

TABLE OF CONTENTS

LIST OF TABLES

Chapter 1

Appendix 2

LIST OF FIGURES

Chapter 1

Chapter 2

Appendix 1

LIST OF SCHEMES

Chapter 1

Chapter 2

LIST OF ABBREVIATIONS

Ac	Acetyl
aq.	Aqueous
BAIB	(Diacetoxyiodo)benzene
CAN	Ceric Ammonium Nitrate
CSA	Camphorsulfonic acid
DIBAL	Diisobutylaluminum hydride
DMAP	4-Dimethylaminopyridine
DMF	*N,N*-Dimethylformamide
DMSO	Dimethyl sulfoxide
dr	Diastereomeric ratio
er	Enantiomeric ratio
ESI	Electrospray ionization
Et_2O	Diethyl ether
HCl	Hydrochloric acid
HMBC	Heteronuclear multiple-bond correlation
HMQC	Heteronuclear multiple-quantum correlation
HRMS	High resolution mass spectrum
IC	Inhibitory concentration
i-Pr	Isopropyl
Ipc	Isopinocamphenyl
LDA	Lithium diisopropylamide
Me	Methyl
MeCN	Acetonitrile

MS	Mass spectrometry
NME	*N*-Methylephedrine
NMR	Nuclear magnetic resonance
NOE	Nucleur Overhauser effect
NOESY	Nucleur Overhauser effect spectroscopy
Nu	Nucleophile
Ph	Phenyl
PMB	*p*-Methoxybenzyl
py	Pyridine
SAR	Structure activity relationship
SEM	2-(Trimethylsily)ethoxymethyl
TAS-F	Tris-(dimethylamino)sulfonium difluorotrimethylsilicate
TBAF	Tetrabutylammonium fluoride
TBS	*tert*-Butyldimethylsilyl
TBSOTf	*tert*-Butyldimethylsilyl trifluoromethanesulfonate
TBTU	*O*-(Benzotriazol-1-yl)-*N,N,N′,N′*-tetramethyluronium tetrafluoroborate
TEMPO	2,2,6,6-tetramethylpiperidine-1-oxyl
Teoc	Trimethylsilylethoxycarbonyl
THF	Tetrahydrofuran
TLC	Thin-layer chromatography

CHAPTER 1 Introduction

1.1 Introduction: The Latrunculin Family of Sponge Metabolites

The protected reefs of the Red Sea (Gulf of Eilat) are populated by red-colored sponges known as the *Latrunculia magnifica* (renamed *Negombata magnifica*).[1] Although clearly visible from the surface and fully exposed, the sponges have not been observed being eaten by fish. Upon further examination, researchers discovered that, as a defense mechanism, the sponges exude a reddish liquid when squeezed that causes nearby fish to flee. If retreat is not possible, the fish suffer hemorrhaging followed by death within minutes after exposure to the red liquid. In 1980, two polyketide natural products, latrunculin A (**1.1**) and latrunculin B (**1.2**), were isolated from *Latrunculia magnifica* and characterized by Kashman *et al.*, utilizing spectroscopic methods and X-ray diffraction of a crystalline derivative of latrunculin A (Figure 1.1).[2,3]

Figure 1.1. Parent Latrunculin Compounds

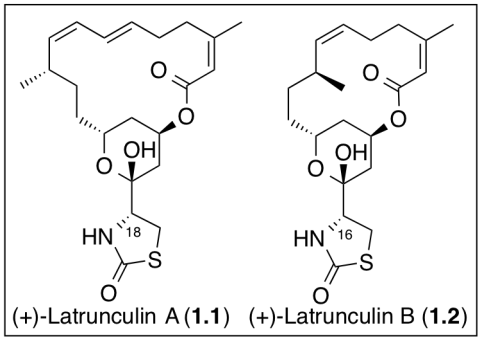

An investigation into the cellular processes affected by the lead compounds revealed the ability of latrunculins to depolymerize selectively the actin cytoskeleton, while leaving the microtubule network unaffected.[4] Actin is *the* most abundant intracellular protein within a eukaryotic cell.[5] As a primary component of the cell cytoskeleton, actin determines the shape of the cell and is directly involved in many vital processes such as intracellular transport, cell

motility and cell division.[6] Actin exists in a dynamic equilibrium of monomeric G-actin and linear polymeric F-actin, continually polymerizing and depolymerizing. A number of toxic natural products are known to interfere with the dynamics of assembly or disassembly of actin subunits, such as rhizopodin,[7] swinholide A,[8] bistramide A,[9] as well as others.[10] Latrunculin A was found to form a 1:1 molar complex with monomeric G-actin, inhibiting repolymerization of the G-actin subunits and effectively resulting in net depolymerization due to the dynamic behavior of the polymeric F-actin.[4,11] Treatment of cultured mouse neuroblastoma and fibroblast cells with submicromolar concentrations of either latrunculin A or latrunculin B result in rapid changes to the cell morphology (i.e., shape) due to depolymerization of the actin cytoskeleton. When the natural product is removed *via* washing, the cell morphology rapidly reassumes the original state, thus demonstrating reversibility of the latrunculin-actin interaction.[1] The striking ability of latrunculin A and latrunculin B to depolymerize selectively the actin cytoskeleton at low concentrations has been widely exploited by researchers to probe the structure and function of actin-dependent cellular processes.[12,13,14] Although cytochalasins were the first natural product "molecular probes" used to test the role of actin in biological processes,[15] due to a better defined mode of action and more potent inhibition, latrunculin A is currently *the* most commonly employed molecular probe of the many natural product actin inhibitors.[16]

The extensive use of latrunculin A as a molecular probe, in combination with the macrolide's interesting architecture, has led to sustained interest from the synthetic community.[17-26] Smith and coworkers completed the first total synthesis of a latrunculin natural product, reporting their total synthesis of latrunculin B (**1.2**) in 1986.[17] In 1990, Smith[18] and White[25] reported back-to-back syntheses of the 16-membered macrolide, latrunculin A (**1.1**) as well as other latrunculin congeners. Recently, Fürstner *et al.* published total syntheses of parent compounds latrunculin A and latrunculin B as well as a multitude of natural and unnatural latrunculin analogs. Fürstner and

coworkers have also spearheaded a detailed structure activity relationship (SAR) study of the latrunculins driven by information from the report of a crystal structure of G-actin bound latrunculin A.[11,22,23] Binding information gathered from the crystal structure is summarized in Figure 1.2.[11,22] The macrocyclic ring of latrunculin A skeleton predominantly fits in a hydrophobic region of the binding site, with carbons 5-7 partly exposed to solvent. An interesting hypothesis from Fürstner was that the stereochemistry at the C-18 position of latrunculin A should have an impact on the binding constant, as this stereogenicity dictates the location of the thiazolidinone in relation to the hydrogen bond donors/acceptors in the binding pocket.[22]

Figure 1.2. Proposed Bonding Interactions between Latrunculin A and G-actin

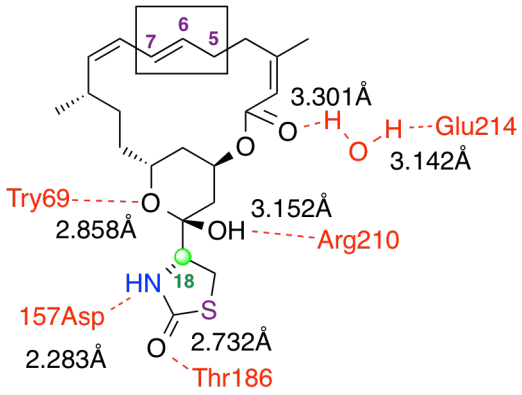

Although the naturally occurring C-16 epimer of latrunculin B (16-*epi*-latrunculin B) was synthesized and proven to inhibit actin polymerization,[22] latrunculin A congeners epimeric at C-18, had not been synthesized or tested prior to the recent report from Crews.[16] The ability of the C-18 stereogenicity to control actin depolymerization was again called into question in 2008, when a new epimeric latrunculin A congener was isolated by Crews and coworkers (*vide infra*).[16]

1.1.1 (+)-18-*epi*-Latrunculol A

Due to the general utility of latrunculin A as a molecular probe, significant efforts have been directed towards the isolation and study of latrunculin analogs. In 2008, Crews and coworkers

isolated 13 latrunculin analogs from two taxonomically unrelated sponges, *Negombata magnifica* and *Cacospongia mycofijiensis*.[16] Upon spectroscopic characterization and initial biological assessment, (+)-18-*epi*-latrunculol A (**1.3**) emerged as an intriguing discovery.

The latrunculin A congener, (+)-18-*epi*-latrunculol A (**1.3**), was characterized *via* extensive 2D NMR analysis involving spectroscopic comparison to a related isolate, latrunculol A (**1.4**), which revealed that the two congeners were epimeric at C-18 (Figure 1.3, **A.**). Latrunculol A (**1.4**) was characterized and assigned in turn through spectroscopic comparison to latrunculin A (**1.1**), which established that both natural products shared the same carbon skeleton and that latrunculol A (**1.4**) contained a vicinal diol in the place of the *E*-olefin in latrunculin A (**1.1**). The stereochemistry of the vicinal diol in **1.4** was elucidated through chemical conversion to the acetonide and NOESY NMR analysis (Figure 1.3, **B.**).

Figure 1.3. A. Comparison of H-18 Between Congeners **B.** NOESY Analysis of Latrunculol A

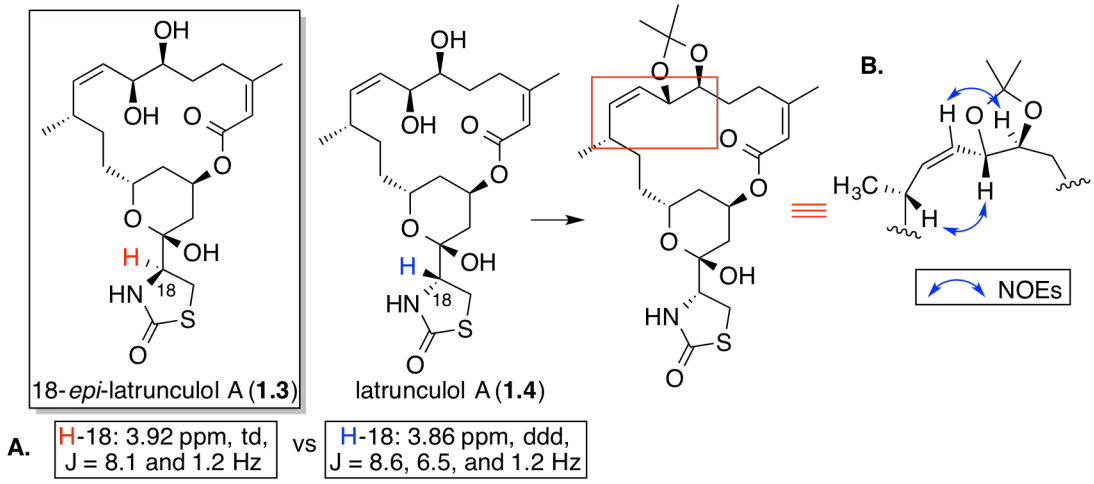

The isolated latrunculin congeners were evaluated first in a disk diffusion soft agar cell-based assay against three murine cell lines: colon 38, L1210, and CFU-GM. The epimeric latrunculin congener, (+)-18-*epi*-latrunculol A (**1.3**) displayed the highest solid tumor selective cytotoxicity profile[27] of all the latrunculin natural products tested against colon 38 and CFU-GM (Z_{C38}–Z_{CFU-}

$_{GM}$ = 15.0 mm). This congener (**1.3**) also demonstrated significant selective cytotoxicity against HCT-116 (5.5 μM) versus MDA-MB-435 (>50 μM) cell lines, and surprisingly did *not* display actin depolymerization activity (Figure 1.4). Interestingly, latrunculol A (**1.4**) proved to be the most cytotoxic latrunculin tested against colon 38 (Z_{C38} = 23.5 mm, at 1.1 μm), being 2.6 and 1.8 times more toxic than parent compounds latrunculin A (**1.1**) and latrunculin B (**1.2**) respectively. Latrunculol (**1.4**) however produced significant actin disruption and did *not* exhibit selective cytotoxicity, bringing the biological significance of C-18 stereogenicity in the latrunculin A framework into light.

Figure 1.4. Microfilament Disrupting Effect of Latrunculin Compounds

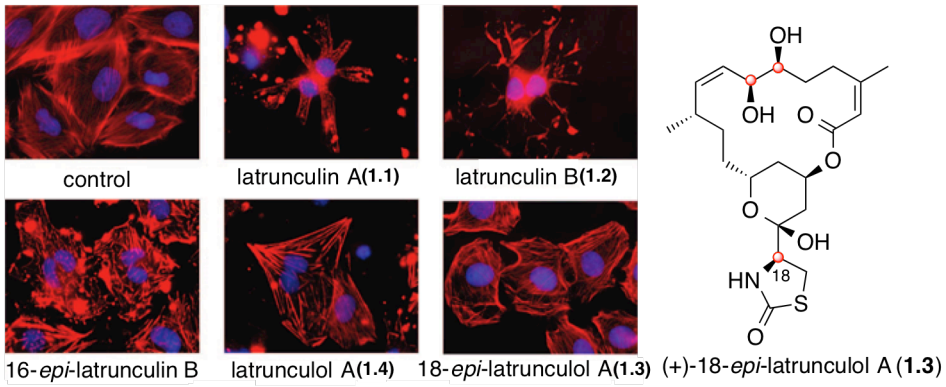

Adapted with permission from Amagata, T.; Johnson, T. A.; Cichewicz, R. H.; Tenney, K.; Mooberry, S. L.; Media, J.; Edelstein, M.; Valeriote, F. A.; Crews, P. *J. Med. Chem.* **2008**, 51, 7234-7242. Copyright 2008 American Chemical Society

Conflicting accounts have been reported concerning the potential of latrunculin A to be a therapeutic agent.[16,28] Due to the ubiquity of actin in living organisms, latrunculin A and latrunculin B display an unselective cytotoxicity profile and thus the parent latrunculins are generally considered not to possess a useful therapeutic index.[28] Indeed, to date cytotoxic actin inhibitors have not been utilized as a therapeutic agent.[16] Thus the selective cytotoxicity profile of (+)-18-*epi*-latrunculol A (**1.3**), as well as the actin-independent mode of cytotoxicity, makes this congener an exciting potential candidate as an anti-cancer therapeutic. In view of the divergent and presently unknown mode of cytotoxicity and the potential of (+)-18-*epi*-latrunculol A (**1.3**) as

a cancer chemotherapeutic agent, we embarked on the development of a scalable total synthesis of this latrunculin congener first to confirm the structure and relative and absolute stereochemistry as well as to provide additional material to facilitate additional biological studies.

1.2 Relevant Synthetic Studies

Although at the outset of this project there were no reported total synthesis of (+)-18-*epi*-latrunculol A, the latrunculin family of natural products had received considerable attention from the synthetic community.[17-26] As (+)-18-*epi*-latrunculol A (**1.3**) shares the (+)-latrunculin A (**1.1**) carbon skeleton, previous total syntheses of parent compound (**1.1**) will be reviewed, as well as the Smith group's seminal report on the total synthesis of (+)-latrunculin B (**1.2**).[17-19]

1.2.1 The Smith Syntheses of (+)-Latrunculin B (1.2) and (+)-Latrunculin A (1.1)

In 1986, Smith *et al.* reported the first total synthesis of (+)-latrunculin B (**1.2**).[17] They proposed a retrosynthetic analysis that would permit access to both (+)-latrunculin B (**1.2**) and (+)-latrunculin A (**1.1**) *via* an advanced common aldehyde **1.6** (Scheme 1.1). In turn, Smith and coworkers envisioned a Mitsunobu macrolactonization to close both the 14-membered macrolactone of (+)-latrunculin B and the 16-membered macrolactone of (+)-latrunculin A, in conjunction with a Wittig olefination to construct the requisite Z-olefin in both latrunculin natural products. The Wittig olefination called for reagents **1.5** and **1.10** to access the complete carbon skeletons of (+)-latrunculin B and (+)-latrunculin A, respectively. The cyclic ketal moiety in **1.6** was anticipated to be accessed *via* an acid-mediated cyclization/equilibration sequence from ketone **1.7** (Scheme 1.2). Construction of the β–hydroxy ketone **1.7**, in turn, was envisioned to utilize an aldol reaction. The requisite aldehyde (i.e., the aldol coupling partner) would arrive *via* orthoester formation of a racemic mixture of lactone **1.8**, employing enantioenriched 2,3-butanediol to provide a mixture of separable diastereomeric orthoesters, followed by ozonolysis

of **1.12**. Methyl ketone **1.9** was anticipated to be readily accessible *via* elaboration of *L*-cysteine.

Scheme 1.1. Smith's Retrosynthetic Analysis of (+)-Latrunculin B and (+)-Latrunculin A

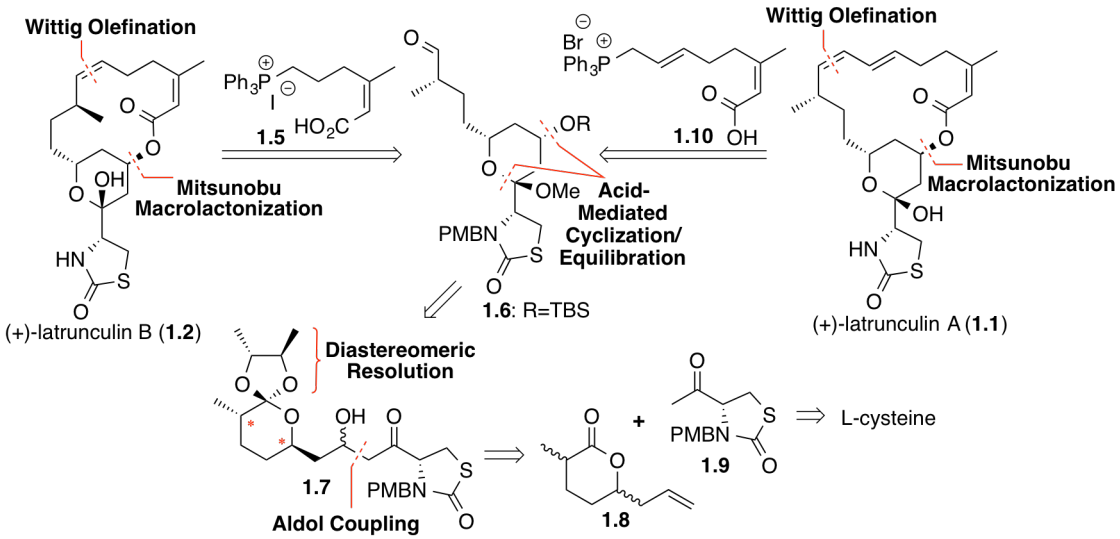

In the forward direction, orthoester **1.12** was isolated as a single diastereomer in three steps from racemic allyl cyclopentanone after preparative HPLC separation of the diastereomeric orthoesters (Scheme 1.2). The aldol reaction afforded a 4:1 mixture of diastereomeric alcohols (**1.7**) that, upon treatment with an aqueous HCl/THF mixture, equilibrated to a 12:1 mixture of lactol diastereomers. Treatment with acidic methanol then afforded ketal **1.14** in 47% from **1.12**.

Scheme 1.2. Smith's Synthesis of Latrunculin A and Latrunculin B

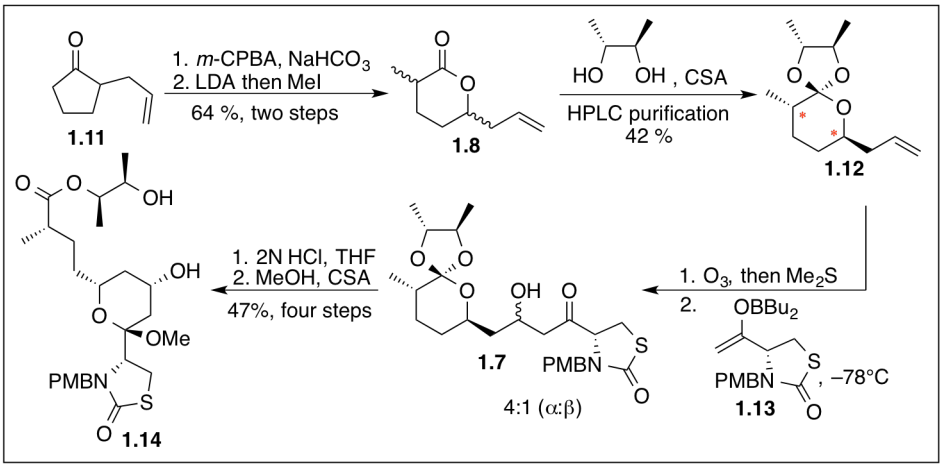

Protection of diol **1.14,** followed by DIBAL reduction delivered the common aldehyde intermediate **1.6** in 53% over two steps (Scheme 1.3). Wittig olefination, employing ylide **1.15** (derived from **1.5**, Scheme 1.1) afforded Z-olefin **1.16** in good yield (81%). Subsequent deprotection with HF•pyridine was followed by Mitsunobu macrolactonization to furnish the 14-membered macrolactone **1.17**. A two-step global deprotection was carried out utilizing ceric ammonium nitrate to achieve oxidative removal of the *p*-methoxy benzyl protecting group and in turn heating the methyl ketal at 60 °C in an aqueous acetic acid/THF mixture afforded (+)-latrunculin B in 46% from 1.16 (Scheme 1.3). The overall yield was 2.5% over the 13 steps.

Scheme 1.3 Smith's Completion of the Total Synthesis of (+)-latrunculin B

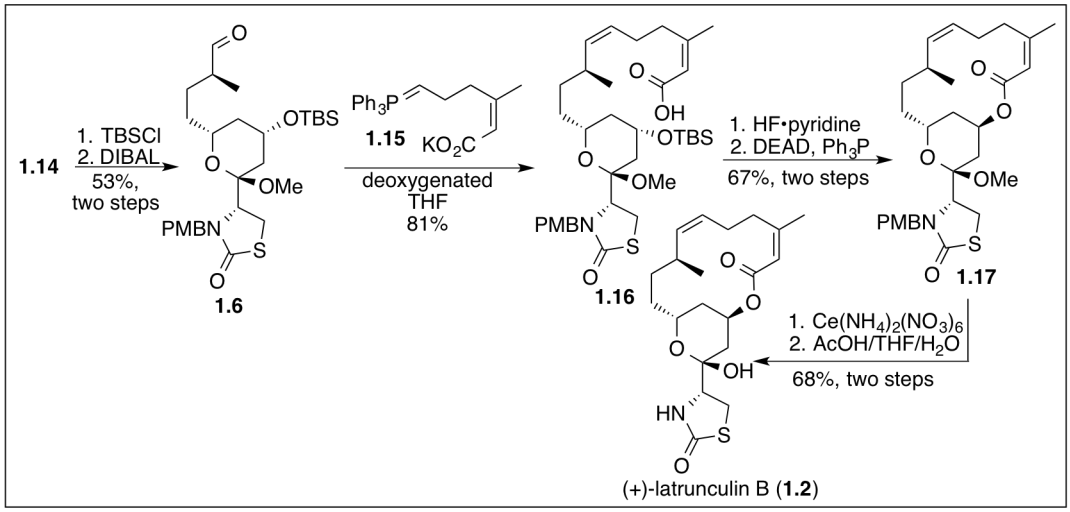

White[26] and Fürstner[20-24] have also reported successful total syntheses of latrunculin B (**1.2**). The truncated latrunculin natural product served as an excellent initial target for their respective synthetic strategies to access the latrunculin family of natural products. As White and Fürstner both also reported total syntheses of latrunculin A that are reviewed (*vide infra*), [20-24,26] their syntheses of latrunculin B will not be reviewed in this thesis.

In 1990, both Smith and White simultaneously reported total syntheses of latrunculin A.[14,21] As the synthesis reported by Smith and coworkers both stems from their initial work on (+)-

latrunculin B and served as the basis for the synthesis of (+)-18-*epi*-latrunculol A (Chapter 2), the Smith synthesis of (+)-latrunculin A will be reviewed first.[18,19,25]

The synthesis of (+)-latrunculin A began with aldehyde intermediate **1.6**, which was also utilized by Smith and coworkers in the synthesis of (+)-latrunculin B. The intended Wittig olefination proceeded in good yield (86%), providing that the reaction mixture was thoroughly deoxygenated (Scheme 1.4). The ensuing 16-membered macrolactonization however was low yielding (31%) and efforts to remove the PMB protecting group were unsuccessful.

Scheme 1.4. Wittig Olefination and Mitsunobu Macrolactonization with PMB

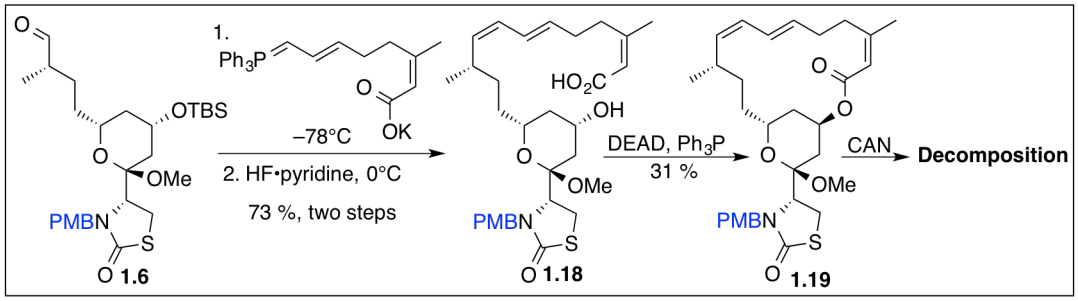

Unable to deprotect advanced intermediate **1.19**, Smith *et al.* implemented a protecting group exchange from PMB to Teoc (Scheme 1.5). Towards this end, the PMB protecting group was removed from ketal **1.20** utilizing a procedure from Williams.[29] Oxidation was, in turn, followed by Teoc protection of the thiazolidinone to provide **1.21** in 37% over three steps. The subsequent Wittig olefination, deprotection, and macrolactonization provided comparable yields to the analogous reactions of PMB-protected substrates (20%, three steps). Removal of the Teoc protecting group in this case, proceeded in good yield (84%) and treatment of the penultimate compound with a 3N HCl/THF mixture delivered (+)-latrunculin A (**1.1**) in a 72% yield.

Scheme 1.5. Protection Group Exchange and Completion of (+)-Latrunculin A

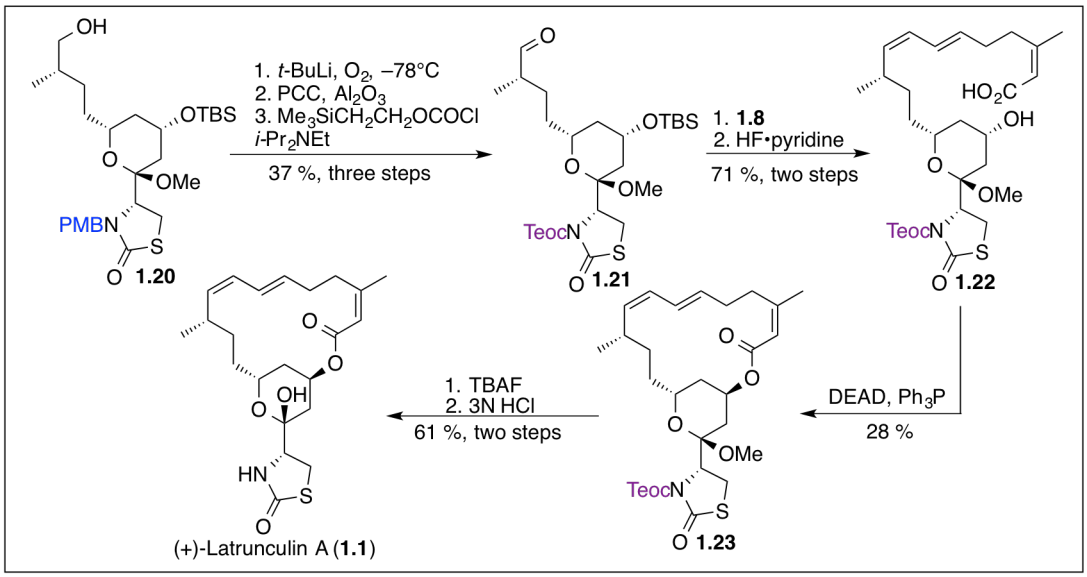

1.2.2 The White Synthesis of (+)-Latrunculin A (1.1)

White and coworkers utilized a multicomponent reaction sequence developed in their lab to construct a large section of the latrunculin skeleton in a single step and achieve their total syntheses of (+)-latrunculin A and (+)-15-*epi*-latrunculin A (Scheme 1.6).[25,26] White envisioned a Mitsunobu macrolactonization to close the 16-membered lactone. Construction of the cyclic acetal was anticipated to arrive *via* an aldol reaction followed by an acid-mediated cyclization.

Scheme 1.6. White's Retrosynthetic Analysis of Latrunculin A

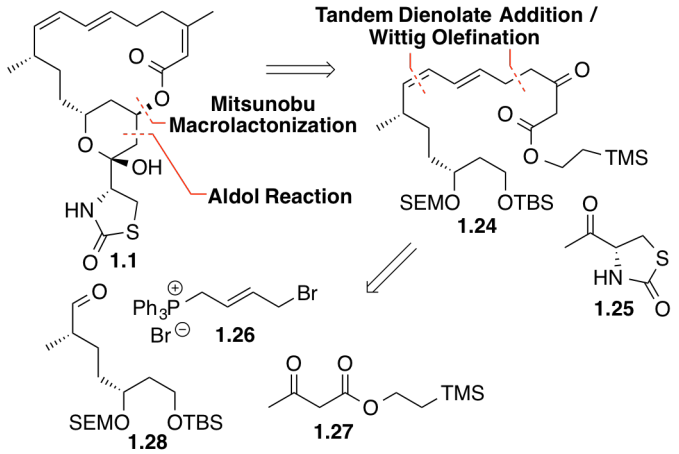

The northern hemisphere carbon skeleton (**1.24**) was constructed by employing the tandem dienolate addition/Wittig olefination one-pot protocol.

The one-pot dienolate addition/Wittig olefination afforded diene **1.24** in 60% yield *via* the sequence outlined in Scheme 1.7. Allylic phosphonium salt **1.26** was first converted to unsaturated phosphonium **1.29** *via* elimination of the allylic bromide with LDA. Addition of dienolate **1.30** to the phosphonium electrophile resulted in ylide **1.31**, which in turn selectively participated in a Wittig reaction with aldehyde **1.28** to construct successfully a large portion of the (+)-latrunculin A (**1.1**) carbon skeleton.

Scheme 1.7. White's Tandem Dienolate Addition/Wittig Olefination

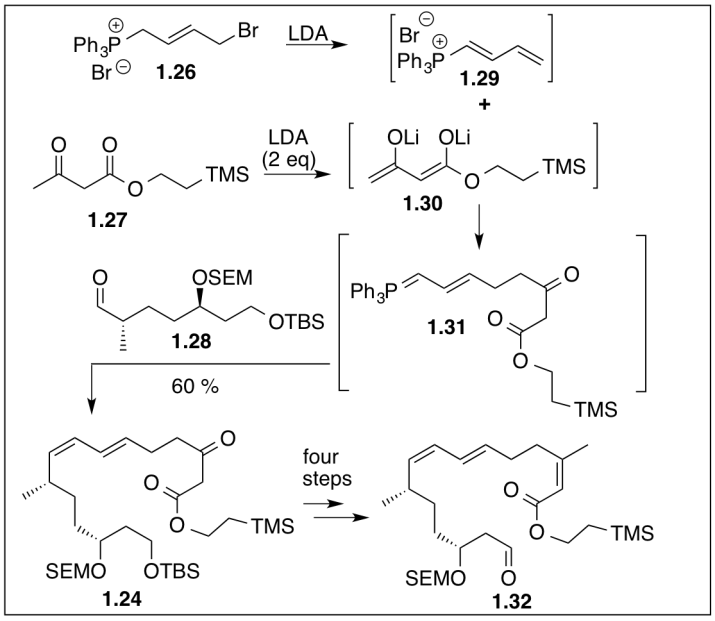

Elaboration of **1.24** over four steps next provided the aldol precursor **1.32**, which after aldol reaction, cyclization, and deprotection furnished two seco-acid diastereomers **1.33** and **1.34** (Scheme 1.8). Seco-acid **1.33** was converted to (+)-latrunculin A in 48% *via* Mitsunobu macrolactonization followed by acidic hydrolysis of the methyl ketal.

Scheme 1.8. White's Completion of (+)-Latrunculin A

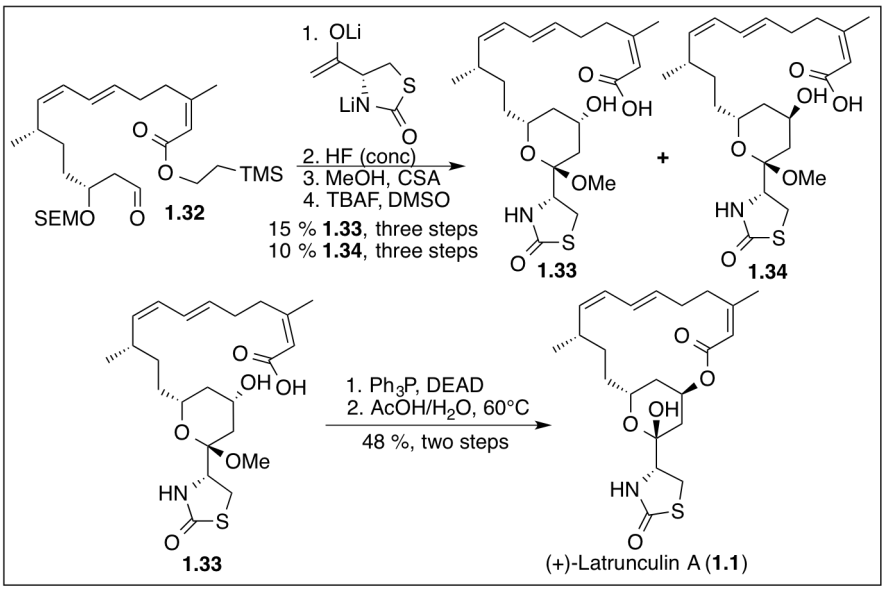

1.2.3 The Fürstner Synthesis of (+)-Latrunculin A (1.1)

In 2005, Fürstner and coworkers reported the total synthesis of (+)-latrunculin A (**1.1**) utilizing ring-closing alkyne metathesis (RCAM) as a key step to close the 16-membered macrolactone (Scheme 1.9).[20-24] Fürstner envisioned an acid-mediated cyclization/equilibration to

Scheme 1.9. Fürstner's Retrosynthetic Analysis of (+)-Latrunculin A

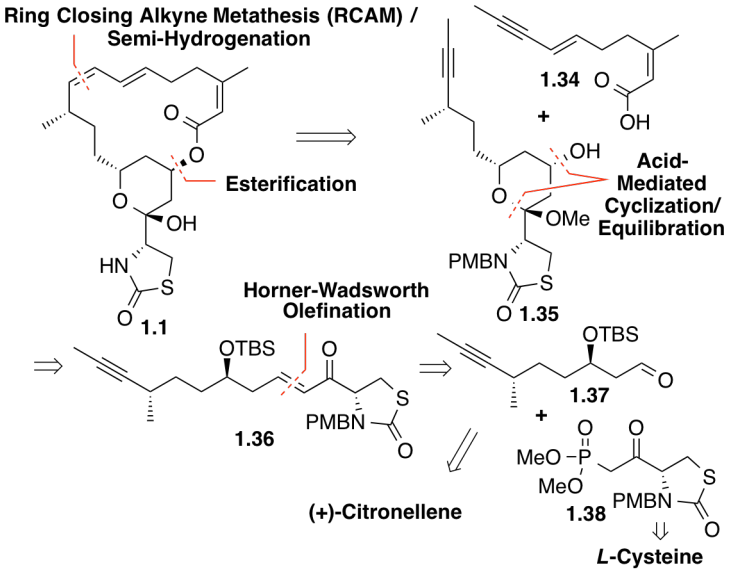

access the cyclic ketal present in (+)-latrunculin A, but interestingly they proposed to utilize δ–hydroxy enone **1.36** as a cyclization precursor (Scheme 1.11), as an alternative to their previously utilized[20,21] yet capricious aldol approach (Scheme 1.10).

Scheme 1.10. Fürstner's Aldol Coupling Approach Toward Latrunculin A

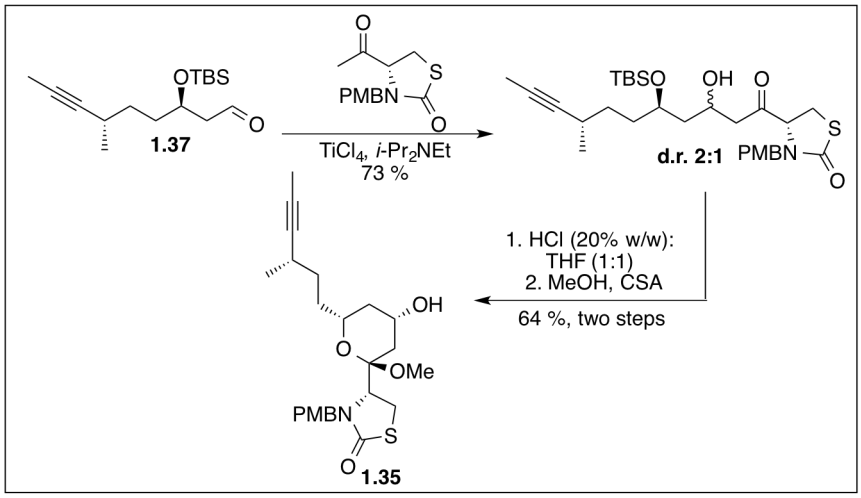

Construction of cyclization precursor **1.36** was achieved in ten steps from (+)-citronellene and employed a Horner-Wadsworth-Emmons reaction to construct the requisite enone (Scheme 1.11). Exposure of enone **1.36** to an aqueous HCl and THF mixture resulted in hydration,

Scheme 1.11. Fürstner's Acid-Mediated Enone Cyclization

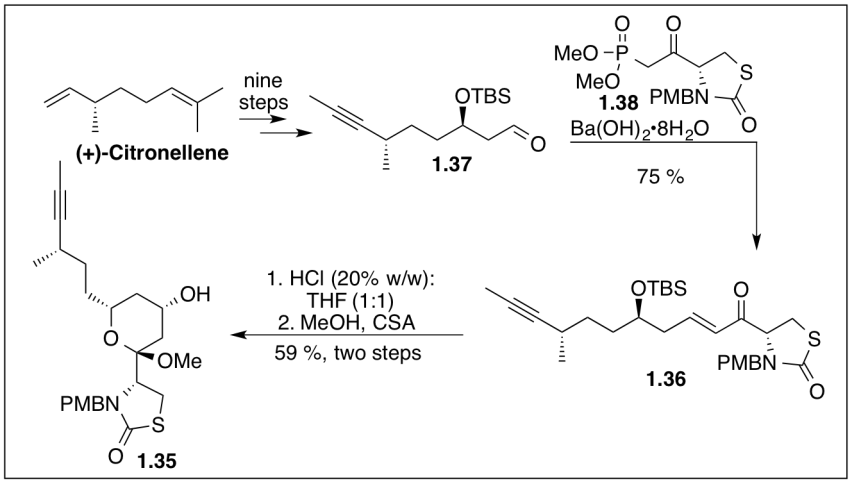

cyclization, and, after treatment with acidic methanol, construction of methyl ketal **1.35** in 59% over the two steps.

Metathesis precursor **1.39** (Scheme 1.12) was synthesized in two steps from alcohol **1.35** *via* triflate formation followed by displacement with the sodium salt of **1.34.** The anticipated ring closing alkyne metathesis (RCAM) provided enyne **1.41** in an unoptimized 36% yield by utilizing complex **1.40.** Decomposition was observed however when **1.36** was treated with ceric ammonium nitrate (CAN) in attempts to remove the robust PMB protecting group. To circumvent the problematic deprotection, the PMB protecting group was removed from RCAM precursor **1.39** using ceric ammonium nitrate and the thiazolidinone was re-protected with the more labile Teoc group, a strategy similar to that employed by Smith and coworkers.[17] With Teoc-protected RCAM precursor **1.42** in hand, molybdenum complex **1.40** was found to deliver macrocyclic enyne **1.43** in good yield (70%). Semi-reduction, using the Lindlar catalyst, was followed by removal of the Teoc group and hydrolysis of the methyl ketal to provide (+)-latrunculin A in 41% from **1.43**.

Scheme 1.12. Fürstner's Synthesis of (+)-Latrunculin A

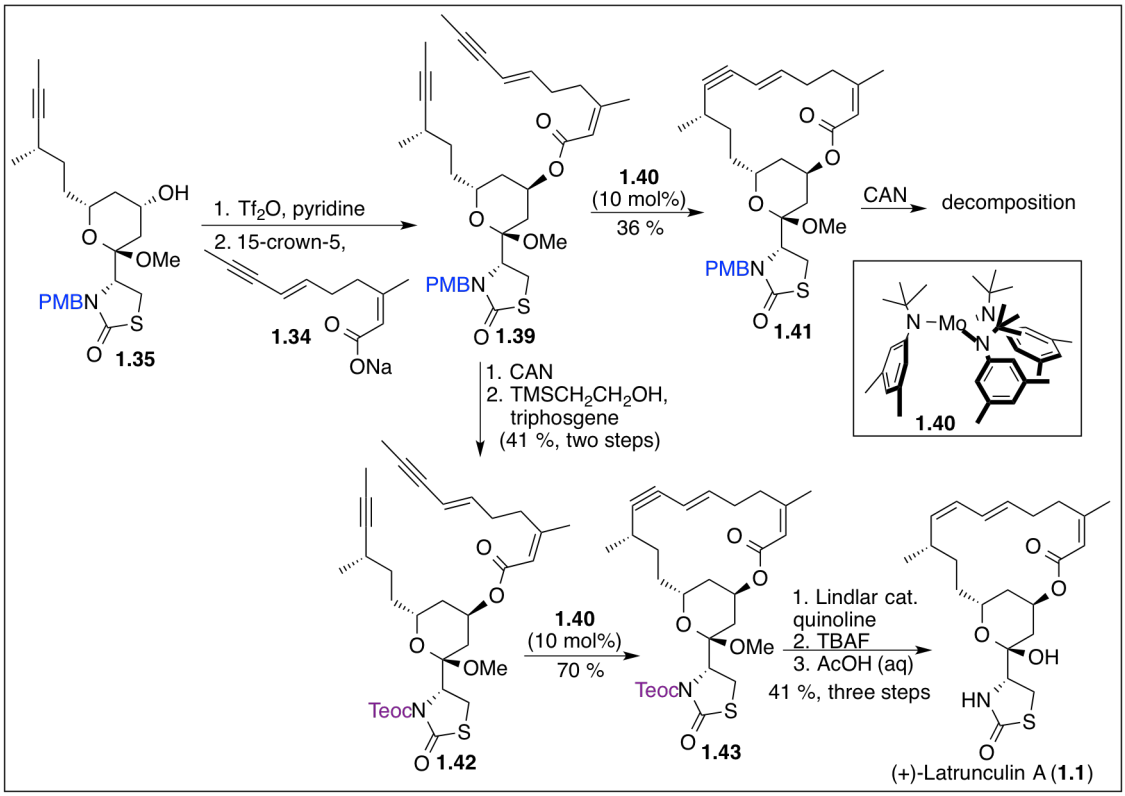

1.3 Summary

The synthetic ventures reviewed (*vide supra*) each developed unique approaches to achieve the total synthesis of latrunculin natural products. While the total syntheses of latrunculin A (**1.1**) resulted in varying efficiencies (Table 1.1), each synthesis provides valuable information concerning the reactivity and sensitivity of latrunculin A intermediates.

Table 1.1. Comparison of the Latrunculin A Total Syntheses

Research Group (year)	Longest Linear Step Count	Overall Yield of Longest Linear Sequence
Smith *et al.* (1990)	17 steps	0.65 %
White *et al.* (1990)	19 steps	0.7 %
Fürstner *et al.* (2005)	20 steps	2.3%

1.4 Chapter 1 References

(1) Spector, I.; Shochet, N.; Kashman, Y.; Groweiss, A. *Science* **1983***, 4584,* 493-495.

(2) Kashman, Y.; Groweiss, A.; Shueli, U.; *Tetrahedron Lett.* **1980**, *21*, 3629-3633.

(3) Neeman, I.; Fishelson, L.; Kashman, Y. *Mar. Biol.* **1975**, 30, 293

(4) Coue, M.; Brenner, S. L.; Spector, I.; Korn, *FEBS Lett.* **1987**, 213, 316-318.

(5) Lodish, H.; Berk, A.; Zipursky, S. L. Section 18.1, The Actin Cytoskeleton. In *Molecular Cell Biology ;* W. H. Freeman, Ed.; 2000; Vol. 4th edition., pp http://www.ncbi.nlm.nih.gov/books/NBK21493/.

(6) Huber, F.; Schnauss, J.; Roenicke, S.; Rauch, P.; Mueller, K.; Fuetterer, C.; Kaes, J. *Adv. Phys.* **2013**, 62, 1-112.

(7) F. Sasse, H.; Steinmetz, G.; Höfle, H. Reichenbach, *J. Antibiot.* **1993**, *46*, 741

(8) Klenchin, V. A.; King, R.; Tanaka, J.; Marriott, G.; and Rayment, I. *Chem. Biol*. **2005**, *12*, 287–291.

(9) Gouiffes, D.; Moreau, S.; Helbecque, N.; Bernier, J. L.; Henichart, J. P.; Barbin, Y.; Laurent, D.; Verbist, J. F. *Tetrahedron,* **1988,** *44* (2), 451-*9*.

(10) Allingham, J. S.; Klenchin, V. A.; Rayment, I. *Cell. Mol. Life Sci.* **2006**, 63, 2119-2134.

(11) Morton, W. M.; Ayscough, K. R.; McLaughlin, P. J. *Nat. Cell Biol.* **2000**, 2, 376-378.

(12) Ayscough, K. R.; Stryker, J.; Pokala, N.; Sanders, M.; Crews, P.; Drubin, D. G. *J. Cell Biol.* **1997**, 137, 399-416.

(13) Wang, J. S.; Sanger, J. M.; Sanger, J. W. *Cell Motil. Cytoskeleton* **2005**, 62, 35-47.

(14) Littlefield, R.; Almenar-Queralt, A.; Fowler, V. M. *Nat. Cell Biol.* **2001**, 3, 544-551.

(15) Sanger, J. W. *Proc. Natl. Acad. Sci. U. S. A.* **1974**, 71, 3621-3625.

(16) Amagata, T.; Johnson, T. A.; Cichewicz, R. H.; Tenney, K.; Mooberry, S. L.; Media, J.; Edelstein, M.; Valeriote, F. A.; Crews, P. *J. Med. Chem.* **2008**, 51, 7234-7242.

(17) Zibuck, R.; Liverton, N. J.; Smith, A. B. *J. Am. Chem. Soc.* **1986**, 108 (9), 2451–2453.

(18) Smith, A. B.; Noda, I.; Remiszewski, S. W.; Liverton, N. J.; Zibuck, R. *J. Org. Chem.* **1990**, 55, 3977-3979.

(19) Zibuck, R.; Liverton, N. J.; Smith, A. B. *J. Am. Chem. Soc.* **1992**, 114, 2995-3001.

(20) Fürstner, A.; De Souza, D.; Turet, L.; Fenster, M. D. B.; Parra-Rapado, L.; Wirtz, C.; Mynott, R.; Lehmann, C. W. *Chem. Eur. J.* **2007**, 13, 115-134.

(21) Fürstner, A.; Nagano, T.; Mueller, C.; Seidel, G.; Mueller, O. *Chem. Eur. J.* **2007**, 13, 1452-1462.

(22) Fürstner, A.; Kirk, D.; Fenster, M. B.; Aissa, C.; De Souza, D.; Nevado, C.; Tuttle, T.; Thiel, W.; Mueller, O. *Chem. Eur. J.***2007**, 13, 135-149.

(23) Fürstner, A.; Kirk, D.; Fenster, M. D. B.; Aissa, C.; De Souza, D.; Muller, O. *Proc. Natl. Acad. Sci. U. S. A.* **2005**, 102, 8103-8108.

(24) Fürstner, A.; Turet, L. *Angew. Chem. Int. Ed.* **2005**, 44, 3462-3466.

(25) White, J. D.; Kawasaki, M. *J. Am. Chem. Soc.* **1990**, 112, 4991-4993.

(26) White, J. D.; Kawasaki, M. *J. Org. Chem*. **1992**, 57, 5292-5300.

(27) Valeriote, F.; Grieshaber Charles, K.; Media, J.; Pietraszkewicz, H.; Hoffmann, J.; Pan, M.; McLaughlin, S. *J. Exp. Ther. Oncol.* **2002**, 2, 228–236.

(28) Newman, D.; Cragg, G. *J. Nat. Prod.* **2004**, 67, 1216-1238.

(29) Williams, R. M.; Kwast, E. *Tetrahedron Lett.* **1989**, *30*, 451

CHAPTER 2 Total Synthesis of (+)-18-*epi*-Latrunculol A (2.1)

2.1 Initial Synthetic Analysis of (+)-18-*epi*-Latrunculol A (2.1)

Figure 2.1. (+)-18-*epi*-Latrunculol A (**2.1**) and (+)-Latrunculin A (**2.2**)

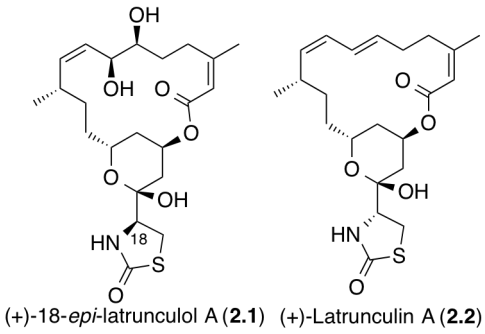

(+)-18-*epi*-latrunculol A (**2.1**) (+)-Latrunculin A (**2.2**)

2.1.1 Retrosynthetic Analysis of (+)-18-*epi*-Latrunculol A (2.1)

Our synthetic approach toward (+)-18-*epi*-latrunculol A (**2.1**), was based on the original Smith *et al.* total synthesis of (+)-latrunculin A (**2.2**),[1,2] with important modifications being made to ensure efficient and asymmetric access (Scheme 2.1). As in the earlier synthesis of (+)-latrunculin A, we envisioned a late-stage Mitsunobu macrolactonization[3] to close the 16-membered macrolactone and a Wittig olefination[4] to unite both northern and southern hemispheres and construct the *Z*-olefin. Wittig reagent (**2.3**) would arise *via* elaboration of cyclic ketal (**2.5**), which in turn would be accessed *via* an acid-mediated cyclization of hydroxy enone (**2.6**), similar to the cyclization employed by Fürstner *et al*.[5] Hydroxy enone (**2.6**) would be obtained through the use of a functional group compatible cross metathesis reaction.[6,7] The cross metathesis reaction was projected to shorten the synthetic route by two steps, compared to Fürstner's route, which utilized a Horner-Wadsworth-Emmons olefination,[5] by circumventing hydroxyl protection and ozonolysis. Cross metathesis partners **2.7** and **2.10** were envisioned to be readily available from known aldehyde (–)-**2.8**[8] and *D*-cysteine (**2.9**) respectively.

Scheme 2.1. Retrosynthetic Analysis of (+)-18-*epi*-Latrunculol A

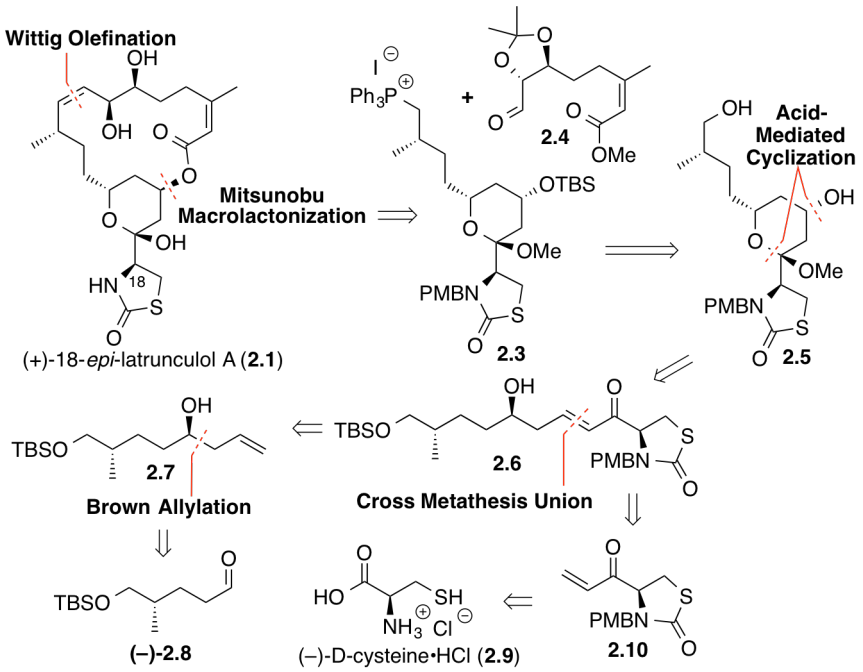

2.1.2 Synthesis of Thiazolidinone Fragment (+)-2.8 and Byproduct

The synthesis of (+)-18-*epi*-latrunculol A (**2.1**) began with the conversion of D-cysteine (**2.9**) to thiazolidinone (+)-**2.11** by employing phenyl chloroformate (Scheme 2.2), followed by chemoselective nitrogen protection using *p*-methoxy benzyl chloride (PMBCl).[9] Amide coupling utilizing TBTU as the coupling reagent furnished the Weinreb amide,[10] which when treated with freshly prepared vinyl Grignard reagent and quenched with 2N HCl furnished enone (+)-**2.10** in 55% from (+)-**2.11**. Interestingly, when the vinyl Grignard reaction was quenched with a saturated aqueous solution of ammonium chloride, a mixture of enone (+)-**2.10** and byproduct (+)-**2.12** was obtained, presumably *via* nucleophilic addition of the released hydroxylamine to the enone product.[11] The structure of (+)-**2.12** was confirmed by single crystal X-ray analysis. Fortunately, rapid acidification (2 N HCl) of the reaction mixture afforded enone (+)-**2.10** as the sole product, likely by protonating the released hydroxylamine and rendering this amine inert to the electrophilic enone.

Scheme 2.2. Synthesis of Enone (+)-**2.10** and Byproduct (+)-**2.12**

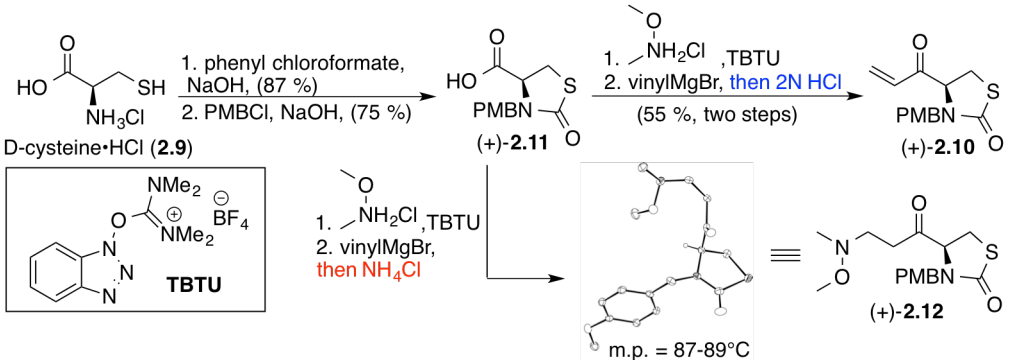

2.1.3 Cross Metathesis Reaction and Acid-Mediated Cyclization

Known alcohol (–)-**2.14** was readily available from 5-hexenoic acid *via* a known, three-step sequence (Scheme 2.3).[12] Protection of the primary alcohol as the TBS ether followed by

Scheme 2.3. Cross Metathesis Union

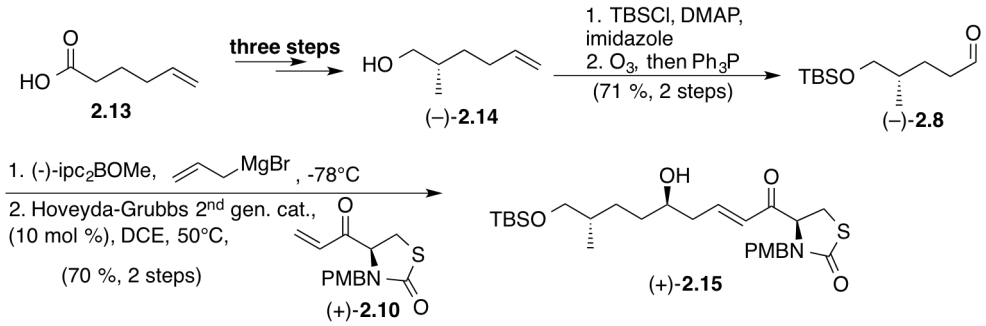

ozonolysis furnished known aldehyde (–)-**2.8** in 71% from alcohol (–)-**2.14**.[8] Brown allylation[13] next provided the requisite homoallylic alcohol, albeit contaminated with a small amount of epimeric homoallylic alcohol byproduct inseparable *via* standard silica gel chromatography. The mixture was treated with three equivalents of enone (+)-**2.10** and the Hoveyda-Grubbs 2nd generation catalyst while sparging with nitrogen to provide pure cyclization precursor (+)-**2.15** in 70% from (–)-**2.8**, as well as a 72% recovery of unreacted cross metathesis partner (+)-**2.10**.

The proposed acid-mediated cyclization/equilibration sequence was achieved by exposure of (+)-**2.15** to a 6N HCl:THF (1:1.3; v:v) mixture, to furnish lactol (+)-**2.18.** Lactol (+)-**2.18** proved to be unstable by slowly isomerizing at room temperature to a mixture of diastereomers; thus

protection as methoxy ketal (+)-**2.5** was therefore carried out immediately following the acid-mediated cyclization in a 43% yield over the two steps (Scheme 2.4). Although extensive experimentation on the acid, solvent, and temperature were carried out, multiple byproducts were always observed, concomitant with product formation. Byproduct formation is attributed to the highly acidic conditions required to hydrate the disubstituted enone (+)-**2.15**. Alternative conditions, explored to achieve the oxa-Michael reaction and ensuing cyclization, will be discussed in Chapter 3.

Scheme 2.4. Acid-Mediated Cyclization/Equilibration Sequence

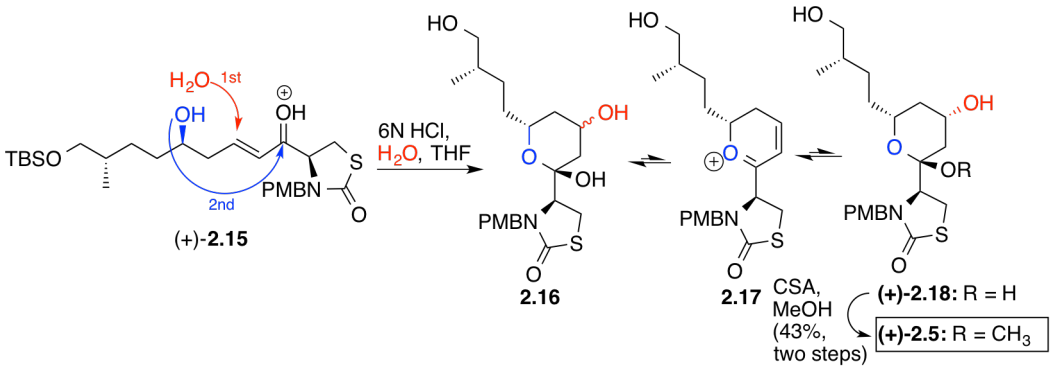

The proposed mechanism for the acid-mediated lactol formation is depicted in Scheme 2.4.[1,5] First, protonation of the carbonyl activates the enone for the intermolecular nucleophilic addition of water, to generate the δ,β–dihydroxy ketone, which cyclizes to lactol **2.16**. The initial addition of water is unselective, generating a ~1:1 mixture of diastereomeric alcohols (*via* TLC analysis); however over time the reaction mixture becomes enriched with the desired α–diastereomer, presumably by equilibration *via* oxonium intermediate **2.17**. Precedent for this equilibration process can be found in the Smith synthesis of (+)-latrunculin A.[1]

2.2 Fragment Union to Complete the Carbon Skeleton of (+)-18-*epi*-Latrunculol A

With the complete southern hemisphere (+)-**2.5** in hand, attention turned to potential methods for fragment union to complete the carbon skeleton of (+)-18-*epi*-latrunculol A (**2.1**). A Wittig olefination was initially envisioned to complete the carbon skeleton and construct the requisite *Z*-olefin. We were cognizant however of both the difficulties that the Wittig reaction presented in the original synthesis of (+)-latrunculin A,[1] and the ease of which (+)-**2.5** could be elaborated to test a variety of coupling procedures (Scheme 2.5). The ensuing section details the research on the final fragment coupling protocol to unite both northern and southern hemispheres of (+)-*epi*-latrunculol A (**2.1**)

Scheme 2.5. Access to Three Coupling Partners from Common Intermediate (+)-**2.5**

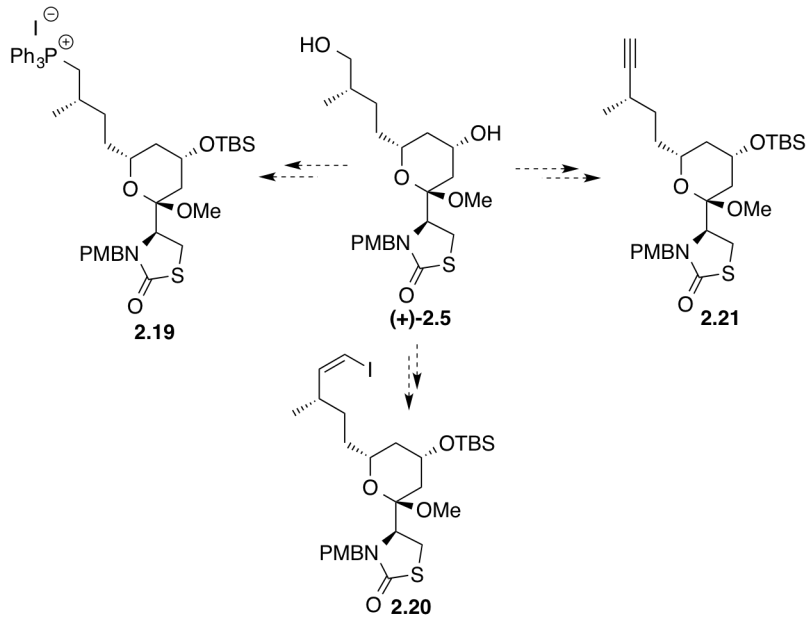

2.2.1 Synthesis of Wittig Reagent and Attempted Model Wittig Reaction

The desired Wittig reagent was readily accessible in three steps from ketal (+)-**2.5** (Scheme 2.6, 55% over three steps). Olefination, with benzaldehyde as the aldehyde coupling partner was first attempted using NaHMDS to deprotonate the unactivated Wittig reagent **2.19**. Full conversion to one product was observed, but to our surprise the product contained no new olefinic

peaks in the NMR spectrum. Moreover, ^{1}H-NMR analysis revealed no incorporation of the elements of benzaldehyde. The molecular weight, acquired *via* HRMS analysis, along with 14

Scheme 2.6. Synthesis of Wittig Reagent and Attempted Olefination

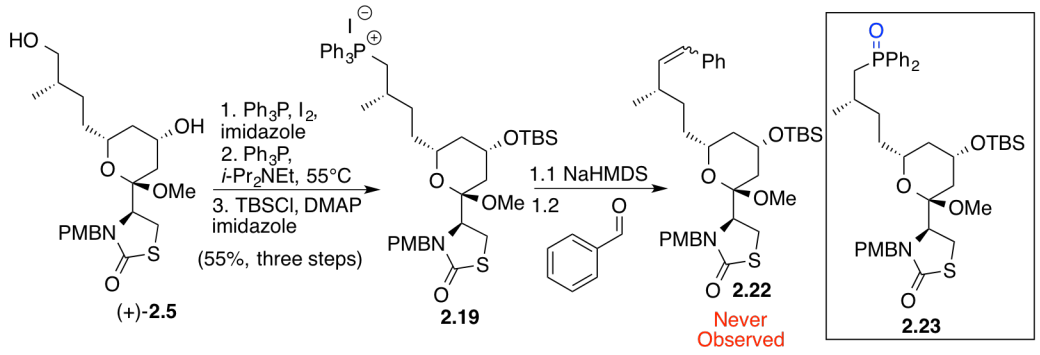

phenyl hydrogens (four being from the PMB group) present in the ^{1}H-NMR spectrum lead to the assignment of the product as phosphine oxide **2.23**. Reports from other research groups[14,15] have also documented the formation of phosphine oxides from unactivated Wittig reagents in the presence of hydroxide. We were aware that our base (NaHMDS) would deprotonate any adventitious water in the reaction mixture, forming hydroxide *in situ* which, in turn could lead to byproduct formation (Scheme 2.7). Therefore to avoid byproduct formation, strictly anhydrous conditions were employed (i.e., flame dried flasks, anhydrous reagents, and addition of 4Å activated molecular sieves). However, even with anhydrous conditions, byproduct **2.23** was the only product isolated. Deoxygenated solvent was also used, employing a freeze, pump, thaw

Scheme 2.7. Proposed Mechanism of Byproduct Formation

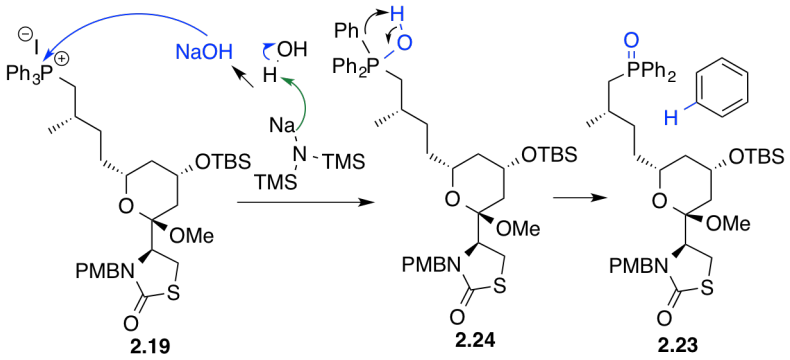

technique, but this also only resulted in formation of **2.23**. At this juncture we decided to test alternative methods for the union of both northern and southern hemispheres of (+)-18-*epi*-latrunculol A (**2.1**).

2.2.2 Synthesis of Vinyl Iodide and An Attempted Chelation-Controlled Addition

Vinyl iodide (+)-**2.20** and terminal alkyne (+)-**2.21** were each constructed in three steps from ketal (+)-**2.5** in 41% and 56% respectively (Scheme 2.8). The structure and absolute stereochemistry of crystalline alkyne (+)-**2.21** was confirmed by single crystal X-ray analysis (Scheme 2.11). The possibility of a utilizing a chelation-controlled addition to generate the necessary stereochemistry was next explored using vinyl iodide (+)-**2.20**.[16,17]

Scheme 2.8. Synthesis of Vinyl Iodide (**2.20**) and Terminal Alkyne (+)-**2.21**

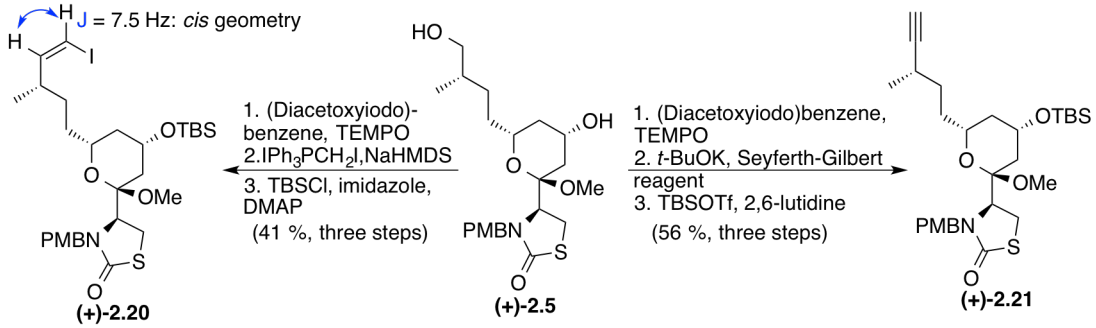

The requisite northern hemisphere aldehyde (+)-**2.25** (Scheme 2.9) was readily constructed in six steps from known alkynyl diol (–)-**2.26**.[18] The synthesis began with a two-step chemoselective protecting strategy on diol (–)-**2.26**, followed by deprotonation of the alkynyl proton with *n*-BuLi and addition of the resulting anion to methyl chloroformate to provide alkynoate (–)-**2.27**. Conjugate addition of Me_2CuLi was then followed in turn by deprotection utilizing acetic acid buffered TBAF and oxidation employing Parikh-Doering conditions[19] to complete construction of

Scheme 2.9. Synthesis of Aldehyde (+)-**2.25**

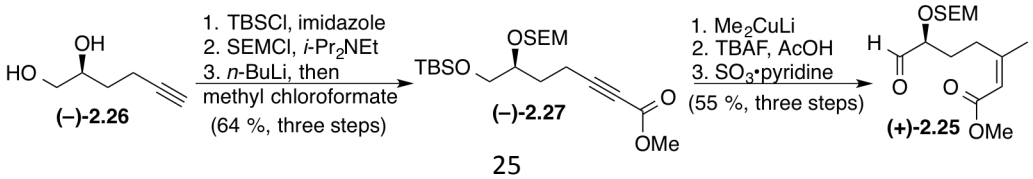

aldehyde (+)-**2.25** in 35% from (–)-**2.26**. Noteworthy here, TBAF, not buffered with acetic acid, led to complete isomerization of the enoate, revealing the base-sensitive nature of this aldehyde.

The chelation-controlled addition of a vinyl nucleophile resulting from metalation of vinyl iodide **2.20** to aldehyde (+)-**2.25** was expected to provide the desired diastereoselectivity *via* coordination of both the aldehyde oxygen and the neighboring oxygen protected by the small SEM protecting group (Scheme 2.10, A.).[16,17,20] The chelation-controlled addition was tested by performing a lithium-halogen exchange between vinyl iodide **2.20** and *t*-BuLi, and then transmetallating to achieve a variety of vinyl nucleophiles. Unfortunately, addition of aldehyde (+)-**2.25** to various metallated species only resulted in protodemetallation and decomposition of aldehyde (+)-**2.25** (Scheme 2.10, **B.**). Decomposition of (+)-**2.25** may be due to incompatibility of the strongly basic vinyl nucleophiles employed and the relatively acidic γ– or α–positions in enoate (+)-**2.25**. Deprotonation of the acidic hydrogens in enoate (+)-**2.25** by the generated vinyl nucleophiles appears to be kinetically more favorable than addition into the aldehyde.

Scheme 2.10. Attempted Chelation-Controlled Addition of Vinyl Iodide (**2.20**)

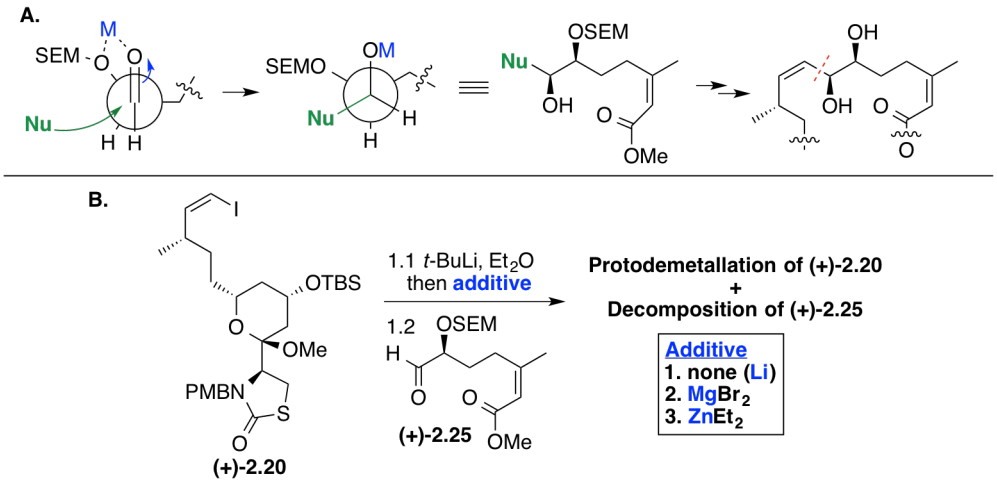

2.2.3 Synthesis of a Terminal Alkyne and Carreira Alkynylation

With renewed awareness of the sensitive nature of aldehyde (+)-**2.25**, a Carriera alkynylation[21] employing alkyne (+)-**2.21** was explored to generate a mild nucleophile that would avoid the competitive deprotonation observed with vinyl nucleophiles. A chiral ligand [(+)-N-methylephedrine] would be employed to dictate the stereochemistry of addition. Initial attempts at the Carreira alkynylation resulted in no reaction, with both alkyne (+)-**2.21** and aldehyde (+)-**2.25** recovered. We discovered however that when prolonged heating under high vacuum (12 h, 120°C, <1 Torr) was employed to activate the requisite $Zn(OTf)_2$, instead of flame drying (30 min), a 69% yield of Carreiera adduct (+)-**2.28** could be obtained. Moreover, when the reaction was permitted to stir for three days, the complete carbon skeleton of (+)-18-*epi*-latrunculol A (**2.1**) was generated in 95% yield (Scheme 2.11). The stereochemistry of the newly formed propargylic alcohol was confirmed *via* conversion to acetonide (+)-**2.29** and subsequent 2D NMR analysis; particularly diagnostic were the NOE correlations illustrated in Scheme 2.11.

Scheme 2.11. Carreira Alkynylation to Construct (+)-18-*epi*-latrunculol (**2.1**) Carbon Skeleton

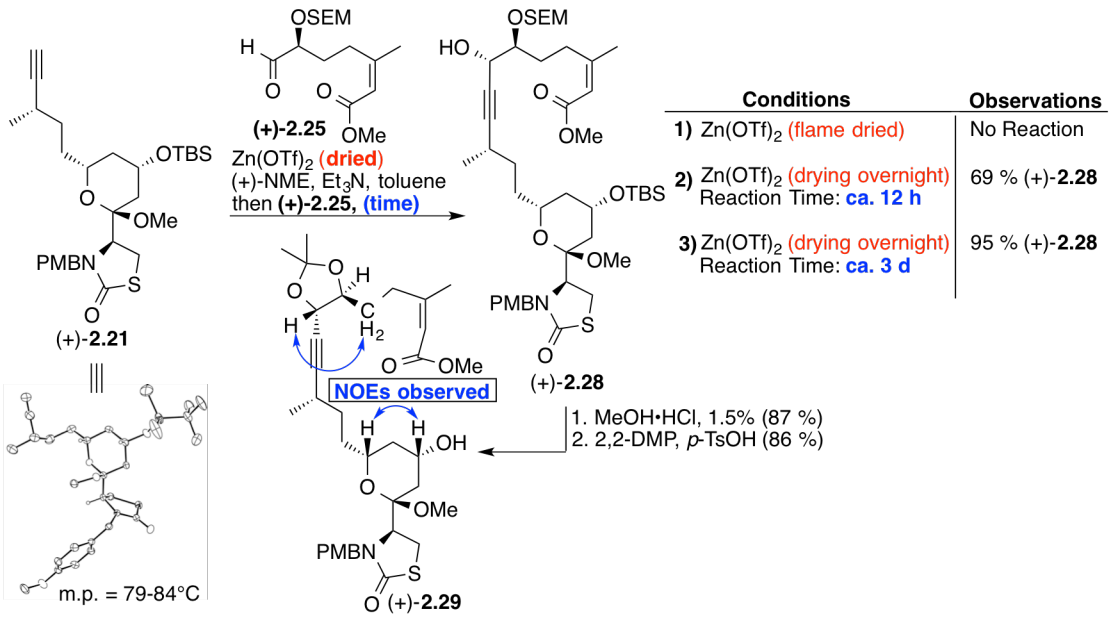

2.2.4 The (+)-18-*epi*-Latrunculol A (2.1) End Game

With the carbon skeleton fully intact we turned to the requisite alkyne semi-reduction. No reduction was observed when (+)-**2.28** was subjected either to Lindlar or P-2 nickel catalysts[22,23] under a hydrogen atmosphere. Molecular mechanics calculations employing MM2 force field were therefore undertaken to aid in visualization of the steric environment around the alkyne. Our strategy quickly changed however when we recognized that the methyl ester in (+)-**2.28** was in nearly the required conformation for the envisioned Mitsunobu macrolactonization. With this information, as well as the knowledge that the semi-reduction of an alkyne imbedded in a 16-membered macrolactone may be expedited by ring strain,[5] we moved forward with the synthesis of an alkyne-containing *seco*-acid. In the MM2 model of (+)-**2.28,** the two adjacent hydroxyls were *anti* to each other, suggesting that individually protecting each hydroxyl, such as with two SEM groups, might facilitate the required conformation for Mitsunobu macrolactonization by allowing free rotation between the hydroxyls, compared to an acetonide protecting group, which would effectively tie the hydroxyls together and prevent rotation.

Implementing our protecting group strategy, propargyl alcohol (+)-**2.28** was protected as bis-SEM ethers (Scheme 2.12). Chemoselective removal of the TBS ether employing acetic acid-buffered TBAF avoided isomerization of the sensitive enoate and hydrolysis of the methyl ester was achieved by heating with NaOH in ethanol to provide *seco*-acid (+)-**2.30** in a high 75% yield over three steps. Ethanol proved essential to achieve a reproducible reaction rate and yield, as the poor solubility of (+)-**2.28** in methanol lead to variability in the reaction. Also important to note is that heating (+)-**2.28** in strongly basic NaOH did not lead to any detectable isomerization of the enoate, thus emphasizing the important effects of the counterion and solvent on reactivity.

Scheme 2.12. Preparation of Seco-Acid (+)-**2.30**

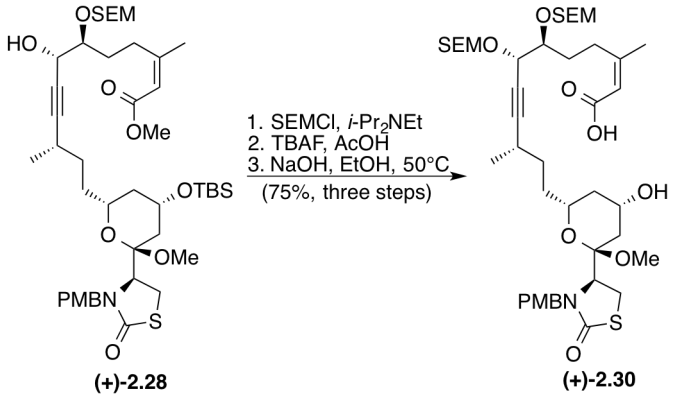

Turning to the highly anticipated Mitsunobu macrolactonization, *seco*-acid (+)-**2.30** was treated with triphenyl phosphine and diisopropyl azodicarboxylate (DIAD) in both toluene and THF solvents (Scheme 2.13). Interestingly, no reaction was observed in THF, however full

Scheme 2.13. Mitsunobu Macrolactonization

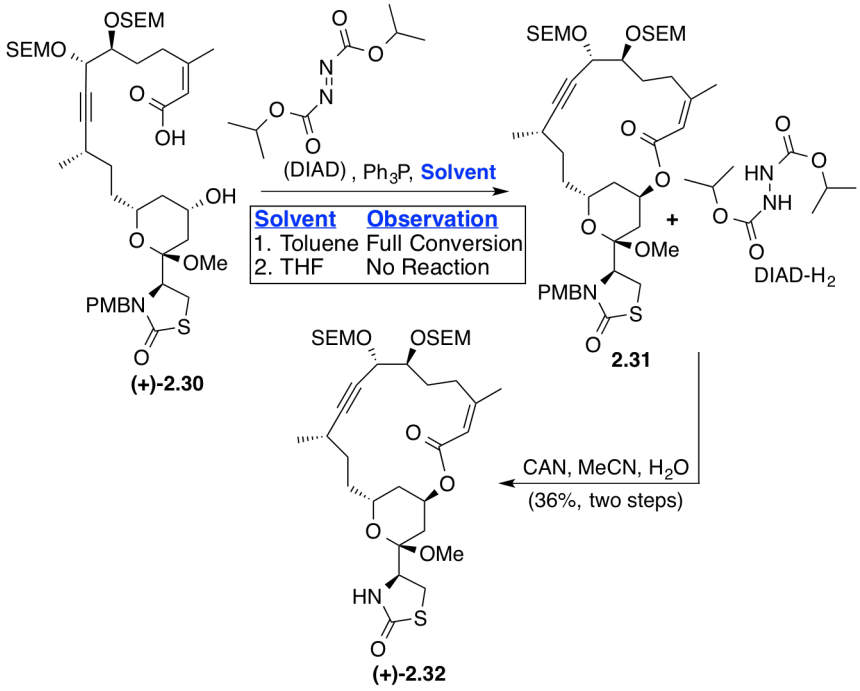

conversion was observed in toluene to provide a mixture of macrolactone and the reduced DIAD byproduct (DIAD-H_2), which proved inseparable *via* standard silica gel chromatography. Fortunately, submitting the mixture of macrolactone **2.31** and byproduct to ceric ammonium

nitrate (CAN), afforded pure deprotected macrolactone (+)-**2.32** in 36% from (+)-**2.30** after separation *via* flash chromatography. For comparison, the Mitsunobu macrolactonization utilized in the original Smith synthesis of (+)-latrunculin A proceeded in only a 31% yield,[1] and the resulting macrolactone proved incompatible with all conditions employed to remove the PMB protecting group. Fürstner *et al.* also observed decomposition of their late stage intermediates when attempting to remove the robust PMB protecting group, and they likewise required a protecting group exchange before the completion of their total synthesis of (+)-latrunculin A (**2.2**).[5] We had reasoned that macrolactone **2.31** might be able to withstand CAN-mediated oxidative removal of the PMB protecting group, as **2.31** lacks the conjugated diene moiety present in (+)-latrunculin A (**2.2**).

Global deprotection was undertaken next and comprised both removal of the two SEM protecting groups and hydrolysis of the methoxy ketal. Towards this end, (+)-**2.32** was treated with aqueous acetic acid with catalytic camphorsulfonic acid (CSA) at 50°C to provide penultimate alkyne (+)-**2.33**. Although global deprotection occurred, acidic removal of the SEM groups required extended reaction times (>12h) at elevated temperature (ca. 50 °C), which led to varying degrees of decomposition and in turn inconsistent yields, ranging from ca. 30% to 50% of (+)-**2.33**. With the expectation of optimizing the global deprotection, a thorough investigation of conditions to provide either global deprotection or selective SEM removal was initiated (Scheme

Scheme 2.14. Representative Deprotection Conditions Screened

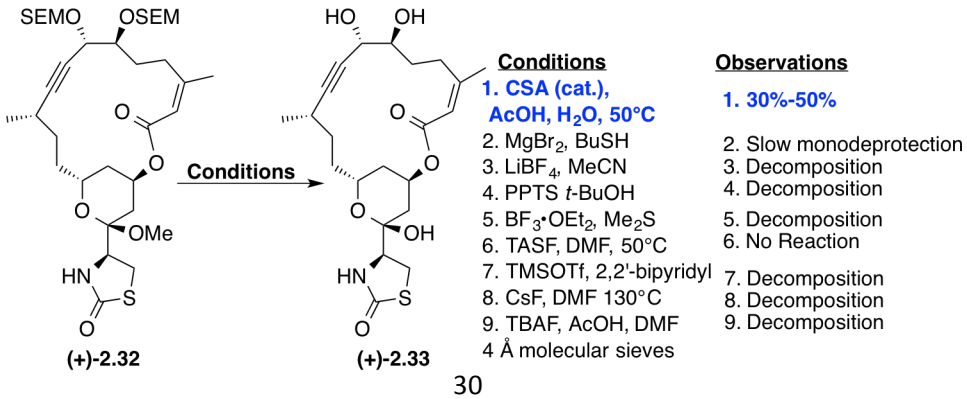

2.14). Unfortunately, all conditions screened resulted in either decomposition of (+)-**2.32**, prohibitively slow deprotection, or no reaction.

Although moderate in yield, the global deprotection provided sufficient penultimate alkyne (+)-**2.33** to test the final semi-reduction (Scheme 2.15). To our surprise, again no reduction was observed utilizing several batches of Lindlar or P-2 nickel catalysts under a hydrogen atmosphere. Other reduction conditions were explored that included: Wilkinson's catalyst,[24] homogeneous palladium catalyzed transfer hydrogenation, Adam's catalyst,[25] and a two-step hydroboration/protodeborylation sequence.[26] All conditions however resulted in either no reaction, over-reduction, or decomposition of starting material (Scheme 2.15). We eventually discovered that catalytic palladium on carbon with *no* poisoning agent, under a hydrogen atmosphere, afforded the desired product with incomplete conversion. The reaction was then repeated with additional catalyst until we found that 1.2 eq of Pd/C (10 wt%) was required to provide full conversion to the product (*via* LCMS analysis). Not withstanding this success, only a 29% isolated yield of (+)-18-*epi*-latrunculol A (**2.1**) was obtained (Scheme 2.15, condition 9). Fortunately, sufficient synthetic material was attained to facilitate a full spectral analysis.

Scheme 2.15. Optimization of the Final Semi-Reduction

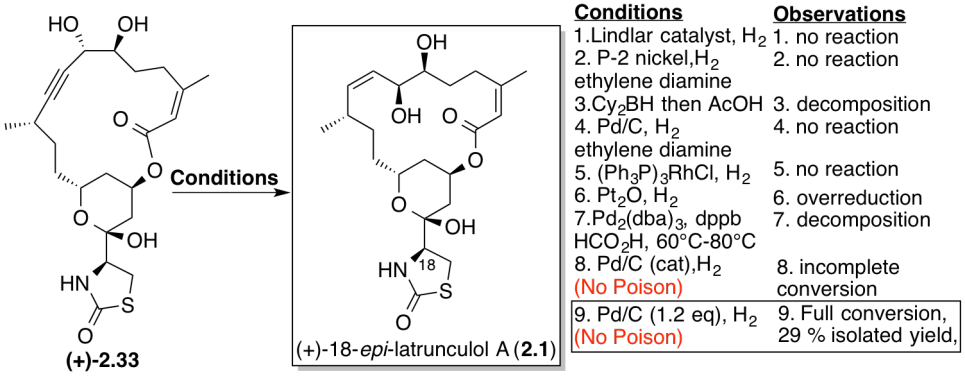

2.2.5. Interpretation of the Synthetic (+)-18-*epi*-latrunculol A (2.1) Spectral Data

All the spectral data of synthetic (+)-18-*epi*-latrunculol A (**2.1**) [i.e., ^{1}H-NMR (500 MHz), HRMS parent ion identification, and chiroptic properties] *except* the ^{13}C-NMR proved identical in all respects to those reported for the natural (+)-18-*epi*-latrunculol A (**2.1**). Alarmingly, the ^{13}C-spectra contained identical peaks to that reported for natural (+)-18-*epi*-latrunculol A (**2.1**),[2] however certain peaks were "doubled," suggestive of a diastereomeric mixture. Initially we feared that the extended reaction time required by the global deprotection was leading to epimerization of the anomeric carbon through the process illustrated in Scheme 2.16. However upon investigation of the ^{13}C NMR spectra of (+)-**2.33**, we observed that (+)-**2.33** was isolated as a single compound and not a mixture of diastereomers.

Scheme 2.16. Epimerization of the Anomeric Carbon

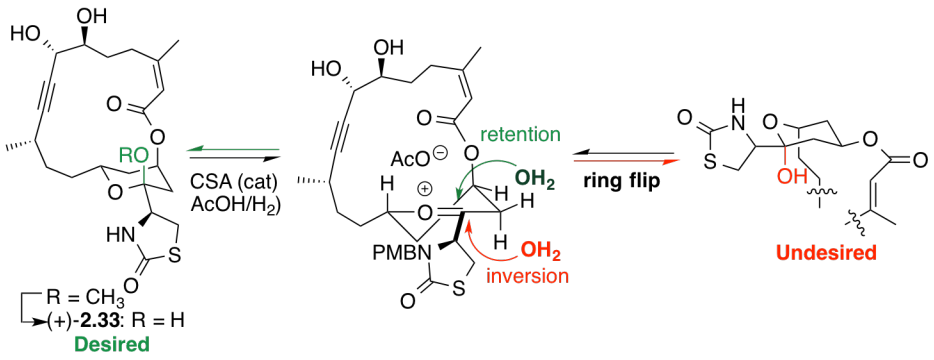

Turning our attention back to the natural product, we analyzed the "mixture" of synthetic (+)-**2.1** by super critical fluid chromatography (SFC) utilizing a chiral stationary phase. To our surprise, only one peak was observed, suggesting that the diastereomers were either not separable *via* the several conditions utilized or that we did not have a mixture of diastereomers. Towards this end, a ^{13}C NMR was taken of synthetic (+)-18-*epi*-latrunculol A (**2.1**) in $CDCl_3$, instead of acetone-d_6 in which the natural product was reported;[2] the spectra now revealed the correct number of carbons. Tracing the problem back to acetone-d_6, we noticed both H_2O and DHO

peaks in the ^{1}H NMR spectra and rationalized that a deuterium exchange, occurring between the solvent and (+)-18-*epi*-latrunculol A (**2.1**), could account for the mixture observed in the ^{13}C NMR. To our delight, handling acetone-d_6 strictly under a nitrogen atmosphere greatly reduced the amount of H_2O and DHO, and although the doubled peaks were still detectable in the ^{13}C spectra, they were now only minor (Figure 2.2, A.). Moreover, adding D_2O to the NMR sample caused the major carbon peaks that had previously appeared doubled to completely convert to the minor peaks resulting in one set of carbon peaks and a clean ^{13}C NMR spectra of deuterated 18-*epi*-latrunculol A (Figure 2.2, B.).

Figure 2.2. ^{13}C NMR (60-80ppm) of synthetic (+)-18-*epi*-latrunculol A (**2.1**) in **A.** acetone-d_6 **B.** acetone-d_6 with D_2O

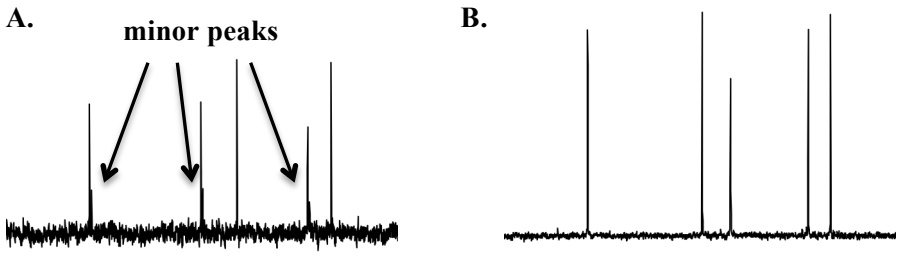

2.3 Protecting Group Exchange and Optimization of the Alkyne Semi-Reduction

Confident we had completed the first total synthesis and structural confirmation of (+)-18-*epi*-latrunculol A (**2.1**), we turned our attention toward optimizing the problematic reactions in the synthesis to enable a preparative scale synthesis of the natural product.

2.3.1 Further Optimization of the Alkyne Semi-Reduction

We reasoned that the low isolated yield from alkyne hydrogenation could be due to the large amount of adsorbing carbon present as the solid catalyst support. By switching to a palladium-mediated hydrogenation utilizing barium carbonate as a less adsorbent solid support, the semi-

reduction of (+)-**2.33** delivered (+)-18-*epi*-latrunculol A (**2.1**) now in a quantitative yield, albeit still requiring a stoichiometric amount of catalyst (Scheme 2.17).

Scheme 2.17. Successful Conditions for the Semi-Reduction

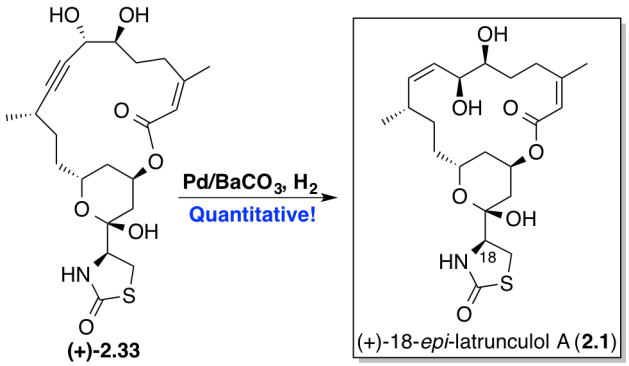

2.3.2 A Useful Protecting Group Exchange

As the investigation of multiple conditions for removal of the SEM groups provided limited success, we decided that switching to an alternative protecting group would offer a chance for improvement. We decided to return to an acetonide as protection for the vicinal diol, as this protecting group exchange would result in the same overall step count as bis-SEM protection, but importantly should be removed much more readily under acidic conditions. The noteworthy difference between SEM and acetonide protecting groups is the relative stability of the oxonium intermediates formed during acid-mediated deprotection (Figure 2.3). Due to the increased hyperconjugation from the geminal dimethyl groups in the acetonide compared to the methylene-centered carbocation, the acetonide is more readily removed under acidic conditions.[20] We were

Figure 2.3. Relative Stabilities of Intermediates Formed in Acidic Deprotection of A. SEM Ether and B. Acetonide

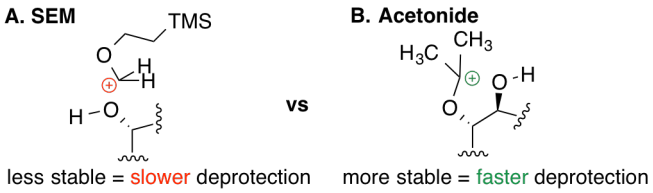

aware that the conformations of the bis-SEM and acetonide protected seco-acids would likely be different, as the bis-SEM ether permitted free rotation between the protected hydroxyls, whereas the acetonide effectively eliminated free rotation, and that these differences might negatively affect the macrolactonization. Nonetheless, we moved forward with a protecting group exchange with the expectation that the mild conditions required by the acetonide protecting group would provide a higher yielding global deprotection.

Treatment of alkyne addition product (+)-**2.28** with acidic methanol afforded removal of both SEM and TBS protecting groups. The vicinal diol in the resulting triol was chemoselectively protected as the acetonide to provide (+)-**2.29** in 77% over the two steps (Scheme 2.18). Fortunately, after hydrolysis, the Mitsunobu macrolactonization and ensuing PMB removal

Scheme 2.18. Protecting Group Exchange and Mitsunobu Macrolactonization

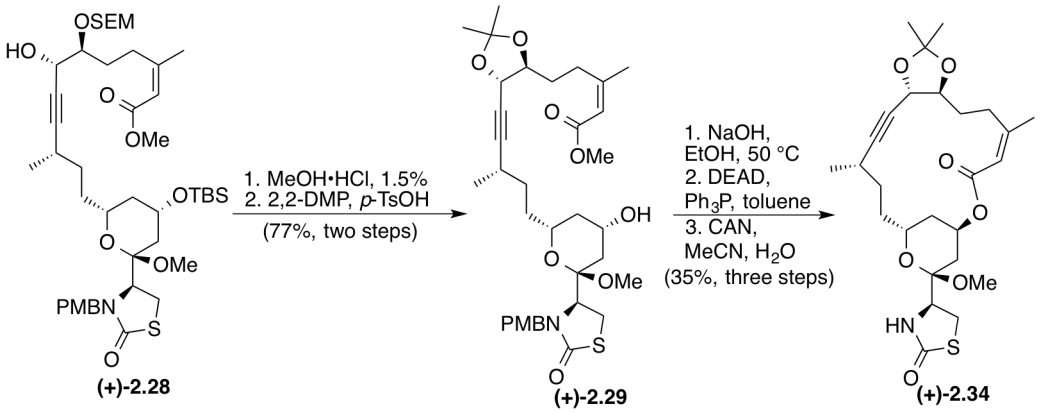

proceeded in comparable yield as with the SEM protected intermediates to provide macrolactone (+)-**2.34** in a 35% yield from methyl ester (+)-**2.29**. We were pleased to find that the anticipated global deprotection now delivered penultimate alkyne (+)-**2.33** in good yield (86%) in only two hours (Scheme 2.19). Synthetic (+)-18-*epi*-latrunculol A (**2.1**) was now obtained in an 86 % yield over the final two steps, a marked improvement from the two-step, 15 % yield provided from the first generation synthetic route.

Scheme 2.19. Revised Global Deprotection and Semi-Reduction

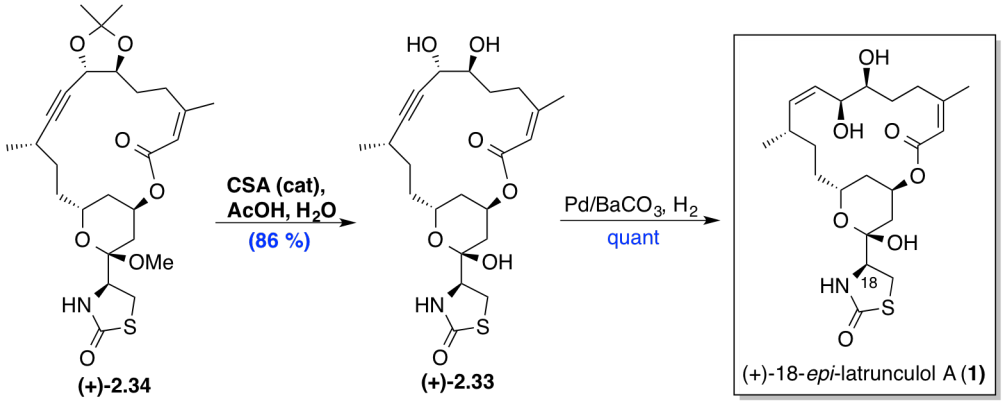

2.4 Summary

In summary, we are pleased to report the first total synthesis, structural validation, and assignment of the relative and absolute stereochemistry of (+)-18-*epi*-latrunculol A (**2.1**), in an overall yield of 3.5 % with a longest linear sequence of 15 steps from known aldehyde (–)-**2.8** as outlined in Scheme 2.20. Key steps in the route include a functional group compatible cross metathesis reaction, which allows the elimination of two steps from the synthetic route, an acid-mediated cyclization/equilibration sequence, a mild Carreira alkynylation, and finally a late-stage Mitsunobu macrolactonization. In addition, successful optimization of the moderate yielding global deprotection and low yielding semi-reduction will now permit preparative access to totally synthetic (+)-18-*epi*-latrunculol A (**2.1**).

Scheme 2.20. Total Synthesis of (+)-18-*epi*-latrunculol A (**2.1**)

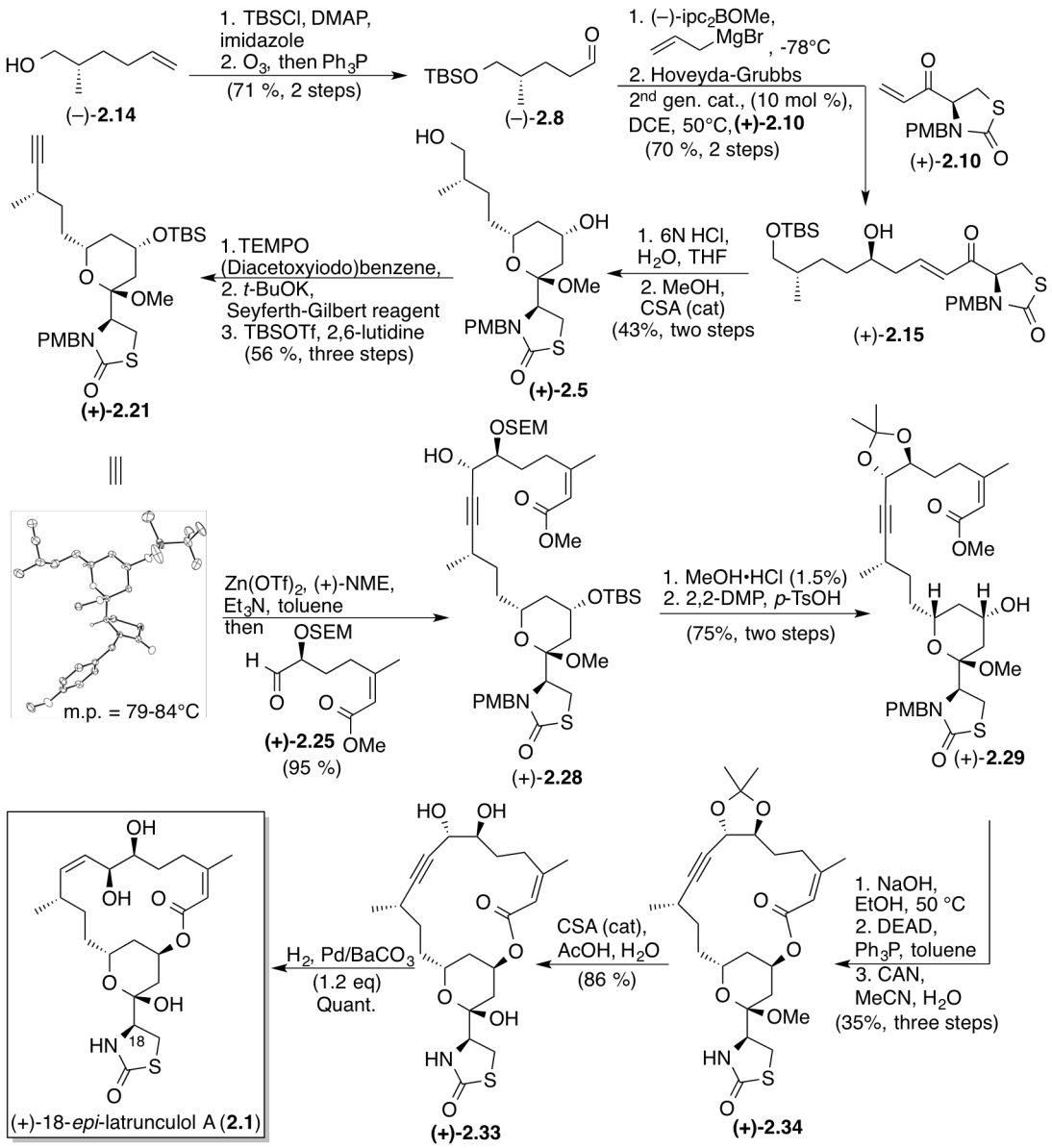

2.5 Chapter 2 References

(1) Smith, A. B.; Noda, I.; Remiszewski, S. W.; Liverton, N. J.; Zibuck, R. *J. Org. Chem.* **1990**, 55, 3977-3979.

(2) Amagata, T.; Johnson, T. A.; Cichewicz, R. H.; Tenney, K.; Mooberry, S. L.; Media, J.; Edelstein, M.; Valeriote, F. A.; Crews, P. *J. Med. Chem.* **2008**, 51, 7234-7242.

(3) Mitsunobu, O. *Synthesis* **1981***, 1,* 1-28.

(4) Wittig, G.; Haag, W. *Chemische Berichte-Recueil* **1955**, 88, 1654-1666.

(5) Fürstner, A.; Turet, L. *Angew. Chem. Int. Ed.* **2005**, 44, 3462-3466.

(6) Kingsbury, J. S.; Harrity, J. P. A.; Bonitatebus, P. J.; Hoveyda, A. H. *J. Am. Chem. Soc.* **1999***, 4,* 791-799.

(7) Chatterjee, A. K.; Choi, T.; Sanders, D. P.; Grubbs, R. H. *J. Am. Chem. Soc*, **2003**, 125 (37), 11360–11370

(8) Marshall, J.; Yanik, M. *J. Org. Chem.* **2001***, 4,* 1373-1379

(9) Seki, M.; Hatsuda, M.; Mori, Y.; Yoshida, S.; Yamada, S.; Shimizu, T. *Chem. Eur. J.* **2004***, 23,* 6102-6110.

(10) Nahm, S.; Weinreb, S. M. *Tetrahedron Lett.* **1981***, 39,* 3815-3818.

(11) Gomtsyan, A. *Org. Lett.* **2000**, 2, 11-13.

(12) Yu, S.; Pan, X.; Ma, D. *Chem. Eur. J.* **2006***, 25,* 6572-6584

(13) Brown, H. C.; Jadhav, P. K. *J. Am. Chem. Soc.* **1983***, 7,* 2092-2093.

(14) Berretta, G.; Coxon, G. D. *Tetrahedron Lett.* **2012***, 2,* 214-216.

(15) Chen, K.; Semple, J.; Joullie, M. *J. Org. Chem.* **1985***, 21,* 3997-4005.

(16) Reetz, M. T. *Acc. Chem. Res.* **1993**, 26, 462-468.

(17) Reetz, M. T. *Angew. Chem. Int. Ed.* **1984**, 23, 556-569.

(18) Ramharter, J.; Mulzer, J. *Org. Lett.* **2009***, 11,* 1151-1153.

(19) Parikh, J.; Doering, W. *J. Am. Chem. Soc.* **1967***, 89,* 5505-5507.

(20) Wuts, P. G. M. and Greene, T. W. *Greene's Protective Groups in Organic Synthesis*, 4th ed.; Wiley: Hoboken, NJ, **2007**

(21) Frantz, D.; Fassler, R.; Carreira, E. *J. Am. Chem. Soc.* **2000***, 8,* 1806-1807.

(22) Brown, C. A.; Ahuja, V. K. *J. Chem. Soc., Chem. Commun.*, **1973**, 553-554

(23) Lindlar, H. *Helv. Chim. Acta* **1952**, 35, 446-456.

(24) Osborn, J. A.; Jardine, F. H.; Young, J. F.; Wilkinson, G. *J. Chem. Soc. A* **1966**, 1711-1732.

(25) Voorhees, V.; Adams, R. *J. Am. Chem. Soc.*, **1922**, *44* (6), 1397–1405

(26) Brown, H. C.; Hamaoka, T.; Ravindran, N. *J. Am. Chem. Soc.*, **1973**, *95*, 6456–6457

CHAPTER 3. An Exploration of Tactics To Achieve the Cyclization of δ−Hydroxy Enones

Concurrent with our synthesis and optimization of the reactions discussed in Chapter 2, was a detailed investigation into the cyclization of δ−hydroxy enones (+)-**3.1** and (+)-**3.7** (products of cross metathesis) to afford cyclic ketal (+)-**3.4** (Scheme 3.1). Research initially focused on the screening and optimization of previously reported methods, but when successful conditions were not uncovered, development of a mild protocol for the cyclization of δ−hydroxy enones to cyclic ketals was determined to be a valuable synthetic contribution. We therefore focused our efforts on the task of developing such a synthetic method.

Scheme 3.1. Cyclization of δ−Hydroxy Enones

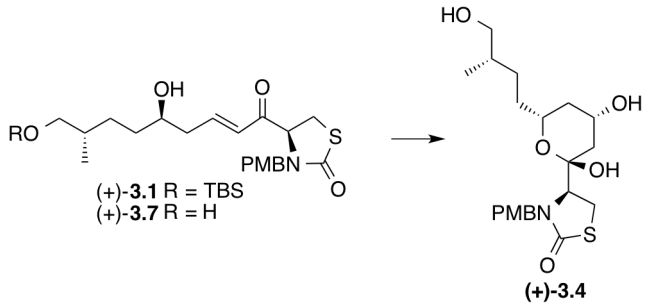

3.1 Known Methods Screened to Achieve Enone Hydration and Cyclization

The use of an acid-mediated enone hydration/cyclization tactic to provide lactol (+)-**3.4** was inspired by the report from Fürstner and coworkers of a similar reaction used their synthesis of the latrunculins.[1] Although the cyclizations used by our group and Fürstner are similar, our yields were consistently ca. 20% lower than those reported by Fürstner. The lower yield can be attributed to the extra hydroxyl group present in our substrate (+)-**3.7** [the TBS group in (+)-**3.1** is quickly removed when exposed to aqueous acid], which can lead to byproduct formation due to preferential protonation of the hydroxyl groups instead of the enone carbonyl (Scheme 3.2).

Scheme 3.2. Acid-Mediated Cyclization of (+)-**3.1**

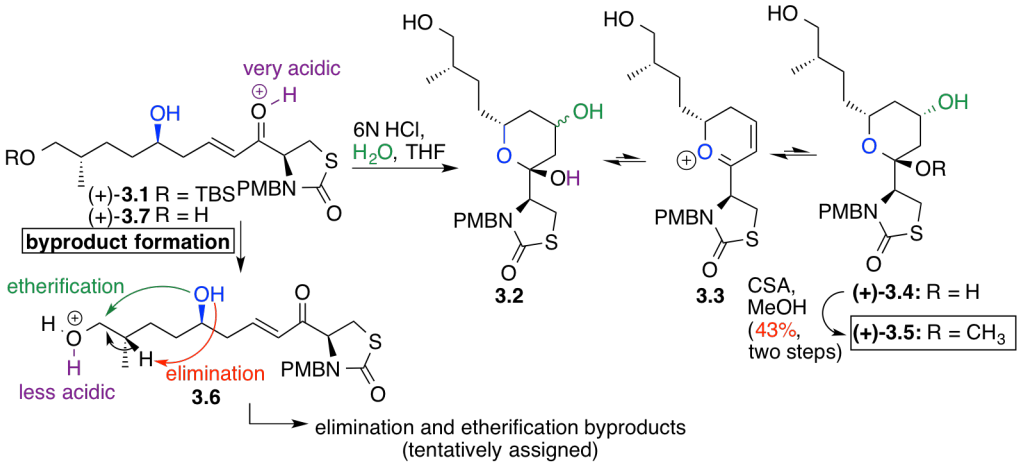

In attempt to optimize the cyclization, we initiated a brief survey of Brønsted acids and solvents. Unfortunately, exposure of enone (+)-**3.1** to dilute acids or small amounts of strong Brønsted acids (i.e., 1 to 3N HCl, TsOH•H_2O, TfOH, HBF_4, 12N HCl) all either failed to hydrate the enone, or rapidly led to the formation of multiple byproducts. Heating the reactions uniformly led to the formation of multiple byproducts and, conversely, slightly cooling the reaction (ca. 20°C) provided the best results (Scheme 3.2, 43% for two steps). Treatment of (+)-**3.1** with sodium hydroxide did not afford hydration or cyclization; moreover, due to the epimerizable stereogenic α–carbon present in (+)-**3.1**, basic conditions were minimally explored. Organocatalytic procedures involving iminium formation likewise were not surveyed. Possible two-step procedures such as copper-catalyzed borylation of the enone, followed by oxidation to afford the aldol product were attempted, but minimal reaction was observed utilizing B_2Pin_2 with CuCl/*t*-BuOK.[2] Two methods for a δ–hydroxy assisted oxa-Michael addition were also tested *via* proposed bismuth catalyzed hemiacetal[3] and aryl boronic ester[4] intermediates but neither reaction afforded the desired product (Scheme 3.3).

Scheme 3.3. Attempted δ–Hydroxy Assisted Oxa-Michael Reactions

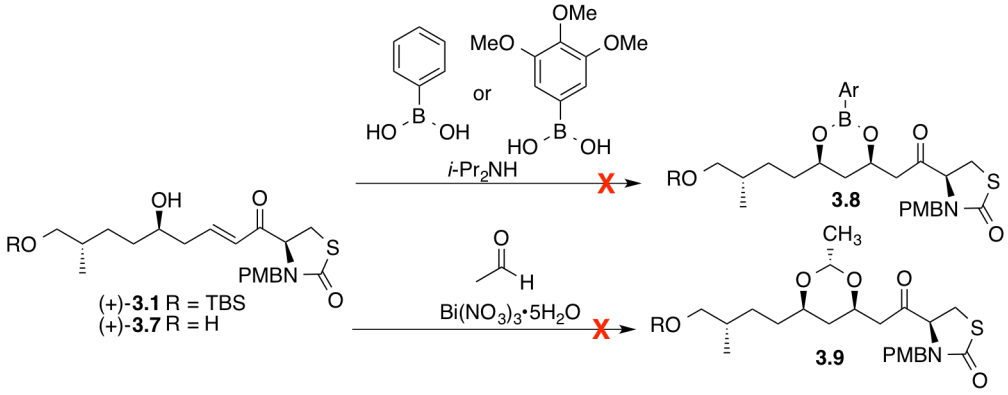

3.2 Exploration of an Addition/Elimination, Two Step Tactic for Cyclization

At this point, we began to formulate ideas for a novel method to achieve the desired cyclization. Reviewing the proposed mechanism for acid-mediated cyclization/equilibration sequence (Scheme 3.2), we postulated that water first hydrates the enone, which we knew was the problematic step as the cyclization of γ, β–dihydroxy ketones (aldol products) proceeds quickly and in much higher yield. After the initial addition of water, lactol formation is followed by ejection of two molecules of water with formation of unsaturated oxonium **3.3**, which permits equilibration to the thermodynamically most stable 2° alcohol. We were interested in the possibility of initially adding a nitrogen, phosphorous, or sulfur-based nucleophile (instead of water) to enone (+)-**3.7**, and then subjecting the adduct to aqueous acid to access intermediate **3.3** and subsequently product (+)-**3.4** (Scheme 3.4).

Scheme 3.4. Bypassing the Initial Oxa-Michael Reaction in Cyclization Cascade

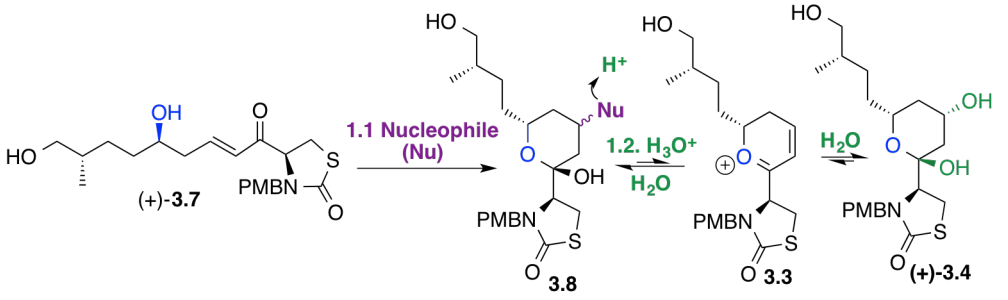

Towards this end, several nucleophiles were found to add readily into enone (+)-**3.7.** Selected examples are depicted in Scheme 3.5 and include pyridine, DMAP, imidazole, thiophenol, and tributyl phosphine. All bracketed compounds in Scheme 3.5 are tentatively assigned based upon LCMS analysis. Each adduct was subjected to a variety of acidic conditions (i.e., 2 to 6N HCl, H_2O/AcOH/Δ) and thiophenol-adduct **3.9** was also subjected to thiophilic reagents such as $HgCl_2$ in attempts to access (+)-**3.4** *via* intermediate **3.3**. Unfortunately, product (+)-**3.4** was never observed *via* TLC or LCMS analysis.

Scheme 3.5. Addition of Nitrogen, Sulfur, and Phosphorous Nucleophiles to (+)-**3.7**

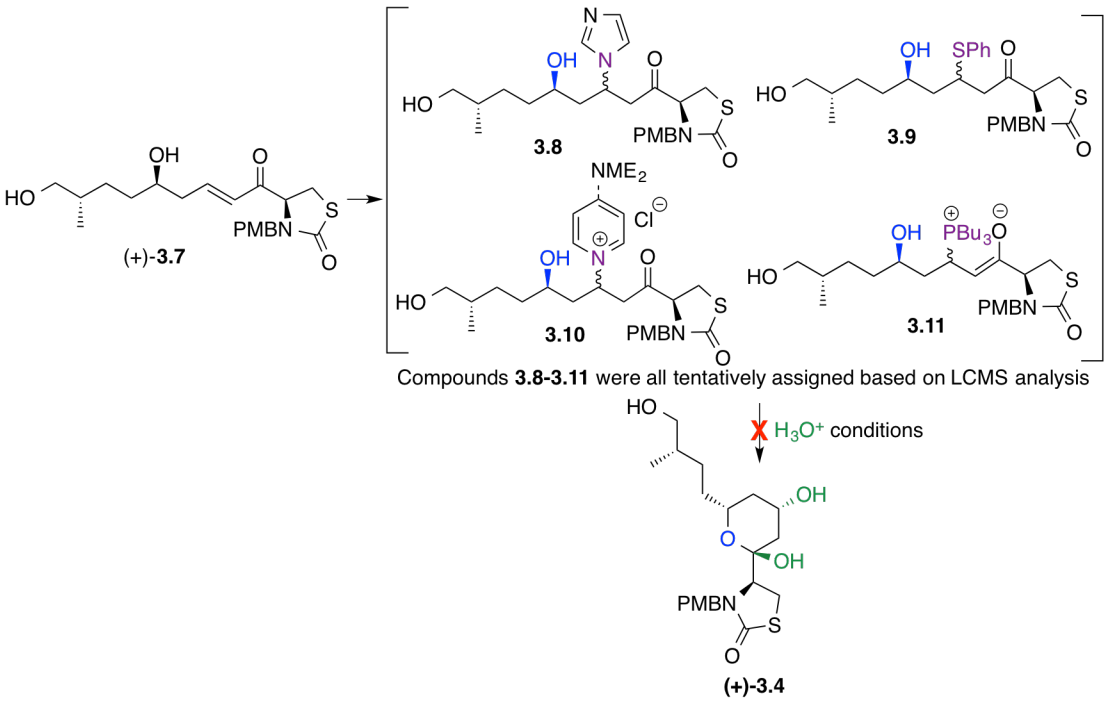

3.3 A Photochemical Isomerization/Cyclization Sequence

3.3.1 Development of a Novel Photochemical Isomerization/Cyclization Sequence

Undaunted, we went back to the mechanism of cyclization. The problematic intermolecular oxa-Michael reaction was the required first step of the reaction sequence, as the ensuing cyclization could not occur when the substrate contains a *trans*-olefin. However, if the substrate contained a *cis*-olefin, cyclization would be facile and more likely to be *catalyzed* by acid than require the super-stoichiometric acids employed by Fürstner.[1] Mindful that the *trans*-enone was more readily accessible than the *cis*-enone, we decided to examine the possibility of isomerizing the enone in the presence of a Brønsted acid to achieve cyclization. We recalled that acyclic enones are notoriously poor substrates for intermolecular photochemical reactions due to their rapid *cis*-*trans* isomerization.[5] We thus turned to photochemistry as a method to achieve isomerization. A simplified mechanistic rational for the proposed cyclization is depicted in Scheme 3.6.[5,6] Near UV radiation (300-400 nm) would be sufficient to promote the enone π–bond to an excited singlet state diradical (*trans**) of identical geometry. As the excited diradical, the vicinal electrons are no longer participating in a constructive bonding interaction and because the exciplex (excited complex) is no longer at an energy minimum, the connecting bond between radicals will rotate to permit the electrons to be at a 90° angle. At this stage, the energy of the excited state is relatively close to the ground state and interconversion (relaxation) can occur to provide a ground state diradical that continues rotation to form a mixture of both *cis* and *trans* olefins (Scheme 3.6, A.). Geometrical isomerization of α,β–enones is well precedented;[5,6] however, we envisioned a dynamic resolution of the mixture of geometrical isomers[7,8] by incorporating acid to achieve preferential cyclization of only the *cis*-isomer, thus funneling both isomers to the desired product (Scheme 3.6, B.).

Scheme 3.6. Proposed Photochemical (**A**) Isomerization and (**B**) Cyclization Cascade

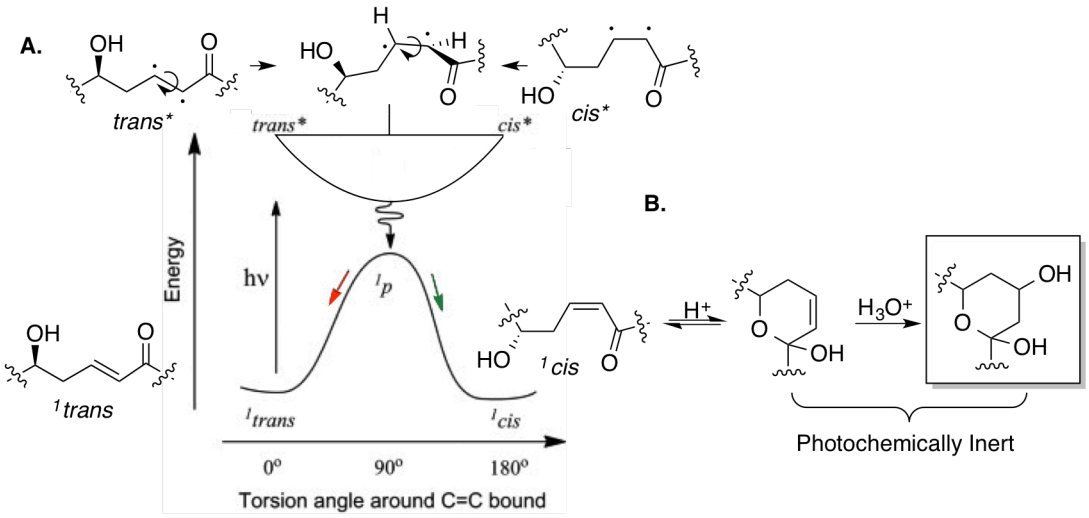

To test our proposal, (+)-**3.7** was first irradiated at 355 nm in THF-d_8 without acid and ^{1}H NMR analysis confirmed isomerization had occurred to give a mixture of *E*- and *Z*-enones. Enone (+)-**3.7** was then irradiated (355 nm) in the presence of various acids (i.e., *p*-toluenesulfonic acid, 2N to 6N HCl) in either THF or acetonitrile. All attempts however resulted in prohibitively slow conversion and/or formation of multiple unidentified byproducts. A breakthrough came when the reaction was carried out in methanol-d_4 with catalytic CSA and we observed complete conversion to a 3.8:1 mixture of diastereomeric dihydropyrans **3.12** (Scheme 3.7). Subsequent attempts to acquire an isolated yield of **3.12** were met with limited success, as the dihydropyran was discovered to react slowly to furnish the bismethoxy adduct *via* a ketal formation, complicating the product analysis.

Scheme 3.7. Successful Photochemical Isomerization/Cyclization

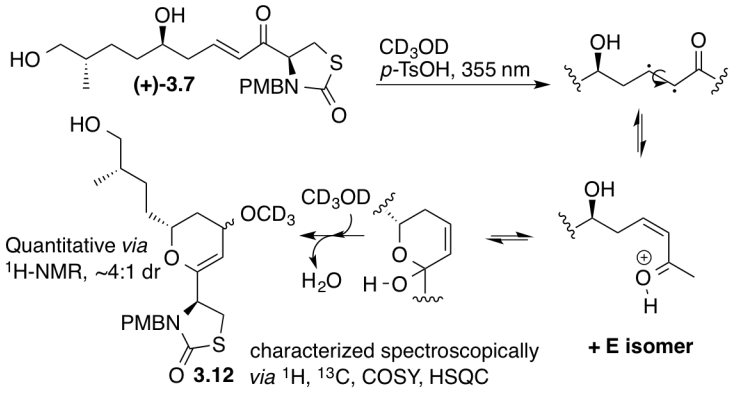

3.3.2 Exploration and Evaluation of the Photochemical Isomerization/Cyclization Sequence

At this juncture, the photochemical method advanced to an individual project. Working with 1st year graduate student (Bo Li), we set out to determine the generality of the reaction, as well as to investigate expansions that would further the application of this method to the synthesis of complex molecules.

Towards this end, preliminary experiments completed by Bo Li have demonstrated generality of the method by applying the photochemical cyclization conditions to racemic **3.13** to generate methyl ketal **3.14** as a single diastereomer in high yield (Scheme 3.8, 91%). An interesting

Scheme 3.8. Model Photochemical Isomerization/Cyclization Sequence

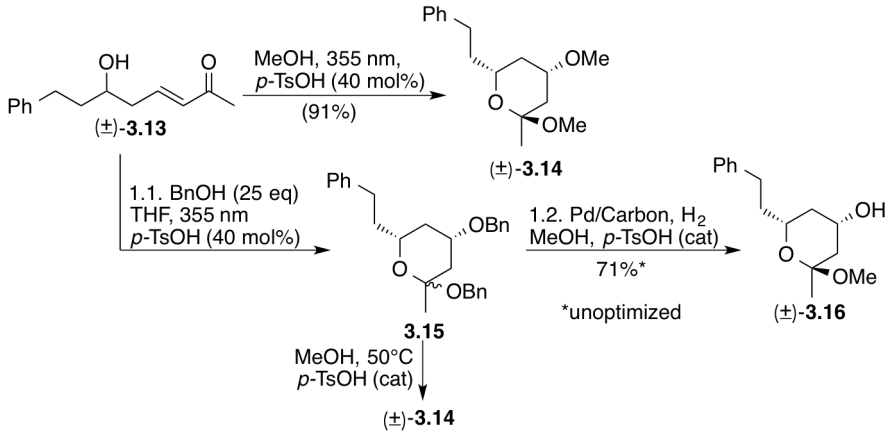

modification has also been implemented to provide a desirable cyclic ketal moiety containing a free hydroxyl in a two-step sequence (Scheme 3.8).

Using THF as solvent, the photochemical cyclization can now be achieved in the presence of 25 eq of benzyl alcohol and 40 mol % of *p*-TsOH•H_2O to generate dibenzylated product **3.15**. Subjecting **3.15**, without purification, to palladium catalyzed hydrogenation conditions in acidic methanol delivers methoxy ketal **3.16** also as a single diastereomer. Noteworthy here is the observation that the hydrogenation conditions not only converts the bis-benzylated diol to a cyclic ketal containing a free hydroxyl as a useful synthetic handle, but also greatly facilitates purification of **3.16** by converting the remaining high-boiling benzyl alcohol to toluene and water, which are both easily removed *in vacuo*. Interestingly, when transacetalization was attempted by heating **3.15** in acidic methanol, **3.14** was obtained thus lending credence to the proposed formation of unsaturated oxonium **3.3** (Scheme 3.2).

3.3.3 Future Directions and Summary

Efforts are currently directed towards optimizing the yield of the two-step benzyl alcohol addition/deprotection sequence, as well as applying these reaction conditions to a diverse set of substrates. Although our photoisomerization/cyclization project is still in its infancy, we can envision several plausible extensions to afford valuable spirocycles (Scheme 3.9). We are also interested in employing chiral Brønsted acids to achieve asymmetric induction and complement the high diastereoselectivity currently observed.

Scheme 3.9. Future Directions for Photoisomerization/Cyclization Method

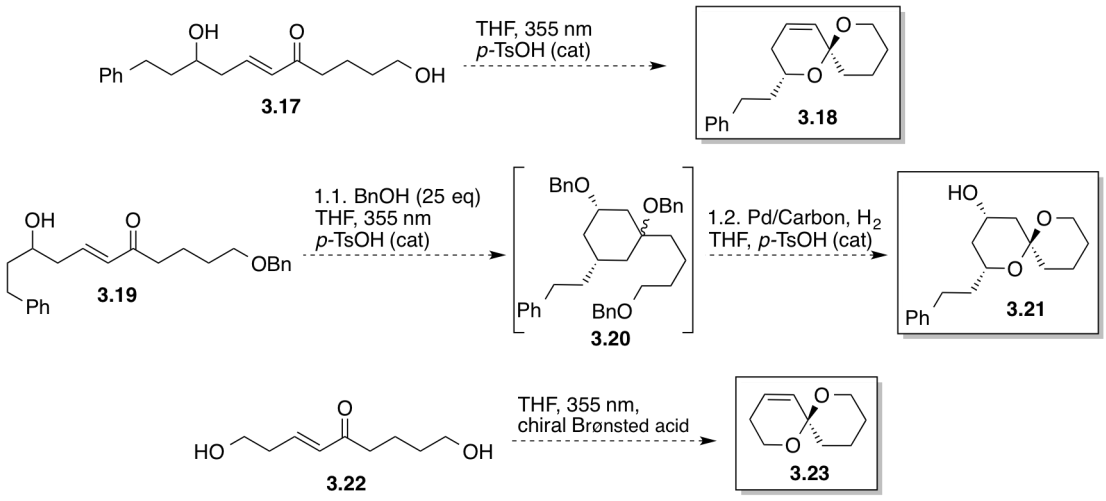

In conclusion, we have developed a novel photochemical isomerization/cyclization utilizing an acid-catalyzed photochemical dynamic resolution of enone geometric isomers. We took the inadequacy of the acid-mediated cyclization encountered in our total synthesis of (+)-18-*epi*-latrunculol A as an impetus to develop a new synthetic method that employs mild conditions to achieve a highly desirable transformation. We are clearly pleased to report success on this front. As this research is presently ongoing, a comprehensive account of this work will be reported in due course.

3.4 Chapter 3 References

(1) Furstner, A.; Turet, L. *Angew. Chem. Int. Ed.* **2005**, 44, 3462-3466.

(2) Sim, H.; Feng, X.; Yun, J. *Chem. Eur. J.* **2009**, 15, 1939-1943.

(3) Evans, P. A.; Grisin, A.; Lawler, M. J. *J. Am. Chem. Soc.* **2012**, 134, 2856-2859.

(4) Li, D. R.; Murugan, A.; Falck, J. R. *J. Am. Chem. Soc.* **2008**, 130, 46-8.

(5) Morrison, H.; Rodriguez, O. J. *Photochem.* 1974, 3, 471–474.

(6) Reguero, M.; Olivucci, M.; Bernardi, F.; Robb, M. A. *J. Am. Chem. Soc.* **1994**, 116, 2103-2114.

(7) Snider, B.; Zhongping S. *J. Am. Chem. Soc.* **1992**, 114, 1790-1800

(8) Huerta, F. F.; Minidisa, A. B. E.; Bäckvall, J. *Chem. Soc. Rev.,* **2001**, 30, 321-331

CHAPTER 4. Experimental Information

4.1 Materials and Methods

Reactions were carried out in flame-dried or oven-dried glassware under a nitrogen atmosphere unless noted otherwise. Anhydrous diethyl ether (Et_2O), tetrahydrofuran (THF), dichloromethane (CH_2Cl_2) and toluene were obtained from a PureSolv™ PS-400 solvent purification system. Triethylamine, diisopropylethylamine and pyridine were freshly distilled from calcium hydride under a nitrogen atmosphere. All chemicals were purchased from Aldrich, Acros or TCI. Reactions were magnetically stirred unless stated otherwise and monitored by thin layer chromatography (TLC) with 0.25 mm Silacycle pre-coated silica gel plates. Silica gel chromatography was performed utilizing ACS grade solvents and silica gel from either Silacycle or Sorbent Technologies. Infrared spectra were obtained using a Jasco FT/IR-480 plus spectrometer. Optical rotations were obtained using a Jasco P2000 polarimeter. All melting points were obtained on a Thomas-Hoover apparatus and are uncorrected. ^{1}H NMR spectra (500 MHz field strength) and ^{13}C NMR spectra (125 MHz field strength) were obtained on a Bruker Avance III 500 MHz spectrometer or a Spectrospin/Bruker cryomagnet (500MHz/52mm) with a 5 mm dual cryoprobe. Chemical shifts are reported relative to chloroform (δ 7.27) or acetone (δ 2.05) for ^{1}H NMR spectra and chloroform (δ 77.23) or methanol (δ 206.68, 29.92) for ^{13}C spectra. High-resolution mass spectra (HRMS) were measured at the University of Pennsylvania on either a Waters LC-TOF mass spectrometer (model LCT-XE Premier) or a Waters GCT Premier Spectrometer.

4.2 Detailed Procedures

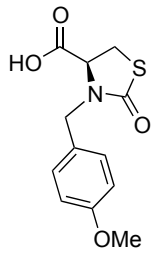

Acid (+)-2.11: To a solution of D-Cysteine hydrochloride hydrate (25 g, 142.34 mmol) in an aqueous sodium hydroxide solution (28.47 g NaOH, 140 mL H_2O) cooled to 0 °C was added phenyl chloroformate (39 ml, 313.15 mmol) in toluene (60 mL) dropwise *via* addition funnel. After the addition was complete, the reaction mixture was allowed to warm to room temperature, where it was stirred overnight and quenched with toluene (60 mL) and H_2O (60 mL). The aqueous layer was washed with toluene (3 x 50 mL). The aqueous layer was acidified by dropwise addition of 1N HCl to a pH < 1 and the solution was extracted with EtOAc (3 x 50 mL). Combined organic layers were washed with brine, dried with Na_2SO_4, filtered, and concentrated *in vacuo* to provide a white solid that was used without further purification.

To a solution of the previously obtained white solid in H_2O (14 mL), DMSO (48 mL), and NaOH (11.1 g, 278 mmol) cooled to 0 °C, was added *p*-methoxybenzyl chloride (25 mL, 184.4 mmol) dropwise. After addition was complete, the ice-water bath was removed and the reaction mixture was stirred at room temperature for 14 h. The reaction mixture became cloudy with white precipitate. The reaction mixture was partitioned between diethyl ether (50 mL) and 0.5 N NaOH (aq) (50 mL). The aqueous layer was separated and washed with diethyl ether (2 x 50 mL). The aqueous layer was acidified to pH<1 by dropwise addition of 6N HCl to the stirring basic aqueous solution. The cloudy white mixture was extracted with EtOAc (3 x 75 mL) and concentrated *in vacuo* to yield (+)-**2.11** (16.0 g, 59.86 mmol, 64% over two steps) as a brown oil:

$[\alpha]_D^{21}$ +53.2 (c .36, $CHCl_3$); IR (neat, cm^{-1}) 2934, 1740, 1612, 1514, 1444, 1396, 1248; ^1H NMR (500 MHz, $CDCl_3$) δ = 7.20 (d, *J* = 8.3 Hz, 2 H), 6.89 (d, *J* = 8.3 Hz, 2 H), 5.15 (d, *J* = 14.5 Hz, 1 H), 4.20 (dd, *J* = 2.8, 8.3 Hz, 1 H), 4.02 (d, *J* = 15.7 Hz, 1 H), 3.81 (s, 3 H), 3.54 (dd, *J* = 9.3, 11.7 Hz, 1 H), 3.42 (dd, *J* = 2.8, 12.3 Hz, 1 H); ^{13}C NMR (125 MHz, $CDCl_3$) δ = 174.5, 172.0, 159.7, 130.1, 127.5, 114.6, 59.0, 55.6, 47.6, 29.2; HRMS (ES) *m/z* $(M+H)^-$ calcd 266.0487 obsd 266.0475.

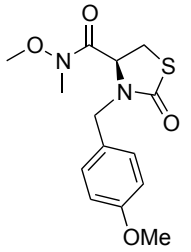

Amide (+)-S1: To a solution of acid (+)-**2.11** (16 g, 59.86 mmol) in CH_2Cl_2 (200 mL) was added *i*-Pr_2NEt (31.4 mL, 179.58 mmol) N,O-dimethylhydroxylamine hydrochloride (9.93 g, 179.58 mmol), and then TBTU (28.8 g, 89.79 mmol) portionwise. The reaction mixture became cloudy with white precipitate and was stirred overnight. The reaction mixture was quenched with 1.2 N HCl (100 mL) and the biphasic mixture was extracted with CH_2Cl_2 (4 x 100 mL). The combined organic layers were washed with 0.5 N NaOH (100 mL) and then concentrated *in vacuo*. Crude mixture was purified *via* column chromatography on SiO_2 (60% EtOAc: hexanes) to provide (+)-**S1** (15.35 g, 49.46 mmol, 83%) as a brown oil: $[\alpha]_D^{21}$ +76.1 (c 1, $CHCl_3$); IR (neat, cm^{-1}) 2935, 1678, 1513, 1444, 1393, 1303; ^1H NMR (500MHz, $CDCl_3$) δ = 7.16 (d, *J* = 8.5 Hz, 2 H), 6.87 (d, *J* = 8.5 Hz, 2 H), 5.15 (d, *J* = 15.3 Hz, 1 H), 4.40 (dd, *J* = 5.7, 8.1 Hz, 1 H), 3.85 (d, *J* = 14.9 Hz, 1 H), 3.80 (s, 3 H), 3.47 (dd, *J* = 8.9, 11.3 Hz, 1 H), 3.38 (s, 3 H), 3.21 (s, 3 H), 3.16 (dd, *J* = 4.8, 11.3 Hz, 1 H); ^{13}C NMR (125 MHz, $CDCl_3$) δ = 172.5, 169.4, 159.6, 130.3, 127.9, 114.4, 61.5, 57.7, 55.5, 47.2, 32.8, 28.3; HRMS (ES) *m/z* $(M+Na)^+$ calcd 333.0885 obsd 333.0887.

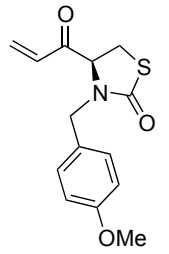

Enone (+)-2.10: To a solution of amide **S1** (316 mg, 1.018 mmol) in THF (3 mL) cooled to 0 °C, was added dropwise a solution of vinyl magnesium bromide in THF (2.1 M, 2.5 mL). Reaction mixture was stirred for 15 min before it was slowly poured into stirring 2 N HCl (10 mL) at room temperature and extracted with CH_2Cl_2 (3 x 15 mL). The combined organic layers were washed with a saturated aq. solution of $NaHCO_3$, dried over Na_2SO_4, decanted, and concentrated *in vacuo*. The crude mixture was purified *via* column chromatography on SiO_2 (60% EtOAc: hexanes) to provide (+)-**2.10** (181 mg, 0.653 mmol, 64%) as a yellow oil: $[\alpha]_D^{21}$ +69.4 (c 0.75, $CHCl_3$); IR (neat, cm^{-1}) 1672, 1612, 1513, 1248, 1175; ^1H NMR (500MHz , $CDCl_3$) δ = 7.12 (d, *J* = 8.9 Hz, 2 H), 6.85 (d, *J* = 8.5 Hz, 2 H), 6.49 (dd, *J* = 11.1, 17.4 Hz, 1 H), 6.36 (dd, *J* = 1.0, 17.0 Hz, 1 H), 5.90 (dd, *J* = 1.0, 10.5 Hz, 1 H), 5.07 (d, *J* = 14.7 Hz, 1 H), 4.34 (dd, *J* = 4.6, 9.3 Hz, 1 H), 3.83 (d, *J* = 15.1 Hz, 1 H), 3.80 (s, 3 H), 3.51 (dd, *J* = 9.7, 11.9 Hz, 1 H), 3.14 (dd, *J* = 4.6, 11.5 Hz, 1 H); ^{13}C NMR (125 MHz, $CDCl_3$) δ = 195.4, 172.0, 159.7, 131.7, 131.4, 130.2, 127.4, 114.4, 63.7, 55.4, 47.4, 27.9; HRMS (ES) *m/z* $(M+Na)^+$ calcd 300.0670 obsd 300.0684.

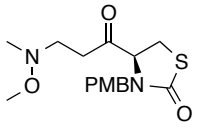

Hydroxylamine (+)-2.12: orange crystalline solid. $[\alpha]_D^{21}$ +40.9 (c 1.0, $CHCl_3$); IR (neat, cm^{-1}) 2935, 1724, 1674, 1611, 1513; ^1H NMR (500MHz , $CDCl_3$) d = 7.13 (d, *J* = 8.5 Hz, 2 H), 6.86 (d, *J* = 8.5 Hz, 2 H), 5.06 (d, *J* = 13.9 Hz, 1 H), 4.19 (dd, *J* = 5.2, 9.3 Hz, 1 H), 3.86 (d, *J* = 13.3 Hz, 1 H), 3.80 (s, 3 H), 3.51 (dd, *J* = 10.3, 11.3 Hz, 1 H), 3.43 (s, 3 H), 3.18 (dd, *J* = 4.0, 12.3 Hz, 1

H), 2.97 - 2.83 (m, 2 H), 2.66 (t, J = 6.3 Hz, 2 H), 2.57 (s, 3 H). ^{13}C NMR (125 MHz, $CDCl_3$) δ = 205.4, 171.9, 159.7, 130.1, 127.6, 114.5, 65.2, 60.0, 55.5, 54.8, 47.5, 45.0, 36.9, 27.9; HRMS (ES) *m/z* $(M+Na)^+$ calcd 339.1379 obsd 339.1374.

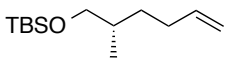

Olefin (-)-S2: To a solution of alcohol **(–)-2.14**[1] (1g, 8.76 mmol) in CH_2Cl_2 (30 mL) at RT was added imidazole (775 mg, 11.39 mmol) followed by TBSCl (1.39 g, 9.2 mmol). The clear reaction mixture became cloudy with white precipitate. After 30 min 0.5 M HCl (20 mL) and CH_2Cl_2 (20 mL) were added. The aqueous layer was separated and extracted with CH_2Cl_2 (2 x 20 mL). Combined organic layers were washed with a saturated aq. solution of $NaHCO_3$ (10 mL) and brine (10 mL) sequentially, and then dried over Na_2SO_4, decanted and concentrated *in vacuo*. The crude mixture was purified *via* column chromatography on SiO_2 (5% Et_2O: hexanes) to provide (-)-**S2** (1.804 g, 7.89 mmol, 90%) as a clear oil. Spectral data matched that previously reported.[2] ^{1}H NMR (500MHz, $CDCl_3$) δ = 5.91 - 5.75 (m, 1 H), 4.98 (dd, J = 15.3, 40.0 Hz, 2 H), 3.46 (dd, J = 5.9, 9.5 Hz, 1 H), 3.39 (dd, J = 6.7, 9.5 Hz, 1 H), 2.20 - 2.08 (m, 1 H), 2.07 - 1.95 (m, 1 H), 1.70 - 1.58 (m, 1 H), 1.57 - 1.46 (m, 1 H), 1.23 - 1.11 (m, 1 H), 0.91 (s, 9 H), 0.89 (d, J = 6.7 Hz, 3 H), 0.05 (s, 6 H); ^{13}C NMR (125 MHz, $CDCl_3$) δ = 139.5, 114.3, 68.5, 35.5, 32.6, 31.5, 26.2, 18.6, 16.8, -5.1.

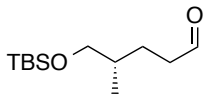

Aldehyde (-)-2.8: Ozone was bubbled through a solution of olefin (-)-**S2** (3.98 g, 17.42 mmol) in CH_2Cl_2 (60 mL) at -78 °C until the reaction mixture appeared blue (3 h). A stream of nitrogen was then bubbled through the reaction mixture until the reaction mixture was again clear and no blue color remained. Triphenylphosphine (4.71 g, 17.94 mmol) was then added in one portion at -

78 °C, after the addition the reaction was allowed to warm to RT and stirred overnight. Et_3N buffered Silica (stirred with 2 mL Et_3N and 100 mL Hexanes) and reaction was concentrated *in vacuo*. The crude mixture was purified *via* column chromatography on SiO_2 (100% hexanes to 5% Et_2O: hexanes) to provide (-)-**2.8** (3.15 g, 13.67 mmol, 79%) as a clear oil.

Spectral data matched that previously reported.[3] ^1H NMR (500MHz, $CDCl_3$) δ = 9.82 - 9.72 (m, 1 H), 3.43 (s, 2 H), 2.53 - 2.38 (m, 2 H), 1.83 - 1.73 (m, 1 H), 1.68 - 1.57 (m, 1 H), 1.50 - 1.39 (m, 1 H), 0.98 - 0.81 (m, 12 H), 0.04 (s, 6 H); ^{13}C NMR (125 MHz, $CDCl_3$) δ = 203.0, 68.0, 41.9, 35.5, 26.1, 25.7, 18.5, 16.7, -5.2, -5.2.

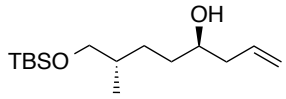

Homoallylic alcohol S3: To a solution of (−)-*B*-Methoxydiisopinocampheylborane (3.72 g, 11.8 mmol) in Et_2O (29 mL) at 0 ^oC was added a 1 M solution of allyl magnesium bromide in Et_2O (11.8 mL, 11.8 mmol). After the addition was complete the ice bath was removed and the reaction mixture was stirred for 1 h at RT. The reaction was cooled to –78 ^oC and a solution of aldehyde (–)-**2.8** (2.58 g, 11.2 mmol) in Et_2O (10 mL) was added dropwise down the side of the flask, additional Et_2O (5 mL) was used to wash any residual aldehyde. The reaction was stirred at –78 ^oC for 3 h and then after allowing it to slowly warm to RT overnight NaOH (3 N, 8 mL) and H_2O_2 (30% w/w, 3 mL) were added and the mixture was refluxed for 2 h. After cooling the mixture was extracted with Et_2O (2 x 100 mL), combined organic layers were dried over Na_2SO_4, decanted and concentrated *in vacuo*. Crude mixture was purified *via* column chromatography on SiO_2 (10% EtOAc: hexanes) to provide allylic alcohol **S3** (3.10 g) contaminated with a minor amount of epimeric alcohol that was used in next reaction without further purification.

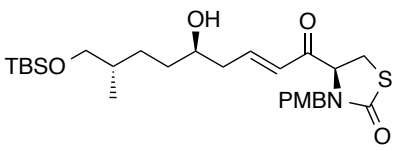

Enone (+)-2.15: To a portion of allylic alcohol **S3** mixture (197 mg) in DCE (4 mL) was added (+)-**2.10** (600 mg, 2.16 mmol, 3 eq) and mixture was sparged with N_2 for 20 min. Hoveyda-Grubbs 2nd gen catalyst (45 mg, 0.072 mmol, 10 mol%) was then added at RT, N_2 sparging was resumed, and reaction was heated to 50 ^{o}C. After 3 h 20 min charcoal (ca 50 mg) was added and reaction mixture was stirred for 1 h, silica (ca 1 g) was then added and solvent was removed *in vacuo*. The crude mixture was purified *via* column chromatography on SiO_2 (10 % EtOAc: CH_2Cl_2) to provide (+)-**2.15** (262 mg, 0.502 mmol, 71% from aldehyde (–)-**2.8**) and recovered (+)-**2.10** (287 mg, 1.04 mmol, 72% recovery); $[\alpha]_D^{21}$ +66.7 (c 0.93, $CHCl_3$); IR (neat) 3459, 2929, 2856, 1682, 1514, 1250; ^{1}H NMR (500MHz, $CDCl_3$) δ = 7.12 (d, *J* = 8.7 Hz, 2 H), 7.03 (dt, *J* = 15.5 Hz, 6.9 Hz, 1 H), 6.84 (d, *J* = 7.9 Hz, 2 H), 6.27 (d, *J* = 15.9 Hz, 1 H), 5.04 (d, *J* = 15.7 Hz, 1 H), 4.30 (dd, *J* = 4.6, 9.3 Hz, 1 H), 3.84 (d, *J* = 15.9 Hz, 1 H), 3.79 (s, 3 H), 3.76 - 3.70 (m, 1 H), 3.49 (dd, *J* = 9.3, 11.7 Hz, 1 H), 3.43 (d, *J* = 5.9 Hz, 2 H), 3.14 (dd, *J* = 4.8, 10.1 Hz, 1 H), 2.47 - 2.39 (m, 1 H), 2.38 - 2.28 (m, 1 H), 1.90 - 1.81 (m, 1 H), 1.66 - 1.59 (m, 1 H), 1.59 - 1.52 (m, 2 H), 1.51 - 1.39 (m, 1 H), 1.18 - 1.09 (m, 1 H), 0.91 - 0.86 (m, 12 H), 0.05 (s, 6 H); ^{13}C NMR (125 MHz, $CDCl_3$) δ = 195.0, 172.2, 159.6, 148.1, 130.2, 127.6, 127.0, 114.4, 71.1, 68.3, 64.1, 55.5, 47.5, 40.6, 35.9, 35.1, 29.3, 28.2, 26.1, 18.5, 17.0, -5.2, -5.2; HRMS (ES) *m/z* $(M+Na)^+$ calcd 522.2709 obsd 522.2688.

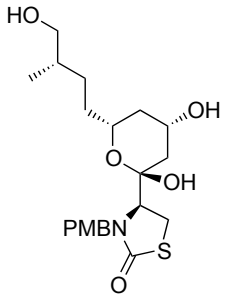

Lactol (+)-2.18: To a solution of enone (+)-**2.15** (25mg, 0.048 mmol) in THF (0.28 mL) was added 6 N HCl (0.21 mL) dropwise at 20 ^{o}C. After reaction mixture was stirred for 19 h, a saturated aq. solution of $NaHCO_3$ (5 mL) was added followed by extraction with CH_2Cl_2 (3 x 10 mL). Combined organic layers were dried over Na_2SO_4, decanted and concentrated *in vacuo*. The crude mixture was purified *via* column chromatography on SiO_2 (100% EtOAc) to provide lactol (+)-**13** (16 mg) as a yellow oil with minor impurities. (+)-**2.18** was used in the following reaction without further purification: $[\alpha]_D^{21}$ +30.0 (c 1.0, $CHCl_3$); IR (neat) 3370, 2934, 1650, 1513, 1444, 1400; ^{1}H NMR (500MHz, $CDCl_3$) δ = 7.2 (d, *J* = 8.2 Hz, 1 H), 6.87 (d, *J* = 8.5 Hz, 1 H), 5.16 (d, *J* = 14.9 Hz, 1 H), 4.45 (d, *J* = 14.3 Hz, 1 H), 4.19-4.11 (m, 1 H), 3.93-3.85 (m, 1 H), 3.81 (s, 3 H), 3.64 (dd, *J* = 5.2, 7.7 Hz, 1 H), 3.45 (d, *J* = 5.7 Hz, 2 H), 3.29-3.23 (m, 2 H), 2.15 (dd, *J* = 4.1, 12.0 Hz, 1 H), 2.0 (d, 12 Hz, 1 H), 1.89 (bs, 2 H), 1.66-1.53 (m, 4 H), 1.35-1.11 (m, 3 H), .92 (d, *J* = 6.5 Hz, 3 H); ^{13}C NMR (125 MHz, $CDCl_3$) δ =174.3, 159.4, 129.8, 128.8, 114.4, 100.5, 70.0, 68.1, 64.7, 64.5, 55.5, 48.4, 40.5, 38.9, 35.9, 33.1, 29.1, 26.7, 16.7; HRMS (ES) *m/z* $(M+Na)^+$ calcd 448.1770 obsd 448.1782.

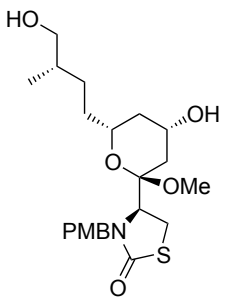

Ketal (+)-2.5: To a solution of **lactol** (+)-**2.18** (16 mg) with minor impurities in MeOH (0.4 mL) was added camphorsulfonic acid (1 mg, 0.004 mmol) and reaction was stirred overnight at RT. The reaction was quenched with a saturated aq. solution of $NaHCO_3$ (5 mL) and was followed by extraction with CH_2Cl_2 (3 x 10 mL). Combined organic layers were dried over Na_2SO_4, decanted and concentrated *in vacuo*. The crude mixture was purified *via* column chromatography on SiO_2 (80 % EtOAc: hexanes) to provide (+)-**2.5** (9 mg, 0.021 mmol, 43% from enone (+)-**2.15** as a clear oil: $[\alpha]_D^{21}$ +46.1 (c 0.95, $CHCl_3$); IR (neat) 3411, 2933, 1655, 1513, 1452, 1396, 1248; ^{1}H NMR (500MHz, $CDCl_3$) δ = 7.15 (d, *J* = 9.1 Hz, 2 H), 6.88 (d, *J* = 8.5 Hz, 2 H), 5.24 (d, *J* = 15.1 Hz, 1 H), 4.22 (d, *J* = 14.9 Hz, 1 H), 4.13 - 4.03 (m, 1 H), 3.95 (dd, *J* = 4.8, 10.3 Hz, 1 H), 3.81 (s, 3 H), 3.56 - 3.49 (m, 1 H), 3.46 (t, *J* = 5.7 Hz, 1 H), 3.41 - 3.26 (m, 2 H), 3.02 (s, 3 H), 2.11 (dd, *J* = 4.6, 11.9 Hz, 1 H), 1.99 (d, *J* = 11.7 Hz, 1 H), 1.73 - 1.43 (m, 8 H), 1.29 - 1.16 (m, 1 H), 1.15 - 1.07 (m, 1 H), 0.91 (d, *J* = 6.5 Hz, 3 H); ^{13}C NMR (125 MHz, $CDCl_3$) δ = 173.4, 159.2, 128.8, 128.6, 114.3, 102.6, 70.5, 68.1, 64.8, 57.0, 55.4, 47.9, 46.9, 40.2, 37.8, 35.8, 33.1, 28.9, 26.4, 16.6; HRMS (ES) *m/z* $(M+H)^+$ calcd 462.1926 obsd 462.1912.

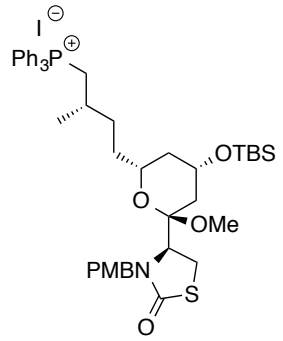

Wittig Reagent 2.19: To a solution of methyl ketal (+)-**2.5** (165 mg, 0.375 mmol) in CH_2Cl_2 (4 mL) was added imidazole (153 mg, 2.25 mmol), triphenyl phosphine (296 mg, 1.13 mmol), and lastly iodine (248 mg, 0.975 mmol). The reaction mixture was stirred overnight at rt. A 1:1 mixture of a 10% aqueous solution of $Na_2S_2O_3$ (5 mL) and a saturated aqueous solution of

sodium bicarbonate (5 mL) was added to quench the reaction mixture. To the resulting biphasic solution was added additional CH_2Cl_2 (5 mL), organic layer was removed and the aqueous layer was extracted with CH_2Cl_2 (2 x 5 mL) and combined organic layers were dried over Na_2SO_4, decanted and concentrated *in vacuo*. Crude mixture was purified *via* column chromatography on SiO_2 (40% EtOAc: hexanes) to provide **iodide** (172 mg, 0.313 mmol, 84%) as a clear oil that was used directly in the next reaction.

To a solution of **iodide** (170 mg, 0.31 mmol) in CH_2Cl_2 (3 mL) was added imidazole (53 mg, 0.78 mmol), DMAP (19 mg, 0.16 mmol), and then TBSCl (71 mg, 0.47 mmol) portionwise. After stirring the reaction mixture overnight, a saturated aqueous solution of sodium bicarbonate (10 mL) was added to quench the reaction mixture. To the resulting biphasic solution was added additional CH_2Cl_2 (15 mL), organic layer was removed and the aqueous layer was extracted with CH_2Cl_2 (2 x 15 mL) and combined organic layers were dried over Na_2SO_4, decanted and concentrated *in vacuo*. Crude mixture was purified *via* column chromatography on SiO_2 (10% EtOAc: hexanes) to provide **iodide-OTBS** (175 mg, 0.264 mmol, 84%) as a clear oil that was used directly in the next reaction.

To a solution of **iodide-OTBS** (108 mg, 0.163 mmol) in acetonitrile (2 mL), was added triphenyl phosphine (640 mg, 2.44 mmol), *i*-Pr_2NEt (0.2 mL, 1.14 mmol), and the reaction mixture was heated to 55°C for 48 h. Reaction mixture was concentrated *in vacuo* to afford an orange oil that was purified *via* filtration through a short pad of SiO_2, washing with EtOAc to remove residual triphenyl phosphine and triphenyl phosphine oxide followed by washing with 5% MeOH/CH_2Cl_2 to provide **Wittig reagent 2.19** as an orange foam (118 mg, 0.13 mmol, 78%). $[\alpha]_D^{21}$ +24.6 (c 1.0, $CHCl_3$); IR (neat, cm^{-1}) 2927, 1667, 1512, 1438; ^1H NMR (500MHz , $CDCl_3$) d = 7.90-7.82 (m, 4 H), 7.71-7.61 (m, 8 H), 7.55 (t, J = 7.7 Hz, 1 H), 7.50-7.44 (m, 2 H), 7.16 (d, J = 8.6 Hz, 2 H), 6.91 (d, J = 8.4 Hz, 2 H), 5.15 (d, J = 16.1 Hz, 1 H), 4.19 (d, J = 16.1 Hz, 1 H),

4.02-3.86 (m, 2 H), 3.81 (s, 3 H), 3.76-3.63 (m, 2 H), 3.40 (t, J = 9.6 Hz, 1 H), 3.27-3.18 (m, 2 H), 2.84 (s, 3 H), 1.86 (dd, J = 4.5, 13.5 Hz, 1 H), 1.86-1.78 (m, 1 H), 1.77-1.65 (m, 4 H), 1.58-1.47 (m, 3 H), 1.25-1.18 (m, 1 H), 1.04 (d, J = 6.4 Hz, 3 H), 0.87, (s, 9 H), 0.06 (s, 6 H); ^{13}C NMR (125 MHz, $CDCl_3$) δ = 173.5, 159.3, 135.2, 133.9 (d, J = 9.6 Hz), 132.3 (d, J = 11.8 Hz),132.1, 130.6 (d, J = 11.8 Hz), 129.0, 128.8 (d, J = 3.2 Hz), 128.6, 119.5, 118.8, 114.4, 102.6, 69.8, 65.2, 57.0, 55.6, 48.3, 46.9, 37.8, 33.7 (d. J = 10.2 Hz), 33.3, 30.3, 29.9, 29.8 (d, J = 3.3 Hz), 26.5, 26.1, 21.0 (d, J = 8.7 Hz), 18.2, -4.3. -4.4; HRMS (ES) *m/z* $(M)^+$ calcd 798.3777 obsd 798.3763.

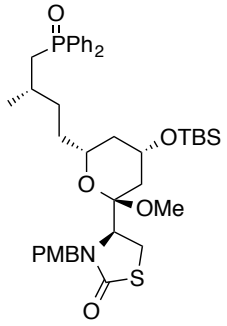

Wittig Reaction Byproduct (+)-2.23: To a solution of **Wittig reagent** (5 mg, 5 μmol) in THF (0.1 mL) at 0°C was slowly added NaHMDS (1M, 50 μl) turning the reaction red. After the reaction was stirred at 0°C for 10 min, benzaldehyde (10 μl, 10 mg, 0.01 mmol) was added. After stirring for 5 min the reaction mixture was quenched with a saturated aqueous solution of ammonium chloride (5 mL). To the resulting biphasic solution was added additional CH_2Cl_2 (5 mL), organic layer was removed and the aqueous layer was extracted with CH_2Cl_2 (2 x 5 mL) and combined organic layers were dried over Na_2SO_4, decanted and concentrated *in vacuo*. LCMS analysis indicated **(+)-2.23** to be a major product in the reaction mixture. The crude mixture was purified *via* column chromatography on SiO_2 (40% EtOAc: hexanes) to provide (+)-**2.23** with an unknown contaminant. The mixture was then further purified *via* preparative TLC (250 μm, 60% EtOAc: hexanes) to provide (+)-**2.23** (1.6 mg, 2.2 μmol) as a clear film. $[\alpha]_D^{21}$ +33.0 (c .11,

$CHCl_3$); IR (neat, cm^{-1}) 2926, 2854, 1673, 1514, 1459, 1386; ^1H NMR (500MHz , $CDCl_3$) δ =7.76-7.69 (m, 4 H), 7.52-7.36 (m, 6 H), 7.15 (d, J = 8.5 Hz, 2 H), 6.89 (d, J = 8.5 Hz, 2 H), 5.19 (d, J = 15.6 Hz, 1 H), 4.21 (d, J = 15.6 Hz, 1 H), 3.96 (sept, J = 5.9 Hz, 1 H), 3.83 (dd, J = 4.4, 9.3 Hz, 1 H), 3.81 (s, 3 H), 3.37-3.20 (m, 3 H), 2.88 (s, 3 H), 2.31-2.22 (m, 1 H), 2.12-2.11 (m, 1 H), 2.08-1.96 (m, 1 H), 1.87 (dd, J = 4.7, 13.1 Hz), 1.72 (app dt. J = 2.2, 12.8 Hz, 1 H), 1.55 (dd, J = 10.4, 13.1 Hz, 2 H), 1.47-1.33 (m, 2 H), 1.15 (q, J = 12.7 Hz, 2 H), 0.98 (d, J = 6.7 Hz, 3 H), 0.88 (s, 9 H), 0.06 (s, 6 H); ^{13}C NMR (125 MHz, $CDCl_3$) δ = 173.6, 159.0, 131.6, 131.6, 130.7 (d, J = 10.4 Hz), 130.6 (d, J = 9.5 Hz), 128.8, 128.7 (d, J = 5.3 Hz), 128.6 (d, J = 5.6 Hz), 128.5, 114.1, 102.5, 69.9, 65.1, 57.0, 55.3, 47.7, 46.7, 40.8, 37.6, 37.1, 36.5, 34.0, 32.7, 29.7, 28.1 (d, J = 3.4 Hz), 26.3, 25.9, 21.5 (d, J = 8.3 Hz), 18.1, -4.5, -4.6 HRMS (ES) *m/z* $(M+H)^+$ calcd 738.3414 obsd 738.3427.

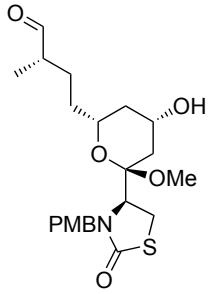

Hydroxy Aldehyde (+)-S4: To a solution of ketal (+)-**2.5** (400mg, 0.91 mmol) in CH_2Cl_2 (9 mL), cooled to 0 °C was added TEMPO (21 mg, 0.137 mmol) followed by (Diacetoxyiodo)benzene (264 mg, 0.819 mmol) portionwise. After 12 h, the reaction mixture was partitioned between CH_2Cl_2 (10 mL) and a saturated aq. solution of $Na_2S_2O_3$ (10 mL). The aqueous layer was extracted with CH_2Cl_2 (3 x 10 mL). Combined organic layers were dried over Na_2SO_4, decanted and concentrated *in vacuo*. Crude mixture was purified *via* column chromatography on SiO_2 (60% EtOAc: hexanes) to provide (+)-**S4** (286 mg, 0.654 mmol, 72%) as a clear oil: $[\alpha]_D^{21}$ +40.9

(c 0.39, $CHCl_3$); IR (neat) 3438, 2929, 2845, 1721, 1669, 1612, 1513, 1456, 1395; ^{1}H NMR (500MHz, $CDCl_3$) δ = 9.59 (d, *J* = 1.6 Hz, 1 H), 7.14 (d, *J* = 8.5 Hz, 2 H), 6.87 (d, *J* = 8.5 Hz, 2 H), 5.22 (d, *J* = 15.3 Hz, 1 H), 4.21 (d, *J* = 14.9 Hz, 1 H), 4.07 (spt, *J* = 4.2 Hz, 1 H), 3.96 (dd, *J* = 3.2, 9.3 Hz, 1 H), 3.80 (s, 3 H), 3.58 - 3.48 (m, 1 H), 3.43 - 3.27 (m, 2 H), 3.00 (s, 3 H), 2.32 (q, *J* = 7.1 Hz, 1 H), 2.10 (dd, *J* = 5.2, 12.5 Hz, 1 H), 1.97 (d, *J* = 12.7 Hz, 2 H), 1.93 - 1.77 (m, 1 H), 1.65 (t, *J* = 11.1 Hz, 1 H), 1.53 (q, *J* = 7.5 Hz, 2 H), 1.40 - 1.30 (m, 1 H), 1.29 - 1.15 (m, 2 H), 1.10 (d, *J* = 7.1 Hz, 3 H), 0.91 - 0.75 (m, 1 H); ^{13}C NMR (125 MHz, $CDCl_3$) δ = 204.8, 173.5, 159.2, 128.7, 128.6, 114.3, 102.7, 70.1, 64.5, 56.9, 55.4, 47.8, 46.8, 46.3, 40.1, 37.7, 33.0, 26.4, 26.3, 13.6; HRMS (ES) *m/z* $(M+H)^+$ calcd 438.1950 obsd 438.1938.

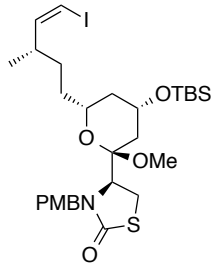

TBS Vinyl iodide (+)-2.20: To a solution of IPh_3PCH_2I (1.26g, 2.38 mmol) in THF (24 mL) was added NaHMDS (1M, 1.9 mL) at rt and reaction mixture was stirred ca 1 min. Reaction mixture was cooled to -60 °C and HMPA (0.66 mL, 3.81 mmol) was added and reaction was further cooled to -78 °C and hydroxy aldehyde **(+)-S5** (104 mg, 0.24 mmol) was added in THF (ca 1 mL) dropwise. After stirring at -78 °C for 1 h, the reaction mixture was quenched by the addition of a saturated aqueous solution of ammonium chloride (5 mL). The biphasic mixture was extracted with diethyl ether (3 x, 5 mL) and combined organic layers were dried over Na_2SO_4, decanted and concentrated *in vacuo*. The crude mixture was purified *via* column chromatography on SiO_2 (45-

50% EtOAc: hexanes) to provide **vinyl iodide** (60 mg, 0.107 mmol, 45%) as a brown foam that was used directly in the next reaction.

To a solution of **vinyl iodide** (60 mg, 0.11 mmol) in CH_2Cl_2 (0.4 mL) was added imidazole (15 mg, 0.214 mmol), DMAP (7 mg, 0.054 mmol), and lastly TBSCl (24 mg, 0.16 mmol) and stirred at rt overnight. The reaction was incomplete after 14 h so again imidazole (15 mg, 0.214 mmol), DMAP (7 mg, 0.054 mmol), and lastly TBSCl (24 mg, 0.16 mmol) were added. After 12 h, a saturated aqueous solution of sodium bicarbonate (ca 5 mL) was added to quench the reaction. The biphasic mixture was extracted with CH_2Cl_2 (3x, 5 mL) and combined organic layers were dried over Na_2SO_4, decanted and concentrated *in vacuo*. The crude mixture was purified *via* column chromatography on SiO_2 (30% EtOAc: hexanes) to provide **TBS vinyl iodide** (+)-**2.20** (74 mg, 0.11 mmol, near quant.) as an oil: $[\alpha]_D^{21}$ +15.4 (c .14, $CHCl_3$); IR (neat, cm^{-1}) 2927, 2856, 1676, 1513, 1457, 1389; ^1H NMR (500MHz , $CDCl_3$) d = 7.16 (d, *J* = 8.7 Hz, 2 H), 6.87 (d, *J* = 8.7 Hz, 2 H), 6.15 (d, 7.1 Hz, 1 H), 5.88 (dd, J = 7.4, 9.0 Hz, 1 H), 5.20 (d, J = 15.3 Hz, 1 H), 4.26 (d, 15.4 Hz, 1 H), 4.02 (sep, J = 5.0 Hz, 1 H), 3.95 (dd, J = 4.0, 9.3 Hz, 1 H), 3.81 (s, 3 H), 3.56-3.50 (m, 1 H), 3.39-3.29 (m, 2 H), 3.04 (s, 3 H), 2.50 (quin, J = 6.0 Hz), 1.92 (dd, J = 1.4, 4.9 Hz, 1 H), 1.81 (dt, J = 2.3, 12.4 Hz, 1 H), 1.59 (dd, J = 10.5, 13.0 Hz, 1 H), 1.52-1.36 (m, 5 H), 1.24 (d, J = 12.2 Hz, 2 H), 0.98 (d, J = 7.1 Hz, 3 H), 0.89 (s, 9 H), 0.076 (s, 6 H). ^{13}C NMR (125 MHz, $CDCl_3$) δ = 173.8, 159.2, 146.5, 129.0, 128.8, 114.4, 102.8, 81.2, 70.0, 65.4, 57.5, 55.5, 48.0, 47.1, 41.0, 39.4, 38.1, 33.2, 31.9, 29.9, 26.5, 26.1, 19.6, 18.3, -4.3, -4.4; HRMS (ES) *m/z* $(M+Na)^+$ calcd 698.1808 obsd 698.1774.

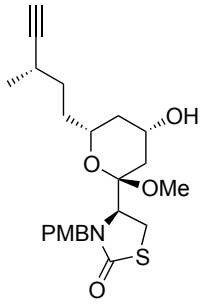

Alkyne (+)-S5: To a 1.0 M solution of *t*-BuOK in THF (4.6 mL, 4.6 mmol) cooled to –78 °C, was added Seyferth-Gilbert reagent (789 mg, 5.26 mmol) in THF (7 mL) down side of the reaction vessel. Reagent was washed with THF (3 mL) and reaction became yellow-orange but remained transparent. After 25 min aldehyde (+)-**S5** (1.15 g, 2.63 mmol) in THF (10 mL) was added to the solution dropwise and then washed with more THF (5 mL). The yellow-orange reaction mixture was quenched with a saturated aq. solution of $NaHCO_3$ (15 mL) and CH_2Cl_2 (20 mL) at –78 °C. The aqueous layer was separated and extracted with CH_2Cl_2 (2 x 30 mL). Combined organic layers were dried over Na_2SO_4, decanted and concentrated *in vacuo*. Crude mixture was purified *via* column chromatography on SiO_2 (50% EtOAc: hexanes) to provide (+)-**S5** (852 mg, 1.97 mmol, 75%) as a white foam: $[\alpha]_D^{21}$ +52.8 (c 0.23, $CHCl_3$); IR (neat) 3416, 2931, 1670, 1513; ^{1}H NMR (500MHz, $CDCl_3$) δ = 7.14 (d, *J* = 8.5 Hz, 2 H), 6.87 (d, *J* = 8.5 Hz, 2 H), 5.22 (d, *J* = 16.1 Hz, 1 H), 4.22 (d, *J* = 15.5 Hz, 1 H), 4.07 (spt, *J* = 4.8 Hz, 1 H), 3.95 (dd, *J* = 4.2, 7.9 Hz, 1 H), 3.80 (s, 3 H), 3.58 - 3.47 (m, 1 H), 3.43 - 3.28 (m, 2 H), 3.01 (s, 3 H), 2.48 - 2.32 (m, 1 H), 2.10 (dd, *J* = 4.2, 12.7 Hz, 1 H), 2.04 (d, *J* = 2.6 Hz, 1 H), 1.98 (d, *J* = 14.9 Hz, 1 H), 1.81 - 1.68 (m, 1 H), 1.67 - 1.54 (m, 3 H), 1.49 - 1.35 (m, 1 H), 1.30 - 1.20 (m, 1 H), 1.17 (d, *J* = 6.9 Hz, 3 H); ^{13}C NMR (125 MHz, $CDCl_3$) δ =173.6, 159.2, 128.8, 128.7, 114.4, 102.7, 88.6, 70.0, 68.9, 64.7, 57.1, 55.5, 47.9, 46.9, 40.3, 37.9, 33.4, 32.5, 26.4, 25.9, 21.1; HRMS (ES) *m/z* $(M+H)^+$ calcd 434.2001 obsd 434.2007.

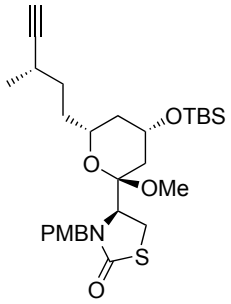

TBS ether (+)-2.21: To a solution of alkyne (+)-**S6** (270 mg, 0.623 mmol) in CH_2Cl_2 (2.1 mL) was added 2,6-lutidine (0.14 mL, 1.246 mmol). Reaction mixture was cooled to 0 °C, and TBSOTf (0.17 mL, 0.747 mmol) was added dropwise. After 1 h, the reaction was diluted with CH_2Cl_2 (5 mL), 0.5 N HCl (5 mL) was added, and aqueous layer was separated and extracted with CH_2Cl_2 (3 x 10 mL). Combined organic layers were dried over Na_2SO_4, decanted and concentrated *in vacuo*. Crude mixture was purified *via* column chromatography on SiO_2 (30% EtOAc: hexanes) to provide (+)-**2.21** (341 mg, 0.623 mmol, near quant.) as white crystals: $[\alpha]_D^{21}$ +16.7 (c 0.69, $CHCl_3$); Melting point = 79 ^oC-84^oC, IR (neat) 3307, 2930, 2856, 1731, 1675, 1513; ^1H NMR (500MHz, $CDCl_3$) δ = 7.16 (d, *J* = 8.3 Hz, 2 H), 6.87 (d, *J* = 8.9 Hz, 2 H), 5.20 (d, *J* = 15.3 Hz, 1 H), 4.26 (d, *J* = 15.9 Hz, 1 H), 4.08 - 3.97 (m, 1 H), 3.94 (dd, *J* = 4.6, 9.7 Hz, 1 H), 3.85 - 3.76 (m, 3 H), 3.56 - 3.46 (m, 1 H), 3.34 (s, 2 H), 2.47 - 2.36 (m, 1 H), 2.04 (d, *J* = 2.2 Hz, 1 H), 1.92 (dd, *J* = 4.4, 12.9 Hz, 1 H), 1.87 - 1.80 (m, 1 H), 1.76 - 1.67 (m, 1 H), 1.62 - 1.55 (m, 5 H), 1.46 - 1.37 (m, 1 H), 1.31 - 1.21 (m, 2 H), 1.18 (d, *J* = 6.9 Hz, 3 H), 0.89 (s, 9 H), 0.08 (s, 6 H); ^{13}C NMR (125 MHz, $CDCl_3$) δ = 173.7, 159.2, 128.9, 128.7, 114.3, 102.7, 88.7, 69.7, 68.9, 65.4, 57.4, 55.5, 47.9, 47.0, 40.9, 38.0, 33.4, 32.5, 26.4, 26.0, 25.9, 21.1, 18.2; HRMS (ES) *m/z* $(M+H)^+$ calcd 548.2866 obsd 548.2878.

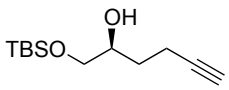

TBS ether (–)-S6: To a solution of diol (–)-**2.26**[4] (0.9 g, 7.89 mmol) in CH_2Cl_2 (80 mL) was added imidazole (1.61 g, 23.67 mmol), cooled to 0 °C and added TBSCl (1.19 g, 7.89 mmol) portionwise. The ice bath was removed after 30 min and the reaction mixture was stirred at room temperature. After 14 h, 0.5 N HCl (40 mL) was added and the aqueous layer was extracted with CH_2Cl_2 (3 x 40 mL). Organic layers were combined and washed sequentially with a saturated aq. solution of $NaHCO_3$ and brine, dried over Na_2SO_4, decanted and concentrated *in vacuo*. Crude mixture was purified *via* column chromatography on SiO_2 (20% to 100% EtOAc: hexanes) to provide (–)-**S6** (1.58 g, 6.9 mmol, 88 %) as a brown oil: $[\alpha]_D^{21}$ -1.1 (c 0.15, $CHCl_3$); IR (neat, cm^{-1}) 3447, 3313, 2118, 1738, 1471, 1256, 1121; ^1H NMR (500MHz , $CDCl_3$) δ = 3.79 (spt, *J* = 4.2 Hz, 1 H), 3.66 (dd, *J* = 3.6, 9.7 Hz, 1 H), 3.45 (dd, *J* = 7.1, 9.9 Hz, 1 H), 2.36 (dt, *J* = 2.1, 7.1 Hz, 2 H), 1.97 (t, *J* = 2.6 Hz, 1 H), 1.72 - 1.57 (m, 2 H), 0.91 (s, 9 H), 0.08 (s, 6 H); ^{13}C NMR (125 MHz, $CDCl_3$) δ = 84.2, 70.7, 68.7, 67.1, 31.8, 26.1, 18.5, 15.0, -5.2, -5.2; HRMS (ES) *m/z* $(M+Na)^+$ calcd 251.1443 obsd 251.1441.

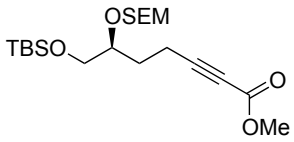

Alkynoate (-)-2.27: To a solution of **TBS ether** (–)-**S6** (556 mg, 2.43 mmol) in CH_2Cl_2 (8 mL), was added *i*-Pr_2NEt (1.7 mL, 9.72 mmol), and SEMCl (0.52 mL, 72.92 mmol) dropwise. An exit needle was placed through septa to allow smoky atmosphere to clear. After 14 h, a saturated aq. solution of $NaHCO_3$ (20 mL) was added to quench the reaction mixture and the aqueous layer was extracted with CH_2Cl_2 (3 x 20 mL). The combined organic layers were washed with 10% citric acid (50 mL) and dried over Na_2SO_4, decanted and concentrated *in vacuo*. Crude mixture was filtered through a pad of SiO_2 to yield a yellow oil that was used without further purification.

To a solution of the previously obtained yellow oil in THF (8 mL), cooled to – 78 °C, was added a solution of *n*-BuLi in THF (2.4M, 1.5 mL) dropwise. After stirring for 20 min methyl chloroformate (0.33 mL, 4.13 mmol) was added dropwise and reaction mixture was stirred for 1 h and dry ice bath was removed. After stirring for 3 h, Et_2O (10 mL) was added followed by a saturated aq. solution of $NaHCO_3$ (10 mL). Aqueous layer was extracted with EtOAc (3 x 20 mL), combined organic layers were washed with brine, dried over Na_2SO_4, decanted and concentrated *in vacuo*. Crude mixture was purified *via* column chromatography on SiO_2 (5% ether: hexanes) to provide protected (–)-**2.27** (737 mg, 1.77 mmol, 73% over two steps) as a free flowing oil: $[\alpha]_D^{21}$ -36.6 (c 1.0, $CHCl_3$); IR (neat, cm^{-1}) 2953, 2239, 1718, 1435, 1253; ^1H NMR (500MHz , $CDCl_3$) δ = 4.78 (d, *J* = 6.7 Hz, 1 H), 4.71 (d, *J* = 6.5 Hz, 1 H), 3.76 (s, 3 H), 3.71 - 3.53 (m, 5 H), 2.53 - 2.44 (m, 2 H), 1.93 - 1.81 (m, 1 H), 1.80 - 1.71 (m, 1 H), 0.95 (t, *J* = 8.3 Hz, 2 H), 0.89 (s, 9 H), 0.06 (s, 6 H), 0.02 (s, 9 H); ^{13}C NMR (125 MHz, $CDCl_3$) δ = 154.4, 94.9, 89.6, 73.2, 65.6, 65.3, 52.7, 30.1, 26.1, 18.5, 18.3, 15.0, -1.2, -5.2. -5.2; HRMS (ES) *m/z* $(M+Na)^+$ calcd 439.2312 obsd 439.2296.

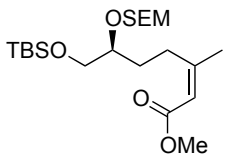

Enoate (–)-S7: To a suspension of CuI (322 mg, 1.69 mmol) in THF (8 mL), cooled to 0 °C was added a solution of MeLi in Et_2O (0.4M, 2.25 mL, 3.38 mmol) was added dropwise turning the reaction mixture orange and then clear. After stirring for 45 min, Me_2CuLi solution was cooled to -78 °C and a solution of alkynoate (–)-**2.27** (587 mg, 1.41 mmol) in THF (8 mL). After 2 h, pH 7 buffer (10 mL) and MeOH (2 mL) were added, and then the reaction was extracted with EtOAc (3 x 20 mL). Combined organic layers were washed with brine, dried over Na_2SO_4, decanted and concentrated *in vacuo*. Crude mixture was purified *via* column chromatography on SiO_2 (10%

ether: hexanes) to provide (–)-**S7** (351 mg, 0.81 mmol, 58%) as an oil: $[\alpha]_D^{21}$ -6.8 (c 0.67, $CHCl_3$); IR (neat, cm^{-1}) 2953, 2929, 2858, 1722, 1649, 1250; ^1H NMR (500MHz , $CDCl_3$) δ = 5.67 (s, 1 H), 4.82 (d, *J* = 7.5 Hz, 1 H), 4.74 (d, *J* = 6.7 Hz, 1 H), 3.71 - 3.59 (m, 6 H), 3.67, (s, 3 H) 2.81 - 2.63 (m, 2 H), 1.90 (s, 3 H), 1.79 - 1.70 (m, 1 H), 1.64 - 1.59 (m, 1 H), 0.96 - 0.94 (m, 1 H), 0.90 (s, 9 H), 0.05 (br. s., 6 H), 0.02 (s, 9 H); ^{13}C NMR (125 MHz, $CDCl_3$) δ = 166.8, 160.8, 116.1, 94.9, 78.5, 65.8, 65.3, 51.0, 30.3, 29.7, 26.1, 25.3, 18.5, 18.3, -1.2, -5.2, -5.2; HRMS (ES) *m/z* $(M+Na)^+$ calcd 455.2625 obsd 455.2638.

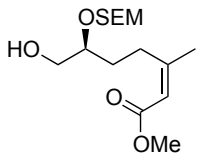

Alcohol (+)-S8: To a solution of enoate (–)-**S7** (351 mg, 0.811 mmol) in THF (8 mL), was added a solution of TBAF in THF (1 M, 1.6 mL) buffered with AcOH (0.12 mL). After 14 h the reaction was quenched with a saturated aq. solution of NH_4Cl (10 mL), aqueous layer was extracted with EtOAc (3 x 20 mL). Combined organic layers were washed with brine, dried over Na_2SO_4, decanted and concentrated *in vacuo*. Crude mixture was purified *via* column chromatography on SiO_2 (20% EtOAc: hexanes) to provide (+)-**S8** (257 mg, 0.807 mmol, 99%) as an oil: $[\alpha]_D^{21}$ +41.7 (c 0.39, $CHCl_3$); IR (neat, cm^{-1}) 3443, 2951, 2891, 1719, 1647, 1436, 1248; ^1H NMR (500MHz , $CDCl_3$) δ = 5.75 - 5.64 (m, 1 H), 4.82 (d, *J* = 7.3 Hz, 1 H), 4.70 (d, *J* = 6.7 Hz, 1 H), 3.84 - 3.74 (m, 1 H), 3.68 (s, 3 H), 3.64 - 3.54 (m, 4 H), 2.79 - 2.68 (m, 1 H), 2.68 - 2.55 (m, 1 H), 1.91 (s, 3 H), 1.76 - 1.58 (m, 2 H), 1.04 - 0.90 (m, 2 H), 0.03 (s, 9 H); ^{13}C NMR (125 MHz, $CDCl_3$) δ = 166.9, 160.6, 116.2, 95.5, 82.2, 65.9, 65.5, 51.1, 30.1, 29.6, 25.4, 18.4, -1.3; HRMS (ES) *m/z* $(M+Na)^+$ calcd 319.1941 obsd 319.1940.

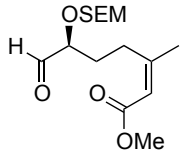

Aldehyde (+)-2.25: To a solution of alcohol (+)-**S9** (149 mg, 0.468 mmol) in CH_2Cl_2 (5 mL), cooled to 0°C was added *i*-Pr_2NEt (0.41 mL, 2.34 mmol) and DMSO (0.33 mL, 4.68 mmol). SO_3 –pyridine (223 mg, 1.4 mmol) was then added in one portion. After 15 min, the reaction mixture was diluted with CH_2Cl_2 (10 mL) and a saturated aq. solution of $NaHCO_3$ (10 mL) was added. The aqueous layer was separated and extracted with CH_2Cl_2 (2 x 15 mL). Combined organic layers were washed with brine, dried over Na_2SO_4, decanted and concentrated *in vacuo*. Crude mixture was purified *via* short column chromatography on SiO_2 (30% EtOAc: hexanes) to provide aldehyde (+)-**2.25** (144 mg, 0.455 mmol, 97%) as a brown oil: $[\alpha]_D^{21}$ +5.2 (c 1.3, $CHCl_3$); IR (neat) 2952, 1719, 1650, 1437, 1378, 1249, 1193; ^{1}H NMR (500 MHz, $CDCl_3$) δ = 9.66 (d, *J*=1.58 Hz, 1 H), 5.70 (s, 1 H), 4.82 (d, *J*=7.13 Hz, 1 H), 4.75 (d, *J*=6.94 Hz, 1 H), 3.94 (ddd, *J*=7.13, 5.15, 1.39 Hz, 1 H), 3.71 - 3.82 (m, 1 H), 3.68 (s, 3 H), 3.58 - 3.67 (m, 1 H), 2.73 - 2.83 (m, 1 H), 2.62 - 2.72 (m, 1 H), 1.90 (s, 3 H), 1.78 - 1.89 (m, 2 H), 0.93 (s, 2 H), 0.02 (s, 9 H); ^{13}C NMR (125 MHz, $CDCl_3$) δ = 202.9, 166.7, 159.3, 116.8, 95.3, 82.4, 66.1, 51.1, 29.2, 28.6, 25.3, 18.2, -1.3; HRMS (ES) *m/z* $(M+Na)^+$ calcd 339.1604 obsd 339.1605.

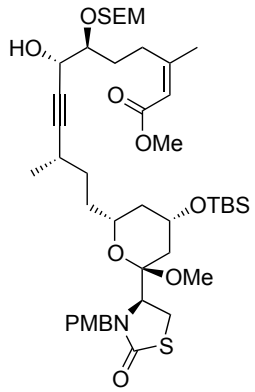

Propargyl Alcohol (+)-2.28: To $Zn(OTf)_2$ (dried overnight at 120 °C under high vacuum, 1.12g, 3.078 mmol), was added (+)-NME (azeotroped 3x with toluene, 600 mg, 3.35 mmol), triethylamine (distilled prior to use, 0.46 mL, 3.35 mmol) in toluene (3.5 mL). Reaction mixture was stirred vigorously for 3 h. Alkyne (+)-**2.21** (300 mg, 0.548 mmol) was then added in toluene (1.3 mL) and stirred for 3 h. Aldehyde (+)-**2.25** (95 mg, 0.300 mmol) was then added in toluene (0.5 mL) and reaction mixture was stirred at room temperature overnight. Reaction was portioned between a saturated aq solution NH_4Cl (10 mL) and EtOAc (10 mL). Aqueous layer was extracted with EtOAc (3 x 20 mL). Combined organic layers were washed with brine, dried over Na_2SO_4, decanted and concentrated *in vacuo*. Crude mixture was purified *via* column chromatography on SiO_2 (20% EtOAc: hexanes) to provide alcohol (+)-**2.28** (247 mg, 0.287 mmol, 95%) as a clear oil: $[\alpha]_D^{21}$ +51.5 (c 0.79, $CHCl_3$); IR (neat) 3440, 2951, 1719, 1678, 1513; ^{1}H NMR (500MHz, $CDCl_3$) δ = 7.15 (d, *J* = 8.5 Hz, 2 H), 6.87 (d, *J* = 8.7 Hz, 2 H), 5.67 (s, 1 H), 5.19 (d, *J* = 15.3 Hz, 1 H), 4.88 (d, *J* = 7.1 Hz, 1 H), 4.69 (d, *J* = 6.9 Hz, 1 H), 4.28 (d, *J* = 6.9 Hz, 1 H), 4.24 (d, *J* = 15.3 Hz, 1 H), 4.01 (spt, *J* = 5.0 Hz, 1 H), 3.93 (dd, *J* = 4.0, 9.5 Hz, 1 H), 3.79 (s, 3 H), 3.77 - 3.69 (m, 1 H), 3.69 - 3.59 (m, 4 H), 3.53 - 3.46 (m, 2 H), 3.38 - 3.28 (m, 2 H), 2.99 (s, 3 H), 2.90 - 2.82 (m, 1 H), 2.64 - 2.55 (m, 1 H), 2.49 - 2.40 (m, 1 H), 1.95 - 1.89 (m, 2 H), 1.88 (d, *J* = 1.0 Hz, 3 H), 1.83 - 1.76 (m, 1 H), 1.75 - 1.63 (m, 2 H), 1.63 - 1.51 (m, 3 H), 1.45 - 1.36 (m, 1 H), 1.29 - 1.20 (m, 2 H), 1.14 (s, 3 H), 0.99 - 0.92 (m, 2 H), 0.88 (s, 9 H), 0.07 (s, 6 H), 0.01 (s, 9 H); ^{13}C NMR (125 MHz, $CDCl_3$) δ = 173.7, 166.7, 160.1, 159.2, 128.9, 128.7, 116.4, 114.3, 102.8, 96.3, 90.5, 84.7, 79.3, 69.8, 66.2, 65.6, 65.4, 57.3, 55.5, 51.0, 47.8, 47.0, 41.0, 37.9, 33.5, 32.5, 30.2, 29.5, 26.5, 26.1, 26.0, 25.1, 21.0, 18.3, 18.2, -1.3, -4.3, -4.4; HRMS (ES) *m/z* $(M+Na)^+$ calcd 886.4391 obsd 886.4396.

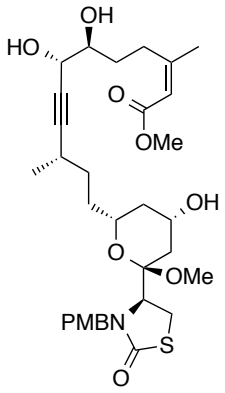

Triol (+)-S9: To propargyl alcohol (+)-**2.28** (43 mg, 0.0498 mmol) was added MeOH•HCl (1.5%) (0.7 mL), followed by CH_2Cl_2 (0.5 mL) to rinse the sides of the flask. After stirring for 3.5 h at RT, a saturated aq. solution $NaHCO_3$ (5 mL) was added to quench the reaction. The resulting mixture was extracted with CH_2Cl_2 (2 x 20 mL). Combined organic layers were dried over Na_2SO_4, decanted and concentrated *in vacuo*. Crude mixture was purified *via* column chromatography on SiO_2 (80%-100% EtOAc: hexanes) to provide (+)-**S9** (27 mg, 0.0436 mmol, 88%) as a clear oil: $[\alpha]_D^{21}$ +58.0 (c 1.0, $CHCl_3$); IR (neat) 3423, 2945, 1651, 1513, 1442, 1395; ^{1}H NMR (500MHz, $CDCl_3$) δ = 7.15 (d, J = 8.5 Hz, 2 H), 6.88 (d, *J* = 8.5 Hz, 2 H), 5.83 - 5.72 (m, 1 H), 5.23 (d, *J* = 16.2 Hz, 1 H), 4.22 (d, *J* = 15.5 Hz, 1 H), 4.19 (br. s., 1 H), 4.12 - 4.05 (m, 1 H), 4.03 (d, *J* = 3.4 Hz, 1 H), 3.95 (dd, J = 2.6, 8.9 Hz, 1 H), 3.80 (s, 3 H), 3.70 (s, 3 H), 3.59 - 3.50 (m, 1 H), 3.50 - 3.43 (m, 1 H), 3.42 - 3.29 (m, 2 H), 3.19 - 3.09 (m, 1 H), 3.00 (s, 3 H), 2.81 (d, *J* = 2.8 Hz, 1 H), 2.45 (q, *J* = 6.1 Hz, 1 H), 2.32 (quin, *J* = 5.5 Hz, 1 H), 2.11 (dd, *J* = 3.2, 12.1 Hz, 1 H), 1.97 (d, *J* = 14.3 Hz, 1 H), 1.91 - 1.88 (m, 3 H), 1.66 (br. s., 2 H), 1.63 (br. s., 3 H), 1.60 - 1.55 (m, 2 H), 1.47 - 1.39 (m, 1 H), 1.25 - 1.20 (m, 1 H), 1.15 (d, *J* = 6.9 Hz, 3 H); ^{13}C NMR (125 MHz, $CDCl_3$) δ = 173.5, 168.2, 160.0, 159.3, 128.8, 128.7, 117.2, 114.4, 102.7, 90.7, 79.2, 73.6, 70.0, 66.3, 64.8, 57.1, 55.5, 51.6, 47.9, 46.9, 40.3, 37.9, 33.4, 32.6, 30.8, 29.3, 26.4, 26.1, 24.9, 21.1; HRMS (ES) *m/z* $(M+Na)^+$ calcd 642.2713 obsd 642.2715.

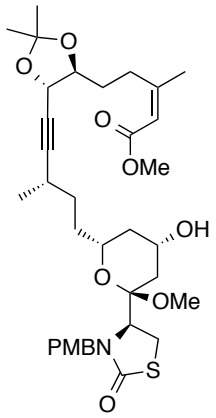

Acetonide (+)-2.29: To a solution of **triol** (+)-**S9** (27 mg, 0.0436 mmol) in 2,2-dimethoxypropane (1 mL) was added acetone (0.2 mL) and a small crystal of *p*-TsOH•H_2O. After the reaction mixture was stirred for 30 min at RT, a saturated aq. solution $NaHCO_3$ (5 mL) was added to quench the reaction. The resulting mixture was extracted with CH_2Cl_2 (2 x 20 mL). Combined organic layers were dried over Na_2SO_4, decanted and concentrated *in vacuo*. Crude mixture was purified *via* column chromatography on SiO_2 (40% EtOAc: hexanes) to provide acetonide (+)-**2.29** (25 mg, 0.0379 mmol, 87%) as a clear oil: $[\alpha]_D^{21}$ +27.5 (c 1.0, $CHCl_3$); IR (neat) 3447, 2944, 1715, 1673, 1513, 1444, 1379; ^{1}H NMR (500MHz, $CDCl_3$) δ = 7.15 (d, J = 8.5 Hz, 2 H), 6.88 (d, J = 8.7 Hz, 2 H), 5.76 - 5.63 (m, 1 H), 5.23 (d, J = 16.6 Hz, 1 H), 4.29 (dd, J = 1.6, 7.3 Hz, 1 H), 4.22 (d, J = 15.1 Hz, 1 H), 4.11 - 4.02 (m, 1 H), 4.02 - 3.91 (m, 2 H), 3.80 (s, 3 H), 3.68 (s, 3 H), 3.58 - 3.48 (m, 1 H), 3.42 - 3.29 (m, 2 H), 3.00 (s, 3 H), 2.88 - 2.77 (m, 1 H), 2.71 - 2.60 (m, 1 H), 2.46 (q, J = 6.1 Hz, 1 H), 2.10 (dd, J = 5.0, 12.7 Hz, 1 H), 1.97 (s, 1 H), 1.91 (d, J = 1.0 Hz, 3 H), 1.81 - 1.72 (m, 3 H), 1.71 - 1.65 (m, 1 H), 1.62 (s, 3 H), 1.60 - 1.56 (m, 1 H), 1.44 (s, 3 H), 1.40 (s, 3 H), 1.25 - 1.19 (m, 1 H), 1.15 (d, J = 6.9 Hz, 3 H); ^{13}C NMR (125 MHz, $CDCl_3$) δ = 173.5, 166.8, 160.0, 159.3, 128.9, 128.7, 116.4, 114.4, 109.8, 102.7, 91.2, 81.8, 77.9, 70.9, 69.9, 64.8, 57.1, 55.5, 51.1, 47.9, 46.9, 40.3, 37.8, 33.4, 32.5, 31.1, 29.8, 27.4, 26.6, 26.4, 26.1, 25.4, 21.0; HRMS (ES) *m/z* $(M+Na)^+$ calcd 682.3026 obsd 682.3026.

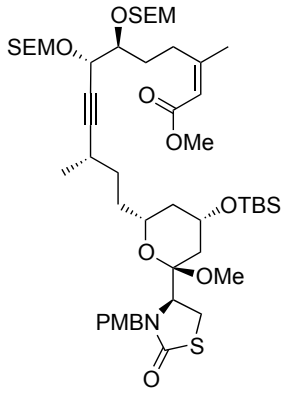

Bis-Sem Ether (+)-S10: To a solution of **alcohol** (+)-**2.28** (208 mg, 0.241 mmol) and *i*-PrNEt$_2$ in CH_2Cl_2 (0.8 mL) was added SEMCl dropwise. After 36 hr, 0.5 N HCl (5 mL) was added. Aqueous layer was extracted with CH_2Cl_2 (3 x 5 mL). Combined organic layers were dried over Na_2SO_4, decanted and concentrated *in vacuo*. Crude mixture was purified *via* column chromatography on SiO_2 (12% EtOAc: hexanes) to provide **SEM ether (+)-S10** (210 mg, 0.211 mmol, 88%) as a clear oil. $[\alpha]_D^{21}$ +98.1 (c 0.3, $CHCl_3$); IR (neat) 2951, 2895, 1719, 1681, 1513, 1456; ^{1}H NMR (500MHz, $CDCl_3$) δ = 7.15 (d, *J* = 8.1 Hz, 2 H), 6.87 (d, *J* = 8.1 Hz, 2 H), 5.65 (s, 1 H), 5.19 (d, *J* = 15.3 Hz, 1 H), 4.91 (d, *J* = 7.1 Hz, 1 H), 4.85 (d, *J* = 8.3 Hz, 1 H), 4.75 (d, *J* = 7.3 Hz, 1 H), 4.66 (d, *J* = 7.1 Hz, 1 H), 4.45 (d, *J* = 4.8 Hz, 1 H), 4.24 (d, *J* = 16.4 Hz, 1 H), 4.02 (spt, *J* = 4.6 Hz, 1 H), 3.94 (dd, *J* = 3.6, 9.1 Hz, 1 H), 3.80 (s, 3 H), 3.66 (s, 7 H), 3.57 - 3.44 (m, 2 H), 3.39 - 3.27 (m, 2 H), 2.98 (s, 3 H), 2.86 - 2.77 (m, 1 H), 2.71 - 2.61 (m, 1 H), 2.48 - 2.39 (m, 1 H), 1.89 (br. s., 1 H), 1.90 - 1.85 (m, 3 H), 1.86 - 1.76 (m, 1 H), 1.55 (br. s., 6 H), 1.44 - 1.36 (m, 1 H), 1.25 - 1.20 (m, 1 H), 1.14 (d, *J* = 6.7 Hz, 3 H), 0.97 - 0.92 (m, 4 H), 0.89 (s, 9 H), 0.07 (s, 6 H), 0.03 - -0.01 (m, 18 H); ^{13}C NMR (125 MHz, $CDCl_3$) δ = 173.8, 166.6, 160.4, 159.2, 128.9, 128.7, 116.2, 114.4, 102.8, 95.6, 92.4, 91.3, 79.7, 77.2, 69.8, 68.4, 65.6, 65.5, 65.4, 57.2,

55.5, 51.0, 47.8, 47.0, 41.0, 37.9, 33.6, 32.7, 29.9, 29.7, 26.5, 26.2, 26.1, 25.2, 21.2, 18.3, -1.2, -4.2, -4.4; HRMS (ES) *m/z* $(M+Na)^+$ calcd 1016.5205 obsd 1016.5207.

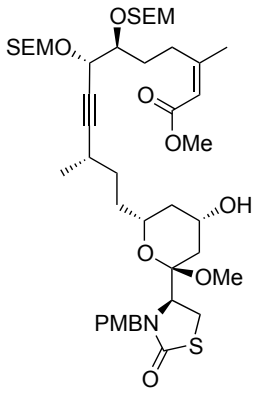

Methyl Ester (+)-S11: To a solution of **bis-SEM ether** (+)-**S11** (346 mg, 0.348 mmol) in THF (1.5 mL) was added a premixed solution of TBAF in THF (1 M, 3.5 mL, 3.5 mmol) and acetic acid (52 mg, 0.87 mmol) at room temperature. After 14 hr, a saturated aq solution NH_4Cl (10 mL) was added and biphasic mixture was extracted with CH_2Cl_2 (3 x 40 mL). Combined organic layers were dried over Na_2SO_4, decanted and concentrated *in vacuo*. Crude mixture was purified *via* column chromatography on SiO_2 (40% EtOAc: hexanes) to provide **Methyl Ester (+)-S11** (305 mg, 0.347 mmol, near quant.) as a clear oil. $[\alpha]_D^{21}$ +50.8 (c 0.2, $CHCl_3$); IR (neat) 3458, 2950, 1718, 1675, 1513, 1249; ^{1}H NMR (500MHz, $CDCl_3$) δ = 7.14 (d, *J* = 8.5 Hz, 2 H), 6.87 (d, *J* = 8.5 Hz, 2 H), 5.66 (s, 1 H), 5.23 (d, *J* = 16.1 Hz, 1 H), 4.90 (d, *J* = 6.7 Hz, 1 H), 4.85 (d, *J* = 6.7 Hz, 1 H), 4.74 (d, *J* = 7.1 Hz, 1 H), 4.66 (d, *J* = 6.5 Hz, 1 H), 4.46 (d, *J* = 4.0 Hz, 1 H), 4.21 (d, *J* = 15.5 Hz, 1 H), 4.11 - 4.02 (m, 1 H), 3.95 (dd, *J* = 3.3, 9.2 Hz, 1 H), 3.80 (s, 3 H), 3.66 (s, 7 H), 3.57 - 3.48 (m, 2 H), 3.41 - 3.29 (m, 2 H), 3.00 (br. s., 3 H), 2.80 (dt, *J* = 6.1, 11.9 Hz, 1 H), 2.69 (dt, *J* = 5.7, 10.9 Hz, 1 H), 2.49 - 2.40 (m, 1 H), 2.10 (dd, *J* = 5.0, 12.9 Hz, 1 H), 1.96 (d, *J* = 12.1 Hz, 1 H), 1.88 (s, 3 H), 1.84 - 1.74 (m, 2 H), 1.68 - 1.55 (m, 4 H), 1.45 - 1.37 (m, 1 H), 1.22 - 1.18 (m, 1 H), 1.14 (d, *J* = 6.7 Hz, 3 H), 0.97 - 0.90 (m, 4 H), 0.83 - 0.78 (m, 1 H), 0.01 (d, *J* =

2.4 Hz, 18 H); ^{13}C NMR (125 MHz, $CDCl_3$) δ = 173.5, 166.8, 160.4, 159.3, 128.8, 128.7, 116.2, 114.4, 102.7, 95.6, 92.4, 91.3, 79.6, 69.9, 68.4, 65.6, 65.6, 64.7, 57.0, 55.5, 51.0, 47.8, 40.3, 37.8, 33.5, 32.6, 29.9, 29.7, 26.4, 26.1, 25.3, 21.2, 18.3, -1.2, -1.2; HRMS (ES) *m/z* $(M+H)^+$ calcd 880.4521 obsd 880.4525.

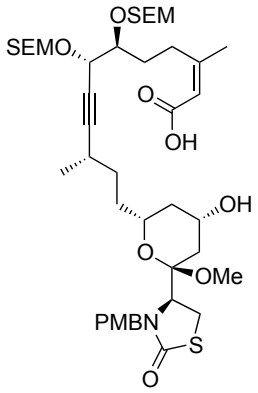

Seco-Acid (+)-2.30: To a vigorously stirring solution of **methyl ester (+)-S12** (24 mg, 0.027 mmol) in EtOH (2.5 mL), at room temperature was added 1 M NaOH (1 mL). Reaction mixture was then stirred at 50 °C for 24 hr. EtOH was removed *in vacuo*, 1N HCl (5 mL) was added and the mixture was extracted with CH_2Cl_2 (3 x 10 mL). Combined organic layers were dried over Na_2SO_4, decanted and concentrated *in vacuo*. Crude mixture was purified by filtering through a SiO_2 plug with EtOAc to yield seco-acid **(+)-2.30** (23 mg, 0.027 mmol, 97%) as a clear oil: $[\alpha]_D^{21}$ +56.0 (c 0.5, $CHCl_3$); IR (neat) 3420, 2951, 2891, 1679, 1513, 1249; ^{1}H NMR (500MHz, $CDCl_3$) δ = 7.14 (d, *J* = 8.5 Hz, 2 H), 6.87 (d, *J* = 8.5 Hz, 2 H), 5.68 (s, 1 H), 5.22 (d, *J* = 16.1 Hz, 1 H), 4.90 (d, *J* = 7.5 Hz, 1 H), 4.84 (d, *J* = 8.7 Hz, 1 H), 4.73 (d, *J* = 7.3 Hz, 1 H), 4.66 (d, *J* = 7.5 Hz, 1 H), 4.45 (d, *J* = 5.9 Hz, 1 H), 4.21 (d, *J* = 13.5 Hz, 1 H), 4.10 - 4.01 (m, 1 H), 3.95 (dd, *J* = 3.8, 9.5 Hz, 1 H), 3.79 (s, 3 H), 3.76 - 3.59 (m, 4 H), 3.53 (d, *J* = 6.1 Hz, 2 H), 3.42 - 3.28 (m, 2 H), 2.98 (s, 3 H), 2.84 - 2.75 (m, 1 H), 2.75 - 2.65 (m, 1 H), 2.50 - 2.40 (m, 1 H), 2.13 - 2.07 (m, 1

H), 2.00 - 1.94 (m, 1 H), 1.95 - 1.88 (m, 3 H), 1.89 - 1.80 (m, 1 H), 1.80 - 1.49 (m, 5 H), 1.45 - 1.39 (m, 1 H), 1.23 - 1.18 (m, 1 H), 1.17 - 1.11 (m, 3 H), 0.98 - 0.89 (m, 4 H), 0.01 (d, J = 3.6 Hz, 18 H); ^{13}C NMR (125 MHz, $CDCl_3$) δ = 173.7, 170.1, 163.0, 159.2, 128.8, 128.7, 116.0, 114.4, 102.7, 95.6, 92.4, 91.4, 79.6, 69.8, 68.5, 65.6, 65.6, 64.8, 60.6, 57.1, 55.5, 47.8, 46.9, 40.0, 37.6, 33.4, 29.8, 29.8, 26.4, 26.1, 25.6, 21.2, 21.2, 18.2, 14.4, -1.2, -1.2; HRMS (ES) *m/z* $(M-H)^-$ calcd 864.4208 obsd 864.4224.

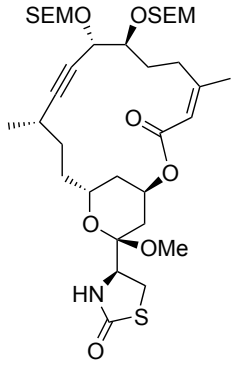

Lactone (+)-2.32: To a solution of seco-acid **(+)-2.30** (139 mg, 0.1605 mmol), and triphenyl-phosphine (210 mg, 0.8023 mmol) in toluene (16 mL). Reaction mixture was cooled to 0 °C, and DIAD was added dropwise. After 14 hr, SiO_2 was added and solvent was removed *in vacuo*. The crude reaction (adsorbed on SiO_2) was purified *via* column chromatography on SiO_2 (20% EtOAc: hexanes) to provide **macrolactone** (140 mg, mixture of macrolactone and DIAD-H_2) as a clear oil that was used directly in the next reaction.

To a solution of the **macrolactone** from the previous step (70 mg) in MeCN (6.4 mL) and H_2O (1.6 mL), cooled to 0 °C, was added CAN (176 mg, 0.321 mmol) in one portion, turning reaction mixture orange. Ice bath was removed after the addition and the reaction mixture was stirred vigorously. After 1.5 hr, a saturated aq solution $NaHCO_3$ (10 mL) was added and aqueous solution was extracted with CH_2Cl_2 (3 x 30 mL). Combined organic layers were dried over Na_2SO_4, decanted and concentrated *in vacuo*. Crude mixture was purified *via* column

chromatography on SiO_2 (25 % EtOAc: hexanes) to provide **lactone (+)-2.32** (21 mg, 0.029 mmol, 36 % for two steps) as an oil. : $[\alpha]_D^{21}$ +20.7 (c 0.2, $CHCl_3$); IR (neat) 3358, 3193, 2924, 2853, 1684, 1463, 1377, 1263; ^{1}H NMR (500MHz, $CDCl_3$) 5.68 (s, 1 H), 5.45 (s, 1 H), 5.10 (br. s., 1 H), 4.91 (t, *J* = 6.3 Hz, 2 H), 4.76 (d, *J* = 8.5 Hz, 1 H), 4.68 (d, *J* = 6.7 Hz, 1 H), 4.26 (d, *J* = 8.7 Hz, 1 H), 4.15 - 4.03 (m, 2 H), 3.80 - 3.67 (m, 2 H), 3.63 - 3.52 (m, 3 H), 3.40 (dd, *J* = 8.7, 12.7 Hz, 1 H), 3.36 - 3.29 (m, 1 H), 3.28 (s, 3 H), 2.72 (dt, *J* = 5.2, 10.7 Hz, 2 H), 2.34 (dt, *J* = 5.2, 11.7 Hz, 1 H), 2.28 (d, *J* = 15.7 Hz, 1 H), 1.96 - 1.91 (m, 1 H), 1.88 (s, 2 H), 1.82 - 1.74 (m, 2 H), 1.71 - 1.63 (m, 2 H), 1.58 - 1.48 (m, 2 H), 1.33 - 1.28 (m, 1 H), 1.18 (d, *J* = 6.7 Hz, 4 H), 1.00 - 0.89 (m, 5 H), 0.03 (d, *J* = 10.5 Hz, 18 H). ^{13}C NMR (125 MHz, $CDCl_3$) δ = 174.1, 167.3, 154.4, 118.5, 99.4, 96.3, 92.8, 90.3, 80.5, 78.8, 70.7, 66.9, 66.0, 65.6, 63.7, 57.7, 48.6, 35.9, 33.0, 31.6, 30.9, 30.8, 29.9, 29.7, 24.6, 24.3, 21.5, 18.3, 18.2, HRMS (ES) *m/z* $(M+Na)^+$ calcd 750.3527 obsd 750.3529.

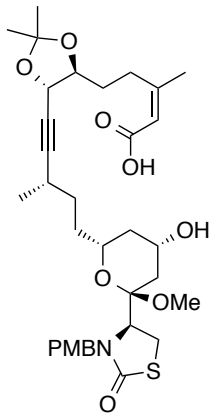

Seco-Acid S12: To a solution of acetonide (+)-**2.29** (13 mg, 0.0227 mmol) in ethanol (1.7 mL) was added an aq. solution of NaOH (1M, 0.7 mL) dropwise. After stirring overnight at 50 °C, the reaction mixture was concentrated under reduced pressure to give ca. 5 mL. An aq. solution of HCl (1 N, 5 mL) was then added to the reaction and the resulting mixture was extracted with CH_2Cl_2 (3 x 10 mL). Combined organic layers were dried over Na_2SO_4, decanted and

concentrated *in vacuo*. Crude mixture was purified *via* SiO_2 plug (EtOAc) to provide seco-acid **S12** (13 mg, 0.0227 mmol, near quant.) as a clear oil that was used in the next reaction without further purification.

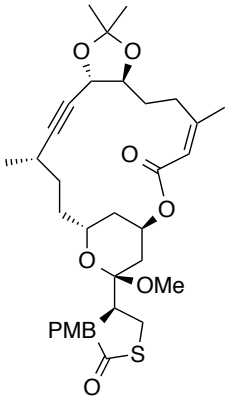

PMB-Macrolactone S13: To a solution of seco-acid **S12** (72 mg, 0.112 mmol) in toluene (11 mL) was added Ph_3P (147 mg, 0.56 mmol) followed by the addition of a 60 % solution of DEAD in toluene (227 mg, 0.78 mmol) dropwise at RT. After the reaction was stirred overnight, SiO_2 was added (ca. 3 g) and the solvent was removed *in vacuo*. Crude mixture was purified *via* column chromatography on SiO_2 (17.5%-20% EtOAc: hexanes) to provide macrolactone **S13** as a mixture contaminated with reduced DEAD (90 mg) that was used in the next reaction without further purification.

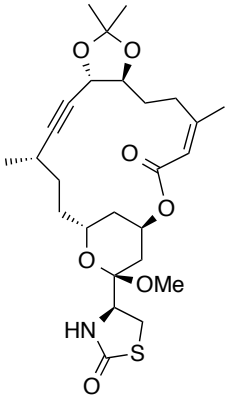

Macrolactone (+)-2.34: The next reaction was split into three batches.

Batch 1: To a solution of the macrolactone **S13** mixture from the previous step (10 mg) in MeCN (1.3 mL) and H_2O (0.3 mL), was added CAN (35 mg, 0.064 mmol) in one portion, turning reaction mixture orange. The reaction mixture was stirred vigorously at RT. After 1 h, a saturated aq solution $NaHCO_3$ (10 mL) was added and aqueous solution was extracted with CH_2Cl_2 (3 x 5 mL). Combined organic layers were dried over Na_2SO_4, decanted and concentrated *in vacuo*.

Batch 2: To a solution of the macrolactone **S13** from the previous step (34 mg) in MeCN (4.3 mL) and H_2O (1.1 mL), was added CAN (119 mg, 0.217 mmol) in one portion, turning reaction mixture orange. The reaction mixture was stirred vigorously at RT. After 1 h 40 min, a saturated aq solution $NaHCO_3$ (10 mL) was added and aqueous solution was extracted with CH_2Cl_2 (3 x 10 mL). Combined organic layers were dried over Na_2SO_4, decanted and concentrated *in vacuo*.

Batch 3: To a solution of the macrolactone **S13** from the previous step (46 mg) in MeCN (5.6 mL) and H_2O (1.4 mL), was added CAN (161 mg, 0.293 mmol) in one portion, turning reaction mixture orange. The reaction mixture was stirred vigorously at RT. After ca. 1 h 30 min, a saturated aq solution $NaHCO_3$ (10 mL) was added and aqueous solution was extracted with CH_2Cl_2 (3 x 10 mL). Combined organic layers were dried over Na_2SO_4, decanted and concentrated *in vacuo*.

The crude mixtures from batches 1, 2 and 3 were combined and then purified *via* column chromatography on SiO_2 (17% EtOAc: hexanes) to provide lactone (+)-**2.34** (20 mg, 0.0394 mmol, 35% over two steps) as a film: $[\alpha]_D^{21}$ +105.1 (c 0.58, $CHCl_3$); IR (neat) 3273, 2935, 1697, 1456, 1378; ^{1}H NMR (500MHz, $CDCl_3$) δ = 5.66 (s, 1 H), 5.53 (s, 1 H), 5.18 - 5.14 (m, 1 H), 4.19 (d, J = 9.1 Hz, 1 H), 4.15 (t, J = 11.5 Hz, 1 H), 4.07 (t, J = 7.9 Hz, 1 H), 3.88 - 3.78 (m, 1 H),

3.44 - 3.36 (m, 1 H), 3.36 - 3.30 (m, 1 H), 3.29 (s, 3 H), 2.82 - 2.74 (m, 1 H), 2.70 (dt, J = 5.4, 11.7 Hz, 1 H), 2.53 (dt, J = 5.2, 11.3 Hz, 1 H), 2.26 (d, J = 14.5 Hz, 1 H), 1.90 (d, J = 0.8 Hz, 3 H), 1.84 (m, 4 H), 1.64 (s, 3 H), 1.61 - 1.53 (m, 2 H), 1.45 (s, 3 H), 1.41 (s, 3 H), 1.19 (d, J = 6.9 Hz, 3 H); ^{13}C NMR (125 MHz, $CDCl_3$) δ = 174.2, 166.8, 154.9, 118.6, 109.9, 99.4, 90.7, 82.5, 77.9, 70.7, 66.7, 64.7, 57.7, 48.7, 36.1, 32.5, 31.0, 30.9, 30.9, 29.7, 29.3, 27.3, 26.7, 24.7, 24.5, 20.8; HRMS (ES) *m/z* $(M+Na)^+$ calcd 530.2188 obsd 530.2184

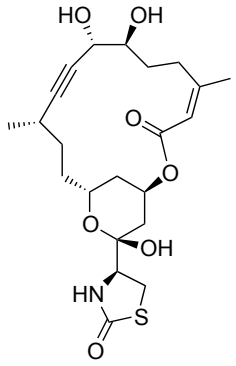

Triol (+)-2.33: To a solution of macrolactone (+)-**2.34** (7mg, 0.0138 mmol) in acetic acid (2.5 mL) and H_2O (1.1 mL) was added camphor sulfonic acid (2 mg). The reaction mixture was stirred at 50 °C. After 1 h, TLC analysis indicated the reaction to be complete. Acetic acid was removed *in vacuo*, a saturated aq. solution $NaHCO_3$ (10 mL) was added and the cloudy aqueous mixture was extracted with CH_2Cl_2 (3 x 20 mL). Combined organic layers were dried over Na_2SO_4, decanted and concentrated *in vacuo*. Crude mixture was purified *via* column chromatography on SiO_2 (75% EtOAc: hexanes) to provide triol (+)-**2.33** (5.4 mg, 0.0138 mmol, 86%) as a white foam: $[\alpha]_D^{21}$ +90.3 (c 0.39, $CHCl_3$); IR (neat) 3395, 2924, 1681, 1279; ^{1}H NMR (500MHz, $CDCl_3$) δ = 6.02 (s, 1 H), 5.71 (s, 1 H), 5.21 (s, 1 H), 4.27 (t, *J* = 11.6 Hz, 1 H), 4.09 (d, *J* = 7.7 Hz, 1 H), 3.85 (t, *J* = 7.8 Hz, 1 H), 3.48 (t, *J* = 8.5 Hz, 1 H), 3.42-3.31 (m, 2 H), 2.84 (td, *J* = 5.3, 11.4 Hz, 1 H), 2.70-2.63 (m, 1 H), 2.35 (td, *J* = 5.0, 12.1 Hz, 1 H), 2.17 (d, J = 14.6 Hz, 1 H), 1.99 (d, *J* = 13.5 Hz, 1H), 1.90 (s, 3 H), 1.83-1.48 (m, 8 H), 1.3-1.27 (m, 1 H), 1.25 (bs, 2 H),

1.17 (d, J = 7.0 Hz, 3 H) ; ^{13}C NMR (125 MHz, $CDCl_3$) δ = 175.8, 166.8, 156.0, 117.8, 96.6, 90.4, 80.0, 75.9, 68.3, 66.9, 62.8, 62.7, 35.5, 32.5, 32.2, 32.0, 30.8, 29.9, 29.2, 24.5, 23.7, 21.3; HRMS (ES) m/z $(M+Na)^+$ calcd 476.1719 obsd 476.1711

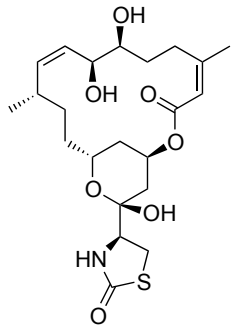

(+)-18-*epi*-latrunculol A (2.1): To a solution of triol (+)-**2.33** (2 mg, 0.0044 mmol) in EtOAc (0.3 mL) was added Pd on $BaCO_3$ (20 mg). The reaction flask was evacuated and refilled with H_2 (3 x) and stirred at room temperature under a balloon of H_2. After 4 h 30 min, a sample of reaction mixture was filtered through celite and LCMS analysis indicated reaction was complete. The reaction mixture was filtered through a pad of Celite with EtOAc and CH_2Cl_2, and the solvent was removed *in vacuo*. Residual catalyst was observed so the crude mixture was filtered through a clean pad of Celite with CH_2Cl_2 to afford (+)-**2.1** (2 mg, 0.0044 mmol, near quant.) as a white foam: $[\alpha]_D^{21}$ +21.3 (c 0.12, MeOH); IR (neat, cm^{-1}) 3418, 2926, 2855, 1681, 1444, 1383, 1289; ^{1}H NMR (500MHz, CD_3COCD_3) δ = 6.58 (s, 1H), 5.63 (t, J=10.5 Hz, 1H), 5.54 (s, 1H), 5.15 (bs, 1H), 5.05 (t, J=10.9 Hz, 1H), 4.87 (s, 1H), 4.39-4.28 (m, 2H), 3.91 (t, J=7.8 Hz, 1H), 3.58 (d, J=6.2Hz, 1H), 3.46 (d, J=7.4 Hz, 1H), 3.43 (dd, J=2.4 Hz, 8.1Hz, 2H), 3.40-3.33 (m, 1H), 2.79-2.73 (m, 1H), 2.68 (td, J=3.6 Hz, 11.8 Hz, 1H), 1.53-1.40 (m, 2 H), 1.10-1.02 (m, 1H), .93 (d, J=6.5Hz, 3H); ^{13}C NMR (125 MHz, CD_3COCD_3)[5] δ = 174.1, 166.7, 158.8, 136.6, 132.4, 118.7, 97.3, 76.7, 70.2, 68.1, 63.9, 62.5, 36.8, 35.4, 33.2, 32.5, 32.2, 31.9, 29.7[6], 29.1[6], 25.6, 23.2

; HRMS (ES) *m/z* $(M+H)^-$ calcd 266.0487 obsd 266.0475. HRMS (ES) *m/z* $(M+Cl)^-$ calcd 478.1875 obsd 478.1861.

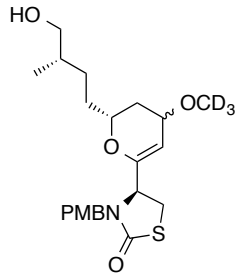

Dihydropyran 3.12: To a solution of **diol (+)-3.7** (5 mg, 0.012 mmol) in MeOD-d_4 (0.75 mL, 0.02 M) was added *p*TsOH•H_2O (1 mg, 0.005 mmol). The reaction was transferred to an NMR tube and irradiated at 355 nm for 1 h and 40 min. ^{1}H-NMR analysis indicated a 3.8:1 mixture of diastereomeric **dihydropyran 3.12**. The structure was assigned spectroscopically *via* ^{1}H, ^{13}C, COSY, and HSQC analysis. ^{1}H NMR (500 MHz, $CDCl_3$)[7] δ = 71.6 (d, J = 8.3 Hz, 2 H), 6.85 (d, J = 8.9 Hz, 2 H), 5.00 (dd, J = 1.2, 5.3 Hz, 1 H), 4.90 (d, J = 14.8 Hz, 1 H), 4.04 (dd, J = 5.5, 8.4 Hz, 1 H), 3.87 (d, J = 14.6 Hz, 1 H), 3.81 (s, 3 H), 3.72-3.69 (m, 1 H), 3.55-3.44 (m, 3 H), 3.32 (dd, J = 8.3, 11.1 Hz, 1 H), 3.28-3.23 (m, 1 H), 1.94 (d, J = 14.6 Hz, 1 H), 1.69-1.56 (m, 7 H), 1.42 (dd, J = 4.2, 12.2 Hz, 1 H), 1.39 (dd, J = 3.9, 12.7 Hz, 1 H), 1.20-1.15 (m, 1 H), 0.95 (d, J = 6.6 Hz, 4 H). ^{13}C NMR (125 MHz, $CDCl_3$) δ = 172.6, 159.4, 153.2, 151.2, 130.2, 129.9, 128.8, 128.6, 128.5, 114.3, 114.2, 102.1, 99.6, 69.0, 68.3, 61.0, 55.5, 46.6, 35.9, 35.8, 33.1, 32.4, 29.6, 28.8, 16.8, 16.7, 1.2 HRMS (ES) *m/z* $(M+Na)^+$ calcd 425.2190 obsd 425.2196.

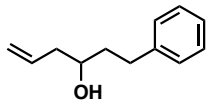

(±)-1-Phenyl-hex-5-en-3-ol (S15):[8] To a solution of 3-phenyl propionaldehyde (1.34 g, 1.3 mL, 10.0 mmol) in ether (33 mL) was added a solution of allyl magnesiumchloride in ether (2 M, 7.5 mL, 15 mmol) at 0°C. The mixture was warmed to room temperature, stirred for 2 h, diluted with

ether and poured into saturated aqueous solution of NH_4Cl (ca. 20 mL). The organic layer was separated, and the aqueous layer was extracted with EtOAc (3 x, ca 20 mL). The combined organic extracts were dried over Na_2SO_4, decanted, and the concentrated *in vacuo*. Purification of the crude reaction mixture *via* flash chromatography on silica gel (hexane/EtOAc 4:1) gave **1-Phenyl-hex-5-en-3-ol (S15)** (1.39 g, 7.89 mmol, 79%) as colorless oil. ^{1}H NMR (500 MHz, $CDCl_3$): δ = 7.32-7.29 (m, 2 H), 7..23-7.19 (m, 3 H), 5.88-5.79 (m, 1 H), 5.18-5.15 (m, 2 H), 3.72-3.67 (m, 1 H), 2.86-2.80 (m, 1 H), 2.74-2.68 (m, 1 H), 2.37-2.32 (m, 1 H), 2.23-2.18 (m, 1 H), 1.83-1.78 (m, 2 H), 1.66 (s, 1 H). ^{13}C NMR (125 MHz, $CDCl_3$): δ = 142.3, 134.8, 128.6, 128.6, 126.0, 118.5, 70.1, 42.3, 38.9, 32.3.

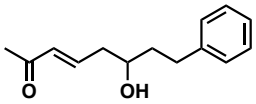

(±)-(E)-6-Hydroxy-8-phenyloct-3-en-2-one (3.13):[9] To a solution of **1-Phenyl-hex-5-en-3-ol** (**S15**) (1.20 g, 6.8 mmol) in dichloromethane (34 mL), **but-3-en-2-one** (2.38 g, 3 mL, 33.9 mmol, 5 eq, filtered through $NaHCO_3$ pad) and 2nd Generation Grubbs-Hoveyda catalyst (128 mg, 0.2 mmol, 3 mol%) were added sequentially. The reaction mixture was stirred overnight at room temperature, added with excess activated charcoal and filtered through celite, which was washed with EtOAc (50 mL). Then combined organic phases were concentrated *in vacuo*. Purification of the crude reaction mixture *via* flash chromatography on silica gel (hexane/EtOAc 4:1 to 3:2) gave **3.13** (1.48 g, 6.78 mmol, quant.) as dark brown oil. ^{1}H NMR (500 MHz, $CDCl_3$) δ= 7.32-7.29 (m, 2 H), 7.22-7.20 (m, 3 H), 6.83 (dt, J = 14.7, 7.1 Hz, 1 H), 6.16 (d, J = 16.0 Hz, 1 H), 3.84-3.79 (m, 1 H), 2.85-2.79 (m, 1 H), 2.74-2.68 (m, 1 H), 2.49-2.44 (m, 1 H), 2.34-2.36 (m, 1 H), 2.26 (s, 3 H), 1.85-1.81 (m, 2 H), 1.65 (br, 1 H). ^{13}C NMR (125 MHz, $CDCl_3$) δ= 198.6, 144.1, 141.7, 133.8, 128.7, 128.6, 126.3, 70.1, 40.7, 39.0, 32.2, 27.2.

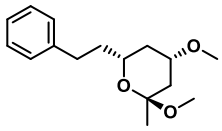

(±)-2, 4-dimethoxy-2-methyl-6-phenethyltetrahydro-2H-pyran (3.14): To a solution of **(E)-6-hydroxy-8-phenyloct-3-en-2-one (3.13)** (124 mg, 0.56 mmol) and MeOH (0.6 mL, 14 mmol, 25 eq) in THF (27 mL) was added *p*-TsOH (44 mg, .22 mmol, 40 mol%) at 20 ^{o}C. After flushing with N_2, the reaction mixture was irradiated with 355nm UV while stirring for 2.5 hr. A saturated aq. solution of $NaHCO_3$ (5 mL) was added followed by extraction with EtOAc (3 x, 10 mL). Combined organic layers were dried over Na_2SO_4, decanted and concentrated *in vacuo*. The crude mixture was purified *via* column chromatography on SiO_2 (10% EtOAc in Hexane) to provide **3.14** (120 mg, 0.45 mmol, 82%) as colorless oil.

OR

(±)-2, 4-dimethoxy-2-methyl-6-phenethyltetrahydro-2H-pyran (3.14): To a solution of **(E)-6-hydroxy-8-phenyloct-3-en-2-one (3.13)** (133 mg, 0.61 mmol) in MeOH (31 mL) was added *p*-TsOH (46 mg, 0.24 mmol, 40 mol%) at 20 °C. After flushed with N_2, the reaction mixture was irradiated with 355nm UV while stirring for 3 hr. A saturated aq. solution of $NaHCO_3$ (5 mL) was added followed by extraction with EtOAc (3 x, 10 mL). Combined organic layers were dried over Na_2SO_4, decanted and concentrated *in vacuo*. The crude mixture was purified *via* column chromatography on SiO_2 (10% EtOAc in Hexane) to provide **3.14** (146 mg, 0.55 mmol, 91%) as colorless oil. ^{1}H NMR (500 MHz, $CDCl_3$) δ= 7.31-7.28 (m, 2 H), 7.23-7.18 (m, 3 H), 3.65 (sep, J = 4.4 Hz, 1 H), 3.61-3.56 (m, 1 H), 3.36 (s, 3 H), 3.18 (s, 3 H), 2.91-2.85 (m, 1 H), 2.70-2.64 (m, 1 H), 2.24-2.20 (m, 1 H), 2.05-2.02 (m, 1 H), 1.94-1.87 (m, 1 H), 1.84-1.77 (m, 1 H), 1.38 (s, 3 H), 1.30 (t, J = 11.3 Hz, 1 H), 1.14 (q, J= 11.7 Hz, 1 H). ^{13}C NMR (125 MHz, $CDCl_3$) δ= 142.3, 128.5, 125.9, 99.7, 73.5, 68.6, 55.6, 47.8, 41.7, 37.8, 37.2, 32.1, 23.0 ppm. IR (neat, cm^{-1}): ν =

2986, 2941, 2825, 1603, 1496, 1453, 1380 cm^{-1}. HRMS (CI, $[M+Na]^+$) calcd for $C_{16}H_{24}O_3$ 287.1725, found 287.1622.

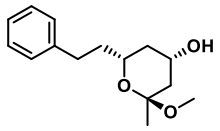

(±)-2-methoxy-2-methyl-6-phenethyltetrahydro-2H-pyran-4-ol (3.16): To a solution of **(E)-6-hydroxy-8-phenyloct-3-en-2-one** (**S15**) (135mg, 0.56 mmol) and BnOH (1.6 mL, 15 mmol, 25eq) in THF (29 mL) was added *p*-TsOH (48 mg, 0.22 mmol, 40mol%) at 20 ^oC. After flushed with N_2, the reaction mixture was irradiated with 355nm UV while stirring for 2.5 hr. The THF was removed *in vacuo*, and then MeOH (29 mL) and 10% Pd/C (84mg, 5 wt% to BnOH) was added. After stirring under an atmosphere of H_2 (balloon) at room temperature for 5 hr, the mixture was filtered through celite, concentrated *in vacuo* and purified *via* column chromatography on SiO_2 (40% EtOAc in Hexane) to provide **3.16** (110 mg, 0.44 mmol, 71%) as colorless oil. ^1H NMR (500 MHz, C_6D_6) δ= 7.18-7.17 (m, 2 H), 7.11-7.06 (m, 3 H), 4.01 (sep, J = 4.6 Hz, 1 H), 3.45-3.40 (m, 1 H), 3.00 (s, 3 H), 2.87-2.81 (m, 1 H), 2.58-2.52 (m, 1 H), 2.10-2.07 (m, 1 H), 1.86-1.78 (m, 1 H), 1.67-1.58 (m, 1 H), 1.24-1.29 (m, 4 H), 1.06 (t, J = 11.3 Hz, 1 H) ppm. ^{13}C NMR (125 MHz, C_6D_6) δ= 143.0, 129.0, 126.4, 128.4, 100.0, 69.0, 65.0, 47.8, 45.9, 41.4, 38.5, 32.8, 24.2 ppm. δ= IR (neat, cm^{-1}): ν = 3392, 3016, 2942, 2825, 1603, 1496, 1453, 1378 cm^{-1}. Awaiting HRMS data.

4.3 References

1. Yu, S.; Pan, X.; Ma, D. *Chemistry-a European Journal* **2006***, 25,* 6572-6584

2. Ramachandran, P. V.; Chandra, J. S.; Prabhudas, B.; Pratihar, D.; Reddy, M. V. R. *Organic & Biomolecular Chemistry* **2005***, 20,* 3812-3824.

3. Marshall, J. A.; Yanik, M. M. *J. Org. Chem.* **2001***, 4,* 1373-1379

4. Ramharter, J; Mulzer, J. *Org. Lett.* **2009**, 11, 1151-1153

5. Minor carbon peaks were observed due to deuterium exchange and not reported here; coalescence was observed upon addition of D_2O, see *deutero*-18-*epi*-latrunculol A (**S12**)

6. Assignments were made from HMBC correlations.

7. Only major peaks are reported.

8. Schmidt, B. *J. Org. Chem.* **2004**, 69, 7672-7687

9. Evans, P. A.; Grisin, A.; Lawler, M. J. *J. Am. Chem. Soc*. **2012**, 134, 2856−2859

Appendix 1: Spectroscopic Data

Figure A2.1. ^{1}H NMR Spectrum (500 MHz) of Compound (+)-**2.11** in $CDCl_3$

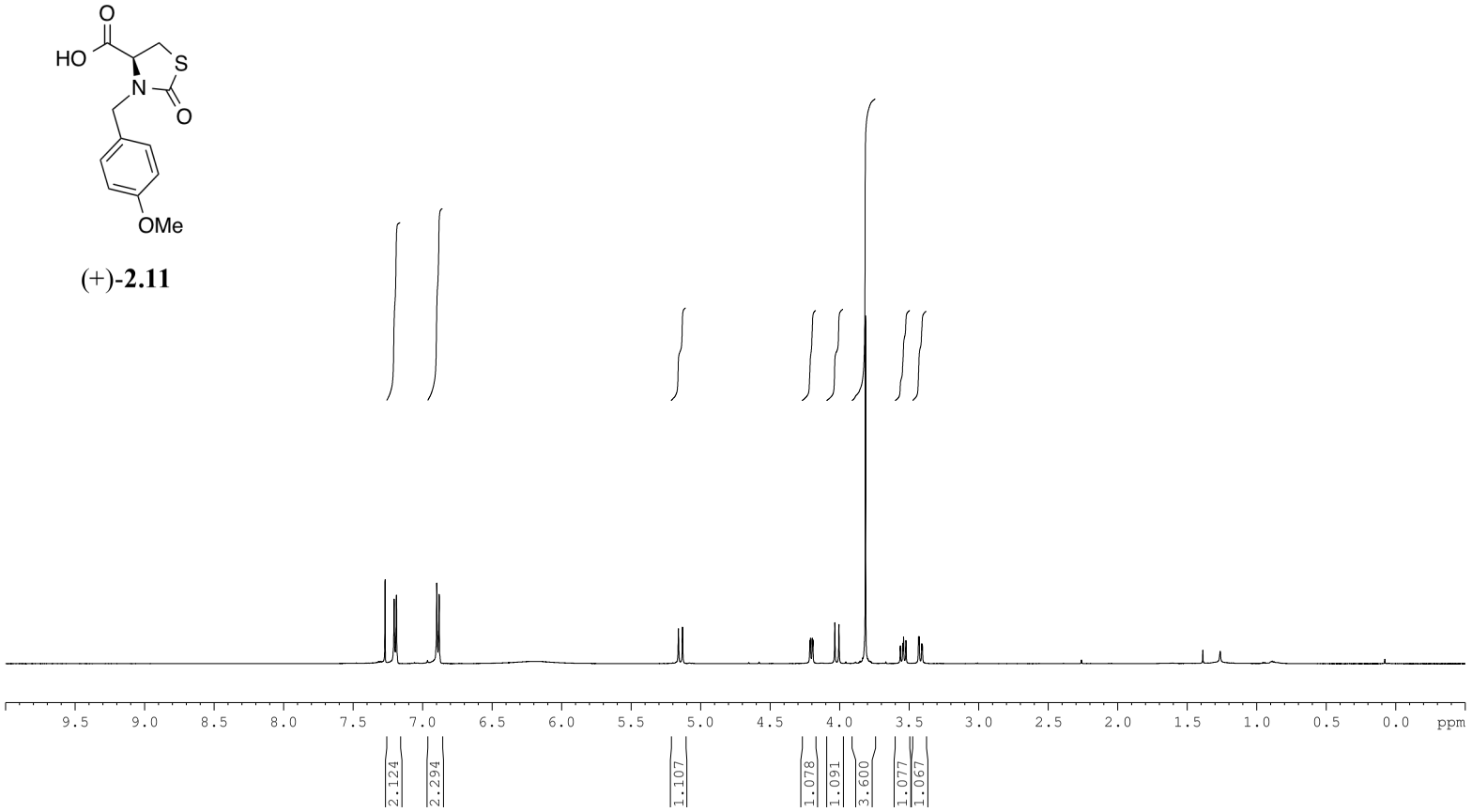

(+)-**2.11**

Figure A2.2. ^{13}C NMR Spectrum (125 MHz) of Compound (+)-**2.11** in $CDCl_3$

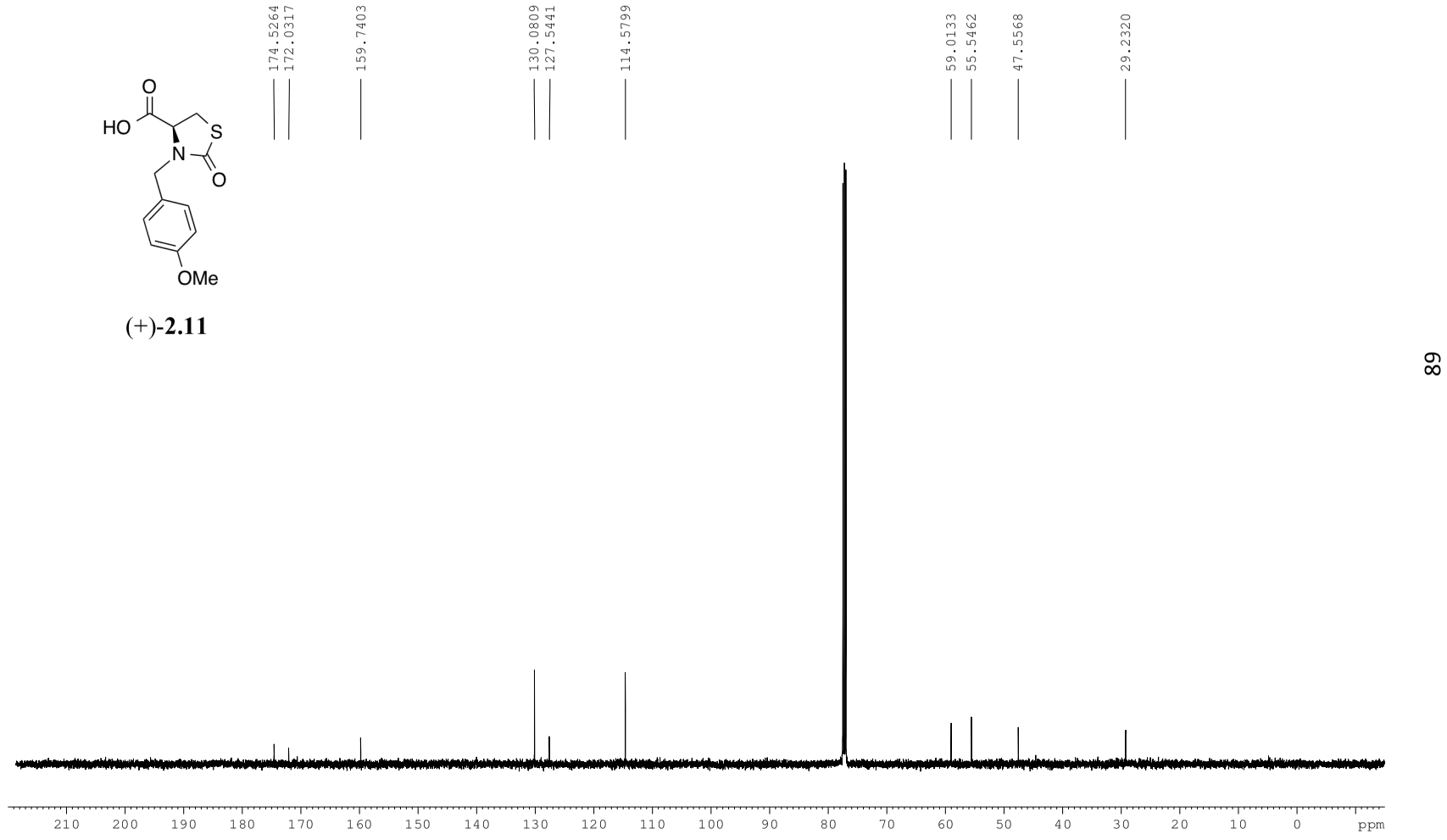

Figure A2.3. ^{1}H NMR Spectrum (500 MHz) of Compound (+)-**S1** in $CDCl_3$

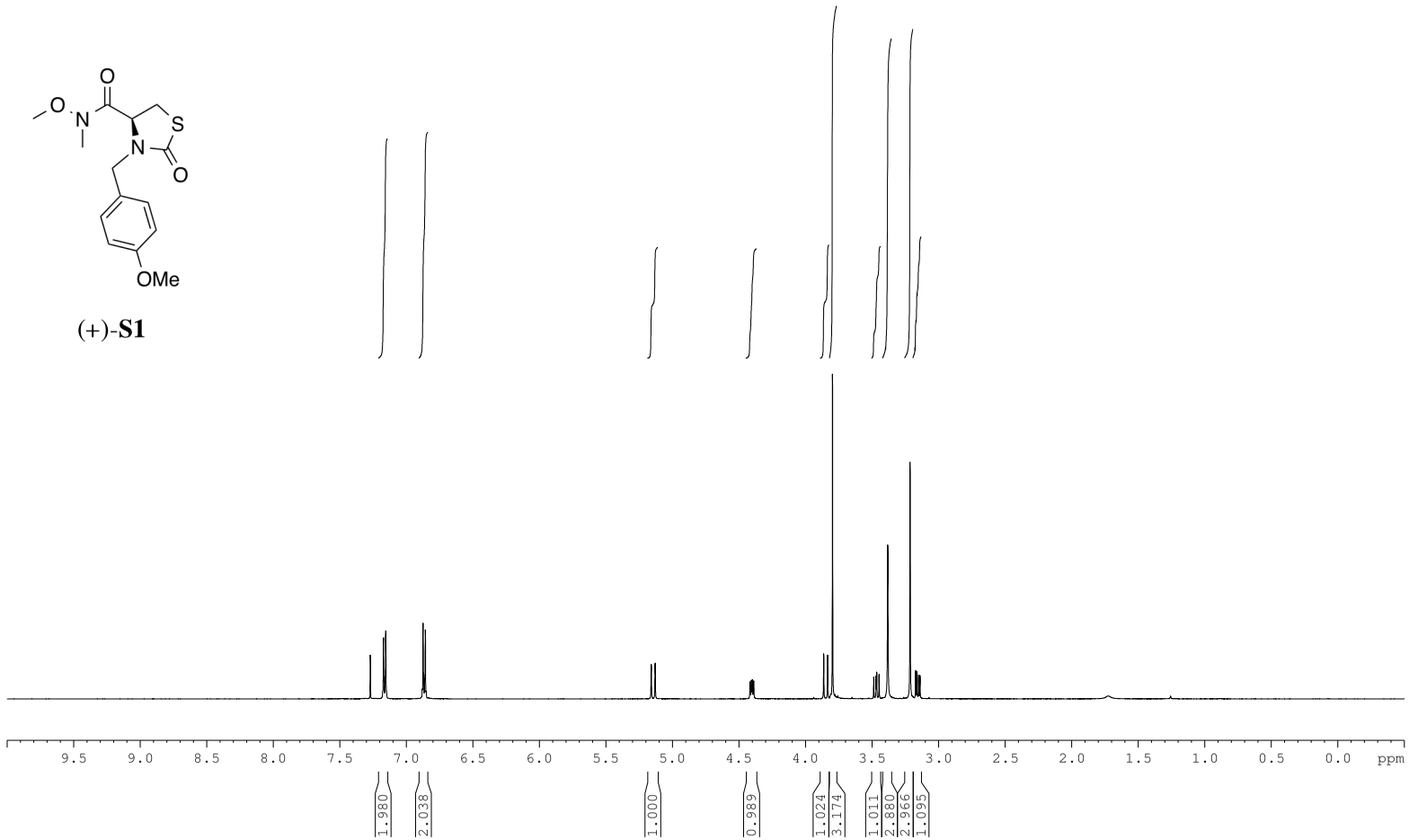

(+)-**S1**

Figure A2.4. ^{13}C NMR Spectrum (125 MHz) of Compound (+)-**S1** in $CDCl_3$

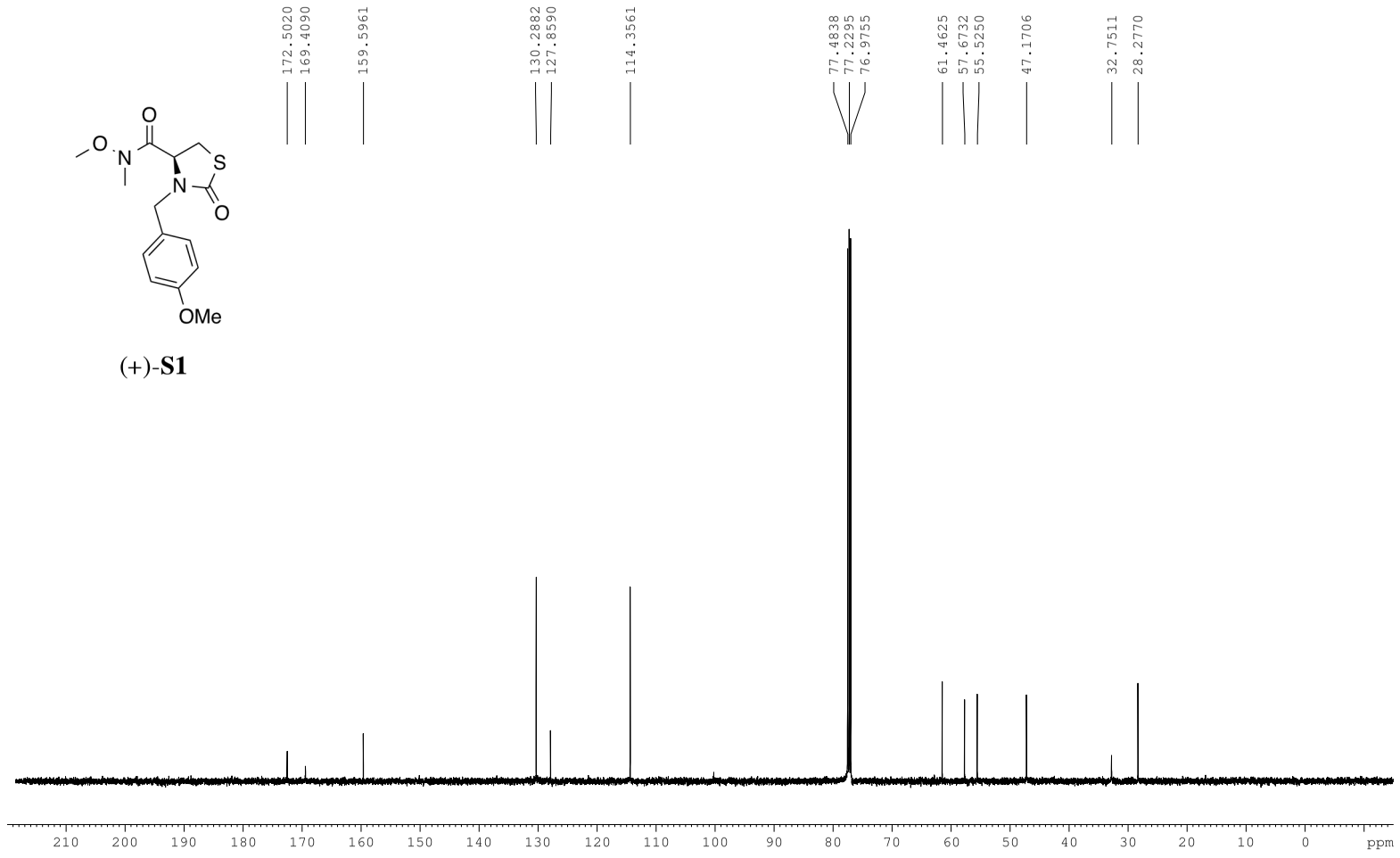

(+)-**S1**

Figure A2.5. ^{1}H NMR Spectrum (500 MHz) of Compound (+)-**2.10** in $CDCl_3$

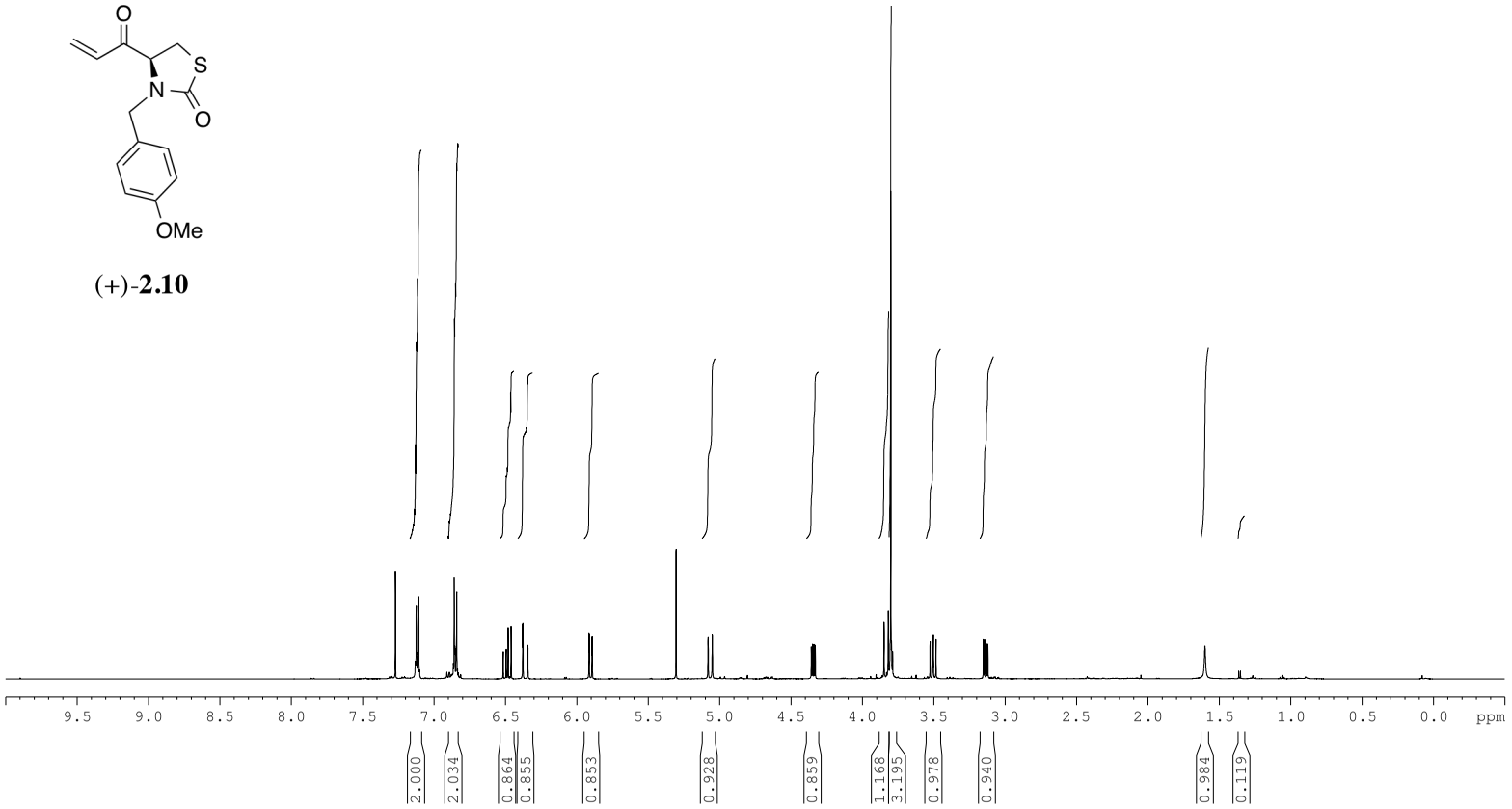

Figure A2.6. ^{13}C NMR Spectrum (125 MHz) of Compound (+)-**2.10** in $CDCl_3$

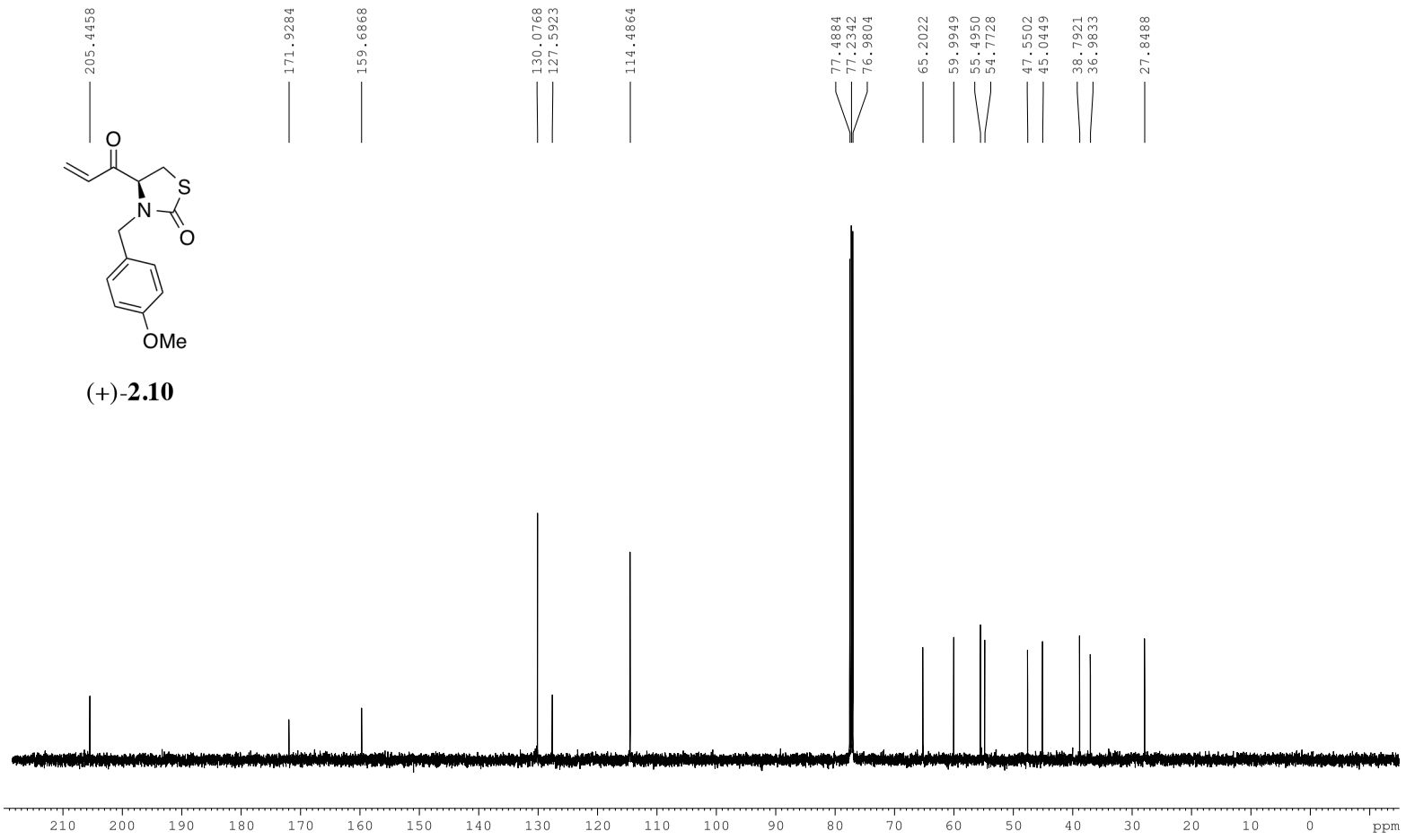

(+)-**2.10**

Figure A2.7. ^{1}H NMR Spectrum (500 MHz) of Compound (+)-**2.12** in $CDCl_3$

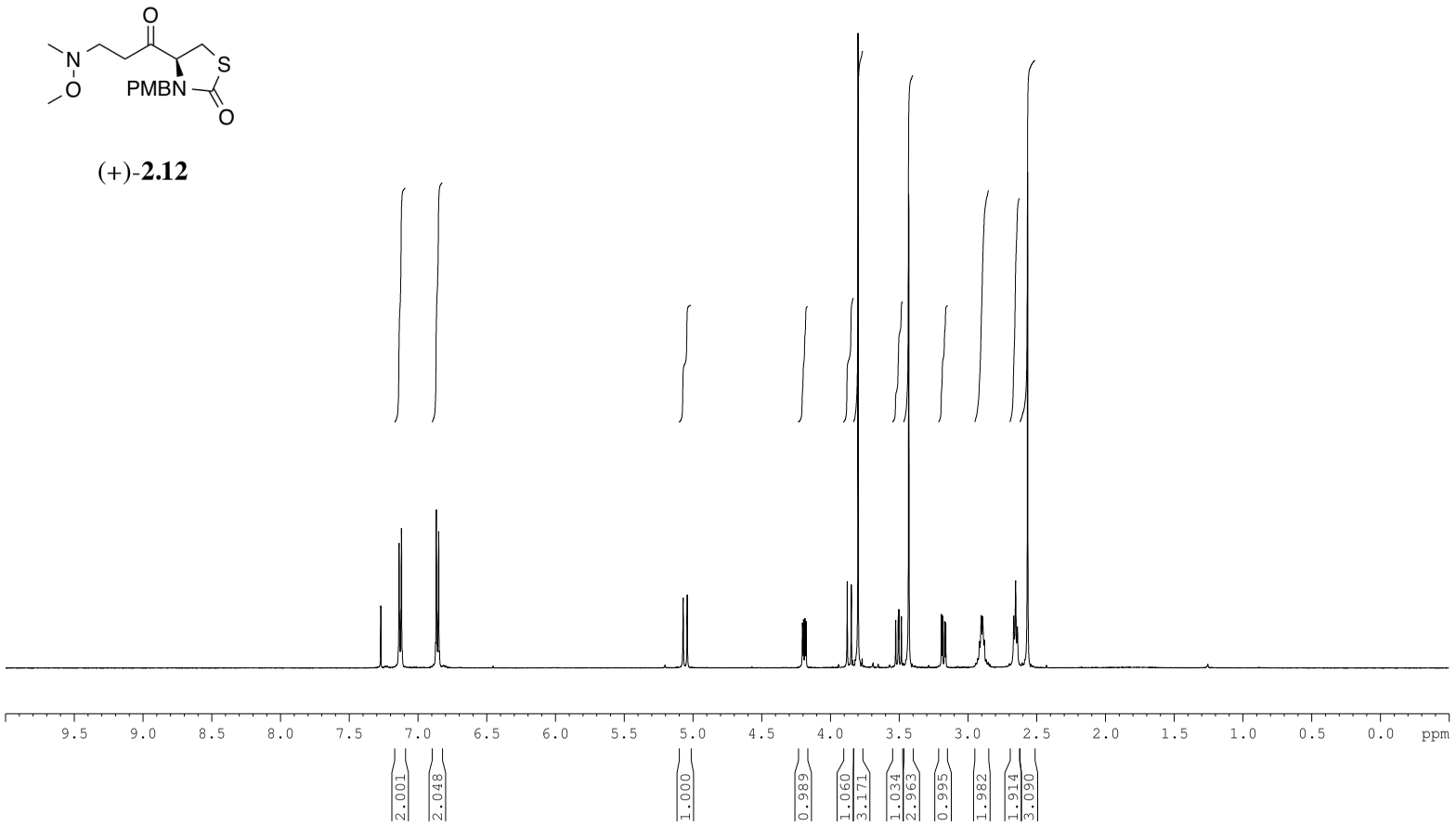

(+)-**2.12**

Figure A2.8. ^{13}C NMR Spectrum (125 MHz) of Compound (+)-**2.12** in $CDCl_3$

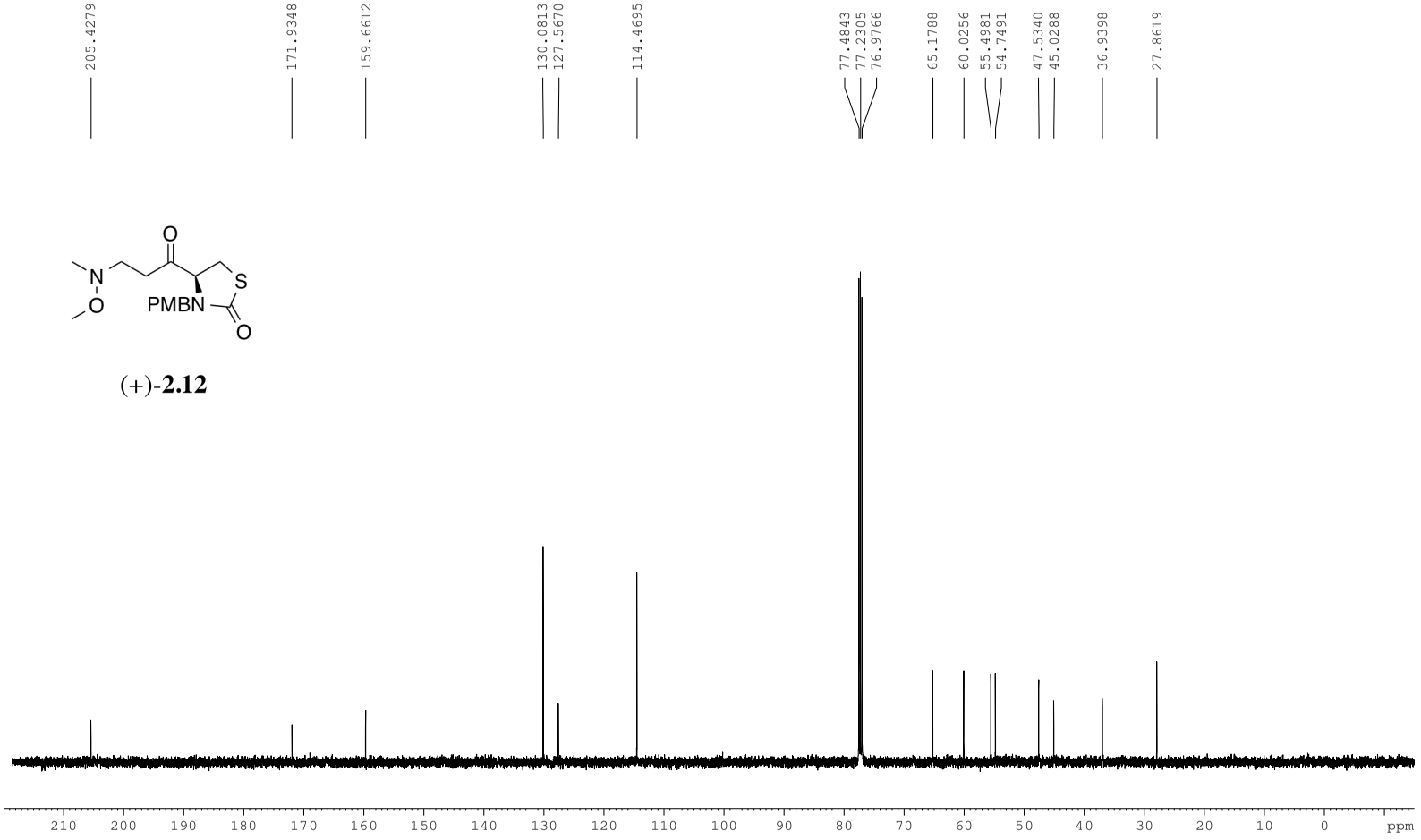

(+)-**2.12**

Figure A2.9. ^{1}H NMR Spectrum (500 MHz) of Compound (–)-**S2** in $CDCl_3$

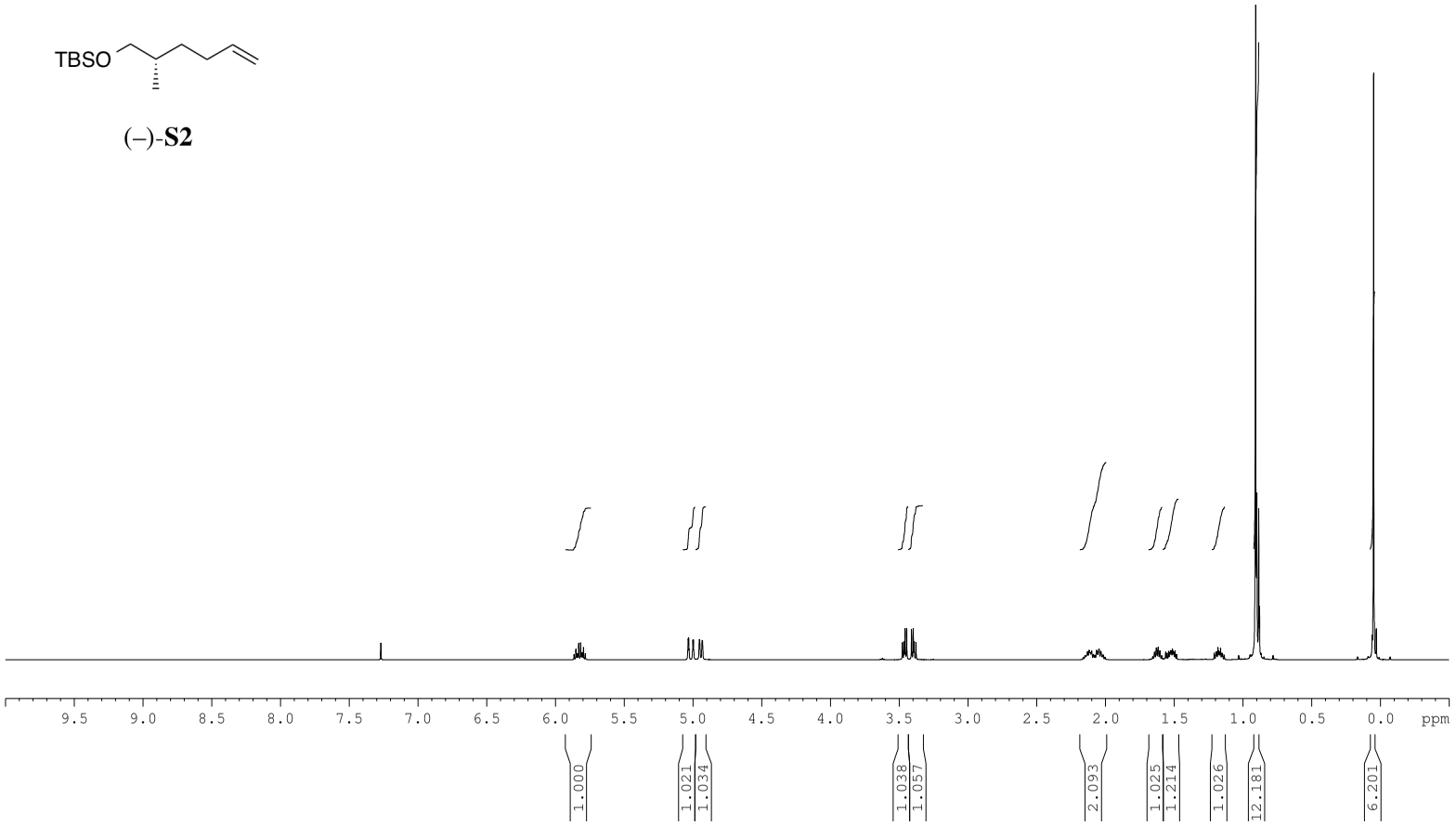

Figure A2.10. ^{13}C NMR Spectrum (125 MHz) of Compound (–)-**S2** in $CDCl_3$

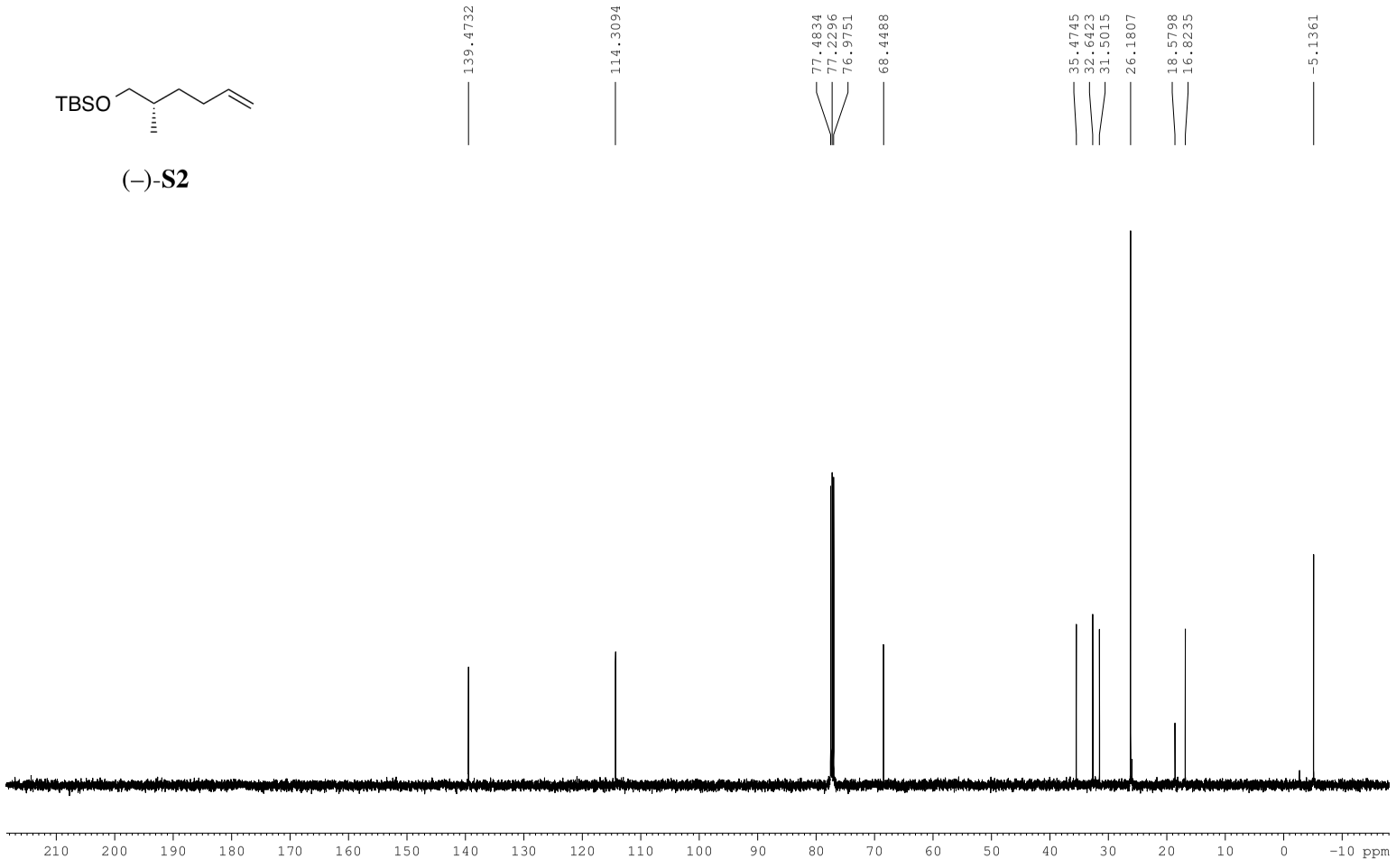

Figure A2.11. ^{1}H NMR Spectrum (500 MHz) of Compound (–)-**2.8** in $CDCl_3$

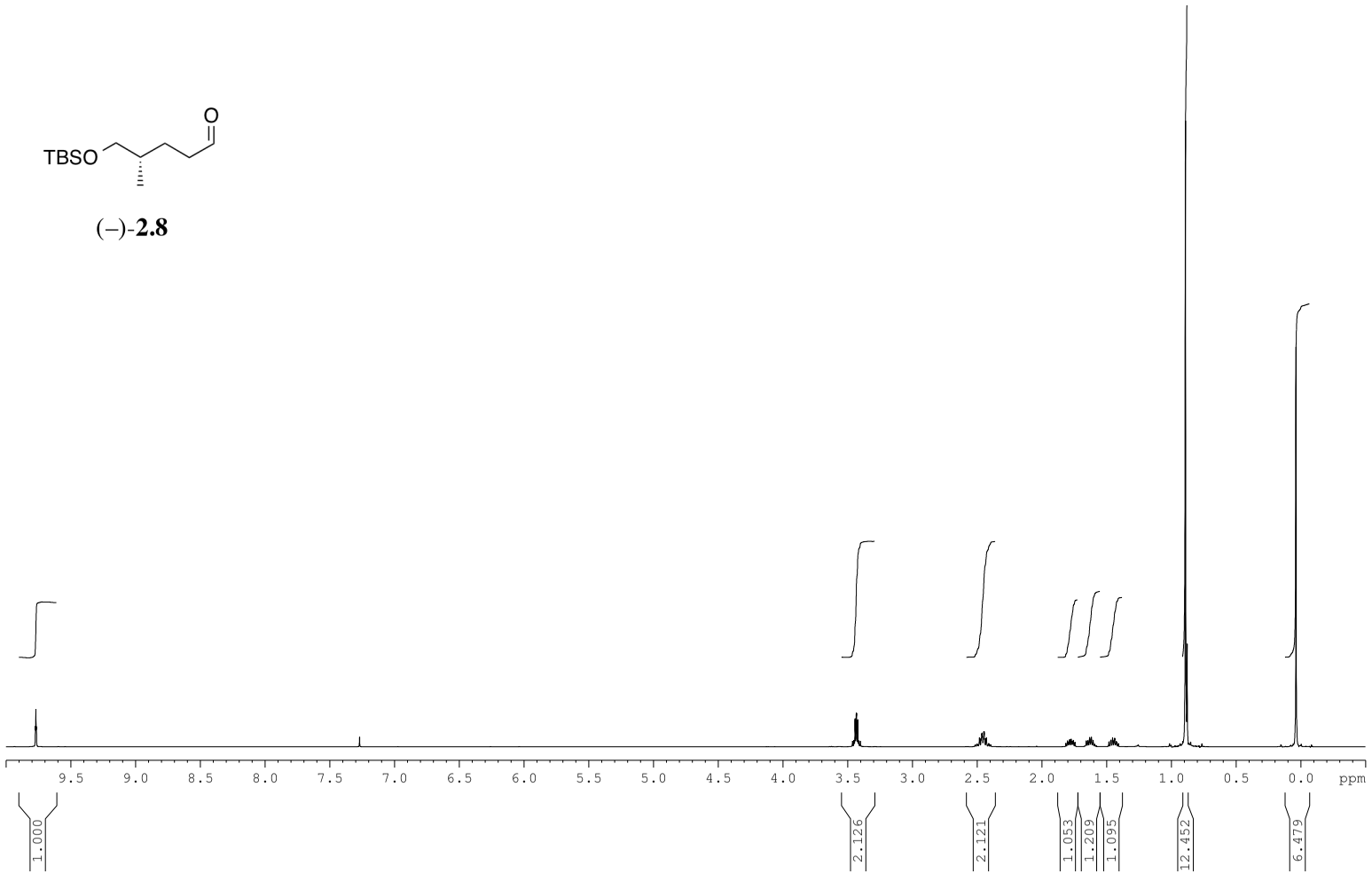

Figure A2.12. ^{13}C NMR Spectrum (125 MHz) of Compound (–)-**2.8** in $CDCl_3$

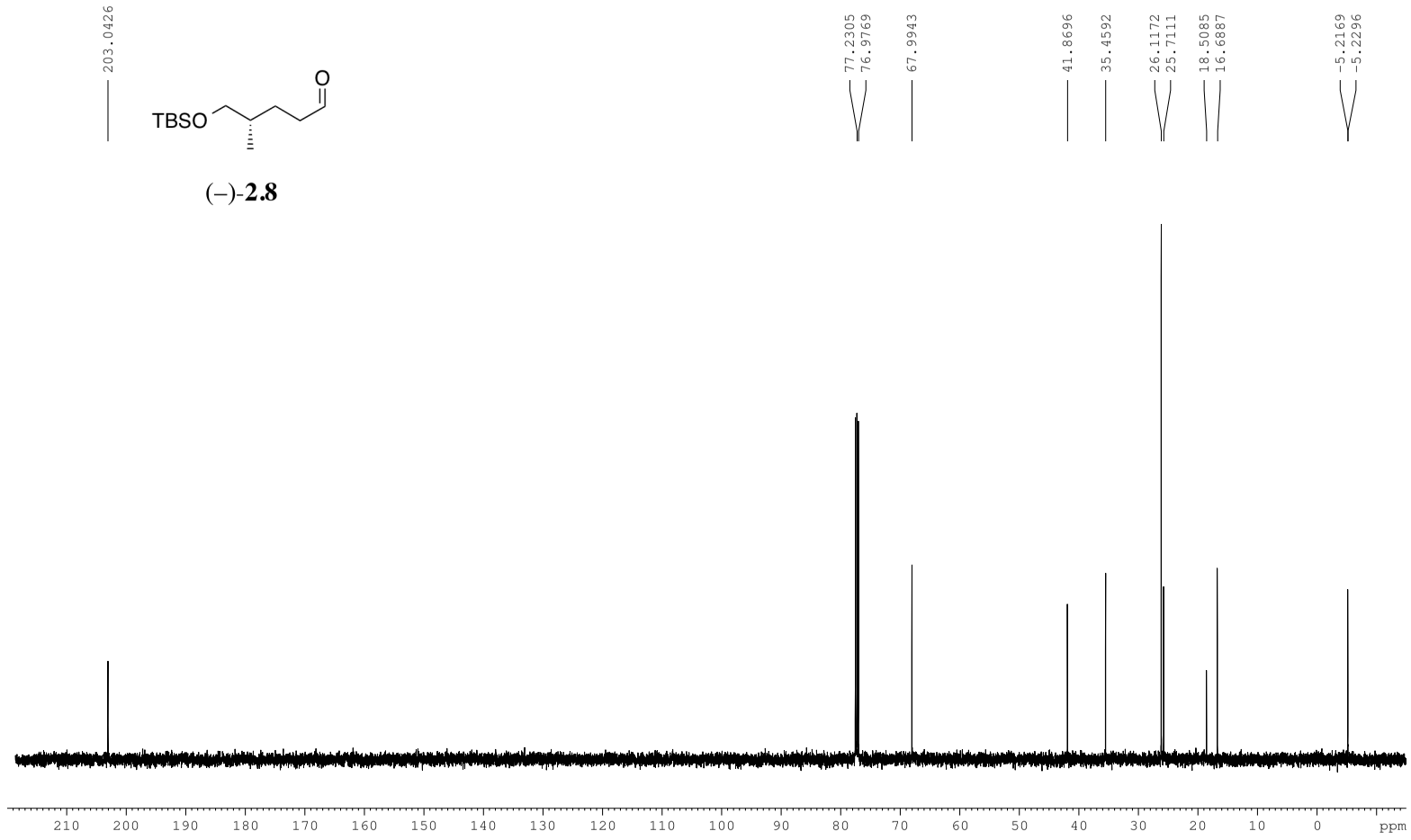

(–)-**2.8**

Figure A2.13. ^{1}H NMR Spectrum (500 MHz) of Compound (+)-**2.15** in $CDCl_3$

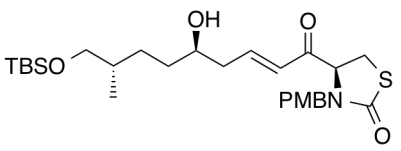

(+)-**2.15**

Figure A2.14. ^{13}C NMR Spectrum (125 MHz) of Compound (+)-**2.15** in $CDCl_3$

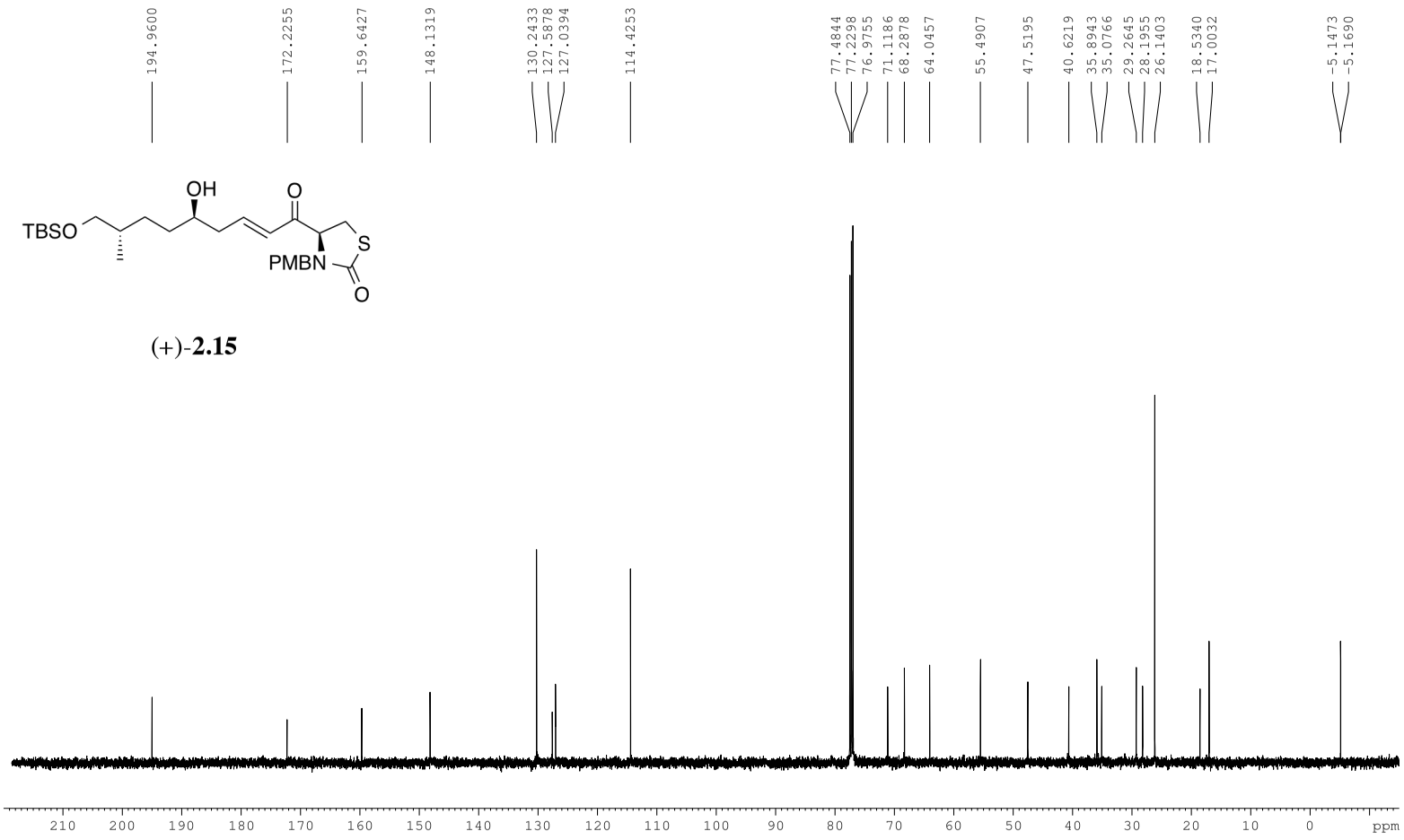

(+)-**2.15**

Figure A2.15. ^{1}H NMR Spectrum (500 MHz) of Compound (+)-**2.18** in $CDCl_3$

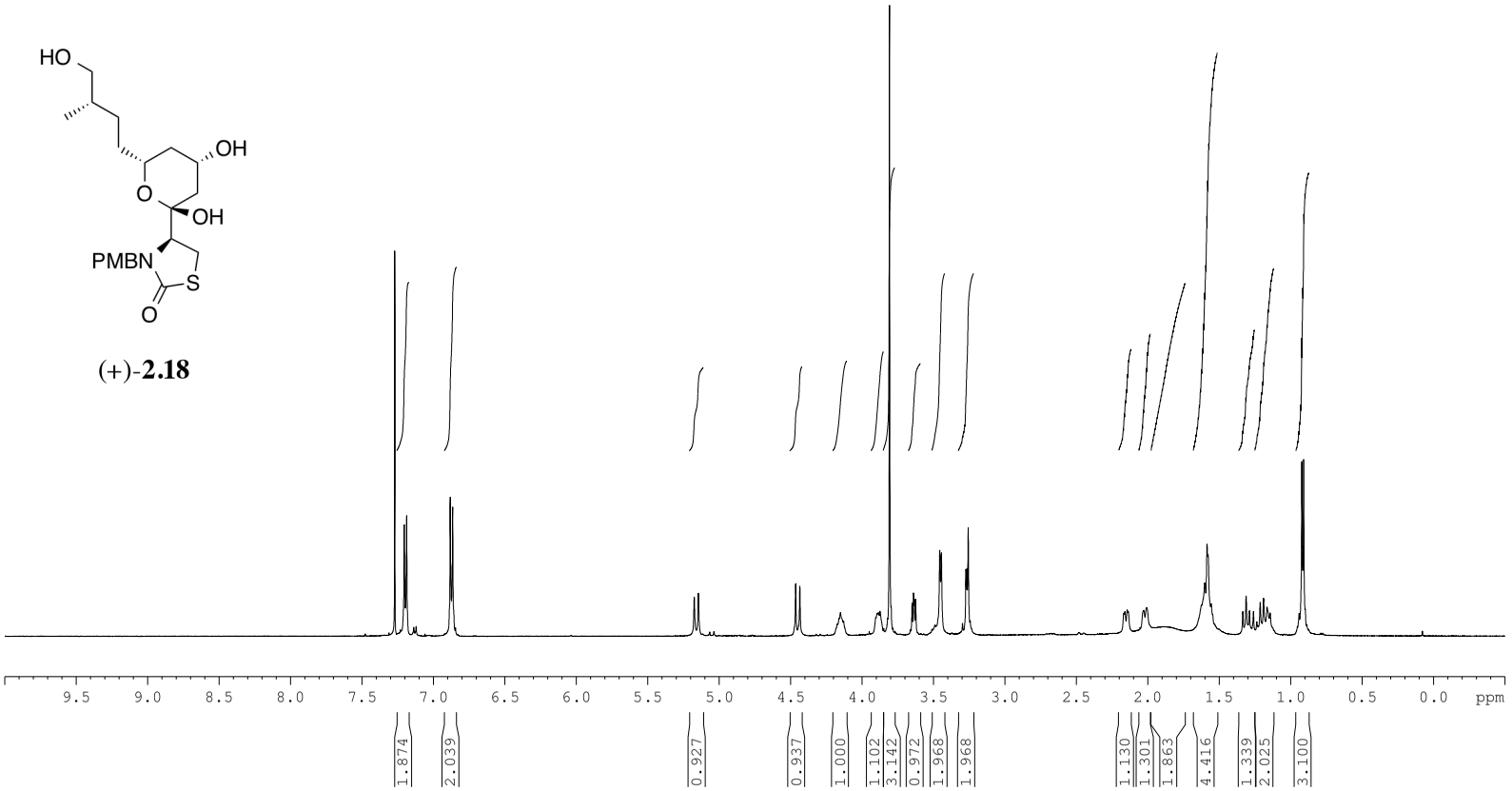

Figure A2.16. ^{13}C NMR Spectrum (125 MHz) of Compound (+)-**2.18** in $CDCl_3$

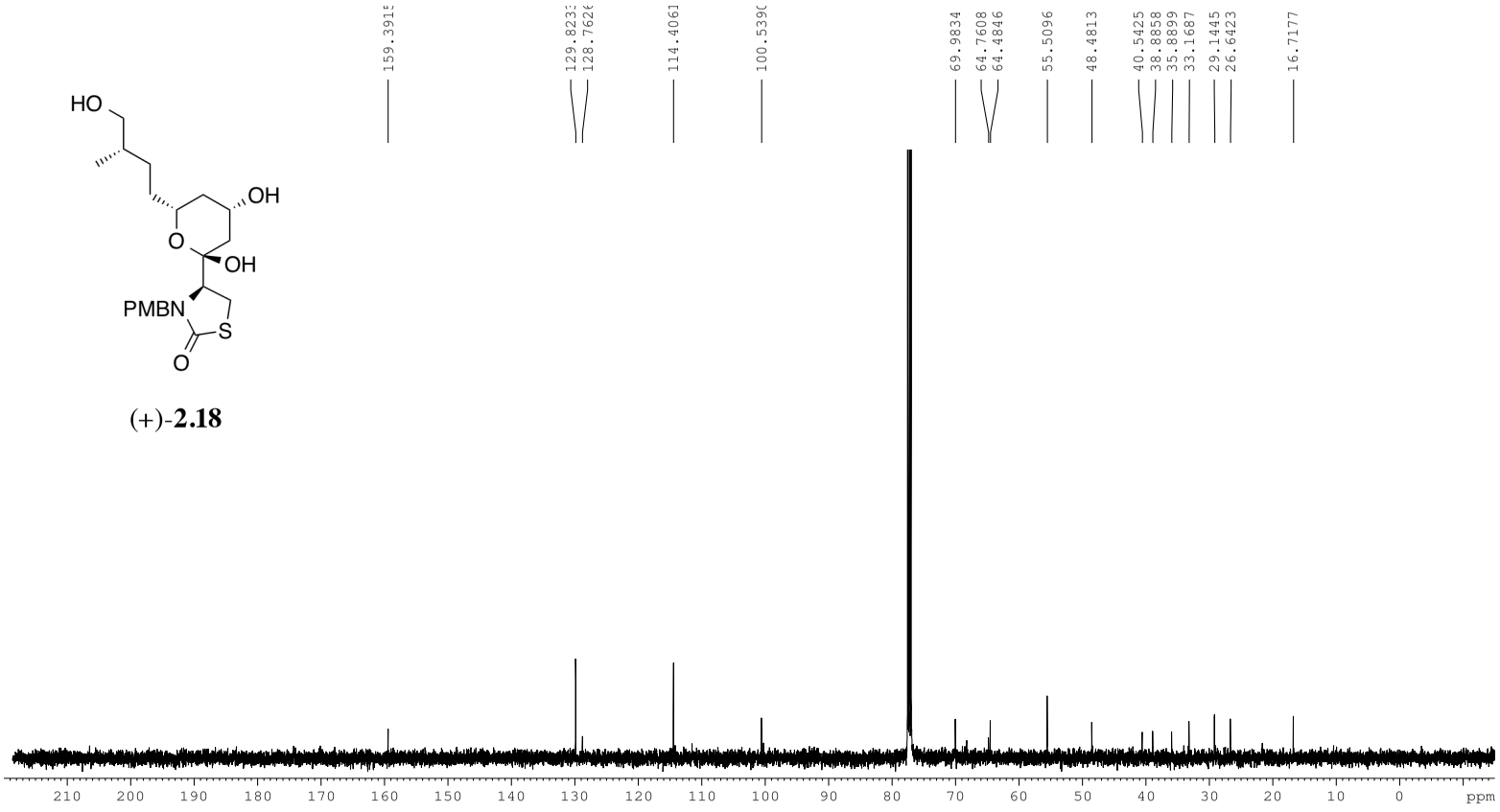

(+)-**2.18**

Figure A2.17. ^{1}H NMR Spectrum (500 MHz) of Compound (+)-**2.5** in $CDCl_3$

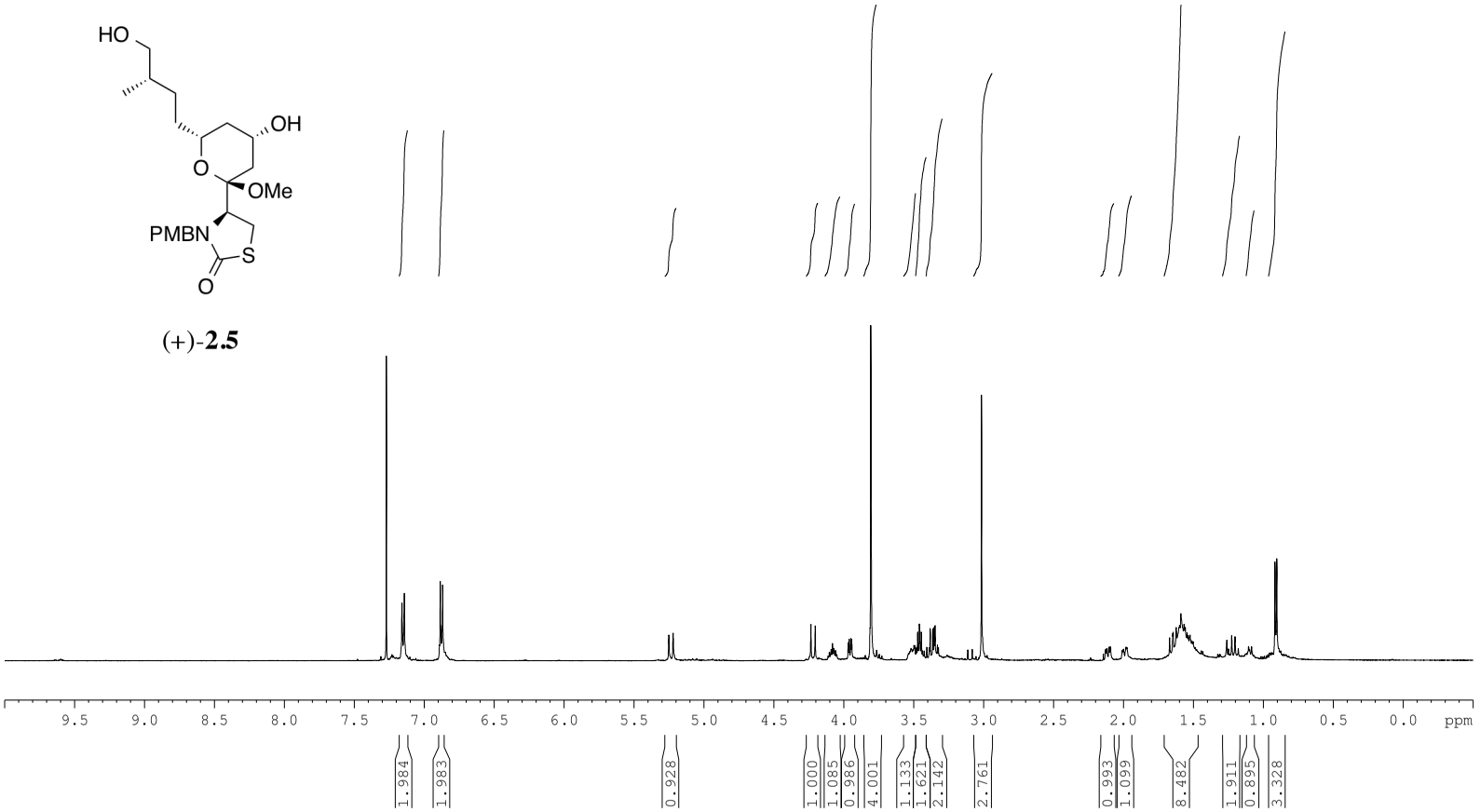

Figure A2.18. ^{13}C NMR Spectrum (125 MHz) of Compound (+)-**2.5** in $CDCl_3$

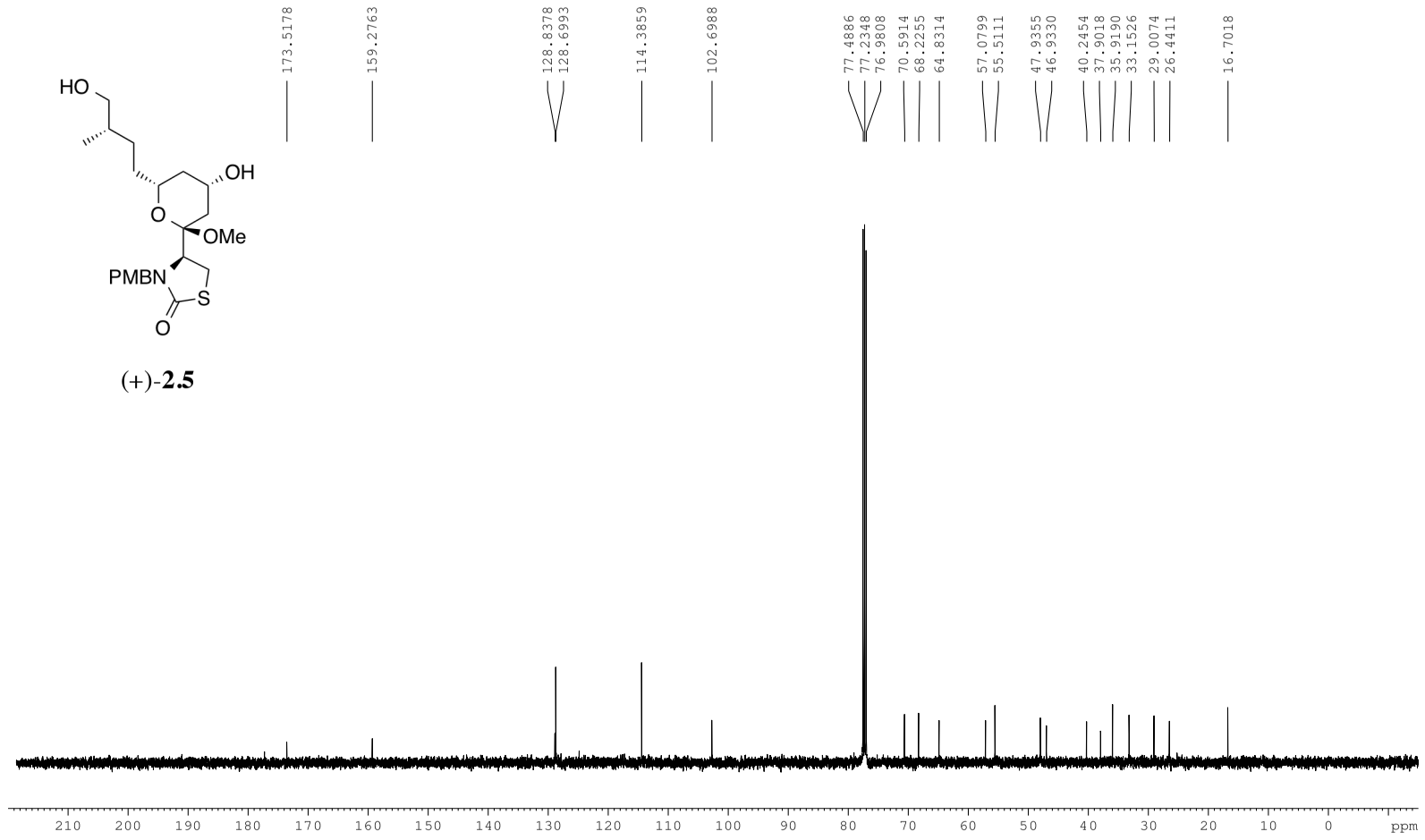

(+)-**2.5**

Figure A2.19. ^{1}H NMR Spectrum (500 MHz) of Compound (+)-**2.19** in $CDCl_3$

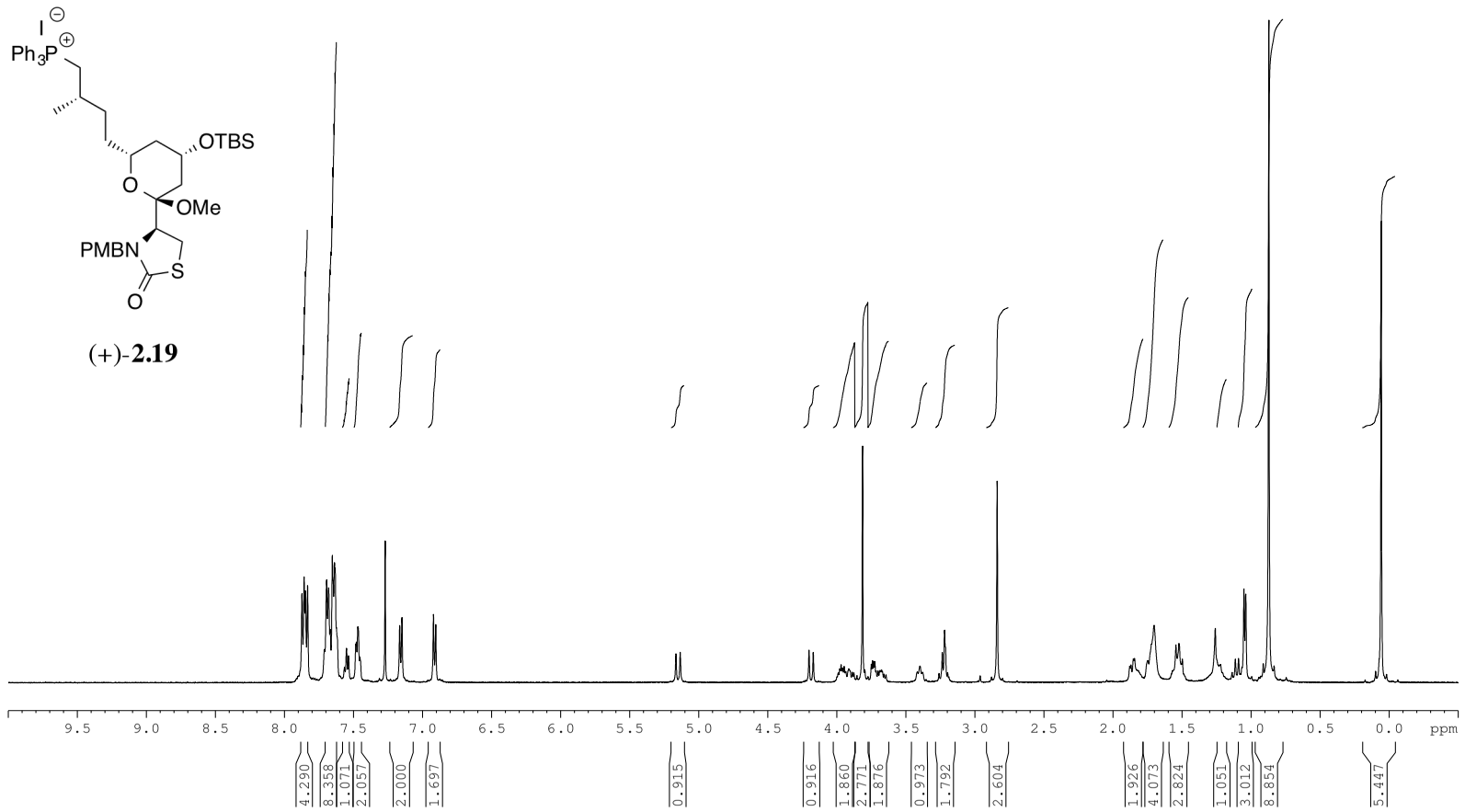

Figure A2.20. ^{13}C NMR Spectrum (125 MHz) of Compound (+)-**2.19** in $CDCl_3$

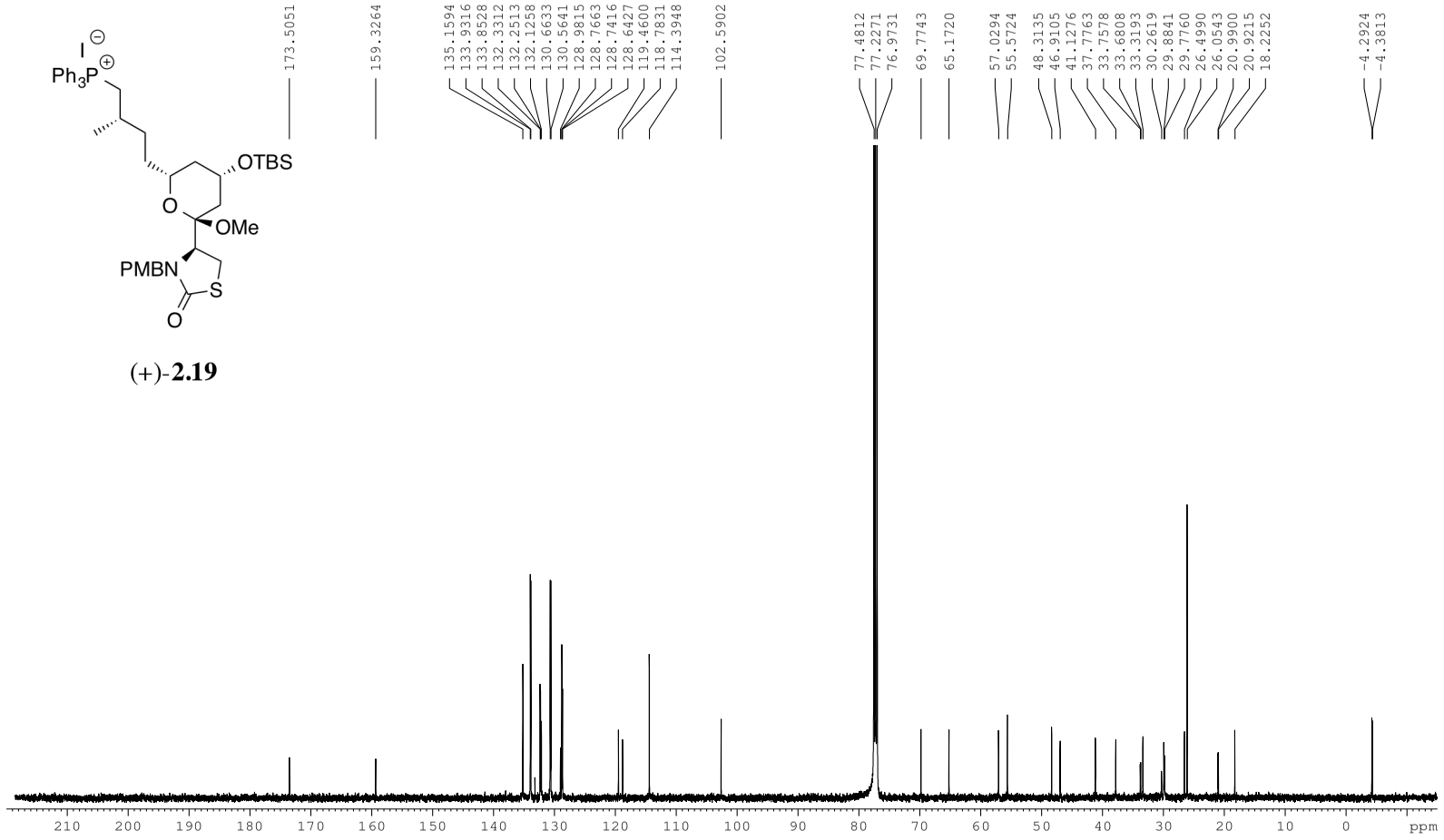

(+)-**2.19**

Figure A2.21. ^{1}H NMR Spectrum (500 MHz) of Compound (+)-**2.23** in $CDCl_3$

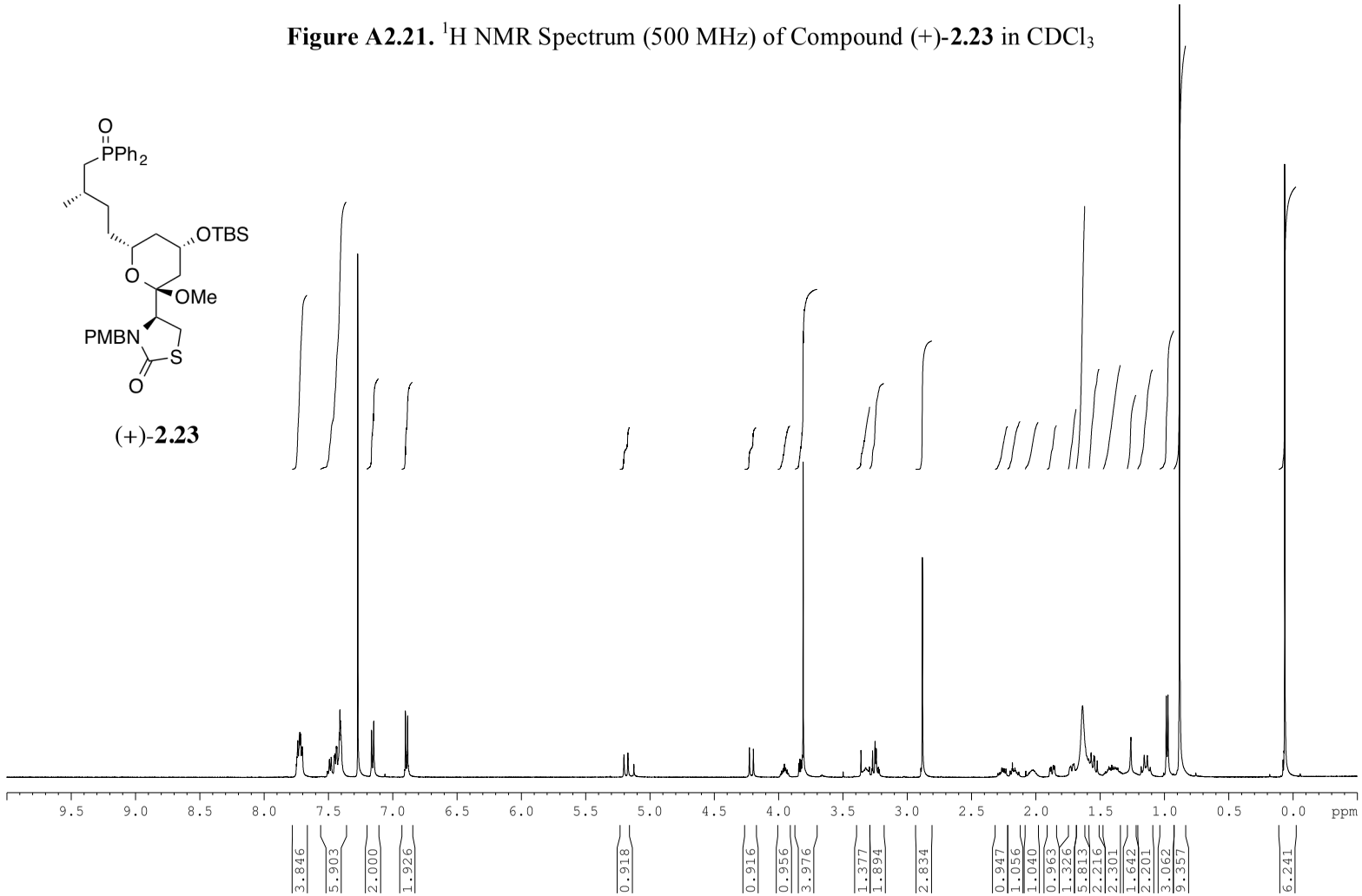

Figure A2.22. ^{13}C NMR Spectrum (125 MHz) of Compound (+)-**2.23** in $CDCl_3$

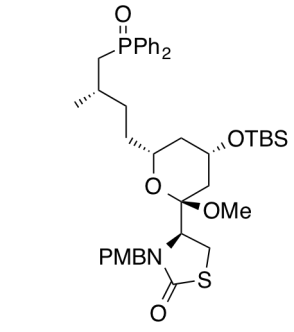

(+)-**2.23**

Figure A2.23. ^{1}H NMR Spectrum (500 MHz) of Compound (+)-**S4** in $CDCl_3$

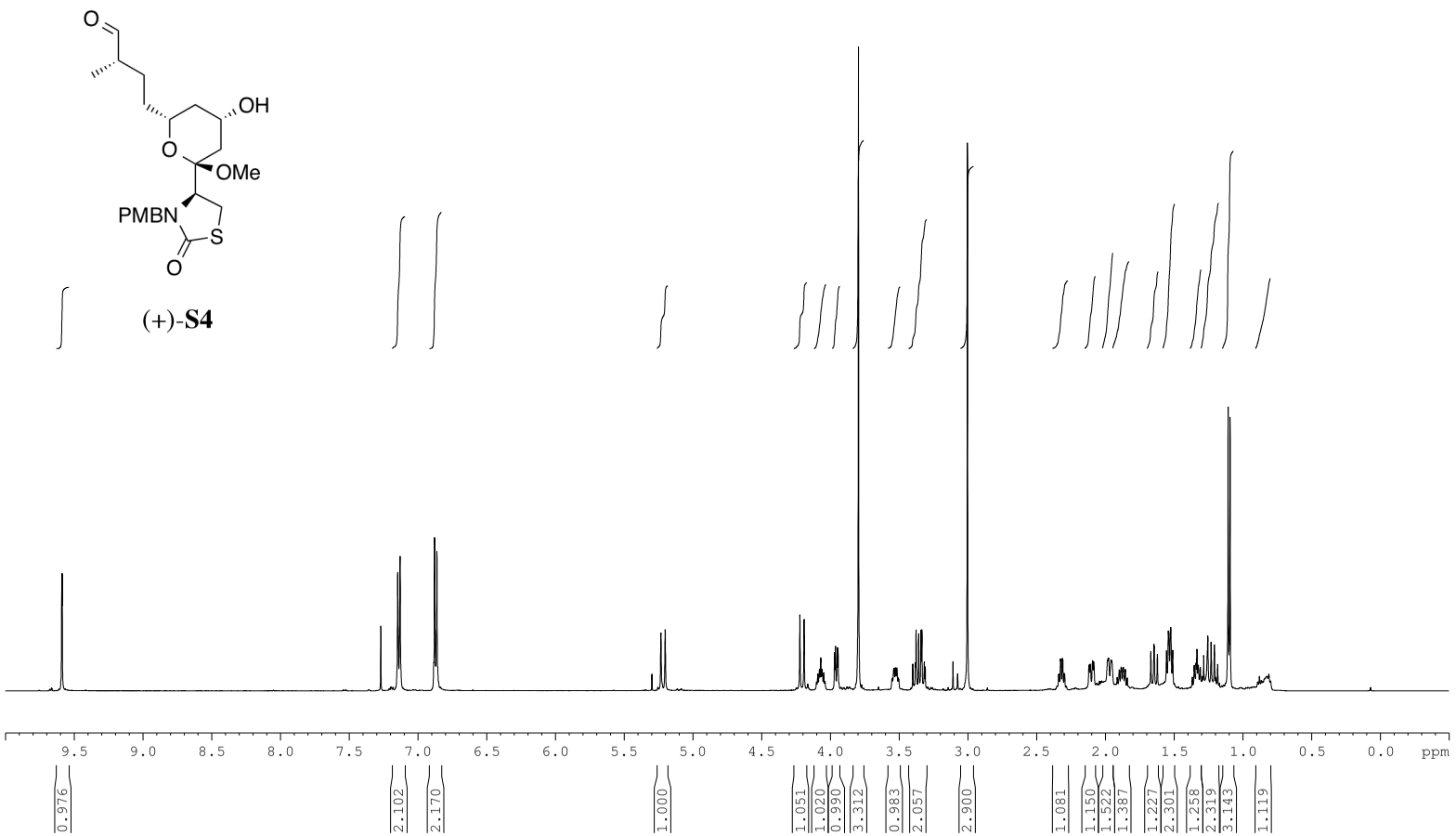

Figure A2.24. ^{13}C NMR Spectrum (125 MHz) of Compound (+)-**S4** in $CDCl_3$

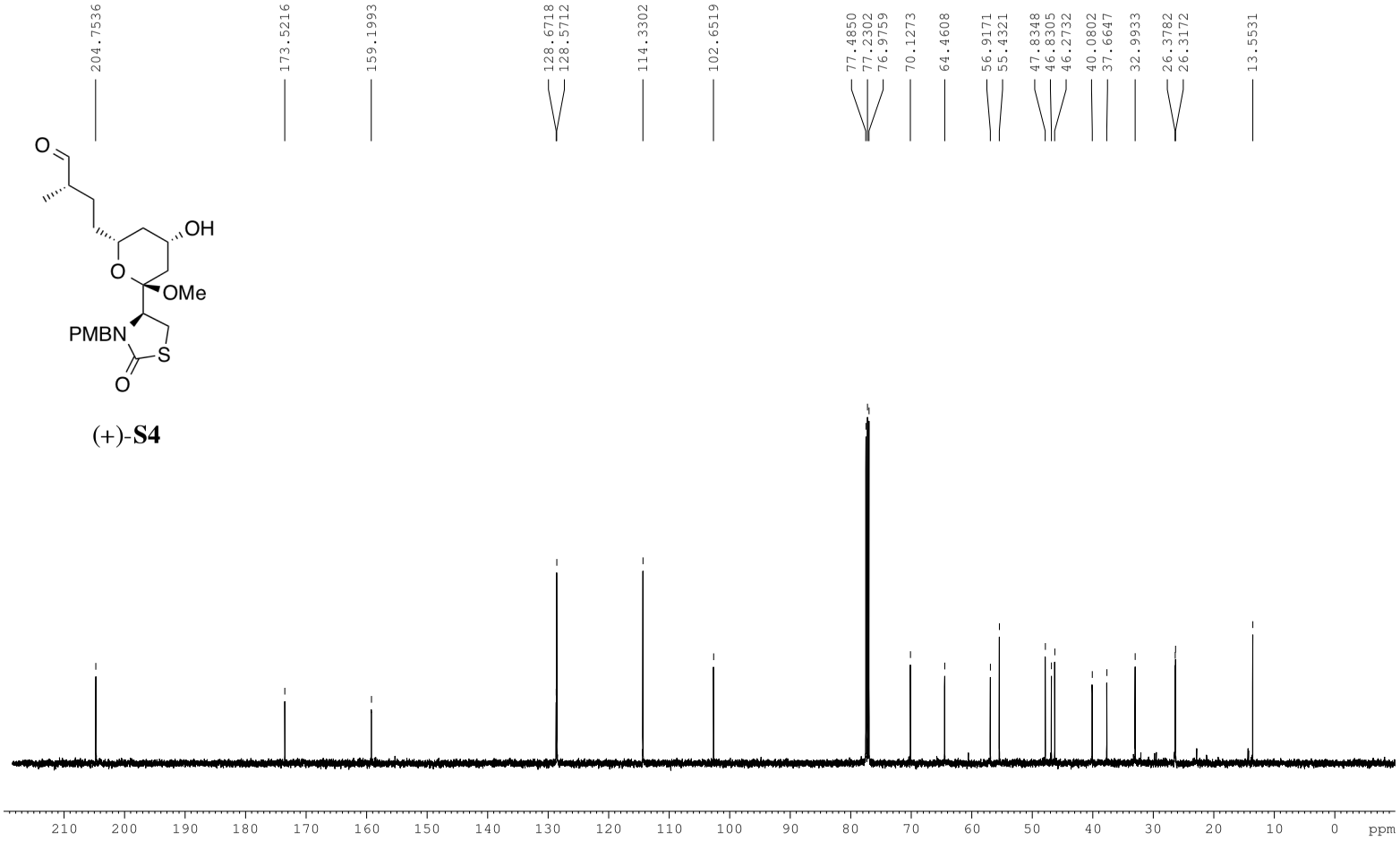

Figure A2.25. ^{1}H NMR Spectrum (500 MHz) of Compound (+)-**2.20** in $CDCl_3$

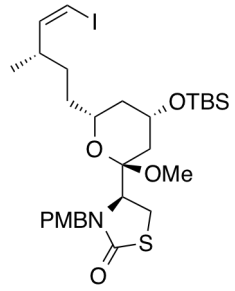

(+)-**2.20**

Figure A2.26. ^{13}C NMR Spectrum (125 MHz) of Compound (+)-**2.20** in $CDCl_3$

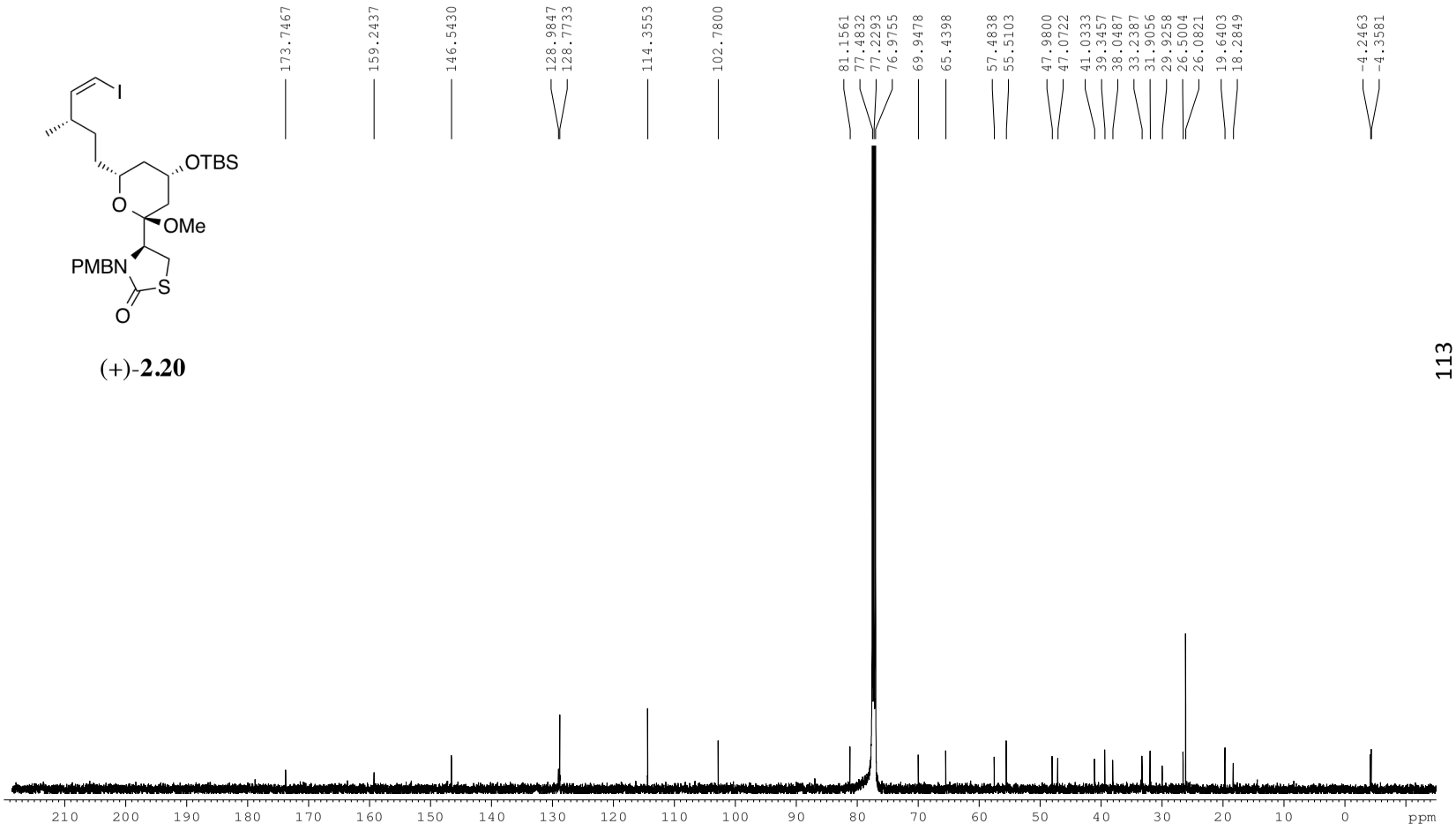

(+)-**2.20**

Figure A2.27. ^{1}H NMR Spectrum (500 MHz) of Compound (+)-**S5** in $CDCl_3$

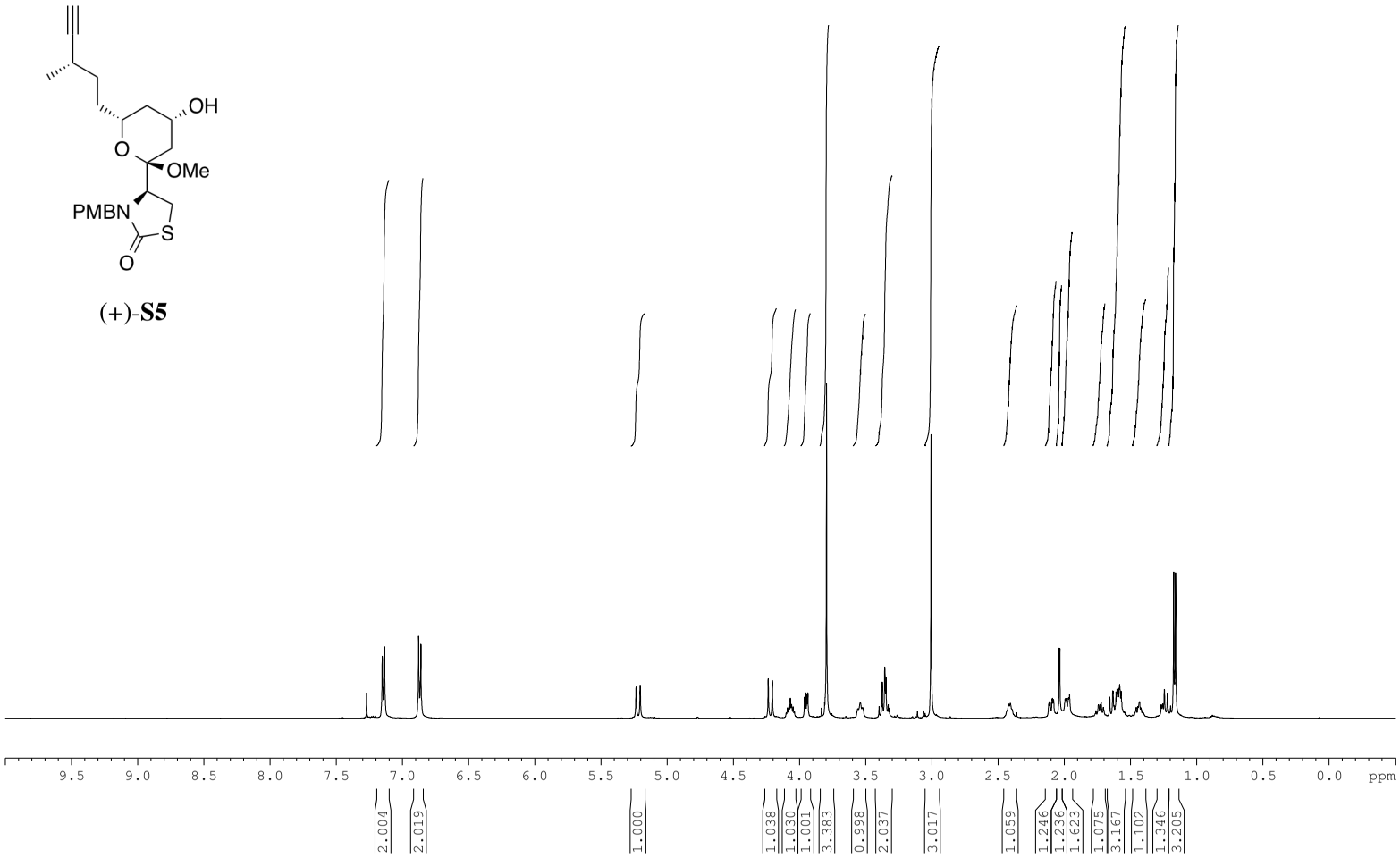

Figure A2.28. ^{13}C NMR Spectrum (125 MHz) of Compound (+)-**S5** in $CDCl_3$

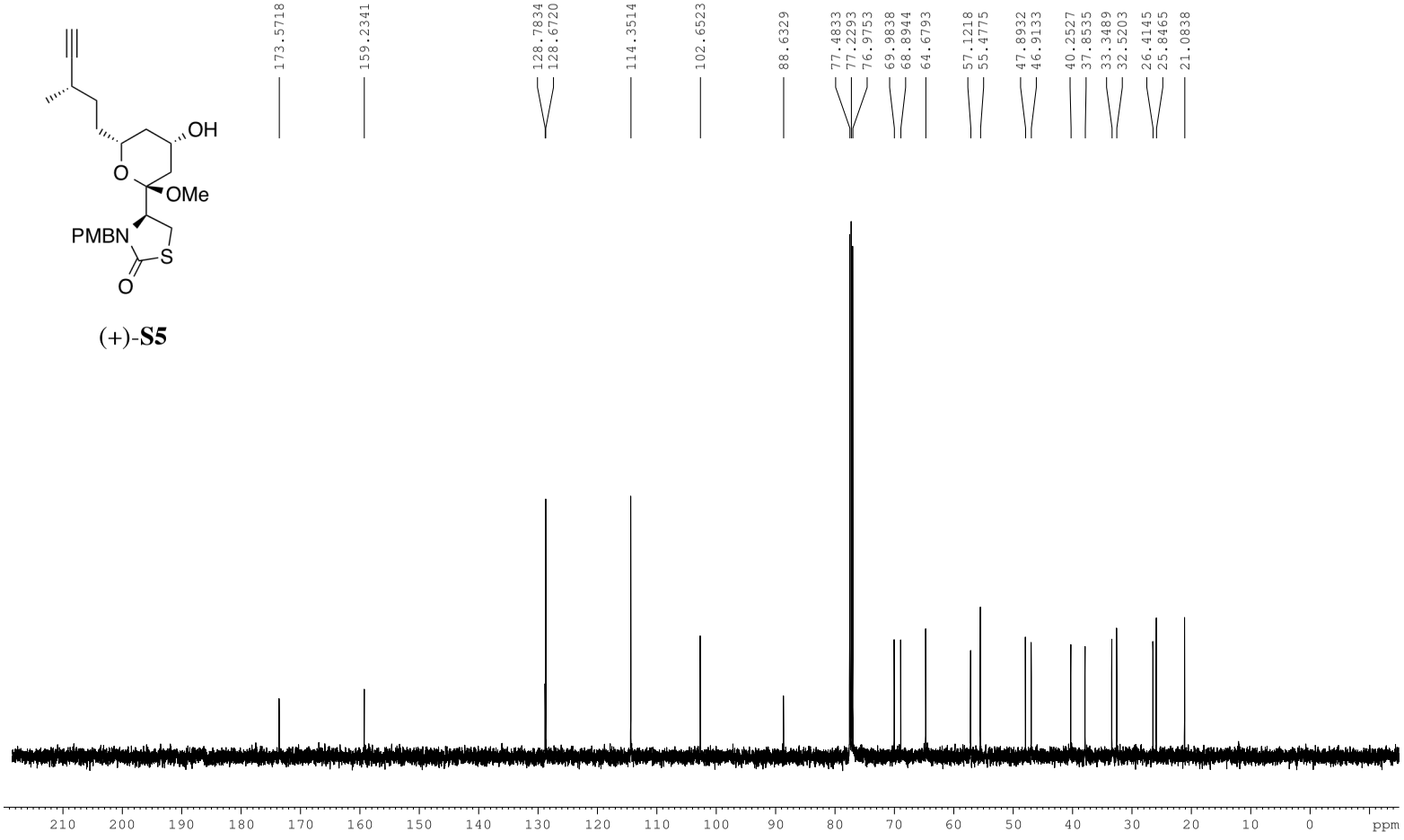

Figure A2.29. ^{1}H NMR Spectrum (500 MHz) of Compound (+)-**2.21** in $CDCl_3$

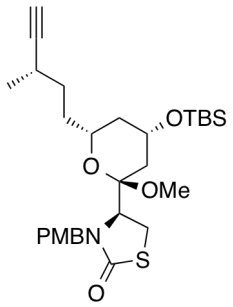

(+)-**2.21**

Figure A2.30. ^{13}C NMR Spectrum (125 MHz) of Compound (+)-**2.21** in $CDCl_3$

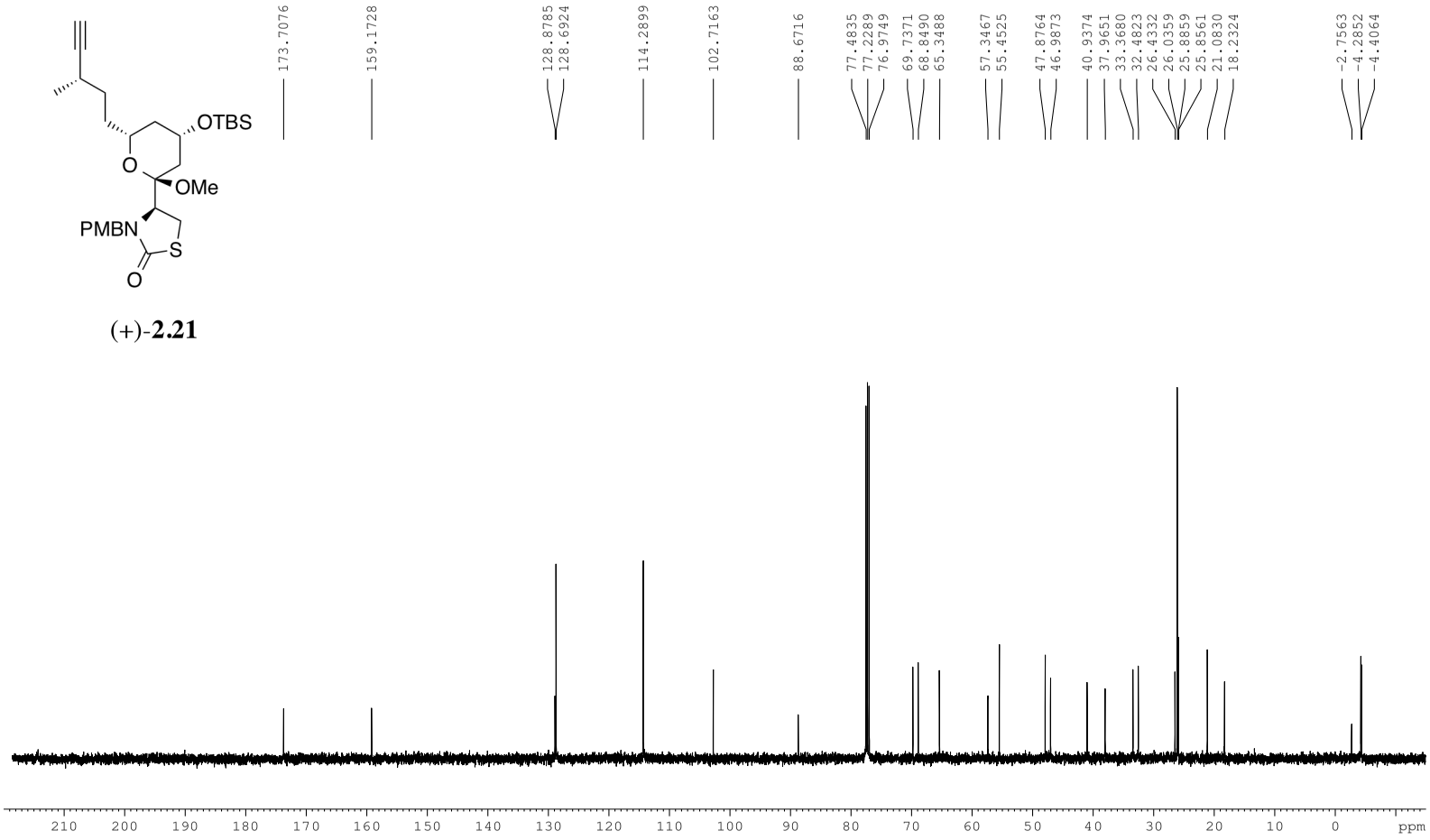

(+)-**2.21**

Figure A2.31. ^{1}H NMR Spectrum (500 MHz) of Compound (–)-**S6** in $CDCl_3$

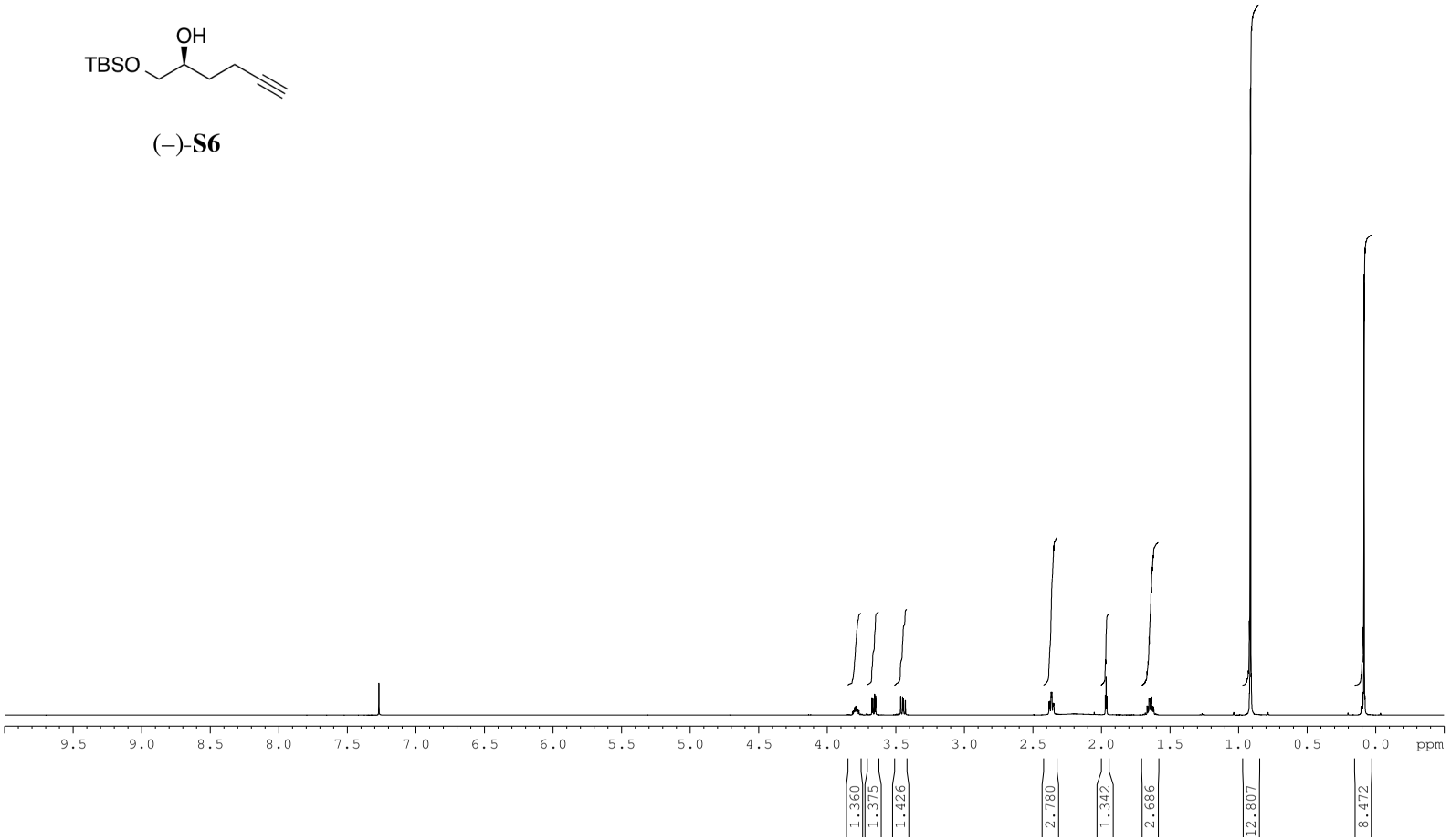

Figure A2.32. ^{13}C NMR Spectrum (125 MHz) of Compound (–)-**S6** in $CDCl_3$

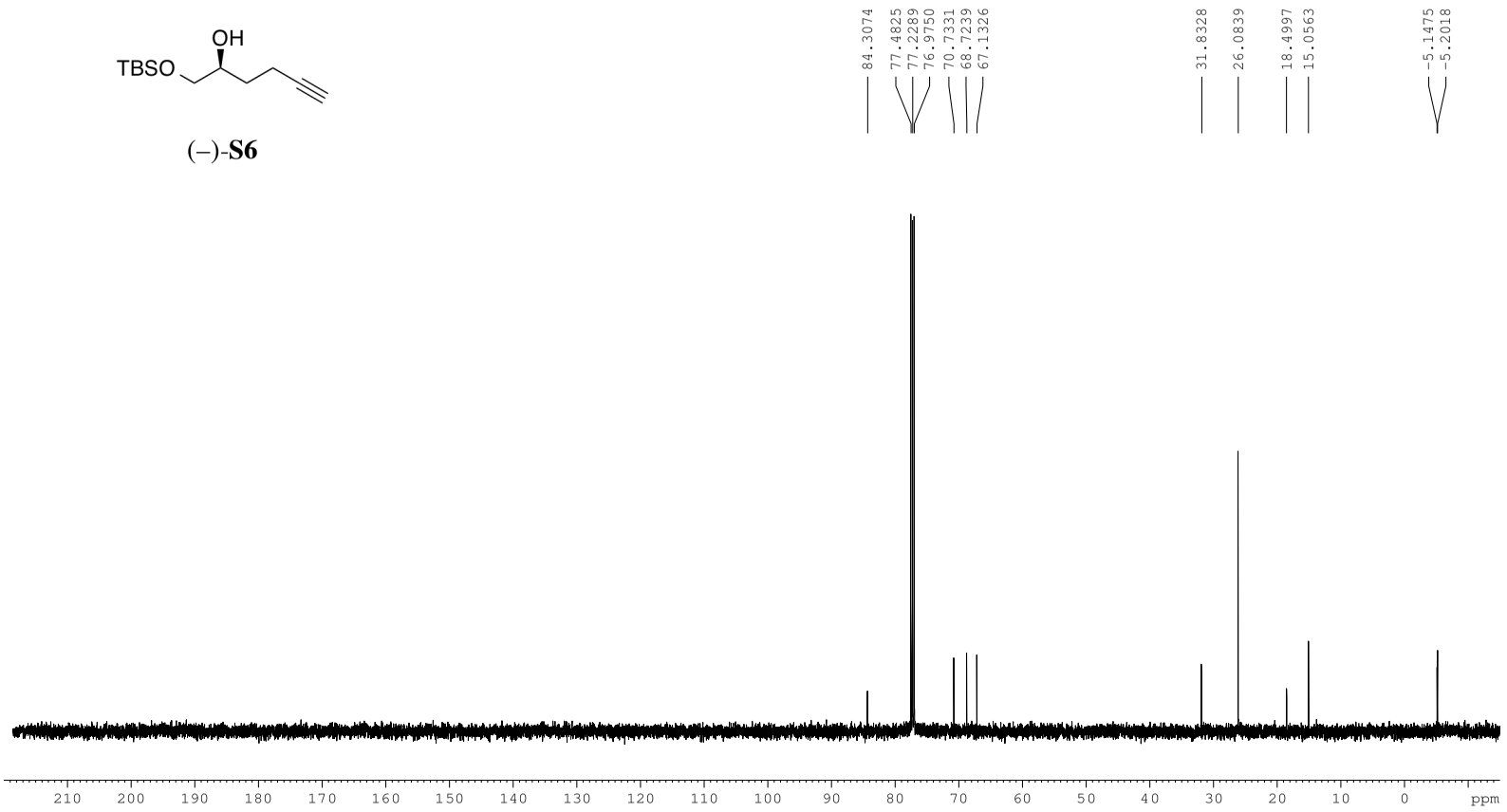

Figure A2.33. ^{1}H NMR Spectrum (500 MHz) of Compound (–)-**2.27** in $CDCl_3$

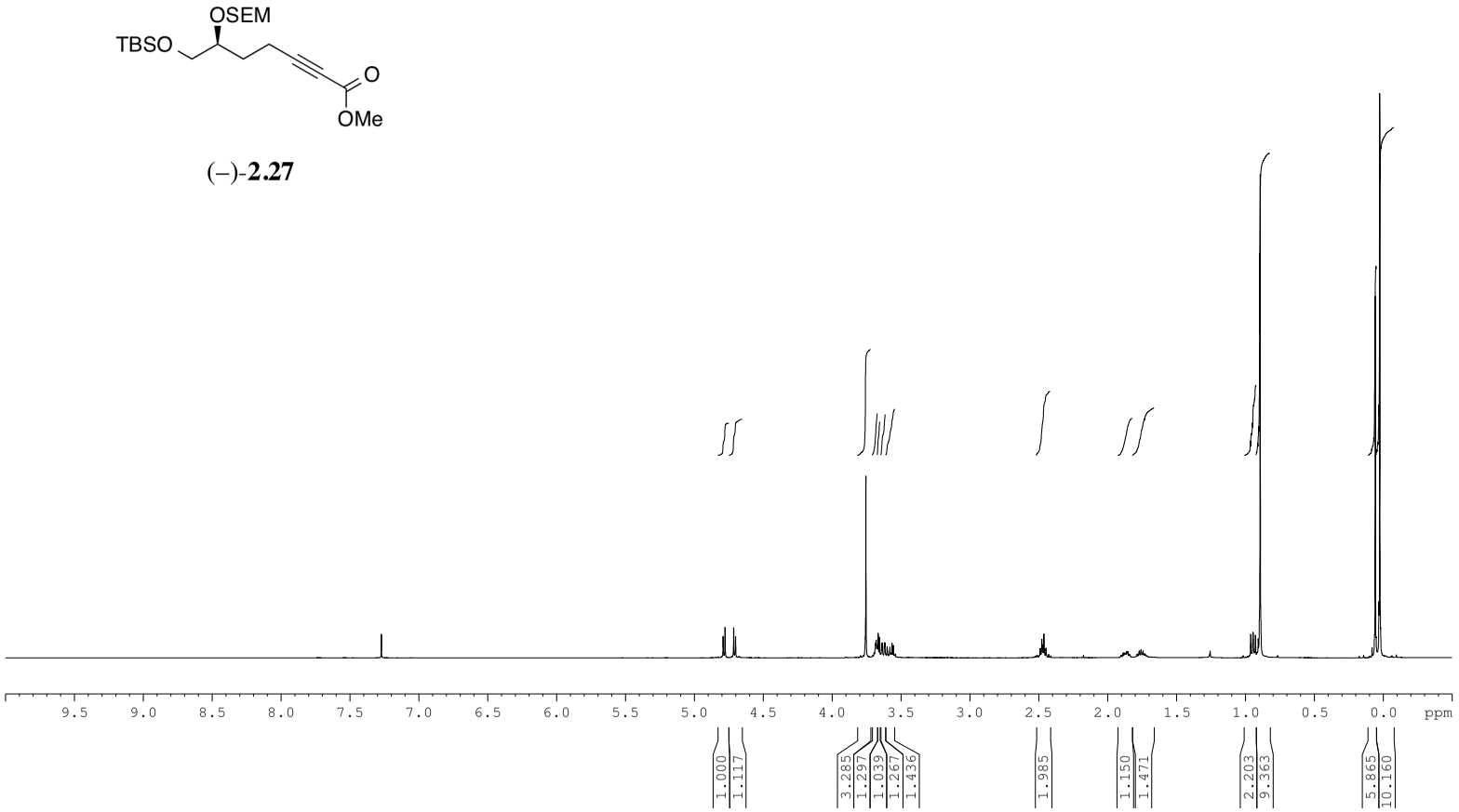

Figure A2.34. ^{13}C NMR Spectrum (125 MHz) of Compound (–)-**2.27** in $CDCl_3$

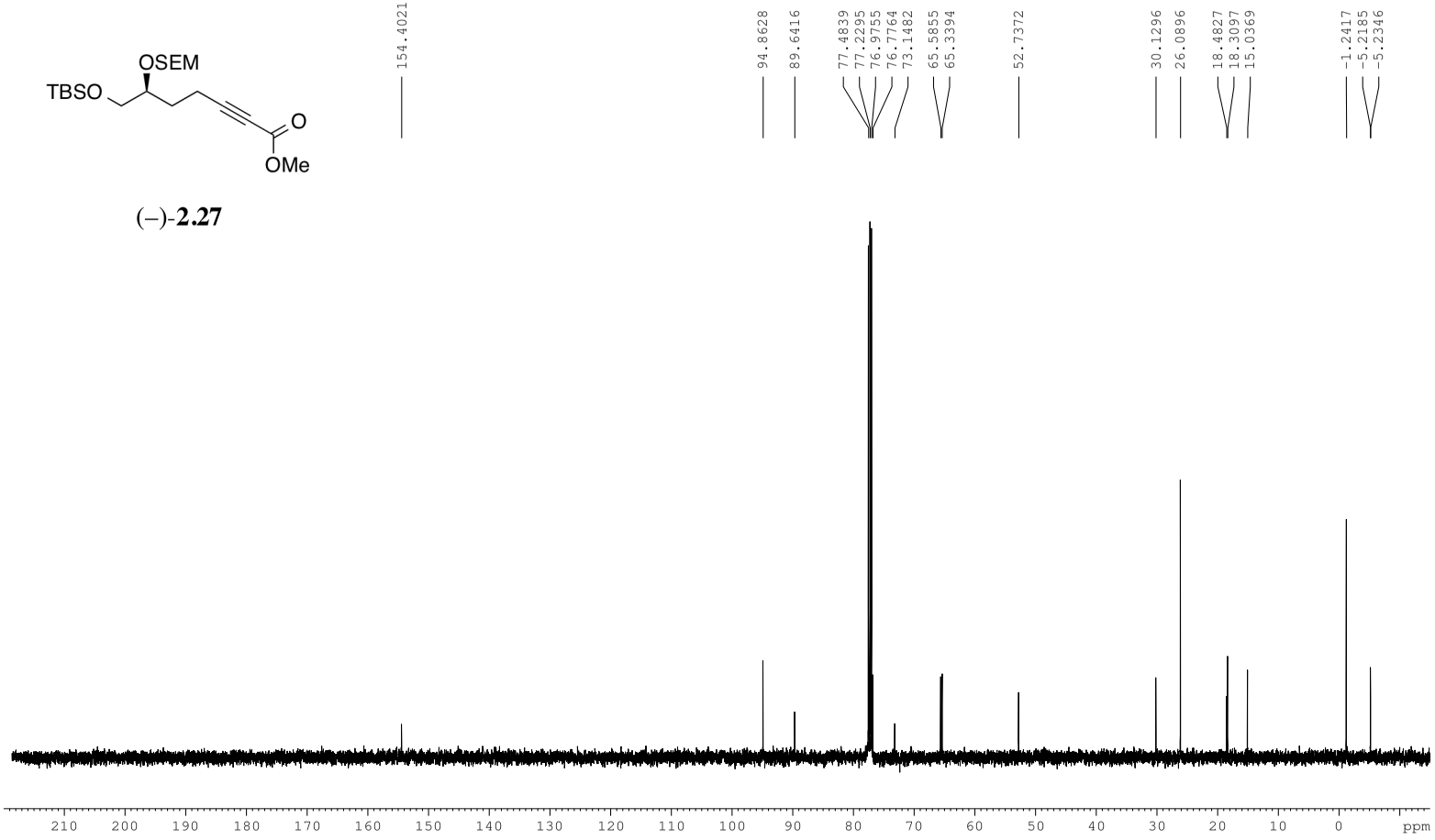

Figure A2.35. ^{1}H NMR Spectrum (500 MHz) of Compound (–)-**S7** in $CDCl_3$

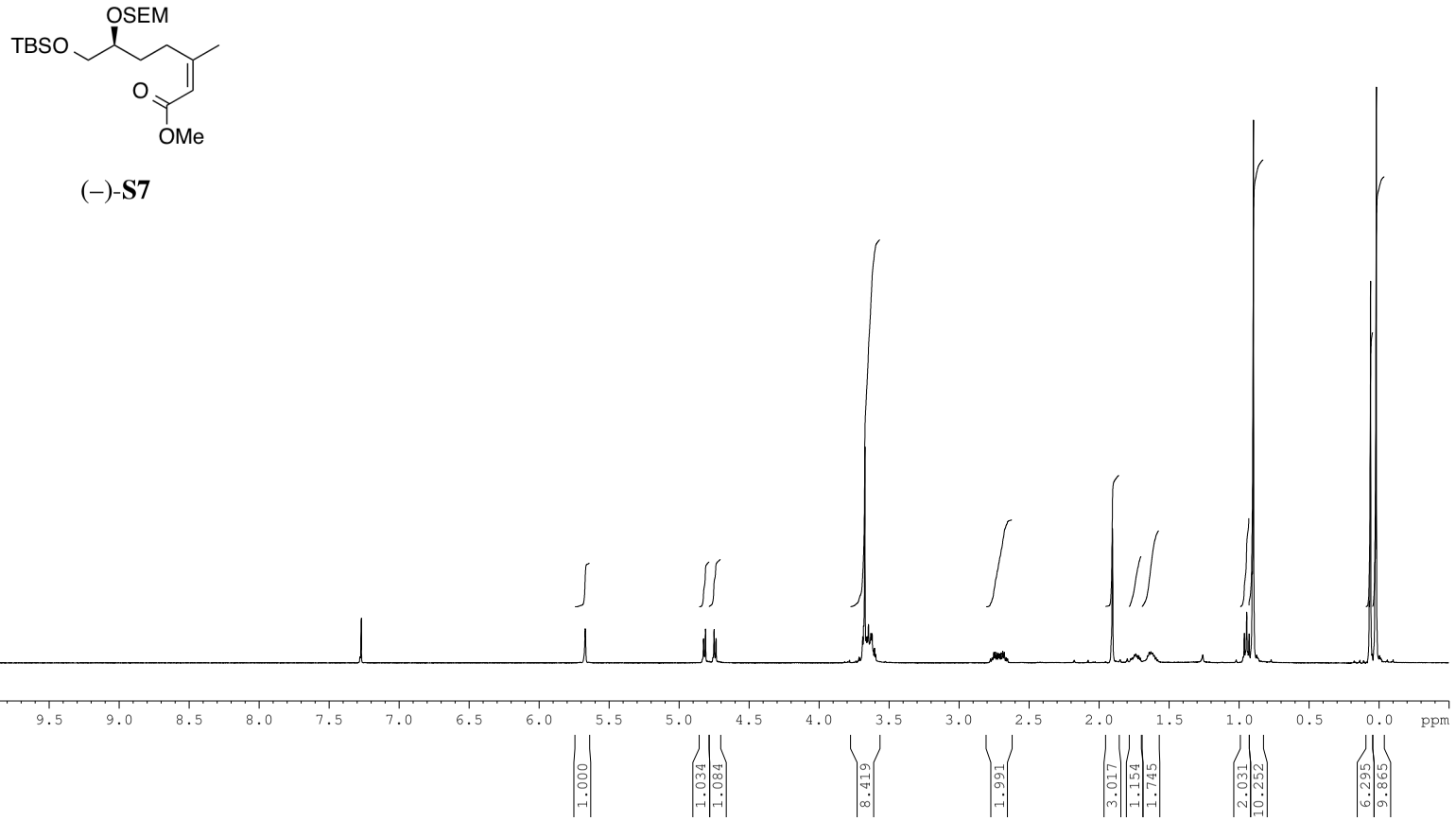

Figure A2.36. ^{13}C NMR Spectrum (125 MHz) of Compound (–)-**S7** in $CDCl_3$

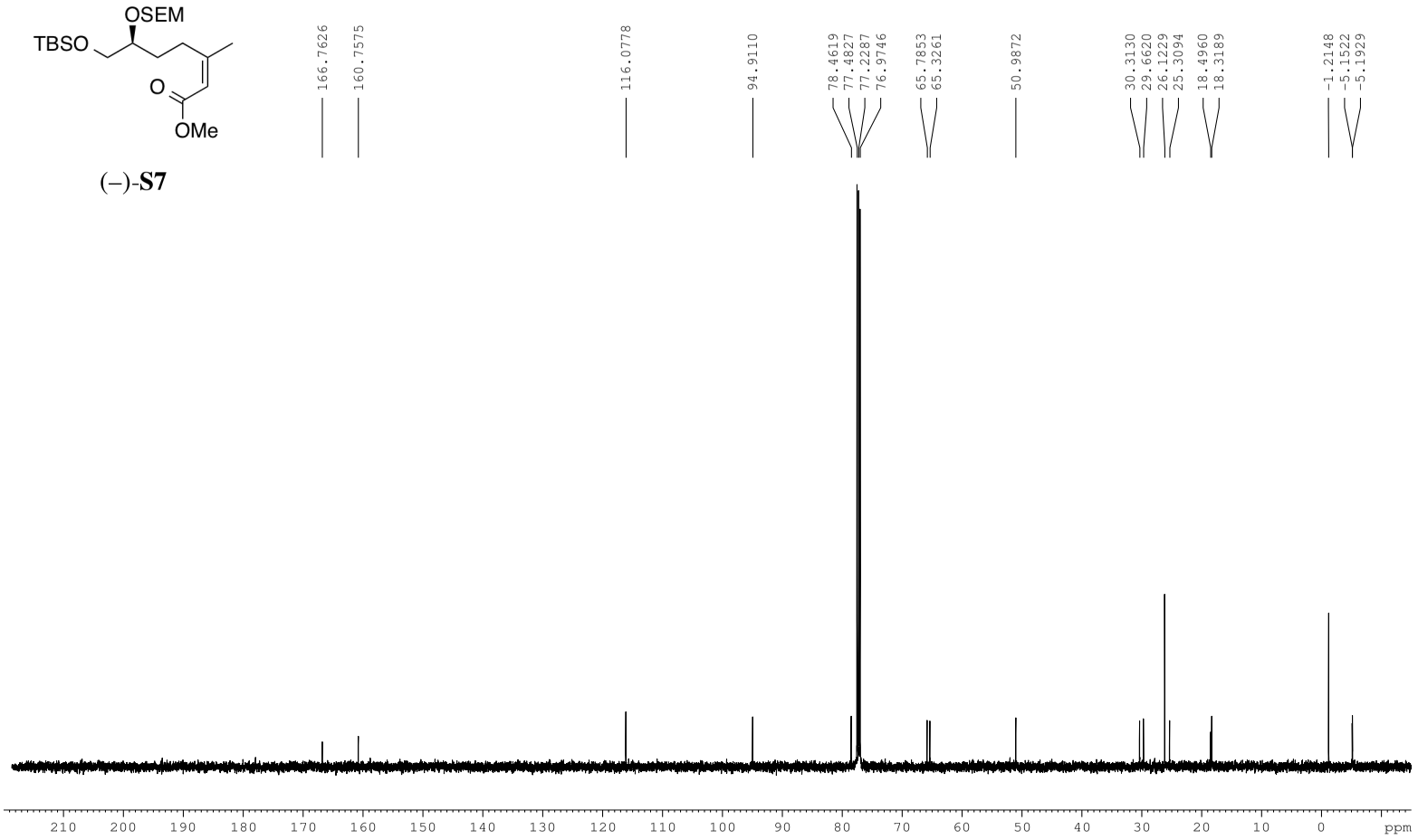

Figure A2.37. ^{1}H NMR Spectrum (500 MHz) of Compound (+)-**S8** in $CDCl_3$

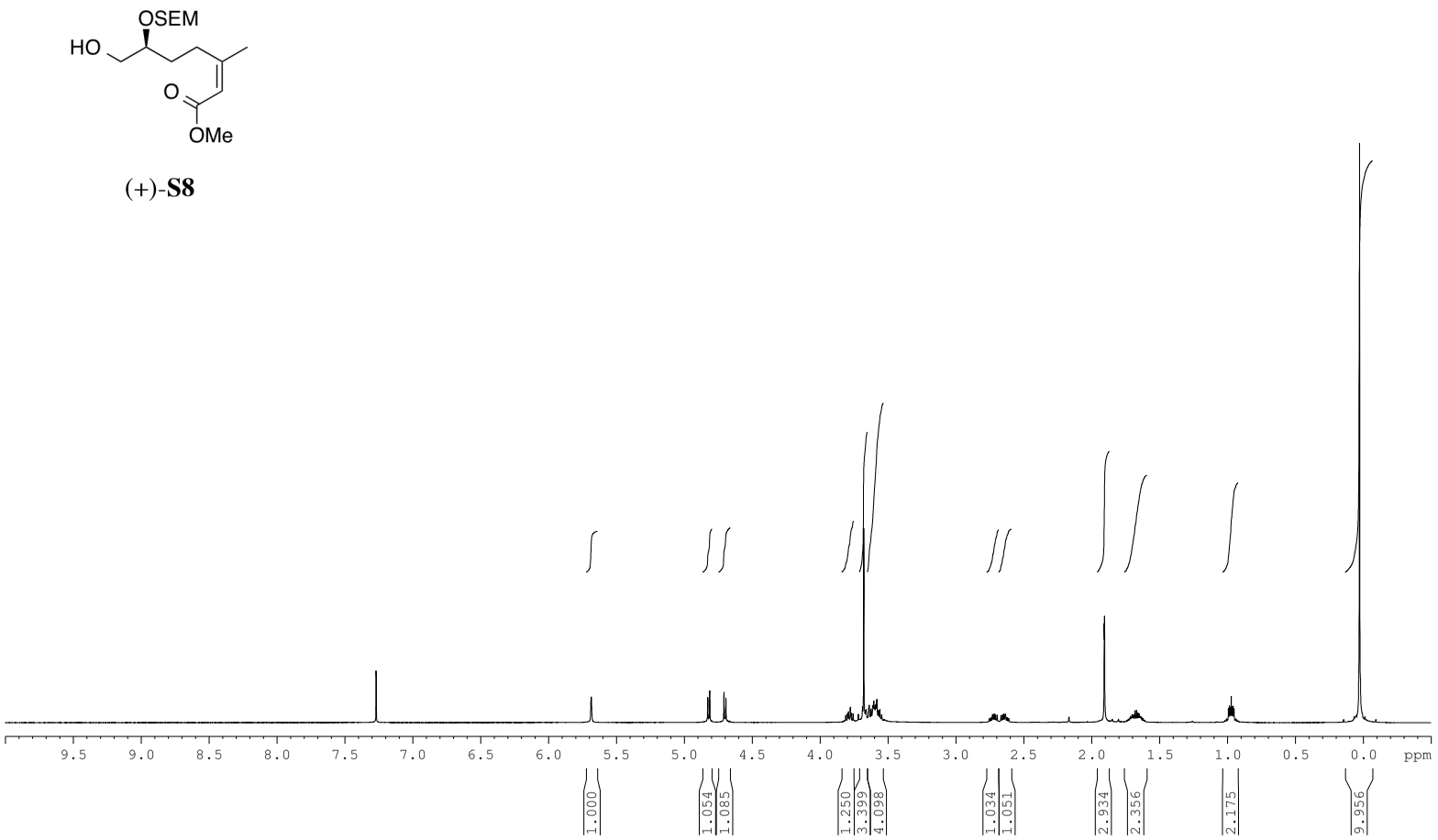

(+)-**S8**

Figure A2.38. ^{13}C NMR Spectrum (125 MHz) of Compound (+)-**S8** in $CDCl_3$

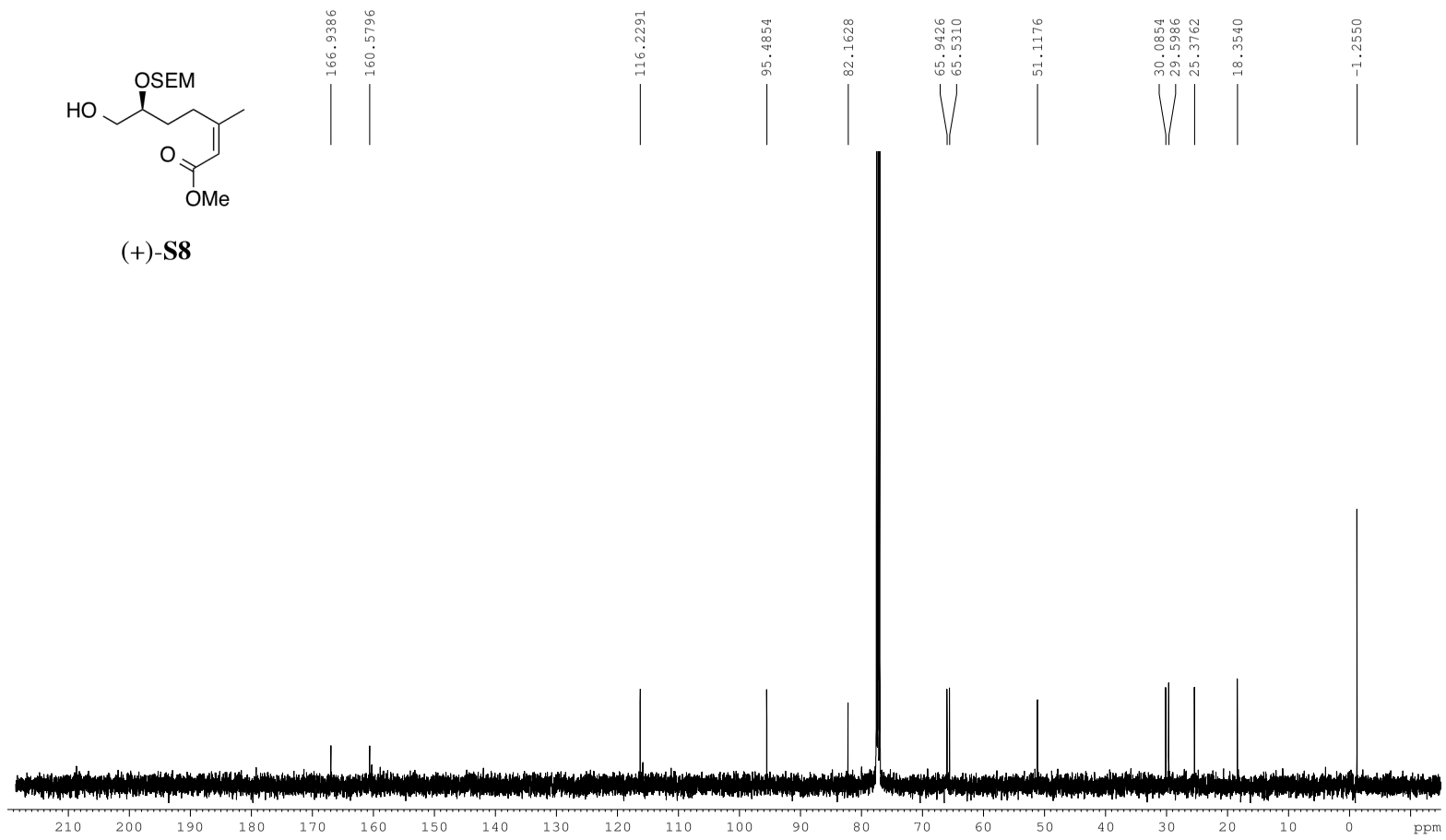

(+)-**S8**

Figure A2.39. ^{1}H NMR Spectrum (500 MHz) of Compound (+)-**2.25** in $CDCl_3$

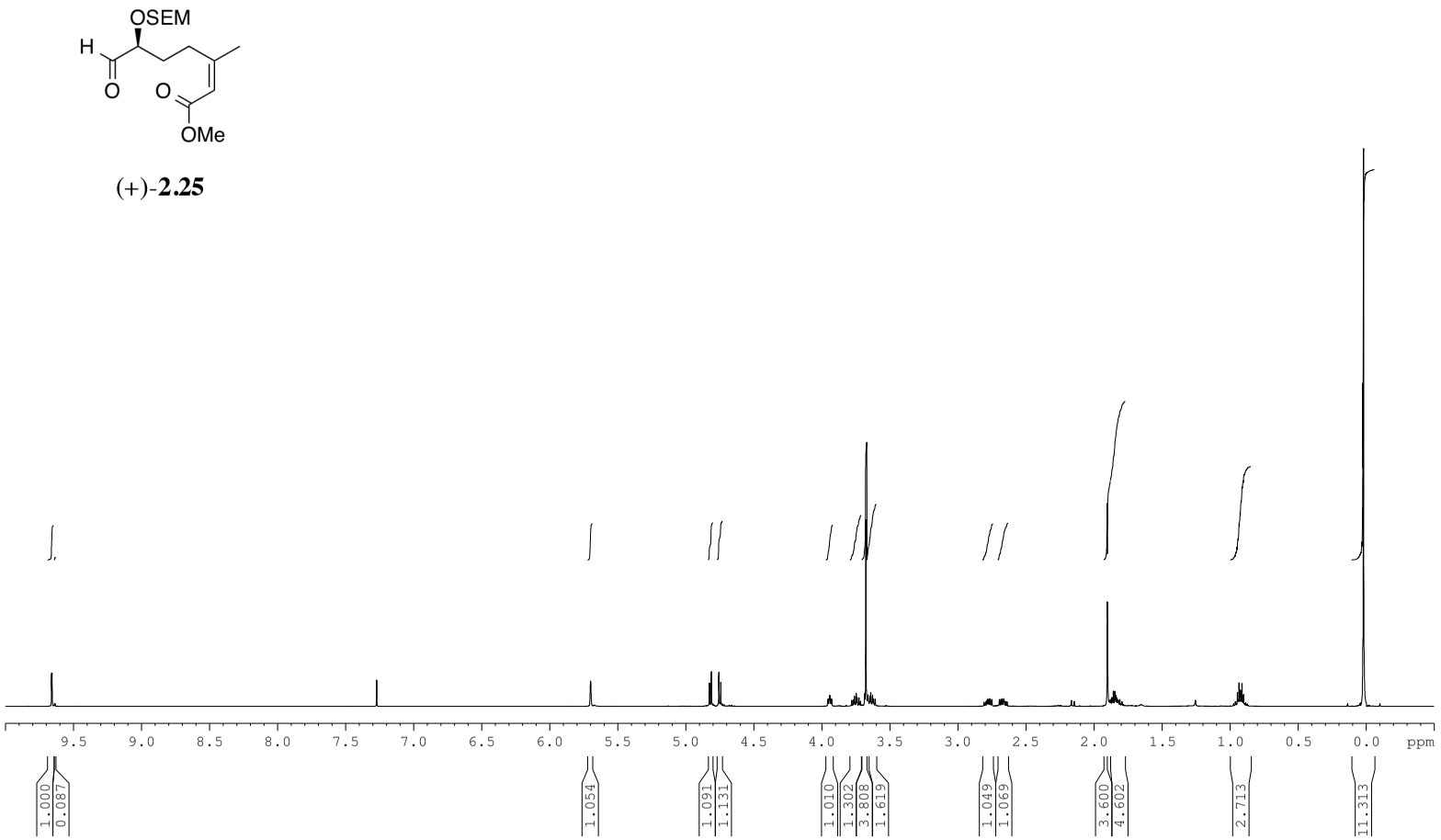

Figure A2.40. ^{13}C NMR Spectrum (125 MHz) of Compound (+)-**2.25** in $CDCl_3$

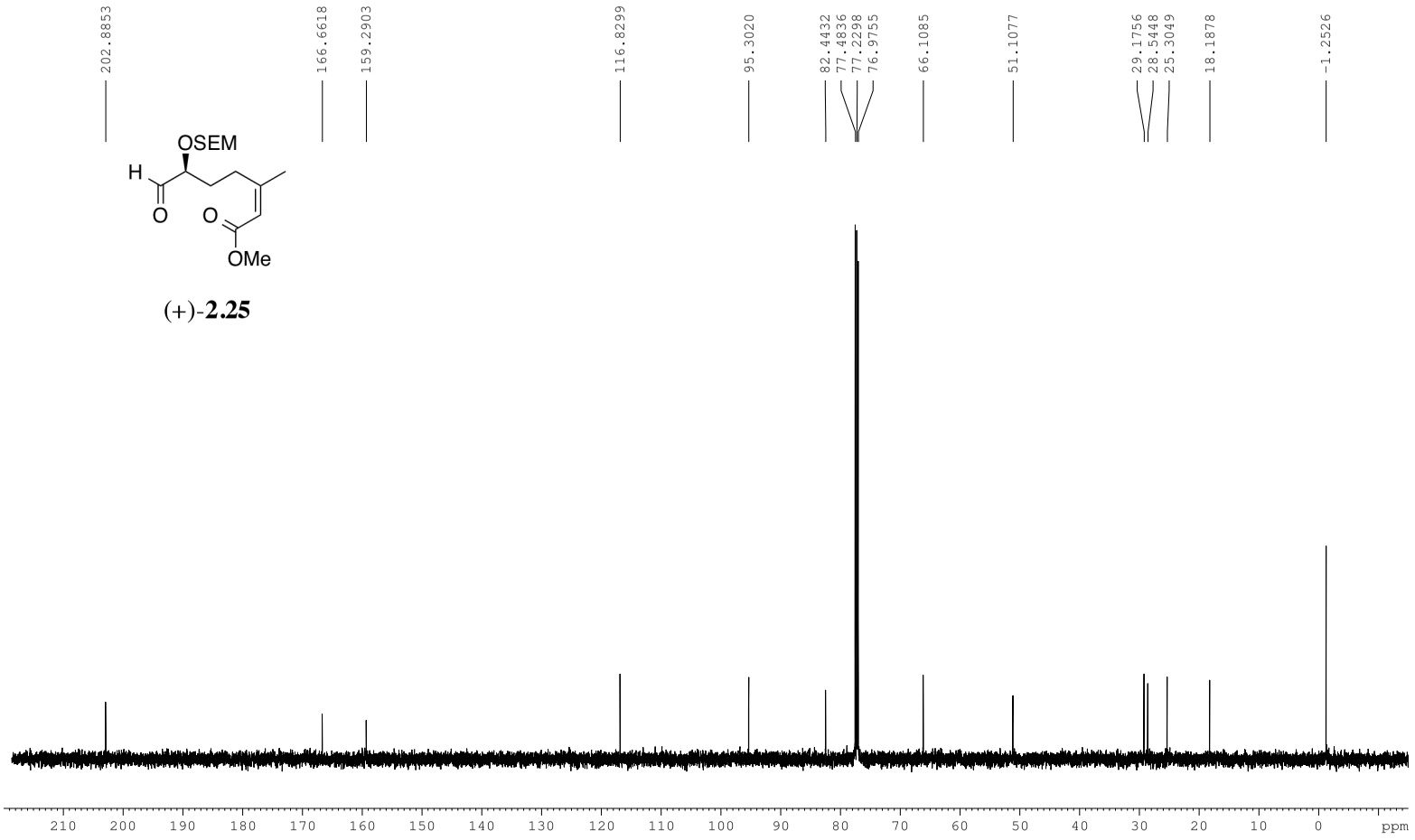

Figure A2.41. ^{1}H NMR Spectrum (500 MHz) of Compound (+)-**2.28** in $CDCl_3$

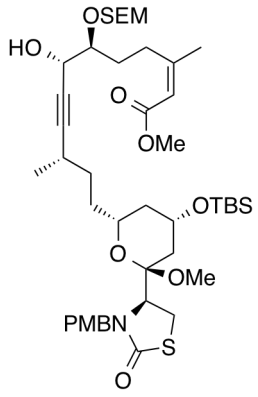

(+)-**2.28**

Figure A2.42. ^{13}C NMR Spectrum (125 MHz) of Compound (+)-**2.28** in $CDCl_3$

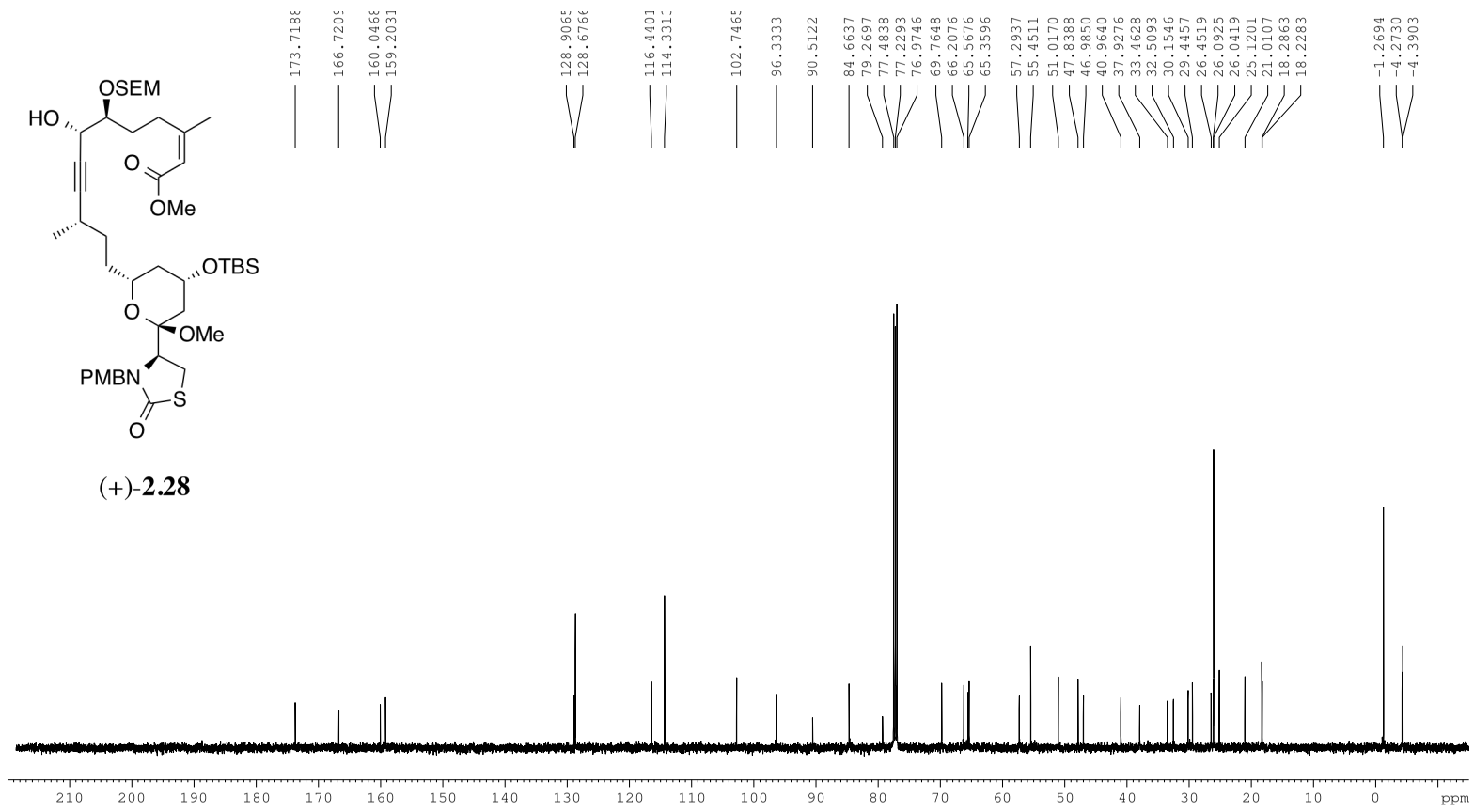

Figure A2.43. ^{1}H NMR Spectrum (500 MHz) of Compound (+)-**S9** in $CDCl_3$

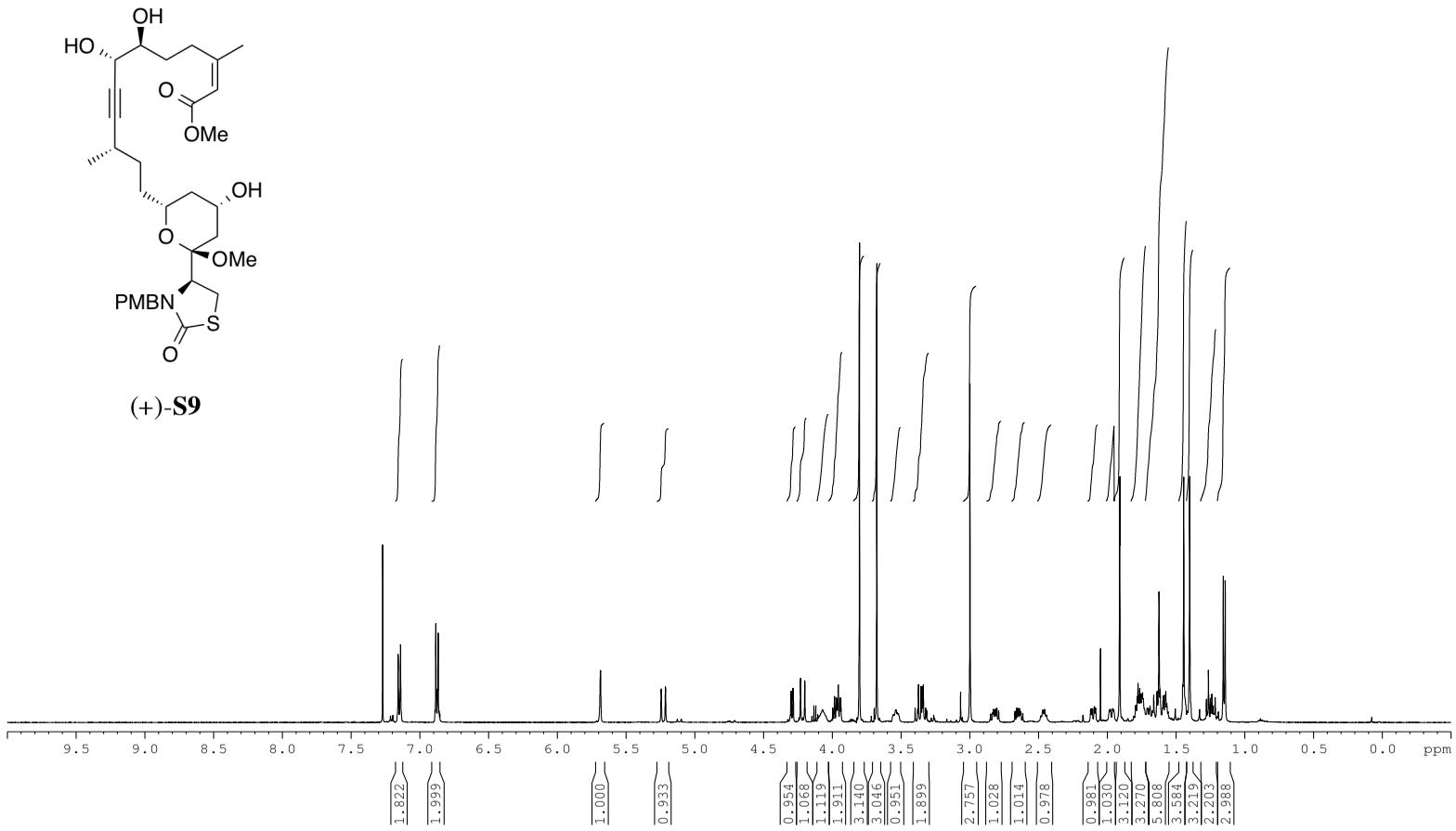

Figure A2.44. ^{13}C NMR Spectrum (125 MHz) of Compound (+)-**S9** in $CDCl_3$

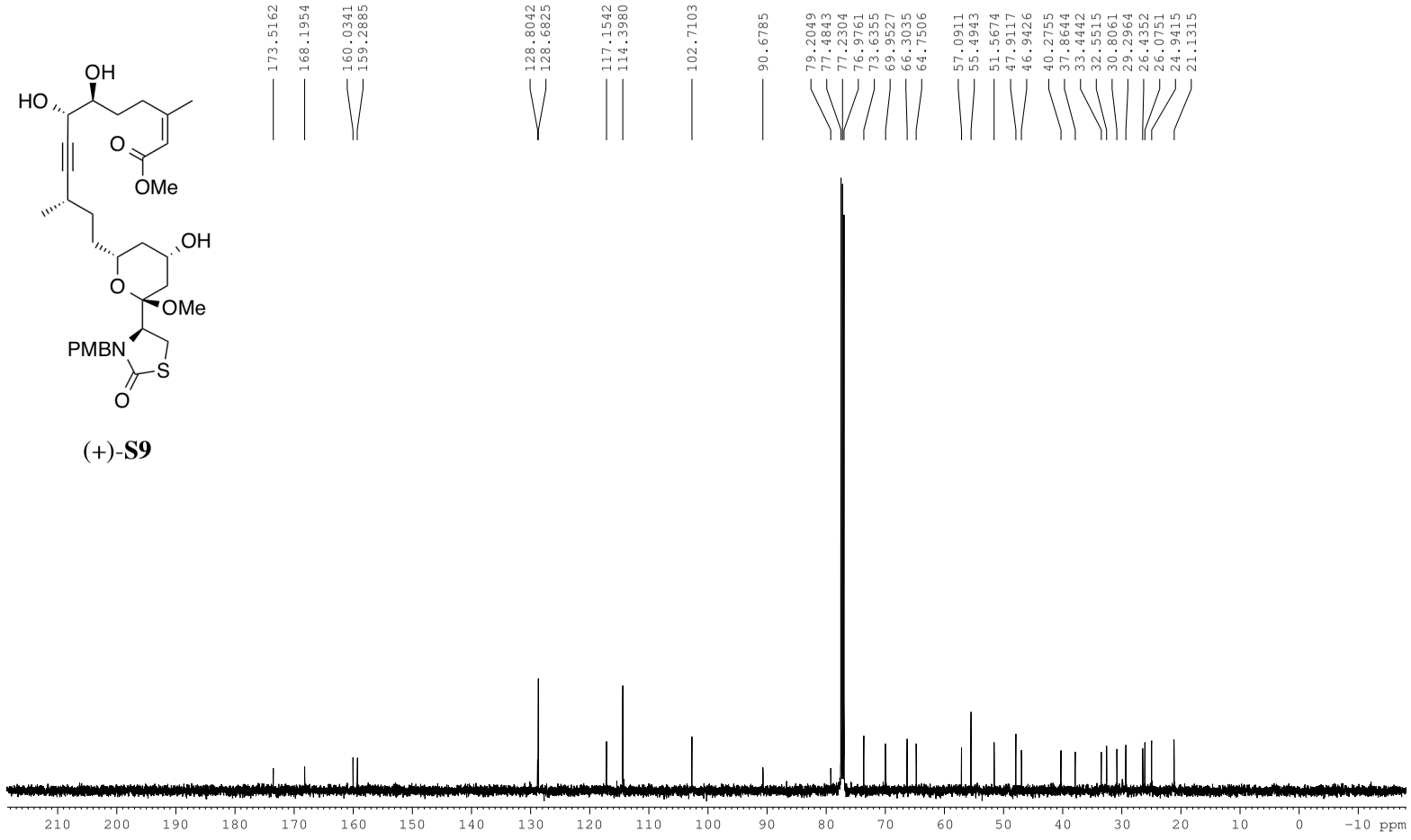

(+)-**S9**

Figure A2.45. ^{1}H NMR Spectrum (500 MHz) of Compound (+)-**2.29** in $CDCl_3$

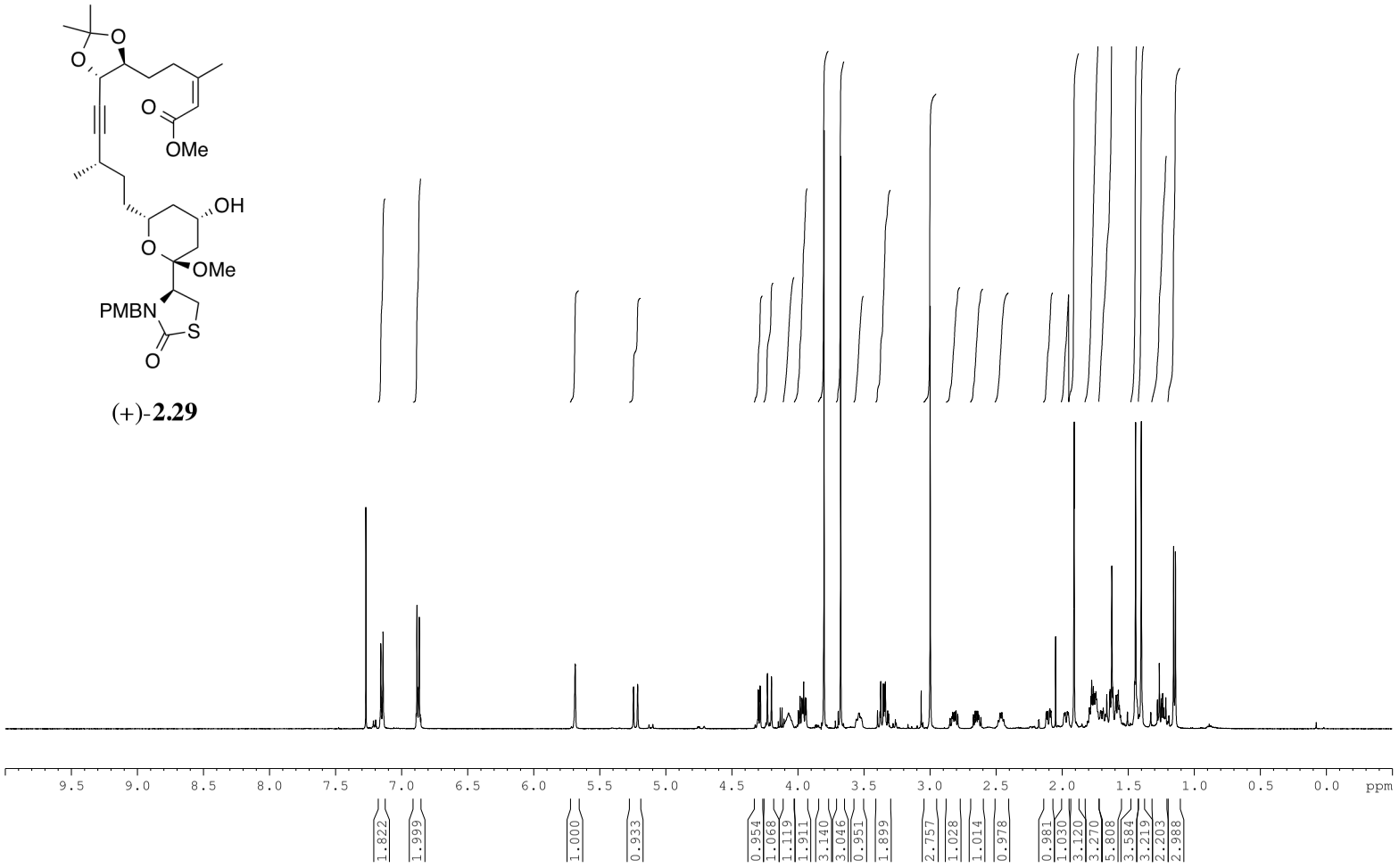

(+)-**2.29**

Figure A2.46. ^{13}C NMR Spectrum (125 MHz) of Compound (+)-**2.29** in $CDCl_3$

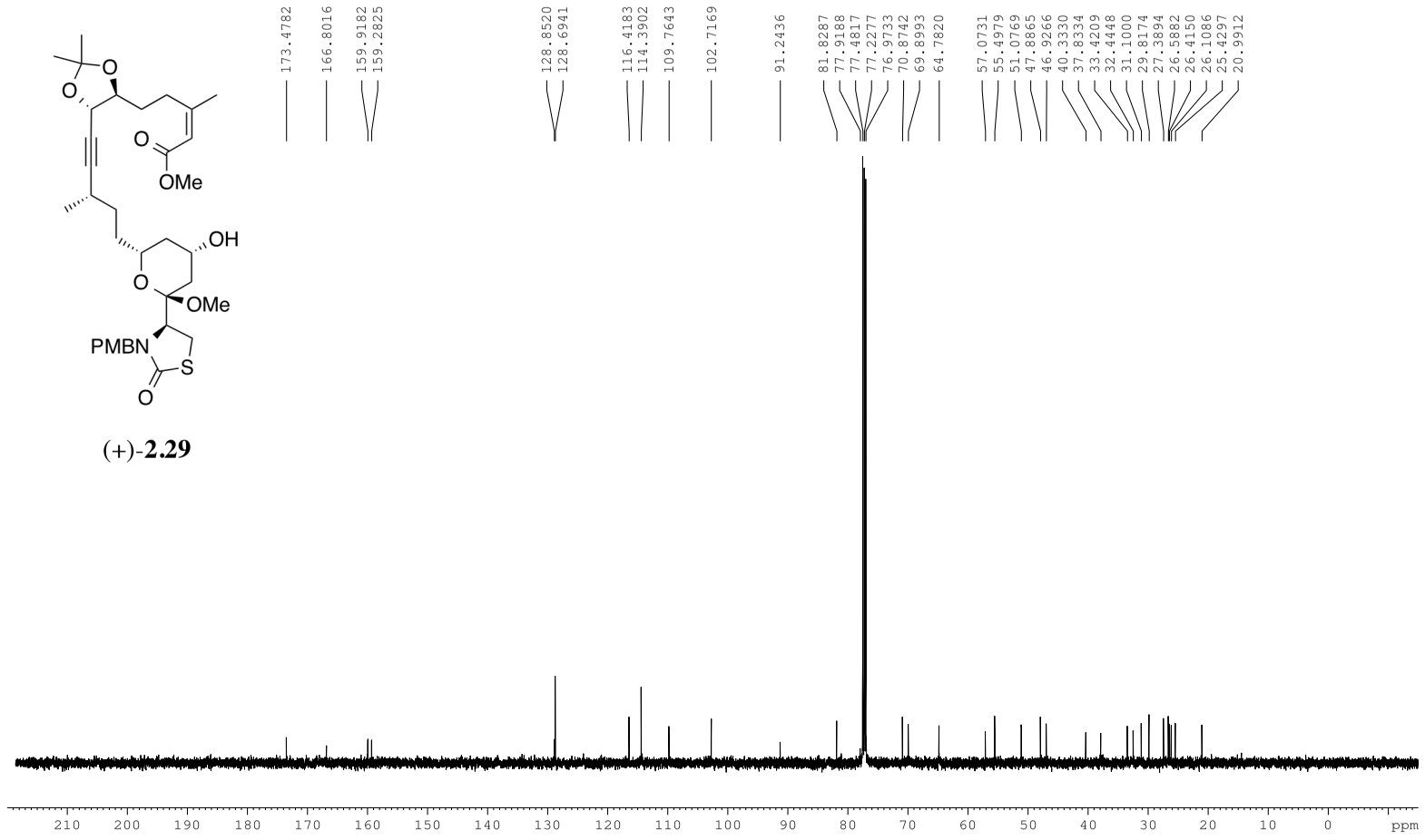

(+)-**2.29**

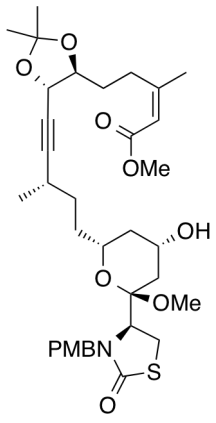

(+)-**2.29**

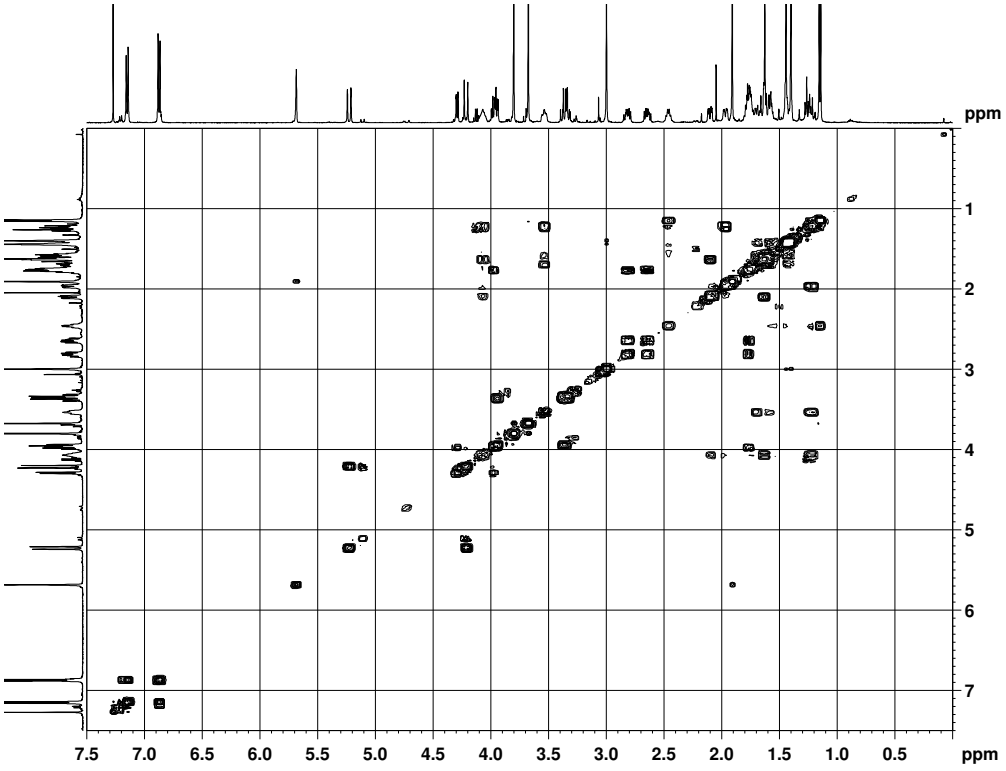

Figure A2.47. COSY Spectrum (500 MHz) of Compound (+)-**2.29** in $CDCl_3$

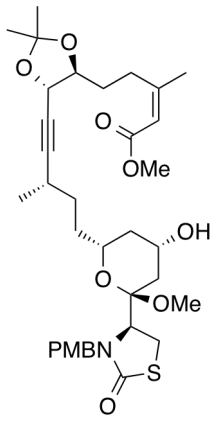

(+)-**2.29**

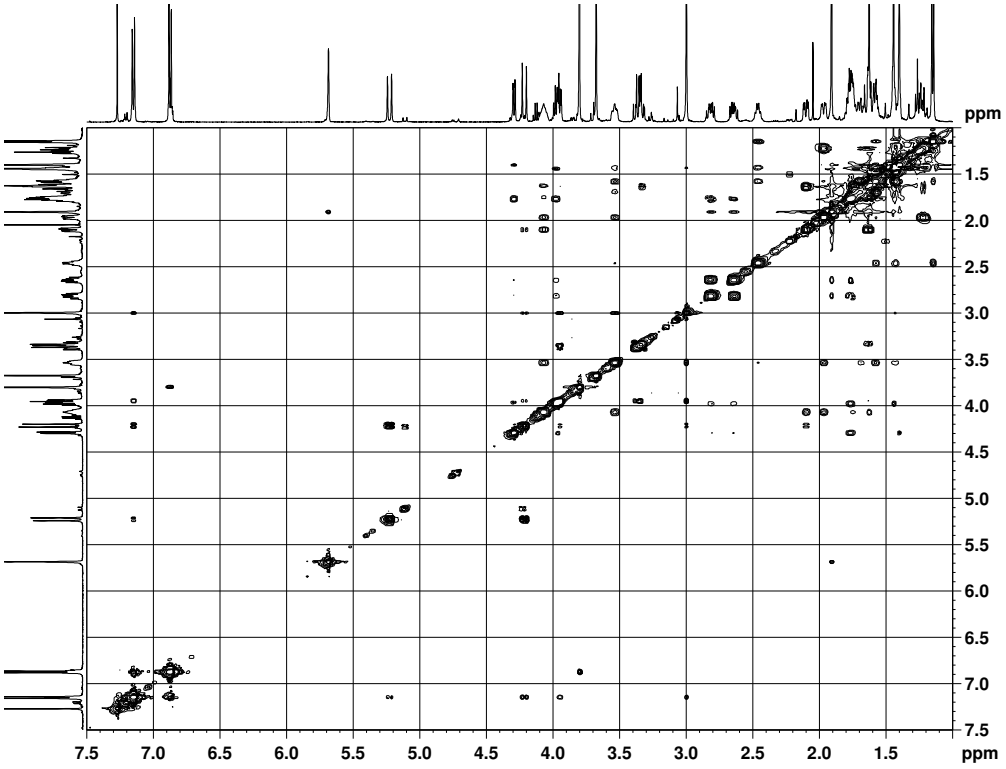

Figure A2.48. NOESY Spectrum (500 MHz) of Compound (+)-**2.29** in $CDCl_3$

Figure A2.49. ^{1}H NMR Spectrum (500 MHz) of Compound (+)-**S10** in $CDCl_3$

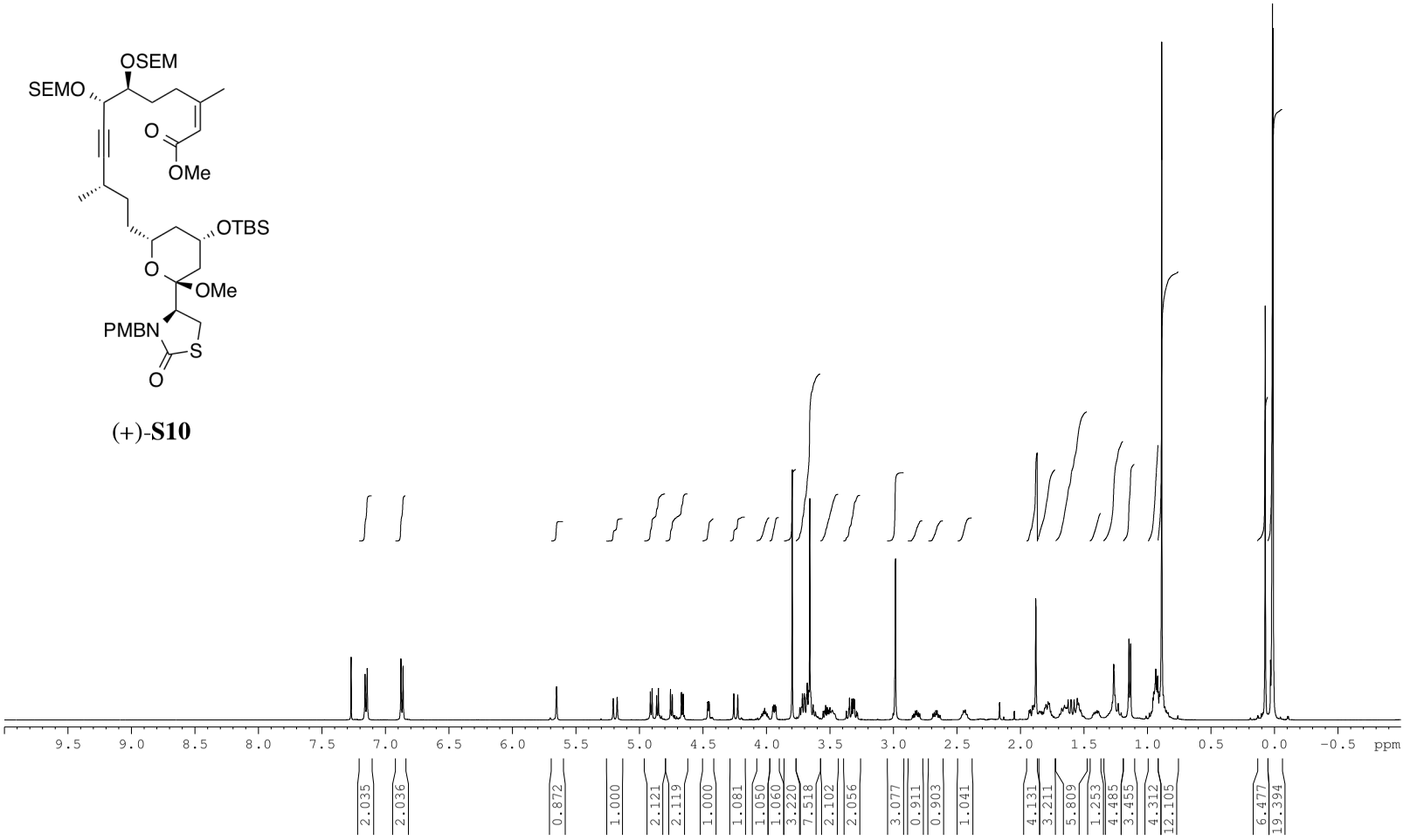

Figure A2.50. ^{13}C NMR Spectrum (125 MHz) of Compound (+)-**S10** in $CDCl_3$

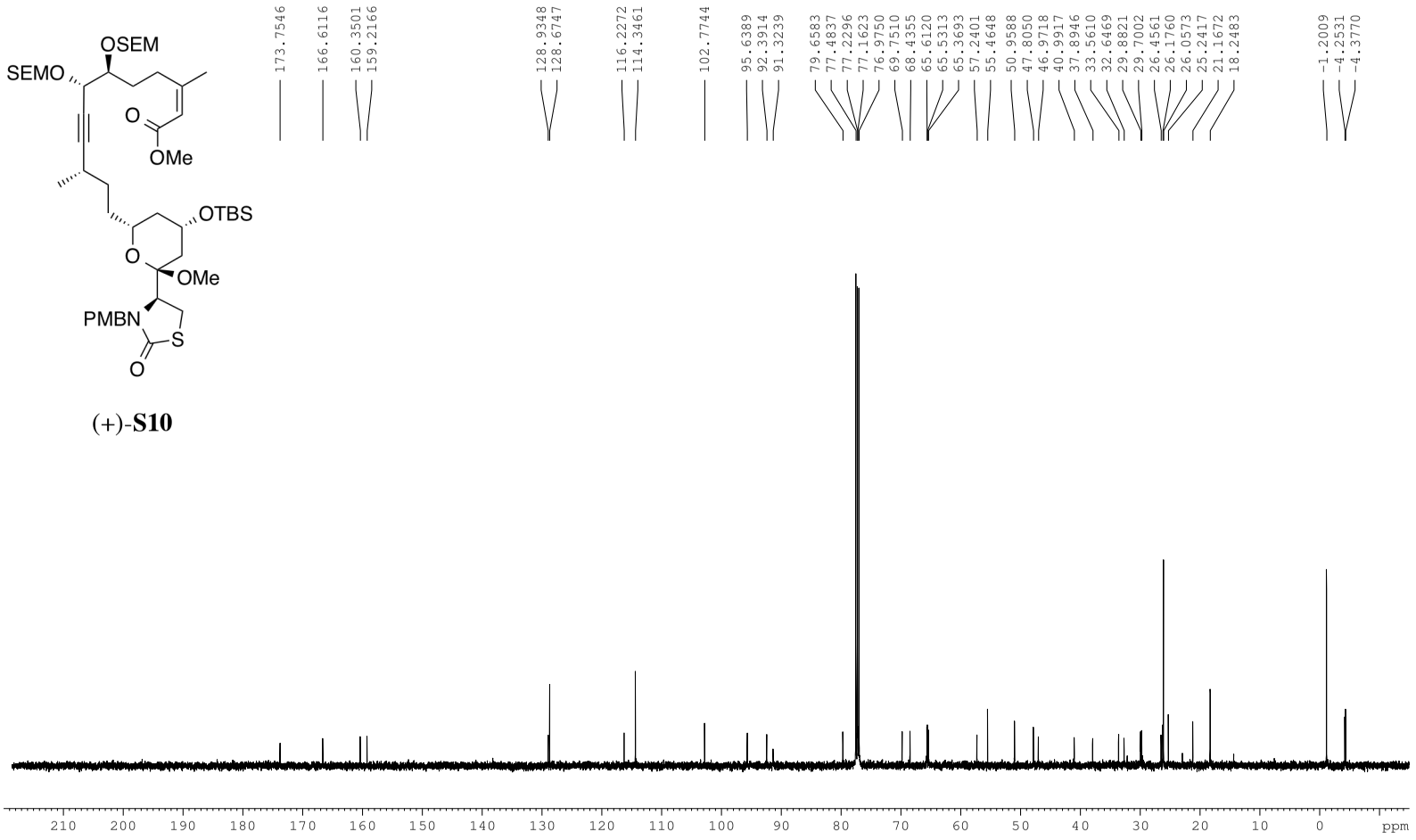

Figure A2.51. ^{1}H NMR Spectrum (500 MHz) of Compound (+)-**S11** in $CDCl_3$

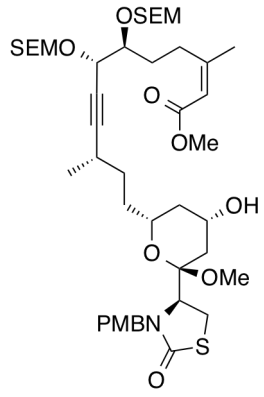

(+)-**S11**

Figure A2.52. ^{13}C NMR Spectrum (125 MHz) of Compound (+)-**S11** in $CDCl_3$

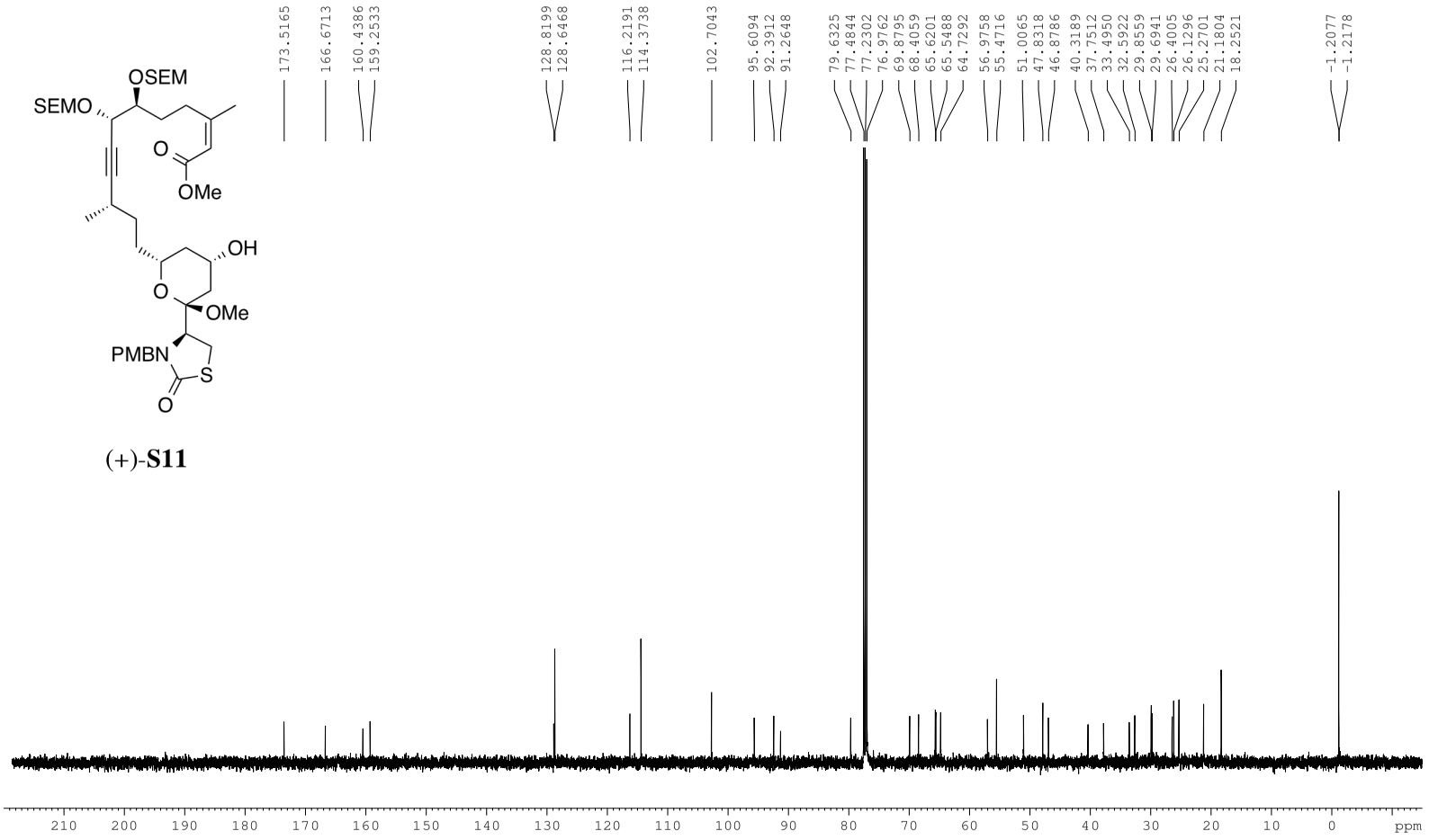

Figure A2.53. ^{1}H NMR Spectrum (500 MHz) of Compound (+)-**2.30** in $CDCl_3$

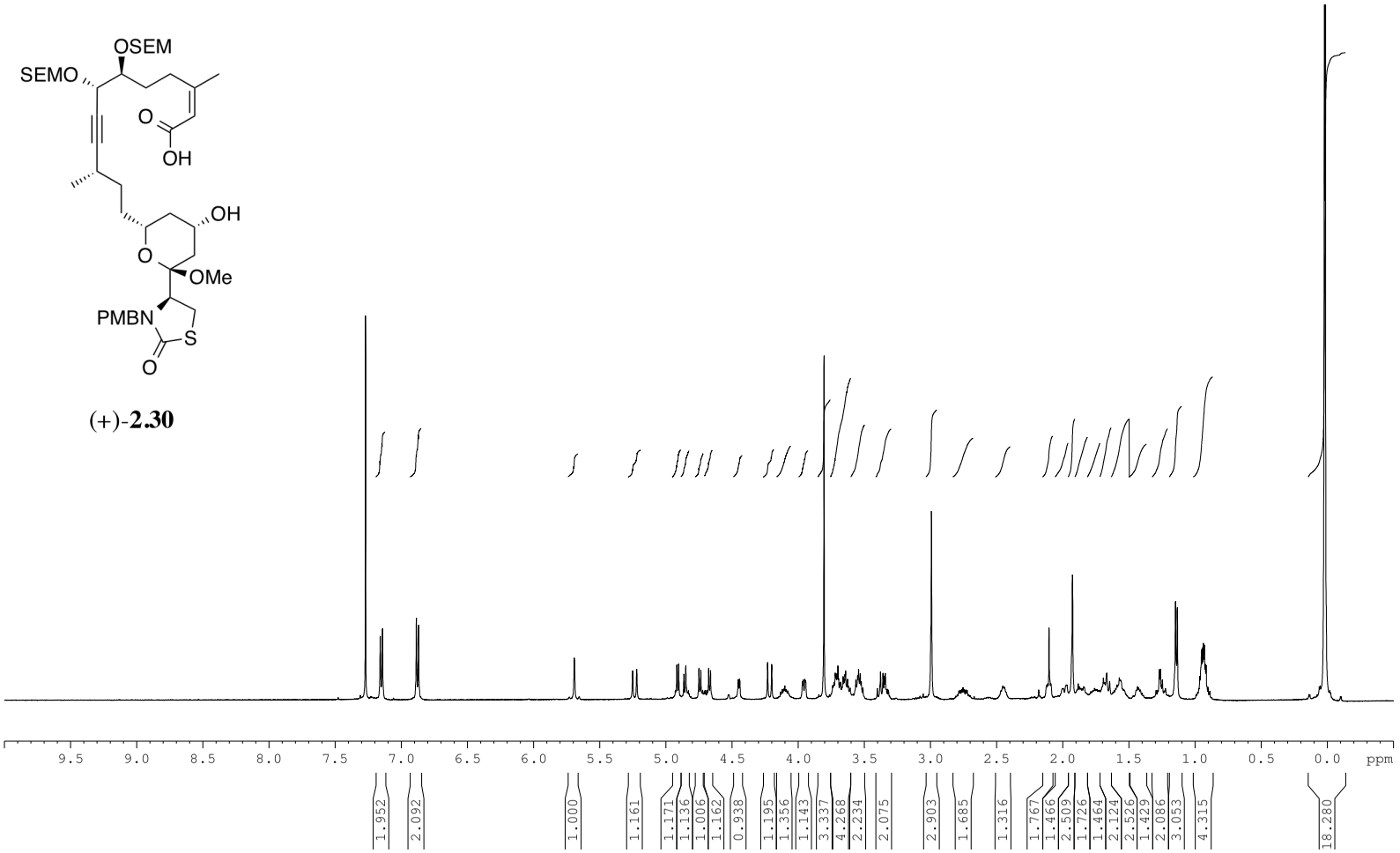

Figure A2.54. ^{13}C NMR Spectrum (125 MHz) of Compound (+)-**2.30** in $CDCl_3$

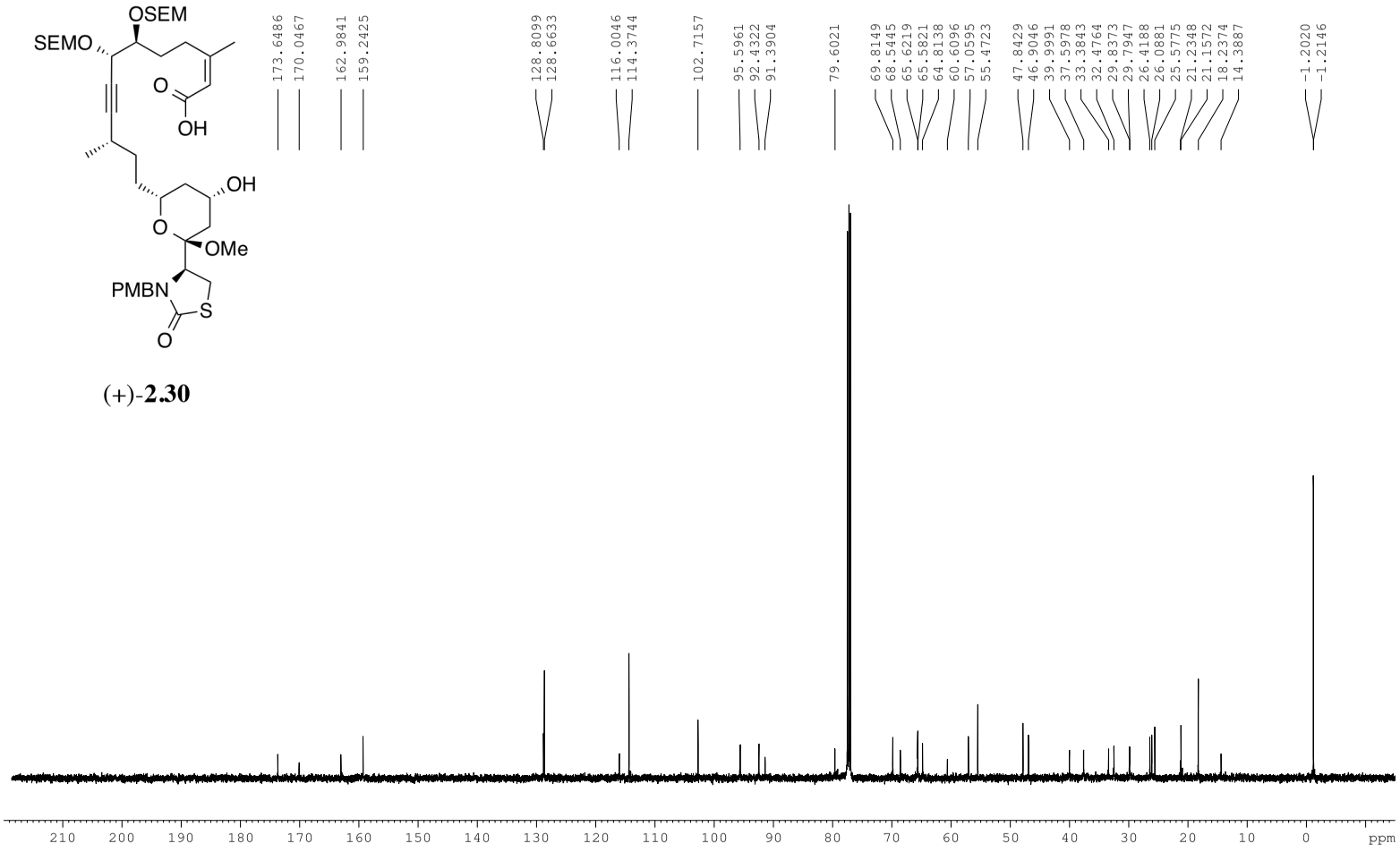

Figure A2.55. ^{1}H NMR Spectrum (500 MHz) of Compound (+)-**2.32** in $CDCl_3$

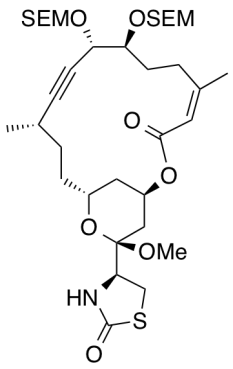

(+)-**2.32**

Figure A2.56. ^{13}C NMR Spectrum (125 MHz) of Compound (+)-**2.32** in $CDCl_3$

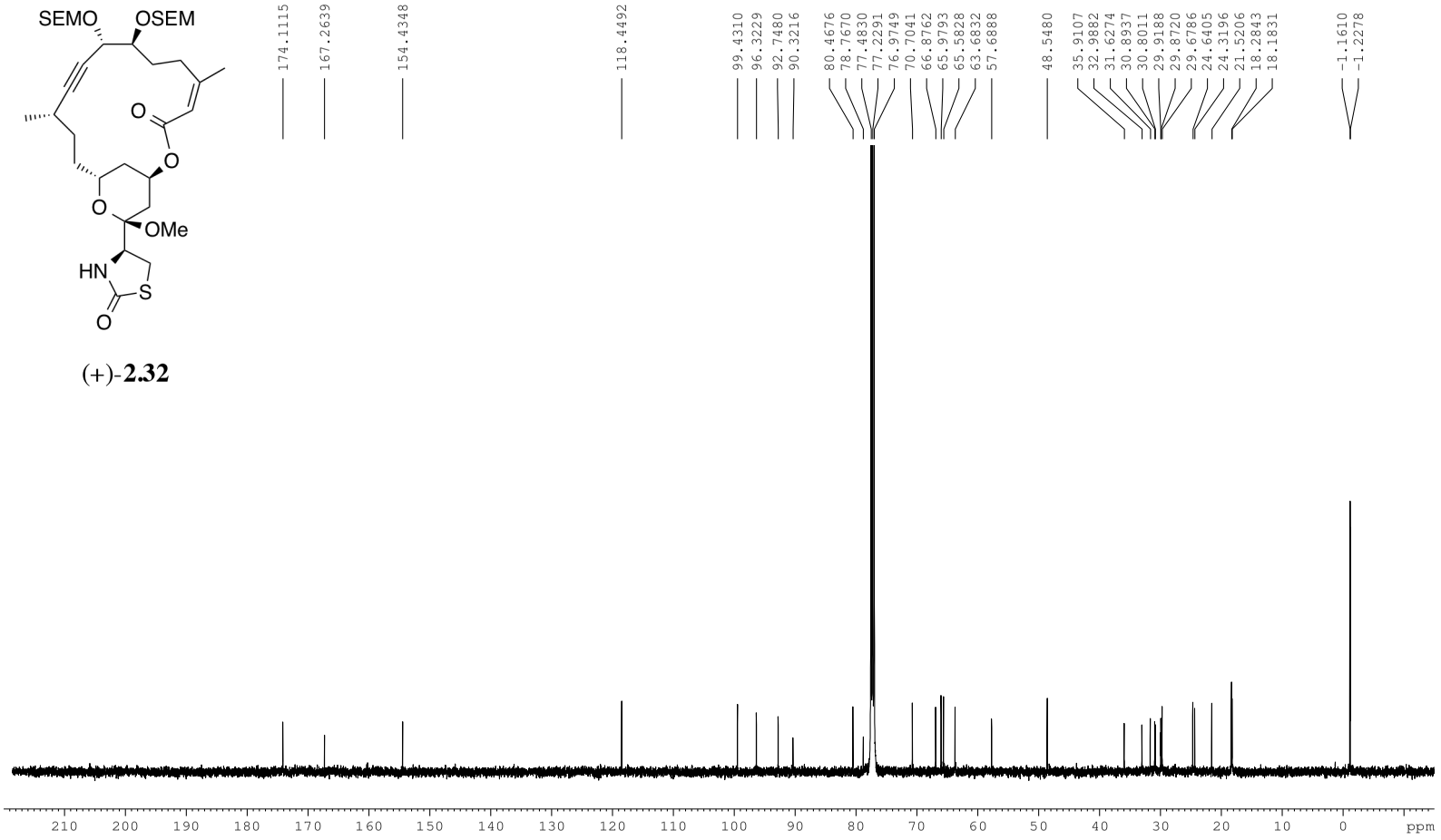

(+)-**2.32**

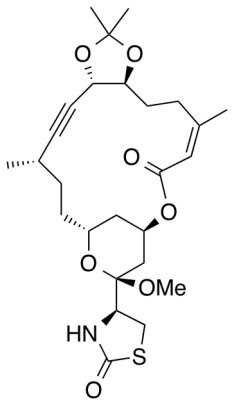

(+)-**2.34**

Figure A2.57. ^{1}H NMR Spectrum (500 MHz) of Compound (+)-**2.34** in $CDCl_3$

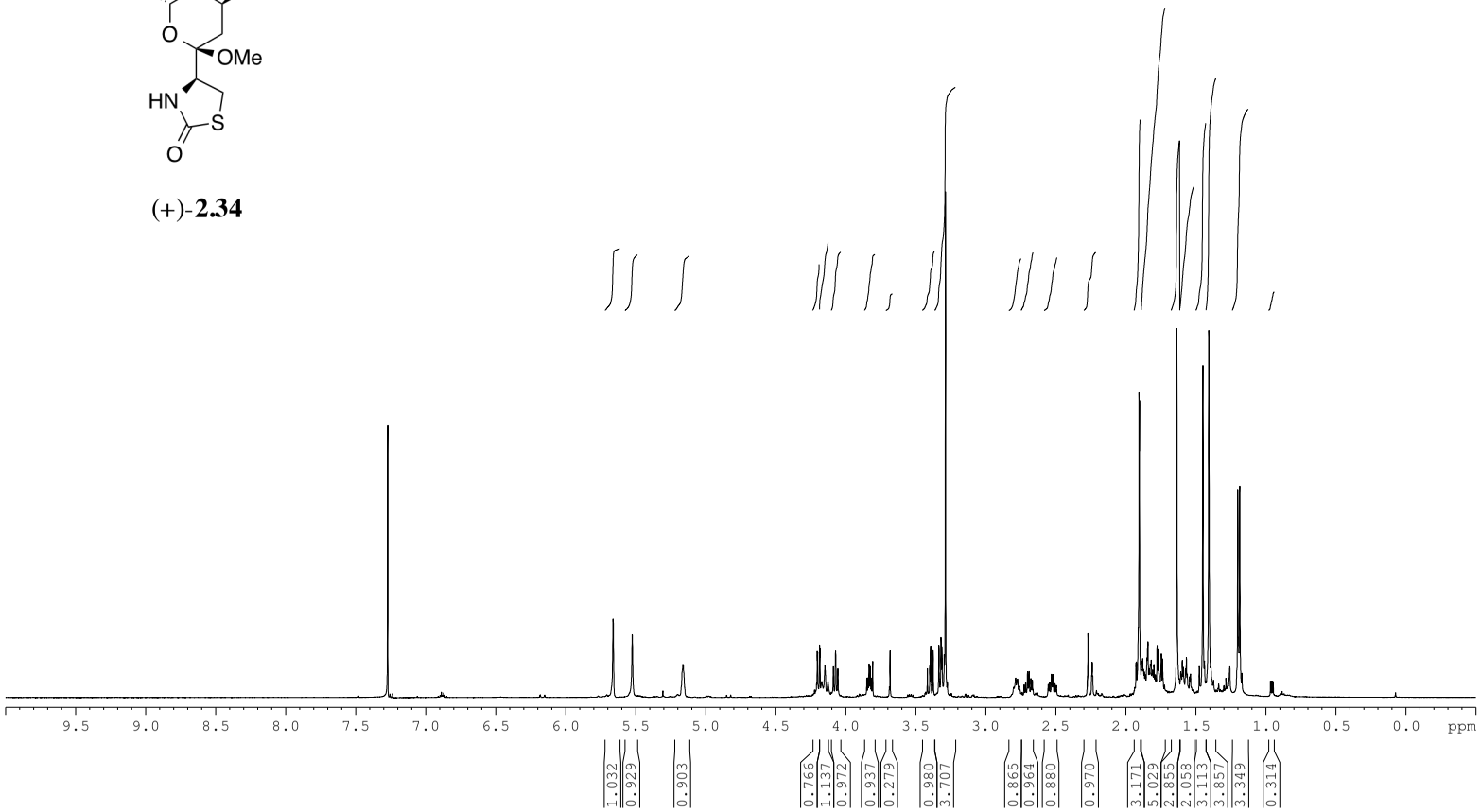

Figure A2.58. ^{13}C NMR Spectrum (125 MHz) of Compound (+)-**2.34** in $CDCl_3$

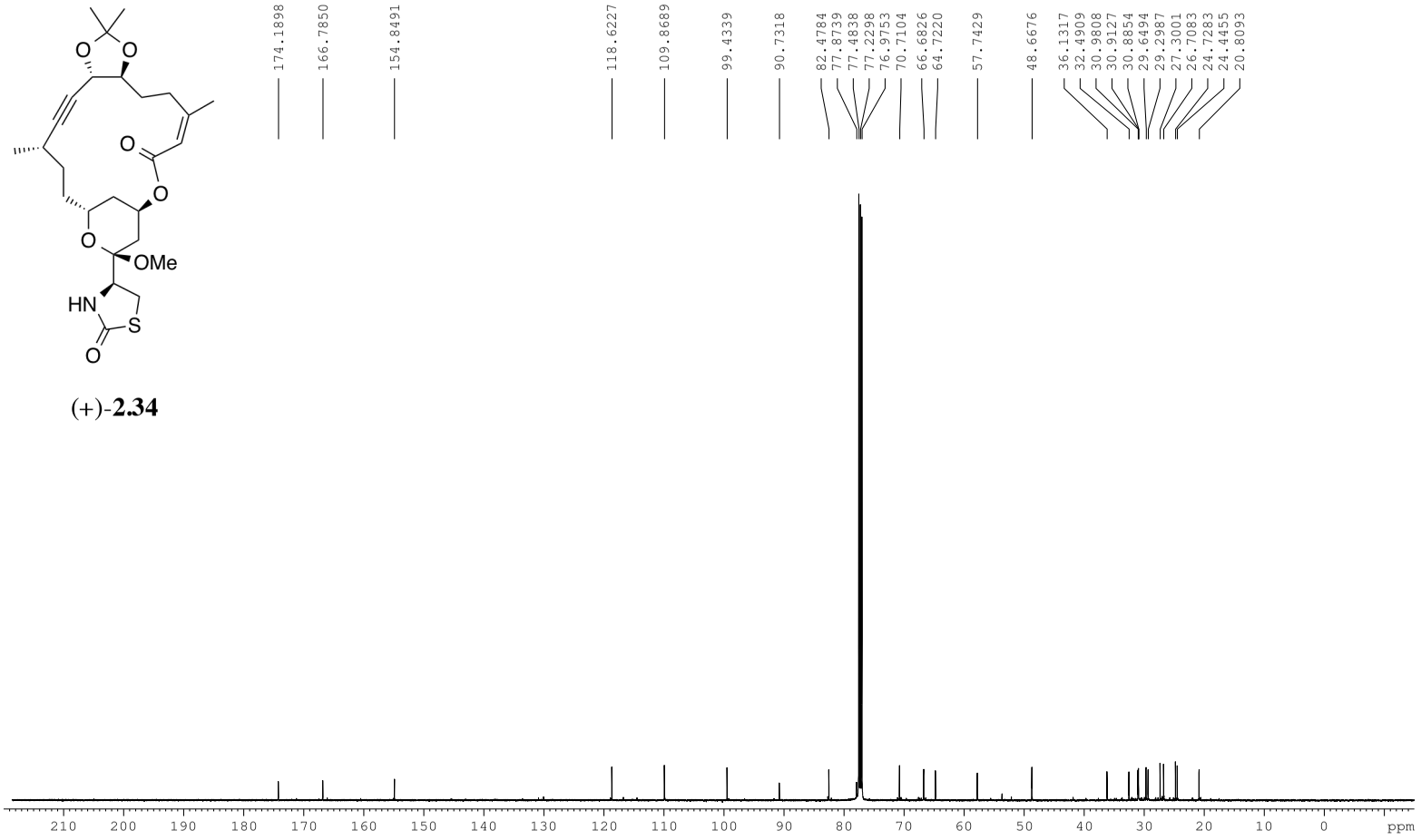

(+)-**2.34**

Figure A2.59. ^{1}H NMR Spectrum (500 MHz) of Compound (+)-**2.33** in $CDCl_3$

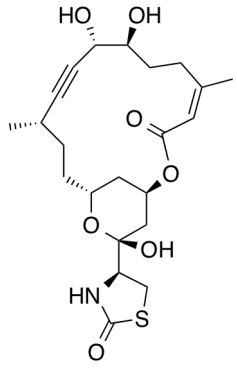

(+)-**2.33**

Figure A2.60. ^{13}C NMR Spectrum (125 MHz) of Compound (+)-**2.33** in $CDCl_3$

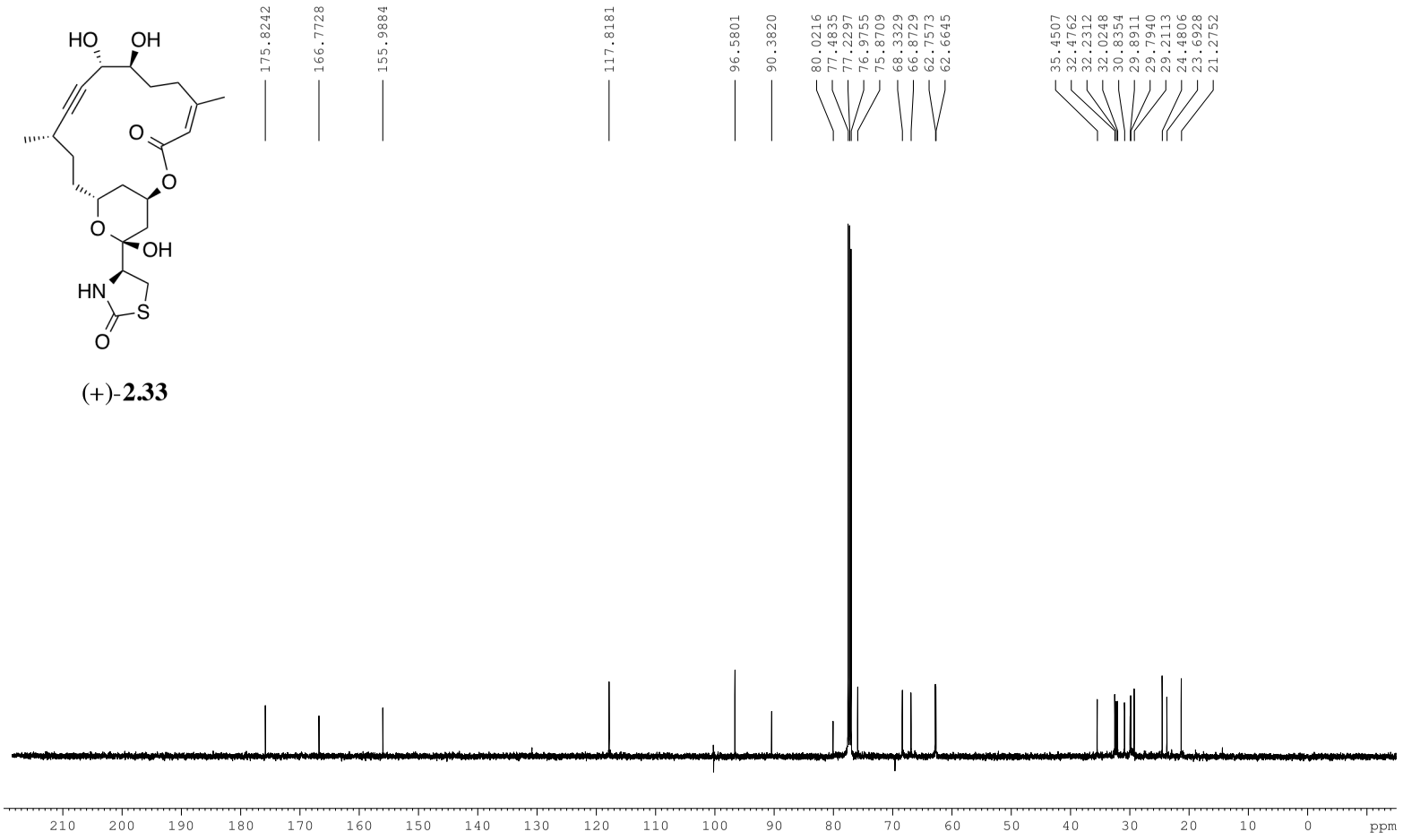

(+)-**2.33**

Figure A2.61. ^{1}H NMR Spectrum (500 MHz) of Compound (+)-**2.1** in acetone-d_6

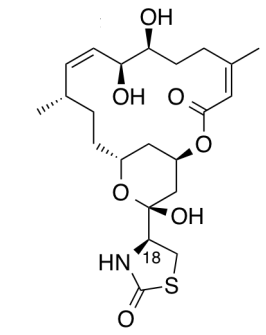

(+)-**2.1**

Figure A2.62. ^{13}C NMR Spectrum (125 MHz) of Compound (+)-**2.1** in acetone-d_6

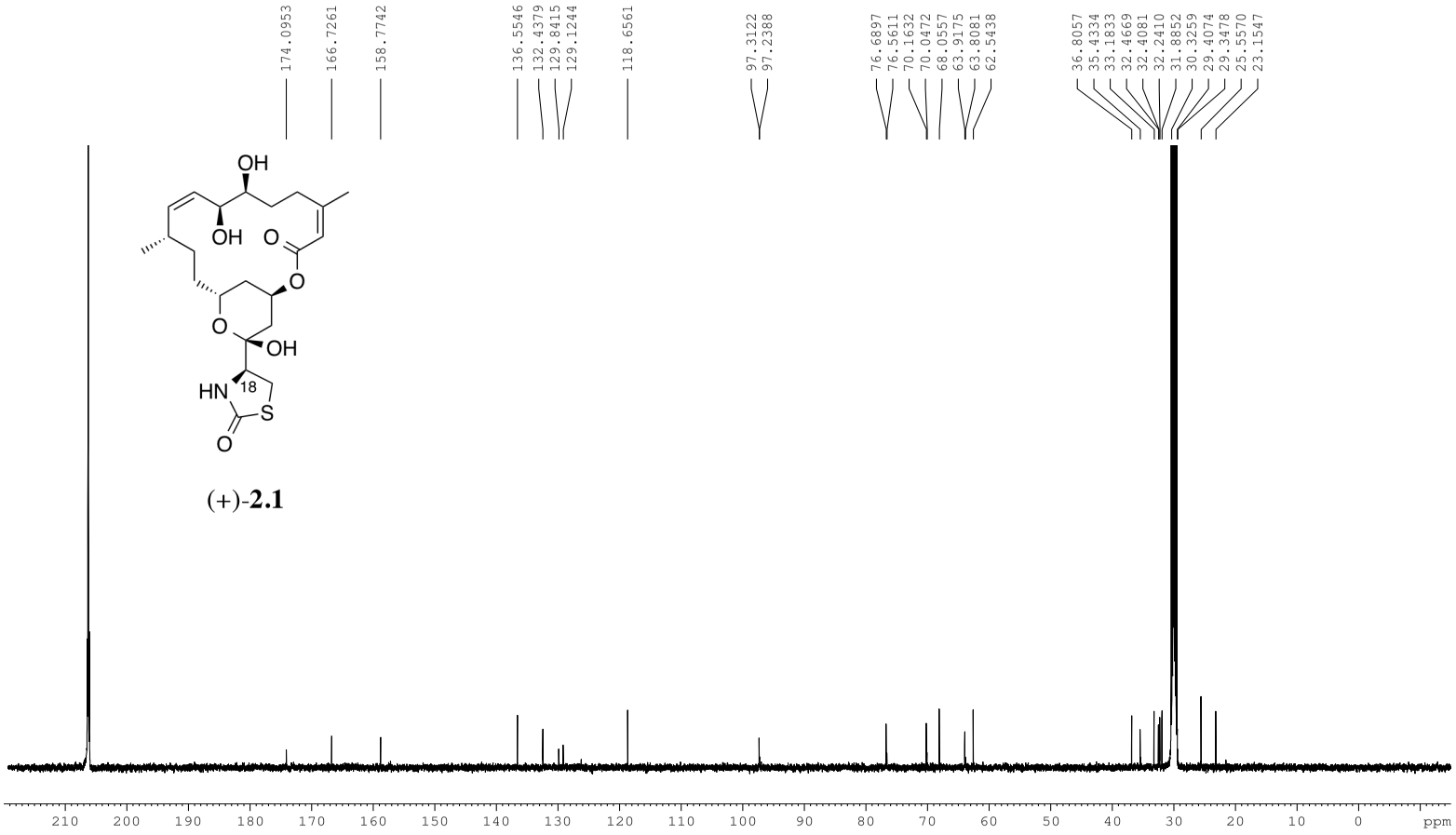

(+)-**2.1**

Figure A2.63. ^{1}H NMR Spectrum (500 MHz) of Compound **S14** in acetone-d_6 with D_2O

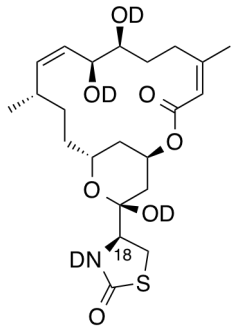

S14

Figure A2.64. ^{13}C NMR Spectrum (125 MHz) of Compound **S14** in acetone-d_6 with D_2O

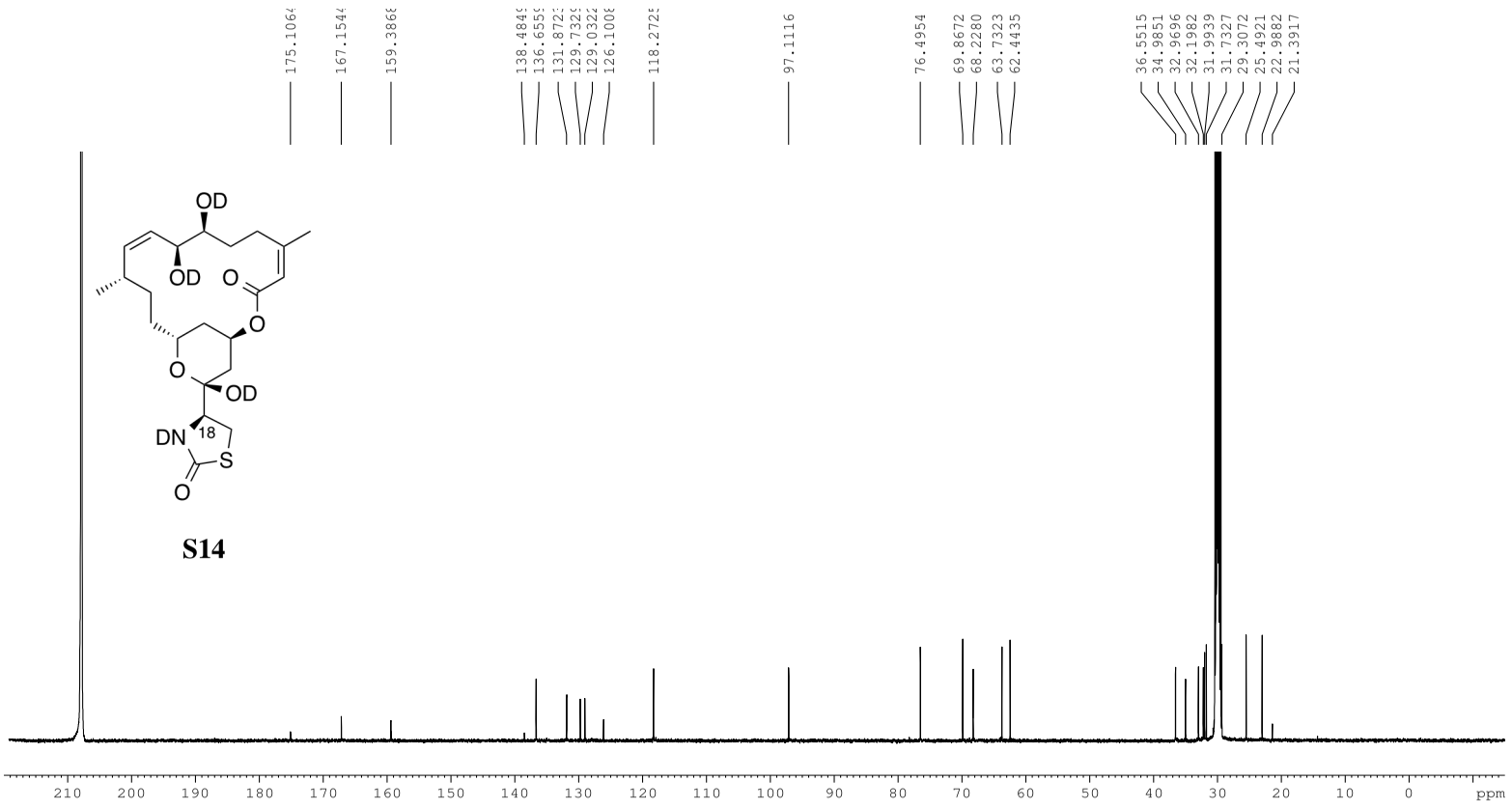

Figure A3.1. ^{1}H NMR Spectrum (500 MHz) of Compound **3.12** in $CDCl_3$

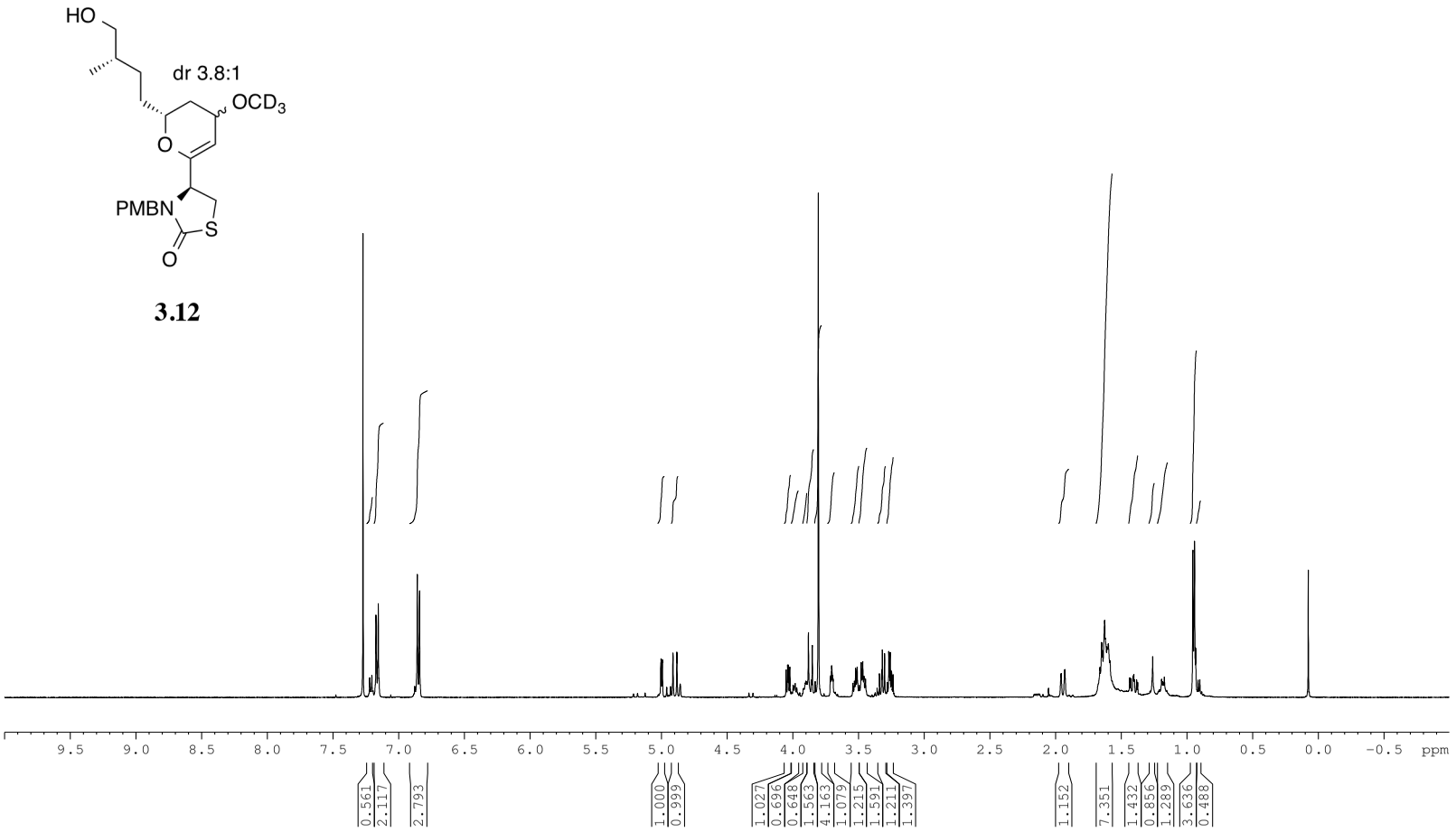

Figure A3.2. ^{13}C NMR Spectrum (125 MHz) of Compound **3.12** in $CDCl_3$

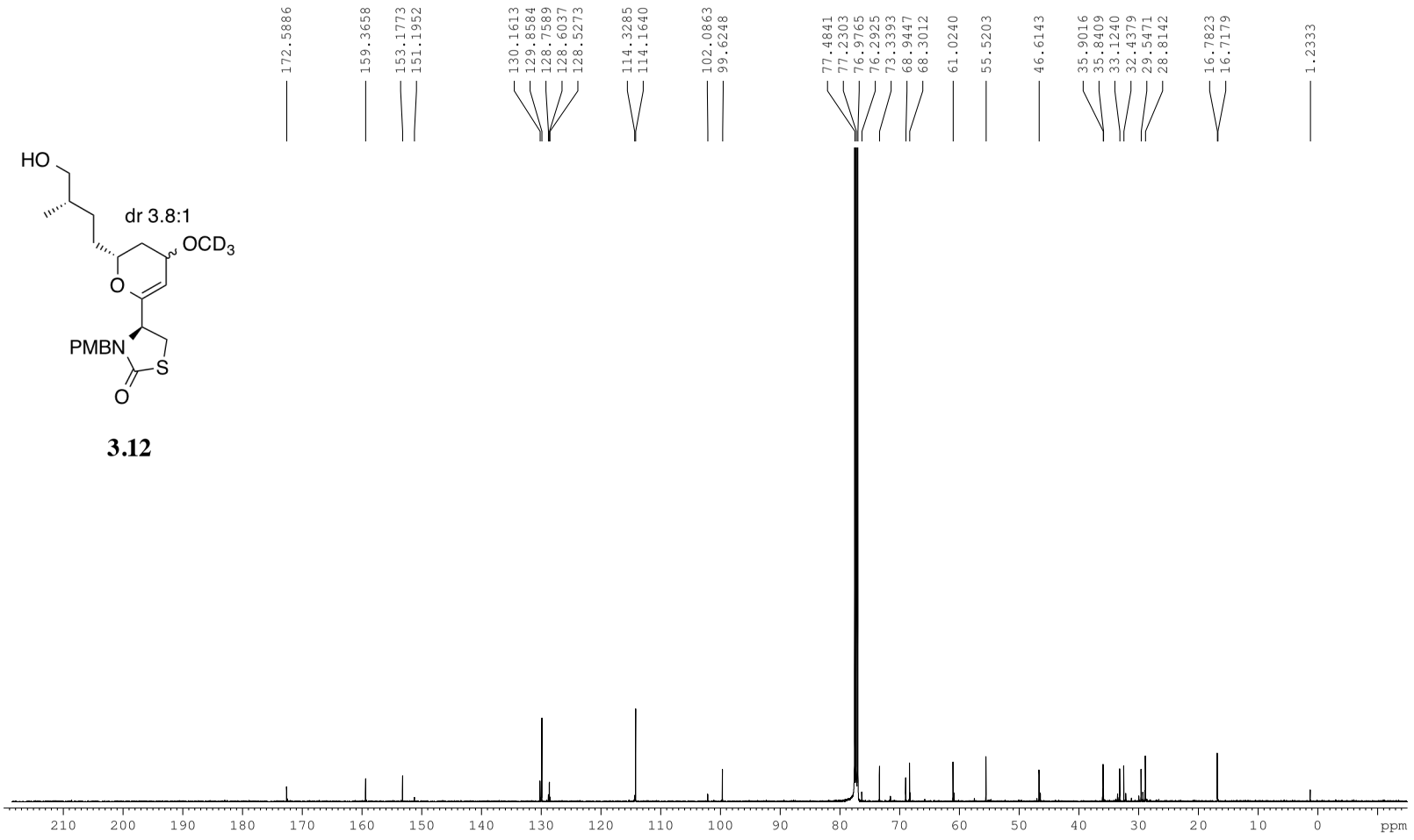

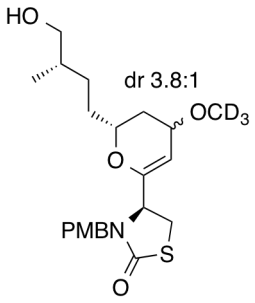

3.12

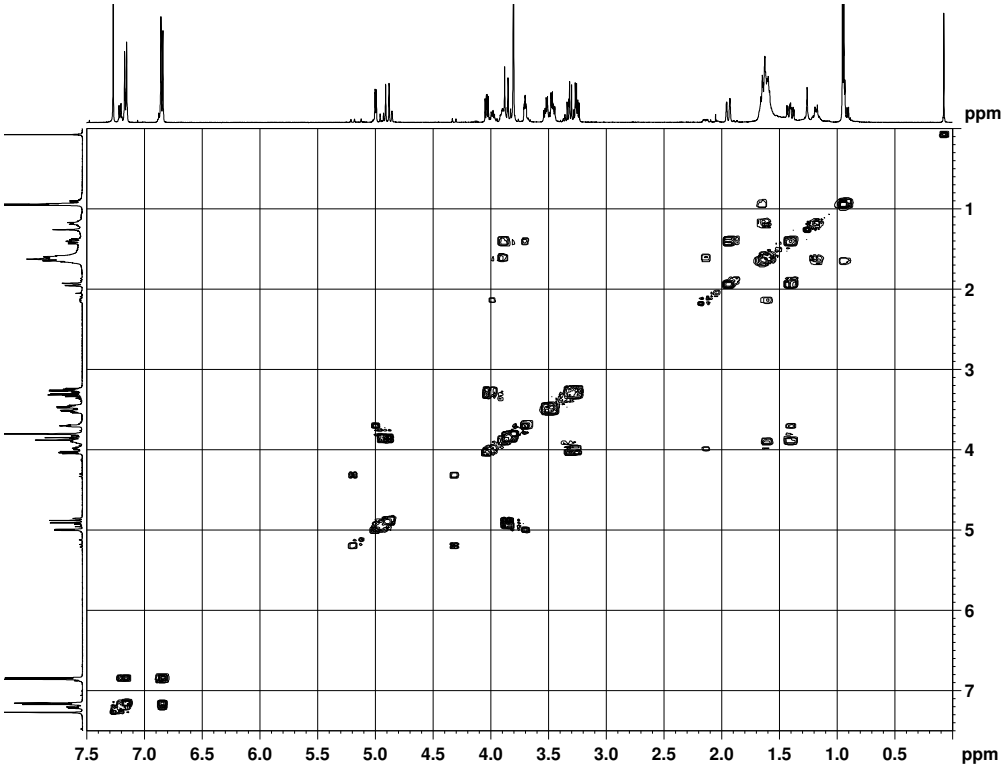

Figure A3.3. COSY Spectrum of Compound **3.12** in $CDCl_3$

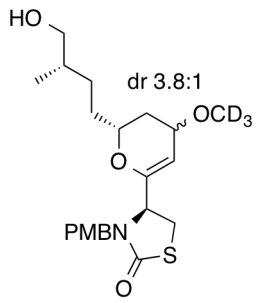

3.12

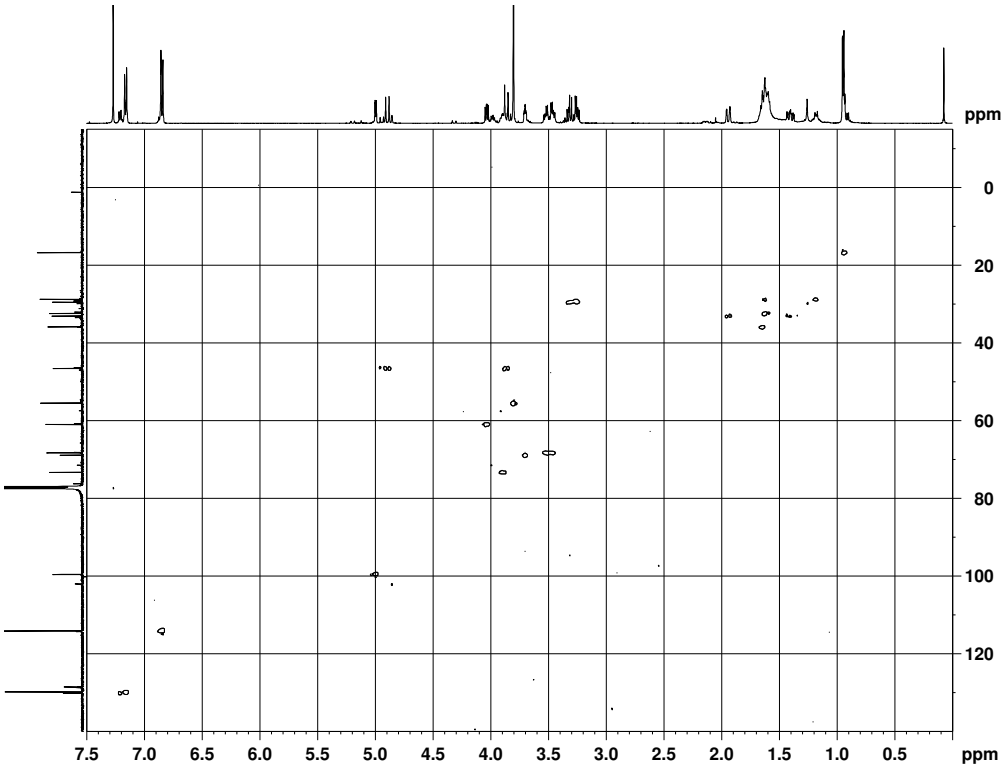

Figure A3.4. HSQC Spectrum of Compound **3.12** in $CDCl_3$

Figure A3.5. ^{1}H NMR Spectrum (500 MHz) of **S15** in $CDCl_3$

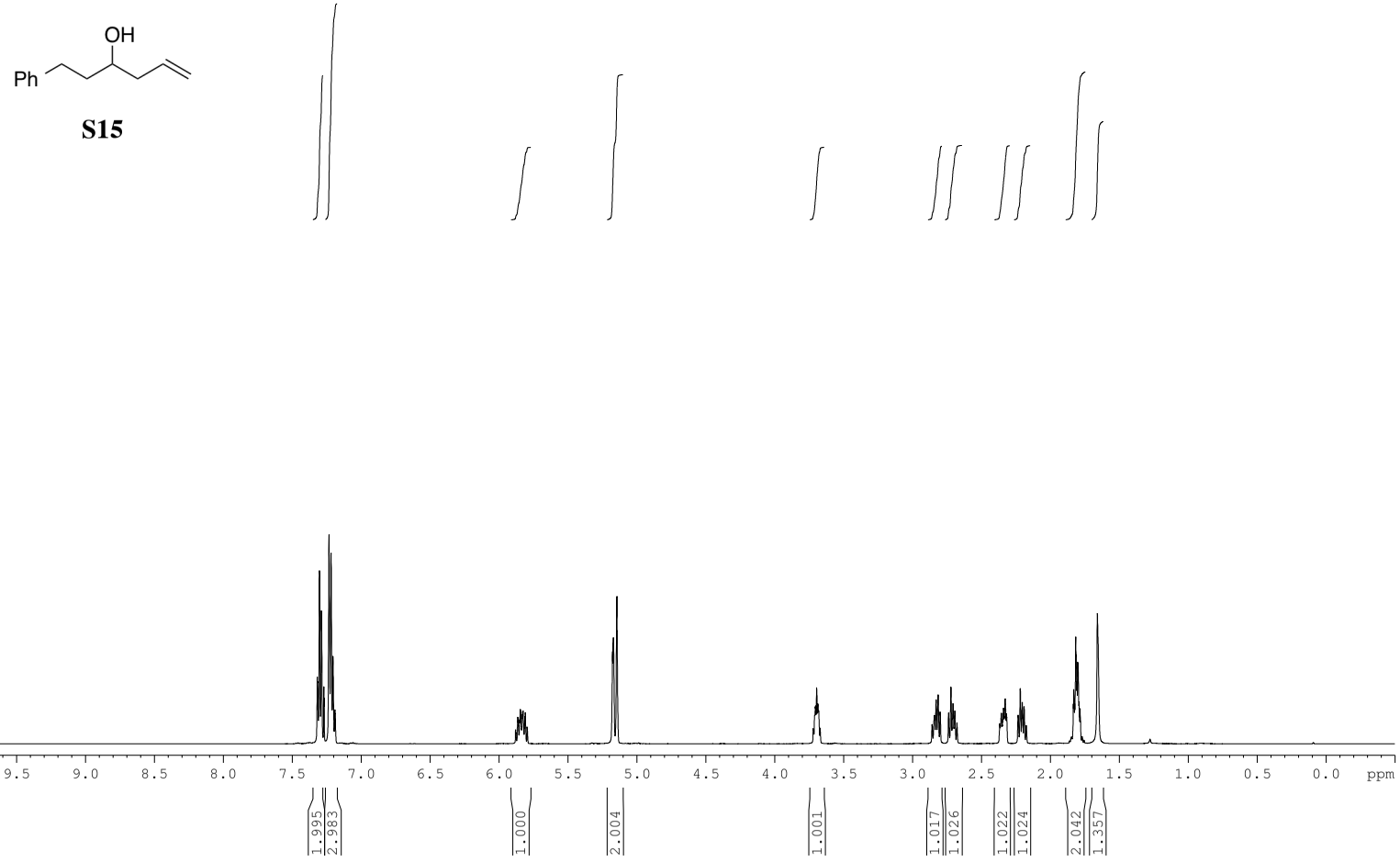

Figure A3.6. ^{13}C NMR Spectrum (125 MHz) of Compound **S15** in $CDCl_3$

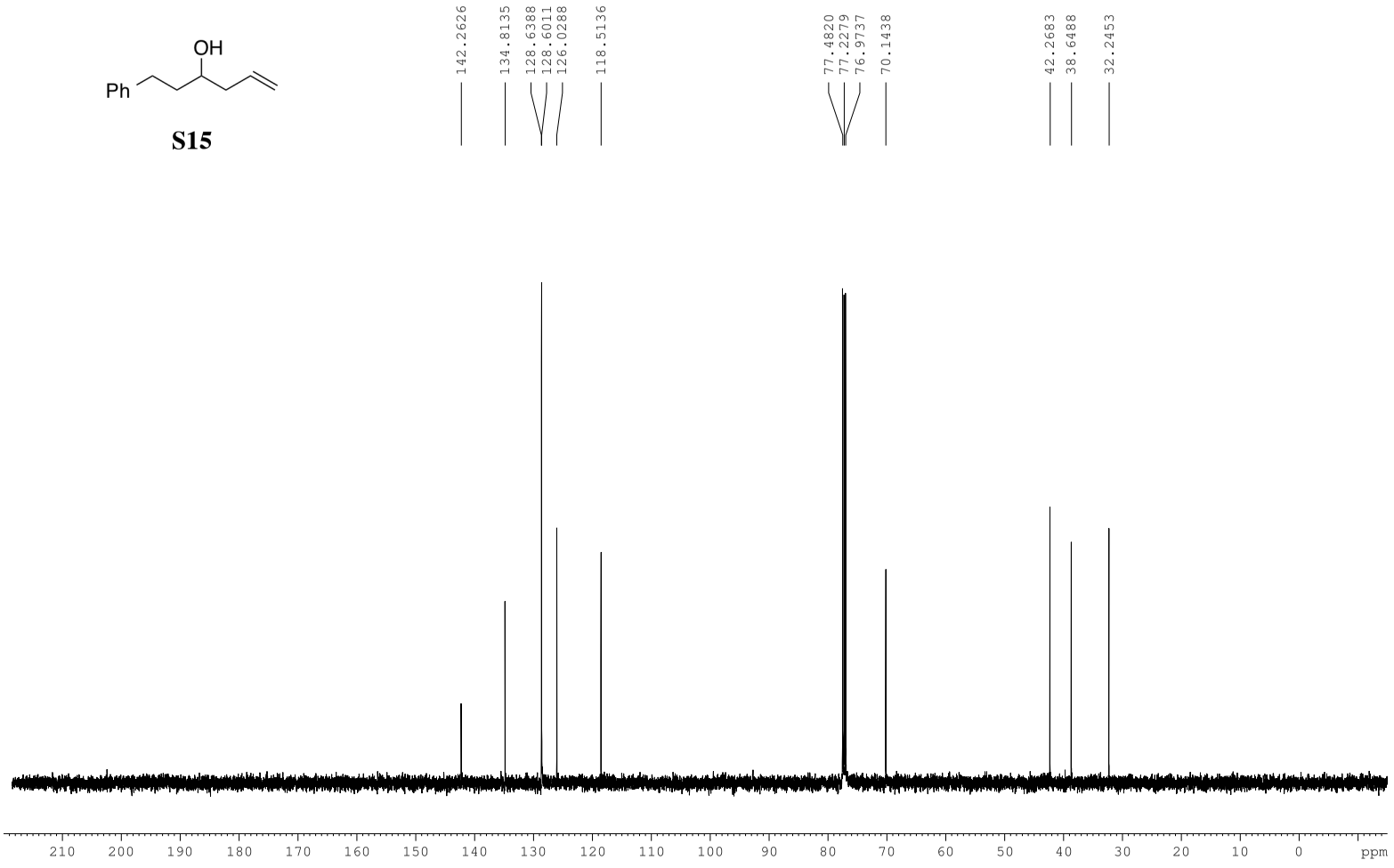

Figure A3.7. ^{1}H NMR Spectrum (500 MHz) of **3.13** in $CDCl_3$

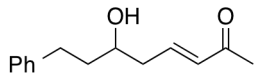

(±)-3.13

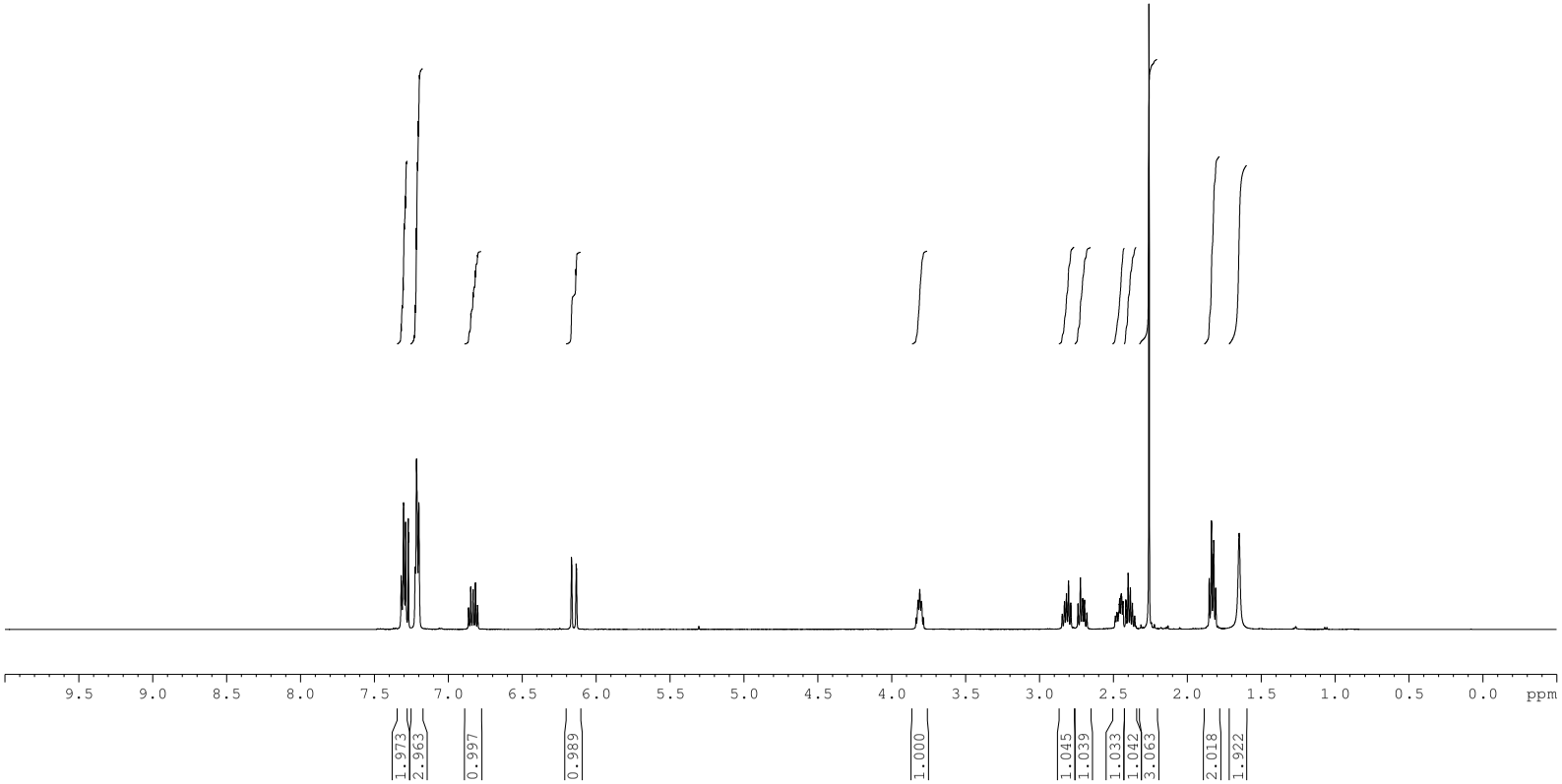

Figure A3.8. ^{13}C NMR Spectrum (125 MHz) of Compound **3.13** in $CDCl_3$

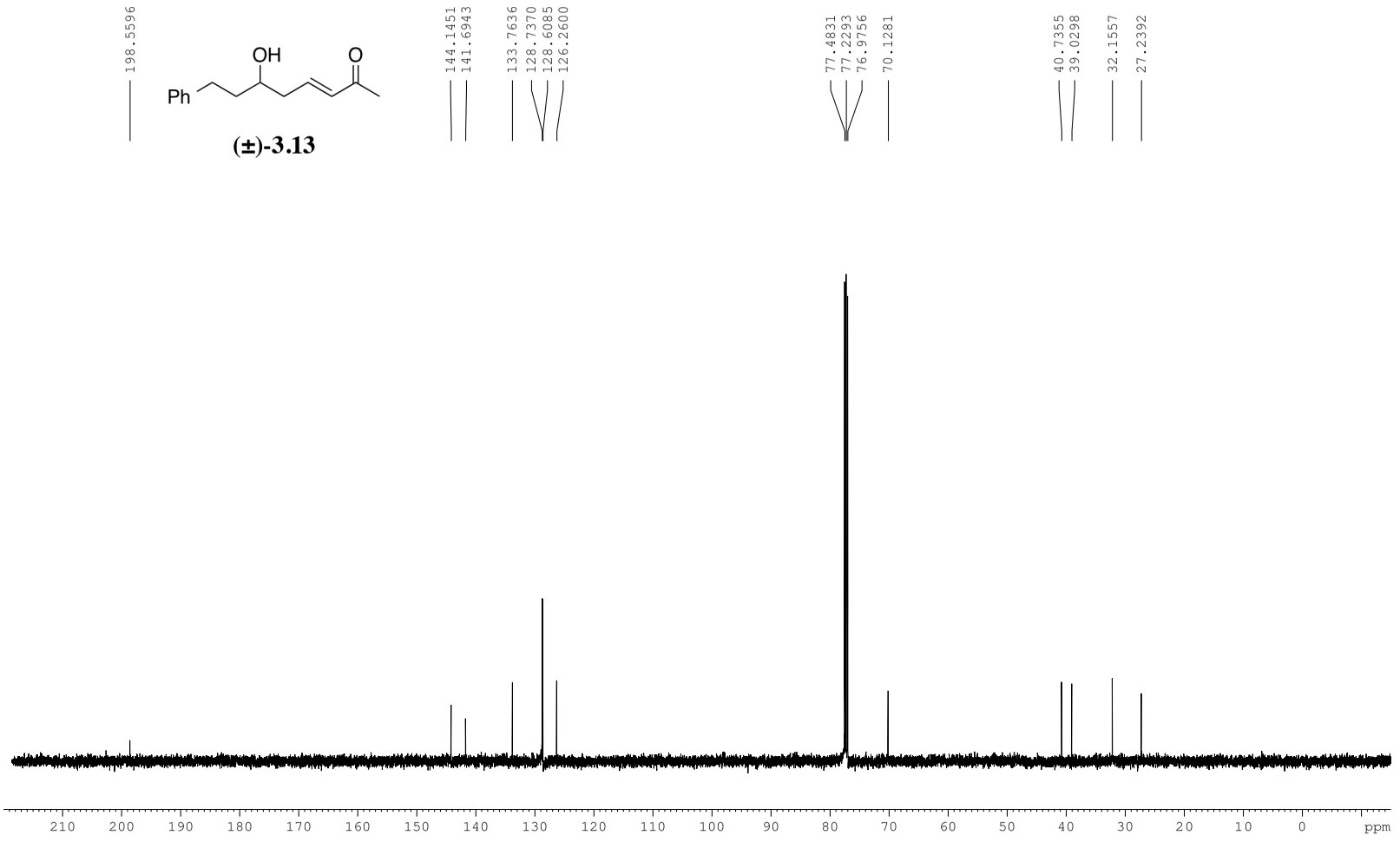

Figure A3.9. ^{1}H NMR Spectrum (500 MHz) of **3.14** in $CDCl_3$

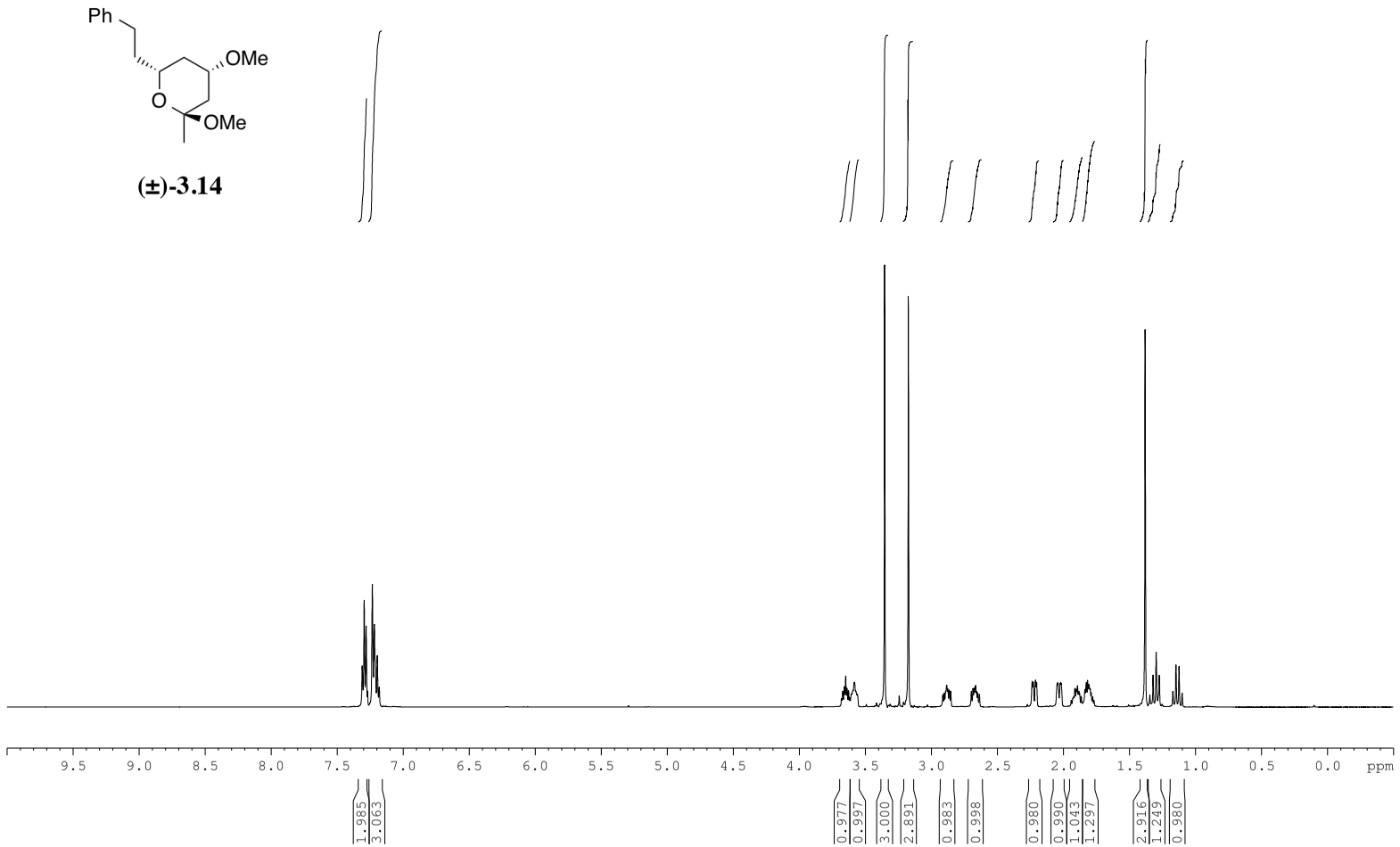

Figure A3.10. ^{13}C NMR Spectrum (125 MHz) of Compound **3.14** in $CDCl_3$

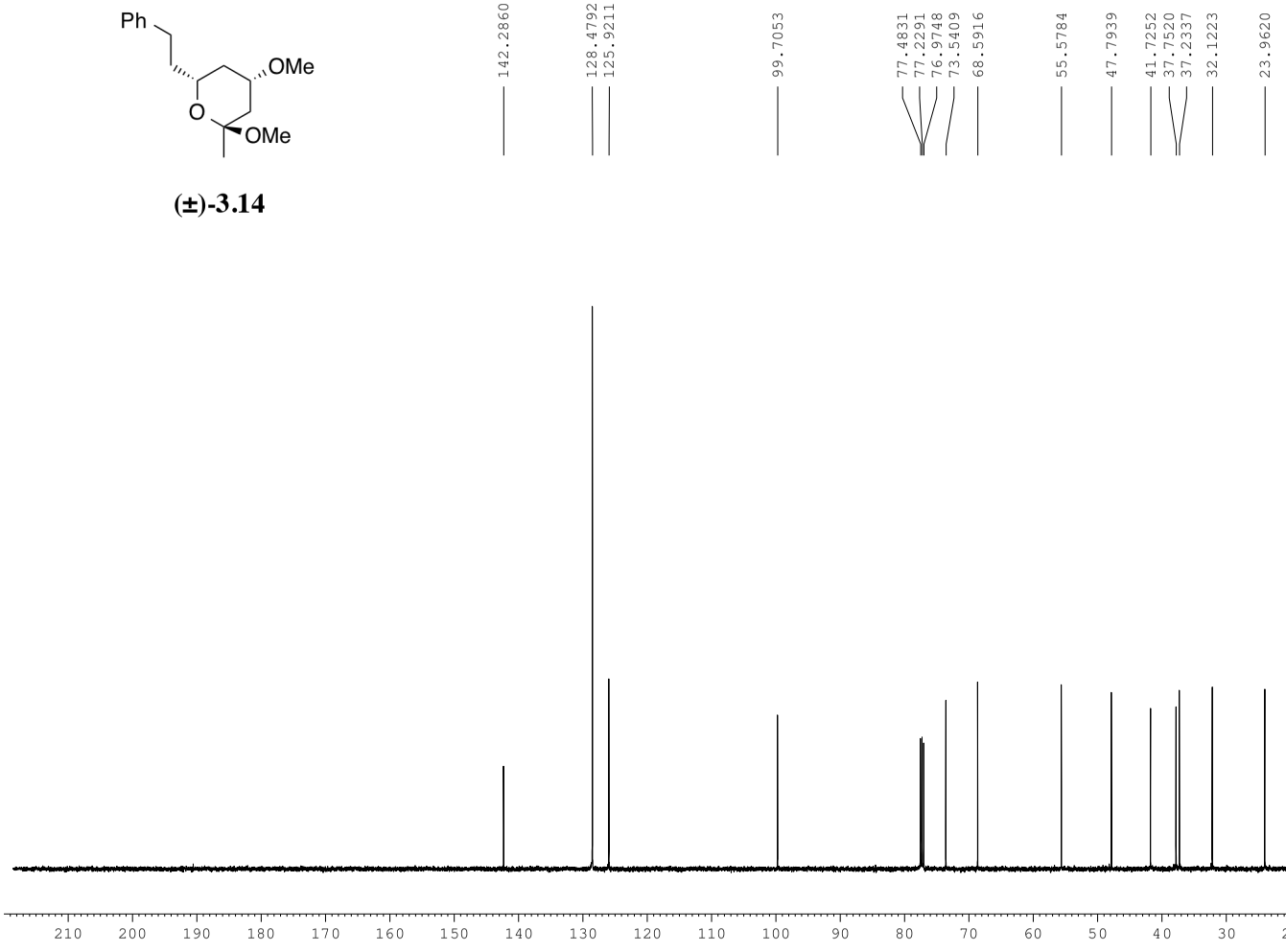

(±)-3.14

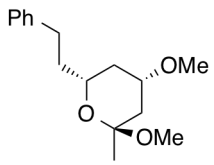

(±)-3.14

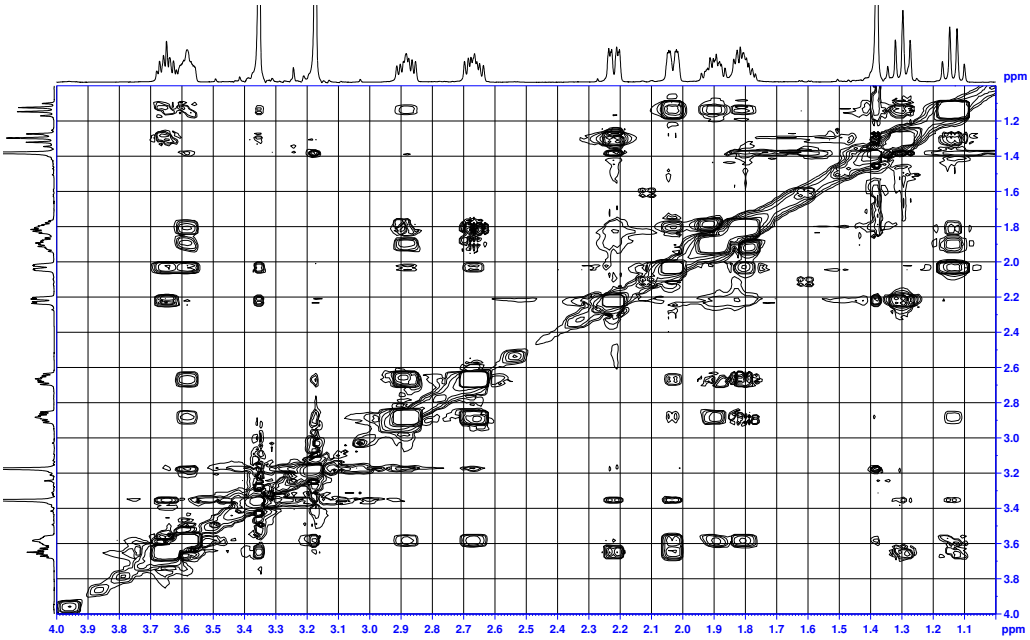

Figure A3.11. NOESY Spectrum of Compound **3.14** in $CDCl_3$

Figure A3.12. ^{1}H NMR Spectrum (500 MHz) of **3.16** in $CDCl_3$

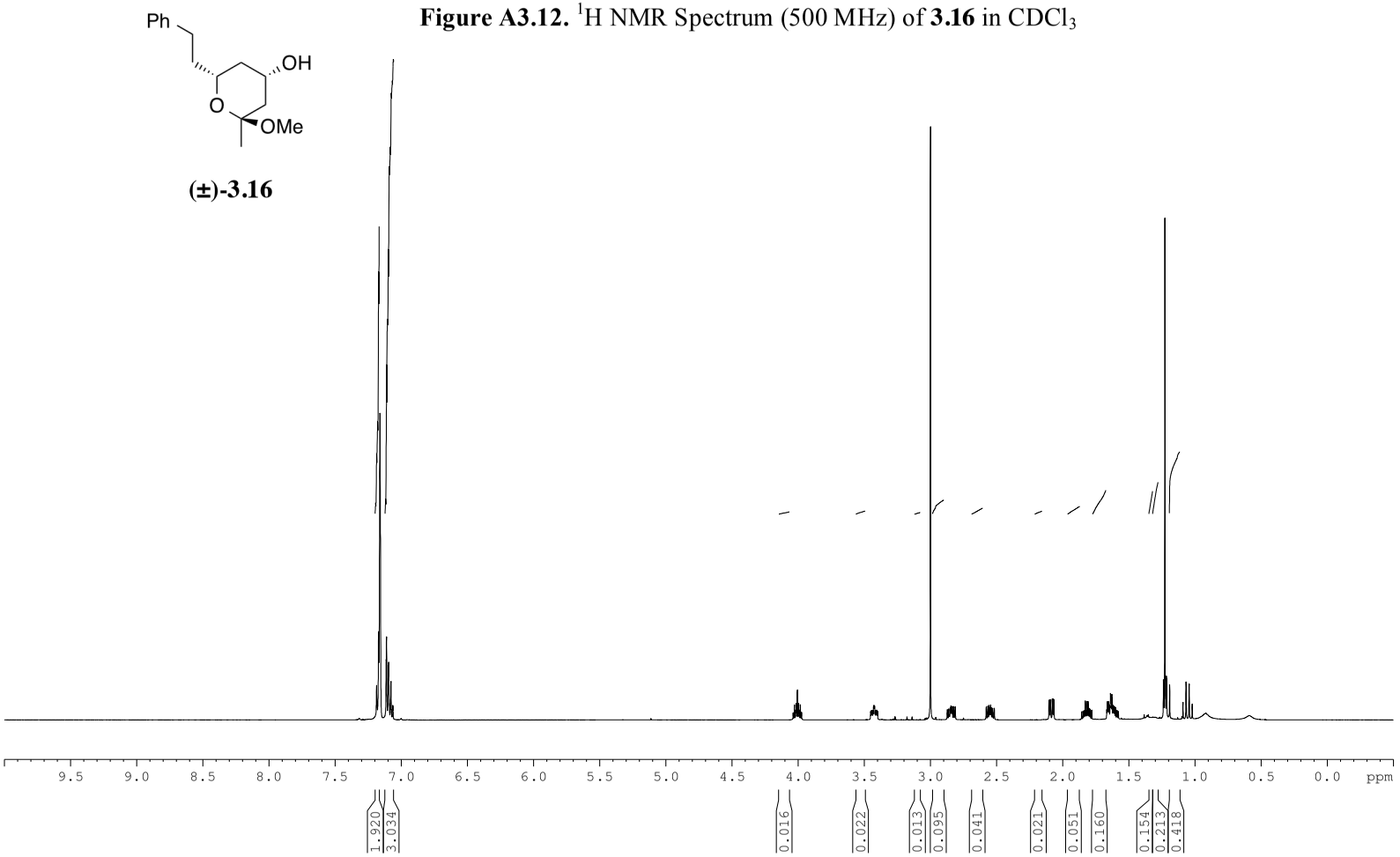

Figure A3.13. ^{13}C NMR Spectrum (125 MHz) of **3.16** in $CDCl_3$

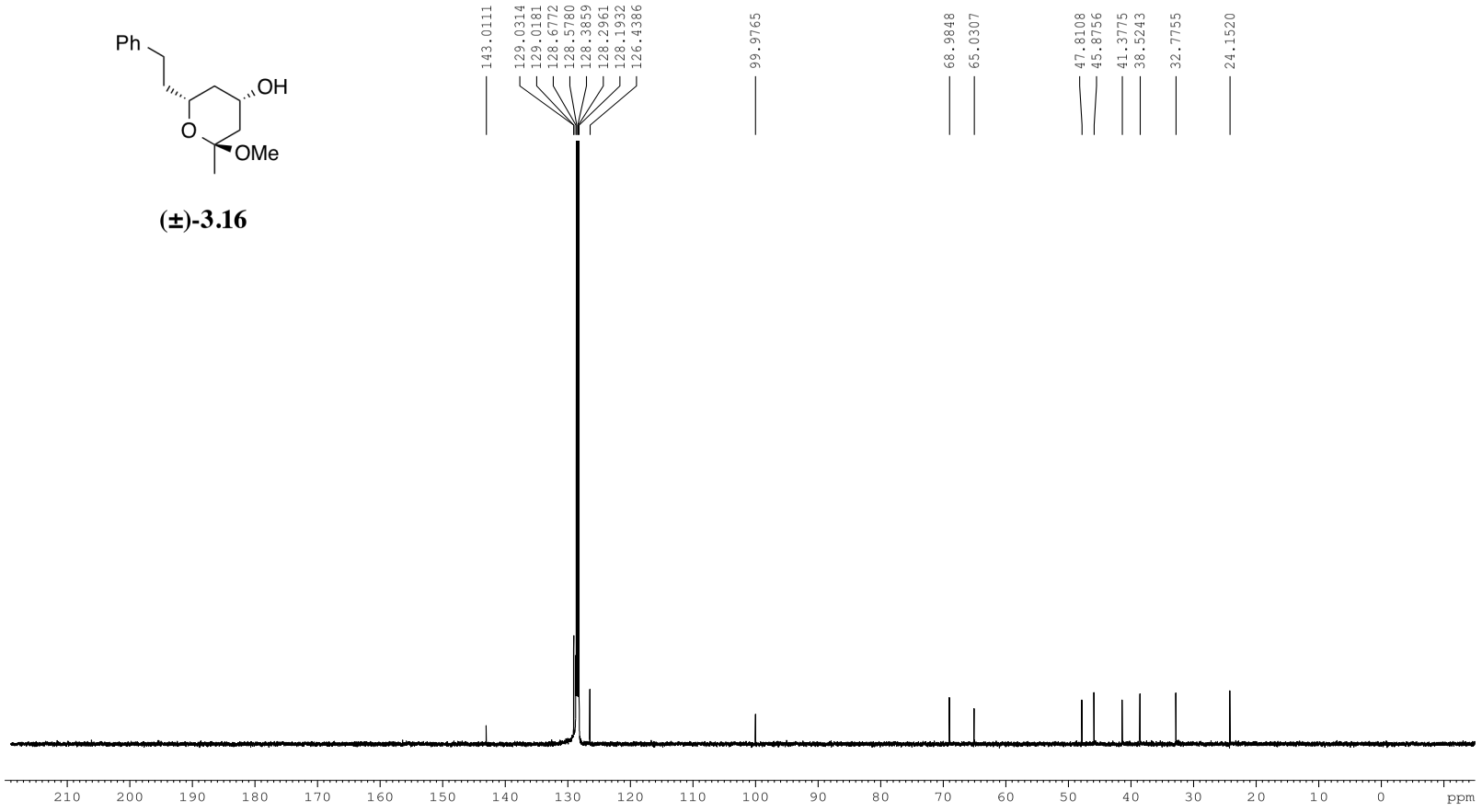

(±)-3.16

Appendix 2: X-ray Data

X-ray Structure Determination of Compound (+)-2.12

Compound (+)-2.12, $C_{16}H_{22}N_2SO_4$, crystallizes in the orthorhombic space group $P2_12_12_1$ (systematic absences h00: h=odd, 0k0: k=odd, and 00l: l=odd) with a=5.13380(10)Å, b=15.8134(4)Å, c=20.2951(5)Å, V=1647.61(7)Å^3, Z=4, and d_{calc}=1.364 g/cm^3 . X-ray intensity data were collected on a Bruker APEXII CCD area detector employing graphite-monochromated Mo-Kα radiation (λ=0.71073 Å) at a temperature of 143(1)K. Preliminary indexing was performed from a series of thirty-six 0.5° rotation frames with exposures of 20 seconds. A total of 1454 frames were collected with a crystal to detector distance of 37.595 mm, rotation widths of 0.5° and exposures of 20 seconds:

scan type	2θ	ω	ϕ	χ	frames
ϕ	-15.50	258.48	-343.84	19.46	715
ϕ	19.50	59.55	-11.29	-26.26	739

Rotation frames were integrated using SAINT[i], producing a listing of unaveraged F^2 and $\sigma(F^2)$ values which were then passed to the SHELXTL[ii] program package for further processing and structure solution. A total of 21759 reflections were measured over the ranges $2.01 \leq \theta \leq 25.06°$, $-6 \leq h \leq 6$, $-18 \leq k \leq 18$, $-23 \leq l \leq 24$ yielding 2910 unique reflections (Rint = 0.0230). The intensity data were corrected for Lorentz and polarization effects and for absorption using SADABS[iii] (minimum and maximum transmission 0.6850, 0.7452).

The structure was solved by direct methods (SHELXS-97[iv]). Refinement was by full-matrix least squares based on F^2 using SHELXL-97.[v] All reflections were used during refinement. The weighting scheme used was $w=1/[\sigma^2(F_o^2)+ (0.0562P)^2 + 0.6677P]$ where $P = (F_o^2 + 2F_c^2)/3$. Non-hydrogen atoms were refined anisotropically and hydrogen atoms were refined using a riding model. Refinement converged to R1=0.0328 and wR2=0.0917 for 2779 observed reflections for which $F > 4\sigma(F)$ and R1=0.0348 and wR2=0.0936 and GOF =1.067 for all 2910 unique, non-zero reflections and 212 variables.[vi] The maximum Δ/σ in the final cycle of least squares was 0.000

and the two most prominent peaks in the final difference Fourier were +0.891 and -0.258 e/Å^3.

Table A-2.1.1. lists cell information, data collection parameters, and refinement data. Final positional and equivalent isotropic thermal parameters are given in Tables 2. and 3. Anisotropic thermal parameters are in Table 4. Tables 5. and 6. list bond distances and bond angles. **Figure A-2.1.1**. is an ORTEP[vii] representation of the molecule with 30% probability thermal ellipsoids displayed.

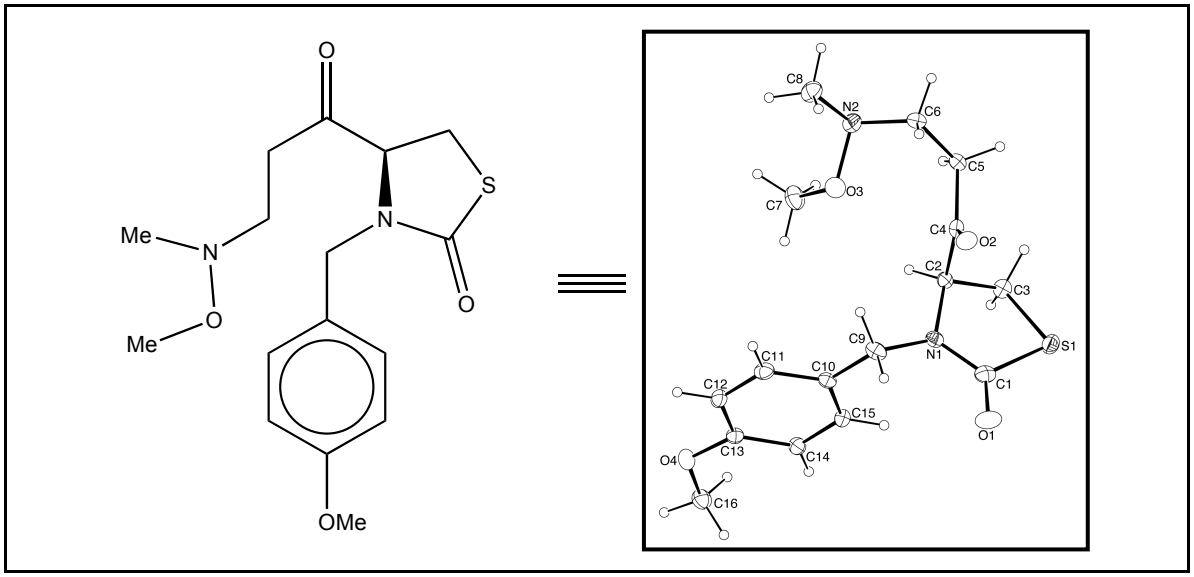

Figure A-2.1.1. ORTEP drawing of (+)-**2.12** with 30% probability thermal ellipsoids.

Table A-2.1.1. Summary of Structure Determination of Compound (+)-2.12

Empirical formula	$C_{16}H_{22}N_2SO_4$
Formula weight	338.42
Temperature	143(1) K
Wavelength	0.71073 Å
Crystal system	orthorhombic
Space group	$P2_12_12_1$
Cell constants:	
a	5.13380(10) Å
b	15.8134(4) Å
c	20.2951(5) Å
Volume	1647.61(7) $Å^3$
Z	4
Density (calculated)	1.364 Mg/m^3
Absorption coefficient	0.218 mm^{-1}
F(000)	720
Crystal size	0.30 x 0.15 x 0.03 mm^3
Theta range for data collection	2.01 to 25.06°
Index ranges	$-6 \le h \le 6$, $-18 \le k \le 18$, $-23 \le l \le 24$
Reflections collected	21759
Independent reflections	2910 [R(int) = 0.0230]
Completeness to theta = 25.06°	99.9 %
Absorption correction	Semi-empirical from equivalents
Max. and min. transmission	0.7452 and 0.6850
Refinement method	Full-matrix least-squares on F^2
Data / restraints / parameters	2910 / 0 / 212
Goodness-of-fit on F^2	1.067
Final R indices [I>2sigma(I)]	R1 = 0.0328, wR2 = 0.0917
R indices (all data)	R1 = 0.0348, wR2 = 0.0936
Absolute structure parameter	0.01(8)
Largest diff. peak and hole	0.891 and -0.258 $e.Å^{-3}$

Table A-2.1.2. Refined Positional Parameters for Compound (+)-2.12

Atom	x	y	z	U_{eq}, A^2
C1	1.0524(4)	0.62084(14)	0.33835(10)	0.0279(5)
C2	0.7930(4)	0.66507(12)	0.24772(10)	0.0208(4)
C3	0.6820(4)	0.57638(13)	0.25899(11)	0.0264(5)
C4	0.9657(4)	0.66593(12)	0.18627(11)	0.0215(4)
C5	0.8329(4)	0.65989(13)	0.11968(10)	0.0235(4)
C6	0.9336(5)	0.72774(13)	0.07314(9)	0.0255(4)
C7	0.5778(5)	0.86525(16)	0.17121(13)	0.0391(6)
C8	0.9230(6)	0.87532(15)	0.04552(12)	0.0377(6)
C9	1.0274(4)	0.77284(14)	0.31757(11)	0.0283(5)
C10	0.8332(4)	0.82437(13)	0.35701(10)	0.0234(4)
C11	0.8233(5)	0.91214(14)	0.34929(10)	0.0278(5)
C12	0.6528(4)	0.96067(13)	0.38572(10)	0.0274(5)
C13	0.4850(4)	0.92319(13)	0.43070(10)	0.0242(5)
C14	0.4946(4)	0.83623(13)	0.43957(10)	0.0244(5)
C15	0.6676(4)	0.78818(13)	0.40261(10)	0.0250(5)
C16	0.1490(5)	0.93992(15)	0.51089(11)	0.0327(5)
N1	0.9422(3)	0.68590(11)	0.30617(8)	0.0239(4)
N2	0.7949(4)	0.80715(12)	0.08224(9)	0.0337(5)
O1	1.2150(4)	0.62468(12)	0.38164(8)	0.0414(4)
O2	1.2001(3)	0.66794(10)	0.19108(8)	0.0278(3)
O3	0.8202(3)	0.82747(10)	0.15091(8)	0.0346(4)
O4	0.3192(3)	0.97644(9)	0.46304(8)	0.0302(4)
S1	0.92494(11)	0.52264(3)	0.30868(3)	0.03006(15)

$U_{eq}={}^{1}/_{3}[U_{11}(aa^*)^2+U_{22}(bb^*)^2+U_{33}(cc^*)^2+2U_{12}aa^*bb^*\cos\gamma+2U_{13}aa^*cc^*\cos\beta+2U_{23}bb^*cc^*\cos\alpha]$

Table A-2.1.3. Positional Parameters for Hydrogens in Compound (+)-2.12

Atom	x	y	z	U_{iso}, A^2
H2	0.6502	0.7056	0.2424	0.028
H3a	0.6563	0.5473	0.2174	0.034
H3b	0.5167	0.5792	0.2820	0.034
H5a	0.6463	0.6664	0.1253	0.031
H5b	0.8649	0.6045	0.1008	0.031
H6a	1.1179	0.7366	0.0810	0.033
H6b	0.9125	0.7088	0.0280	0.033
H7a	0.5518	0.9173	0.1477	0.059
H7b	0.5831	0.8765	0.2177	0.059
H7c	0.4370	0.8272	0.1618	0.059
H8a	0.8411	0.9282	0.0559	0.057
H8b	0.9080	0.8646	-0.0009	0.057
H8c	1.1037	0.8777	0.0575	0.057
H9a	1.0558	0.8002	0.2754	0.037
H9b	1.1924	0.7720	0.3409	0.037
H11	0.9334	0.9382	0.3191	0.037
H12	0.6503	1.0190	0.3801	0.036
H14	0.3858	0.8103	0.4701	0.033
H15	0.6721	0.7299	0.4088	0.033
H16a	0.0407	0.8982	0.4901	0.049
H16b	0.0417	0.9833	0.5298	0.049
H16c	0.2504	0.9136	0.5450	0.049

Table A-2.1.4. Refined Thermal Parameters (U's) for Compound (+)-2.12

Atom	U_{11}	U_{22}	U_{33}	U_{23}	U_{13}	U_{12}
C1	0.0221(11)	0.0394(12)	0.0222(10)	0.0006(9)	0.0052(9)	0.0041(10)
C2	0.0173(9)	0.0223(10)	0.0229(10)	-0.0022(8)	-0.0019(9)	0.0032(8)
C3	0.0228(10)	0.0274(11)	0.0289(11)	0.0010(8)	0.0007(9)	-0.0006(9)
C4	0.0199(11)	0.0176(9)	0.0270(10)	0.0003(8)	-0.0005(9)	0.0005(8)
C5	0.0238(10)	0.0241(10)	0.0225(10)	-0.0045(8)	-0.0005(9)	-0.0011(9)
C6	0.0251(10)	0.0318(11)	0.0196(10)	-0.0023(8)	-0.0004(9)	-0.0002(10)
C7	0.0381(13)	0.0345(12)	0.0449(14)	-0.0063(10)	0.0097(12)	0.0051(12)
C8	0.0439(14)	0.0342(12)	0.0352(12)	0.0077(10)	0.0034(12)	-0.0014(12)
C9	0.0250(11)	0.0338(12)	0.0261(11)	-0.0058(9)	0.0028(9)	-0.0065(9)
C10	0.0235(10)	0.0263(10)	0.0205(10)	-0.0035(8)	-0.0042(8)	-0.0023(9)
C11	0.0313(12)	0.0293(11)	0.0228(10)	0.0043(9)	0.0009(9)	-0.0080(9)
C12	0.0345(12)	0.0197(10)	0.0282(11)	0.0017(8)	-0.0052(9)	-0.0022(9)
C13	0.0258(11)	0.0246(10)	0.0221(10)	-0.0004(8)	-0.0065(8)	0.0005(9)
C14	0.0276(12)	0.0220(10)	0.0238(10)	0.0005(8)	0.0032(8)	-0.0046(8)
C15	0.0295(11)	0.0197(9)	0.0258(10)	0.0017(8)	-0.0011(9)	0.0006(9)
C16	0.0328(13)	0.0343(12)	0.0310(12)	-0.0043(10)	0.0035(10)	0.0054(10)
N1	0.0231(8)	0.0274(9)	0.0210(8)	-0.0028(7)	0.0018(8)	0.0013(8)
N2	0.0438(12)	0.0288(10)	0.0285(10)	0.0042(8)	0.0030(10)	0.0025(9)
O1	0.0360(9)	0.0601(11)	0.0280(8)	0.0034(8)	-0.0086(8)	0.0028(9)
O2	0.0186(8)	0.0372(8)	0.0275(7)	0.0038(7)	0.0014(7)	0.0006(6)
O3	0.0329(9)	0.0357(9)	0.0352(9)	-0.0030(7)	-0.0031(8)	0.0029(8)
O4	0.0331(8)	0.0229(7)	0.0345(8)	-0.0032(7)	0.0031(7)	0.0018(7)
S1	0.0331(3)	0.0269(3)	0.0302(3)	0.0049(2)	0.0043(3)	0.0068(2)

The form of the anisotropic displacement parameter is:

$\exp[-2\pi^2(a^{*2}U_{11}h^2+b^{*2}U_{22}k^2+c^{*2}U_{33}l^2+2b^*c^*U_{23}kl+2a^*c^*U_{13}hl+2a^*b^*U_{12}hk)]$

Table A-2.1.5. Bond Distances in Compound (+)-2.12, Å

C1-O1	1.213(3)	C1-N1	1.343(3)	C1-S1	1.790(2)
C2-N1	1.450(3)	C2-C4	1.530(3)	C2-C3	1.531(3)
C3-S1	1.815(2)	C4-O2	1.207(3)	C4-C5	1.517(3)
C5-C6	1.520(3)	C6-N2	1.455(3)	C7-O3	1.441(3)
C8-N2	1.466(3)	C9-N1	1.461(3)	C9-C10	1.516(3)
C10-C15	1.381(3)	C10-C11	1.398(3)	C11-C12	1.379(3)
C12-C13	1.388(3)	C13-O4	1.365(3)	C13-C14	1.388(3)
C14-C15	1.389(3)	C16-O4	1.428(3)	N2-O3	1.436(3)

Table A-2.1.6. Bond Angles in Compound (+)-2.12, °

O1-C1-N1	127.1(2)	O1-C1-S1	122.59(18)	N1-C1-S1	110.30(16)
N1-C2-C4	111.01(17)	N1-C2-C3	106.40(16)	C4-C2-C3	110.22(16)
C2-C3-S1	104.84(14)	O2-C4-C5	121.5(2)	O2-C4-C2	120.8(2)
C5-C4-C2	117.69(17)	C4-C5-C6	110.87(17)	N2-C6-C5	111.33(18)
N1-C9-C10	113.10(18)	C15-C10-C11	117.7(2)	C15-C10-C9	122.41(19)
C11-C10-C9	119.88(19)	C12-C11-C10	121.0(2)	C11-C12-C13	120.6(2)
O4-C13-C14	124.8(2)	O4-C13-C12	116.09(18)	C14-C13-C12	119.1(2)
C13-C14-C15	119.7(2)	C10-C15-C14	121.93(19)	C1-N1-C2	116.51(17)
C1-N1-C9	121.16(18)	C2-N1-C9	120.09(17)	O3-N2-C6	105.78(16)
O3-N2-C8	106.75(18)	C6-N2-C8	110.51(19)	N2-O3-C7	106.98(18)
C13-O4-C16	117.30(17)	C1-S1-C3	91.84(10)		

References:

[i]Bruker (2009) SAINT. Bruker AXS Inc., Madison, Wisconsin, USA.

[ii]Bruker (2009) SHELXTL. Bruker AXS Inc., Madison, Wisconsin, USA.

[iii]Sheldrick, G.M. (2007) SADABS. University of Gottingen, Germany.

[iv]Sheldrick, G.M. (2008) Acta Cryst. A64,112-122.

[v]Sheldrick, G.M. (2008) Acta Cryst. A64,112-122.

[vi]$R1 = S||F_o| - |F_c|| / S |F_o|$

$wR2 = [Sw(F_o^2 - F_c^2)^2/Sw(F_o^2)^2]^{½}$

$GOF = [Sw(F_o^2 - F_c^2)^2/(n - p)]^{½}$

where n = the number of reflections and p = the number of parameters refined.

[vii]"ORTEP-II: A Fortran Thermal Ellipsoid Plot Program for Crystal Structure Illustrations". C.K. Johnson (1976) ORNL-5138.

X-ray Structure Determination of Compound (+)-2.21

Compound (+)-2.21, $C_{29}H_{45}SiNSO_5$, crystallizes in the monoclinic space group $P2_1$ (systematic absences 0k0: k=odd) with a=7.9222(4)Å, b=9.8530(4)Å, c=20.0514(10)Å, β=92.404(2)°, V=1563.78(13)Å^3, Z=2, and d_{calc}=1.163 g/cm^3 . X-ray intensity data were collected on a Bruker APEXII CCD area detector employing graphite-monochromated Mo-Kα radiation (λ=0.71073 Å) at a temperature of 143(1)K. Preliminary indexing was performed from a series of thirty-six 0.5° rotation frames with exposures of 25 seconds. A total of 1904 frames were collected with a crystal to detector distance of 37.600 mm, rotation widths of 0.5° and exposures of 25 seconds:

scan type	2θ	ω	ϕ	χ	frames
ϕ	-15.50	258.48	8.97	19.46	681
ϕ	-8.00	-39.98	-206.70	55.93	485
ϕ	19.50	59.55	-11.22	-26.26	739

Rotation frames were integrated using SAINT[vii], producing a listing of unaveraged F^2 and $\sigma(F^2)$ values which were then passed to the SHELXTL[vii] program package for further processing and structure solution. A total of 26518 reflections were measured over the ranges $2.30 \leq \theta \leq 25.07°$, $-9 \leq h \leq 9$, $-11 \leq k \leq 10$, $-23 \leq l \leq 23$ yielding 5405 unique reflections (Rint = 0.0182). The intensity data were corrected for Lorentz and polarization effects and for absorption using SADABS[vii] (minimum and maximum transmission 0.6977, 0.7452).

The structure was solved by direct methods (SHELXS-97[vii]). Refinement was by full-matrix least squares based on F^2 using SHELXL-97.[vii] All reflections were used during refinement. The weighting scheme used was $w=1/[\sigma^2(F_o^2)+ (0.0675P)^2 + 0.6644P]$ where $P = (F_o^2 + 2F_c^2)/3$. Non-hydrogen atoms were refined anisotropically and hydrogen atoms were refined using a riding model. Refinement converged to R1=0.0413 and wR2=0.1108 for 5055 observed reflections for

which F > 4σ(F) and R1=0.0453 and wR2=0.1146 and GOF =1.037 for all 5405 unique, non-zero reflections and 343 variables.[vii] The maximum Δ/σ in the final cycle of least squares was 0.005 and the two most prominent peaks in the final difference Fourier were +0.653 and -0.286 e/Å^3.

Table A-2.2.1. lists cell information, data collection parameters, and refinement data. Final positional and equivalent isotropic thermal parameters are given in Tables 2. and 3. Anisotropic thermal parameters are in Table 4. Tables 5. and 6. list bond distances and bond angles. **Figure A-2.2.1**. is an ORTEP[vii] representation of the molecule with 30% probability thermal ellipsoids displayed.

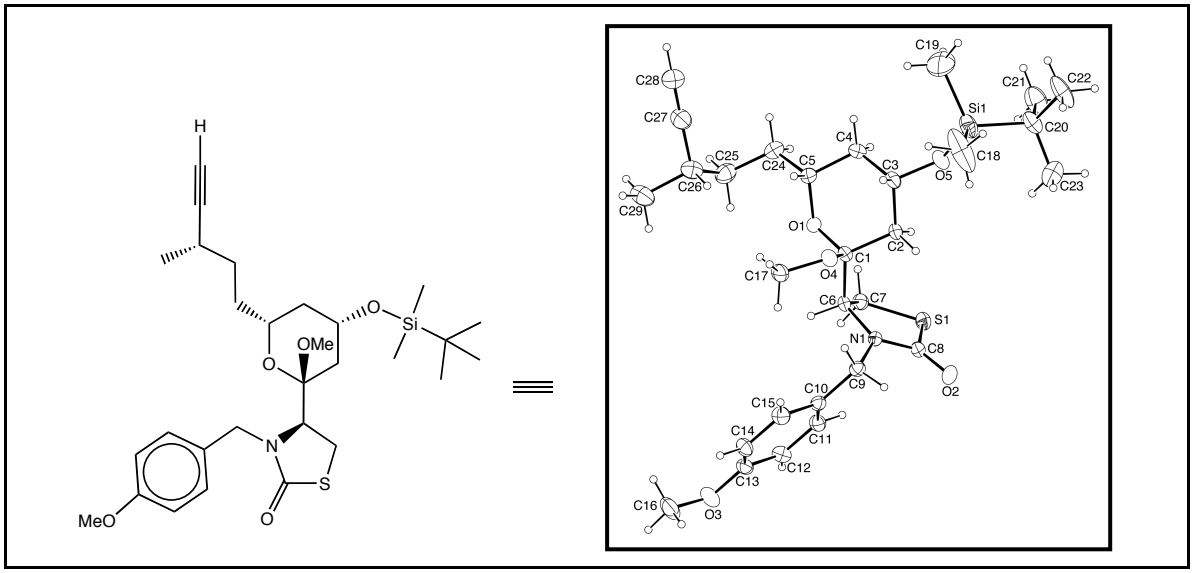

Figure A-2.2.1. ORTEP drawing of the Compound (+)-**2.21** with 30% probability thermal ellipsoids.

Table A-2.2.1. Summary of Structure Determination of Compound (+)-2.21

Empirical formula	$C_{29}H_{45}SiNSO_5$
Formula weight	547.81
Temperature	143(1) K
Wavelength	0.71073 Å
Crystal system	monoclinic
Space group	$P2_1$
Cell constants:	
a	7.9222(4) Å
b	9.8530(4) Å
c	20.0514(10) Å
β	92.404(2)°
Volume	1563.78(13) $Å^3$
Z	2
Density (calculated)	1.163 Mg/m^3
Absorption coefficient	0.177 mm^{-1}
F(000)	592
Crystal size	0.45 x 0.10 x 0.05 mm^3
Theta range for data collection	2.30 to 25.07°
Index ranges	$-9 \le h \le 9$, $-11 \le k \le 10$, $-23 \le l \le 23$
Reflections collected	26518
Independent reflections	5405 [R(int) = 0.0182]
Completeness to theta = 25.07°	99.9 %
Absorption correction	Semi-empirical from equivalents
Max. and min. transmission	0.7452 and 0.6977
Refinement method	Full-matrix least-squares on F^2
Data / restraints / parameters	5405 / 1 / 343
Goodness-of-fit on F^2	1.037

Final R indices [I>2sigma(I)]	R1 = 0.0413, wR2 = 0.1108
R indices (all data)	R1 = 0.0453, wR2 = 0.1146
Absolute structure parameter	0.02(8)
Largest diff. peak and hole	0.653 and -0.286 e.Å^{-3}

Table A-2.2.2. Refined Positional Parameters for Compound (+)-2.21

Atom	x	y	z	U_{eq}, A^2
C1	0.6869(3)	0.5587(3)	0.31046(12)	0.0315(5)
C2	0.5299(3)	0.5016(3)	0.27326(12)	0.0325(5)
C3	0.5569(3)	0.4901(3)	0.19894(12)	0.0360(5)
C4	0.6172(3)	0.6261(3)	0.17233(12)	0.0409(6)
C5	0.7712(4)	0.6773(3)	0.21214(13)	0.0418(6)
C6	0.6587(3)	0.5935(3)	0.38480(11)	0.0314(5)
C7	0.5264(3)	0.7026(3)	0.39484(13)	0.0358(6)
C8	0.4421(3)	0.4643(3)	0.43650(12)	0.0325(5)
C9	0.7289(3)	0.3800(3)	0.45318(12)	0.0325(5)
C10	0.8331(3)	0.4465(3)	0.50883(12)	0.0320(5)
C11	0.7676(3)	0.5479(3)	0.54818(13)	0.0365(6)
C12	0.8636(3)	0.6091(3)	0.59870(12)	0.0409(6)
C13	1.0306(4)	0.5684(3)	0.61088(13)	0.0405(6)
C14	1.0981(3)	0.4688(3)	0.57227(14)	0.0435(6)
C15	0.9997(3)	0.4091(3)	0.52132(14)	0.0420(6)
C16	1.2910(4)	0.6057(5)	0.67301(19)	0.0701(10)
C17	0.9785(3)	0.4936(4)	0.32871(14)	0.0489(7)
C18	0.4860(6)	0.1885(6)	0.1243(4)	0.133(3)
C19	0.4358(8)	0.4235(10)	0.0279(2)	0.156(3)
C20	0.1316(4)	0.3187(3)	0.10072(17)	0.0551(8)
C21	0.0397(5)	0.4497(4)	0.0842(2)	0.0777(11)
C22	0.0881(6)	0.2134(4)	0.0460(3)	0.0930(16)
C23	0.0746(6)	0.2688(6)	0.1686(3)	0.0969(16)

C24	0.8193(4)	0.8216(4)	0.19183(15)	0.0541(8)
C25	0.9666(4)	0.8823(3)	0.23067(17)	0.0567(8)
C26	1.1380(4)	0.8203(4)	0.21775(15)	0.0545(8)
C27	1.1823(4)	0.8330(4)	0.14723(16)	0.0579(8)
C28	1.2173(5)	0.8403(5)	0.09099(18)	0.0688(10)
C29	1.2800(5)	0.8929(4)	0.26179(17)	0.0674(10)
N1	0.6068(2)	0.4732(2)	0.42160(10)	0.0304(4)
O1	0.7363(2)	0.68346(19)	0.28261(8)	0.0362(4)
O2	0.3745(2)	0.3684(2)	0.46237(10)	0.0438(5)
O3	1.1170(3)	0.6373(2)	0.66120(11)	0.0562(6)
O4	0.8117(2)	0.4579(2)	0.30462(9)	0.0393(4)
O5	0.3974(2)	0.4546(2)	0.16727(9)	0.0442(5)
S1	0.33204(7)	0.61662(7)	0.41375(3)	0.03750(16)
Si1	0.36412(11)	0.34500(10)	0.10758(5)	0.0584(3)

$U_{eq}={}^{1}/_{3}[U_{11}(aa^*)^2+U_{22}(bb^*)^2+U_{33}(cc^*)^2+2U_{12}aa^*bb^*\cos\gamma+2U_{13}aa^*cc^*\cos\beta+2U_{23}bb^*cc^*\cos\alpha]$

Table A-2.2.3. Positional Parameters for Hydrogens in Compound (+)-2.21

Atom	x	y	z	U_{iso}, A^2
H2a	0.5042	0.4127	0.2910	0.043
H2b	0.4342	0.5605	0.2804	0.043
H3	0.6405	0.4194	0.1907	0.048
H4a	0.6448	0.6160	0.1259	0.054
H4b	0.5269	0.6923	0.1745	0.054
H5	0.8666	0.6161	0.2057	0.056
H6	0.7663	0.6255	0.4050	0.042
H7a	0.5102	0.7568	0.3547	0.048
H7b	0.5620	0.7621	0.4314	0.048
H9a	0.8036	0.3464	0.4198	0.043
H9b	0.6693	0.3029	0.4709	0.043
H11	0.6562	0.5754	0.5403	0.049

H12	0.8173	0.6770	0.6245	0.054
H14	1.2094	0.4413	0.5802	0.058
H15	1.0469	0.3424	0.4950	0.056
H16a	1.3025	0.5117	0.6849	0.105
H16b	1.3368	0.6611	0.7088	0.105
H16c	1.3511	0.6231	0.6333	0.105
H17a	1.0023	0.5855	0.3163	0.073
H17b	1.0590	0.4339	0.3095	0.073
H17c	0.9860	0.4854	0.3764	0.073
H18a	0.6041	0.2065	0.1197	0.199
H18b	0.4498	0.1196	0.0931	0.199
H18c	0.4677	0.1580	0.1689	0.199
H19a	0.3771	0.5076	0.0200	0.234
H19b	0.4118	0.3626	-0.0086	0.234
H19c	0.5552	0.4404	0.0318	0.234
H21a	0.0748	0.4833	0.0420	0.117
H21b	0.0659	0.5156	0.1183	0.117
H21c	-0.0798	0.4334	0.0817	0.117
H22a	-0.0323	0.2041	0.0408	0.140
H22b	0.1372	0.1275	0.0584	0.140
H22c	0.1325	0.2430	0.0046	0.140
H23a	0.1106	0.3323	0.2027	0.145
H23b	0.1239	0.1817	0.1782	0.145
H23c	-0.0463	0.2614	0.1674	0.145
H24a	0.8449	0.8210	0.1449	0.072
H24b	0.7220	0.8800	0.1967	0.072
H25a	0.9464	0.8737	0.2779	0.075
H25b	0.9711	0.9785	0.2205	0.075
H26	1.1359	0.7239	0.2297	0.072
H28	1.2449	0.8461	0.0465	0.091
H29a	1.3860	0.8482	0.2561	0.101

H29b	1.2521	0.8888	0.3079	0.101
H29c	1.2885	0.9861	0.2483	0.101

Table A-2.2.4. Refined Thermal Parameters (U's) for Compound (+)-2.21

Atom	U_{11}	U_{22}	U_{33}	U_{23}	U_{13}	U_{12}
C1	0.0279(12)	0.0357(13)	0.0307(12)	-0.0005(10)	-0.0031(10)	-0.0015(10)
C2	0.0296(12)	0.0336(14)	0.0340(12)	-0.0026(10)	-0.0032(10)	-0.0062(10)
C3	0.0322(12)	0.0404(14)	0.0350(12)	-0.0068(11)	-0.0049(10)	-0.0018(11)
C4	0.0434(14)	0.0510(16)	0.0280(12)	0.0005(12)	-0.0028(10)	-0.0025(14)
C5	0.0416(15)	0.0536(16)	0.0303(13)	0.0000(12)	0.0038(11)	-0.0106(13)
C6	0.0261(11)	0.0364(15)	0.0311(11)	0.0002(10)	-0.0041(8)	-0.0078(10)
C7	0.0394(14)	0.0325(14)	0.0353(13)	-0.0002(10)	-0.0017(10)	-0.0045(11)
C8	0.0294(12)	0.0370(14)	0.0310(12)	-0.0019(10)	-0.0013(9)	-0.0040(11)
C9	0.0330(12)	0.0315(13)	0.0332(12)	0.0034(10)	0.0021(10)	0.0019(10)
C10	0.0302(12)	0.0334(13)	0.0323(12)	0.0072(10)	0.0012(9)	0.0011(10)
C11	0.0300(13)	0.0415(15)	0.0378(13)	0.0023(11)	-0.0013(10)	0.0054(11)
C12	0.0481(15)	0.0387(15)	0.0354(13)	-0.0014(12)	-0.0025(11)	0.0048(13)
C13	0.0454(15)	0.0405(15)	0.0347(13)	0.0066(11)	-0.0087(11)	-0.0063(11)
C14	0.0304(13)	0.0519(18)	0.0474(15)	0.0051(13)	-0.0091(11)	0.0045(12)
C15	0.0371(14)	0.0437(16)	0.0451(15)	0.0009(12)	0.0017(11)	0.0090(12)
C16	0.063(2)	0.072(2)	0.071(2)	0.010(2)	-0.0357(17)	-0.012(2)
C17	0.0294(13)	0.075(2)	0.0421(15)	0.0022(14)	-0.0003(11)	0.0029(14)
C18	0.079(3)	0.089(4)	0.225(7)	-0.087(4)	-0.066(4)	0.037(3)
C19	0.162(6)	0.256(9)	0.053(3)	-0.041(4)	0.039(3)	-0.094(6)
C20	0.0540(17)	0.0479(18)	0.0615(19)	-0.0112(15)	-0.0199(15)	0.0003(15)
C21	0.068(2)	0.056(2)	0.106(3)	-0.002(2)	-0.027(2)	0.0090(19)
C22	0.082(3)	0.069(3)	0.123(4)	-0.042(3)	-0.053(3)	0.001(2)
C23	0.077(3)	0.115(4)	0.099(3)	0.023(3)	0.010(2)	-0.032(3)
C24	0.0574(18)	0.062(2)	0.0437(16)	0.0097(15)	0.0062(13)	-0.0108(16)

C25	0.070(2)	0.0450(18)	0.0562(18)	0.0028(14)	0.0106(15)	-0.0072(15)
C26	0.0636(19)	0.0537(19)	0.0457(16)	0.0038(14)	-0.0023(14)	0.0061(16)
C27	0.0525(17)	0.068(2)	0.0526(19)	-0.0064(16)	-0.0026(14)	0.0046(16)
C28	0.070(2)	0.086(3)	0.050(2)	0.0036(19)	0.0045(16)	-0.005(2)
C29	0.063(2)	0.084(3)	0.0532(19)	-0.0055(18)	-0.0113(16)	0.0132(19)
N1	0.0272(9)	0.0339(11)	0.0301(10)	0.0039(8)	-0.0003(8)	-0.0040(8)
O1	0.0372(9)	0.0418(10)	0.0297(9)	-0.0003(8)	0.0017(7)	-0.0128(8)
O2	0.0370(10)	0.0429(12)	0.0519(11)	0.0064(9)	0.0047(8)	-0.0103(8)
O3	0.0598(13)	0.0542(14)	0.0525(12)	-0.0010(10)	-0.0221(10)	-0.0100(11)
O4	0.0290(9)	0.0507(12)	0.0381(9)	-0.0030(8)	-0.0006(7)	0.0033(8)
O5	0.0380(10)	0.0517(12)	0.0420(10)	-0.0131(9)	-0.0092(8)	-0.0014(9)
S1	0.0290(3)	0.0408(3)	0.0425(3)	-0.0030(3)	-0.0007(2)	0.0005(3)
Si1	0.0450(5)	0.0675(6)	0.0622(5)	-0.0332(5)	-0.0043(4)	-0.0038(4)

The form of the anisotropic displacement parameter is:
$\exp[-2\pi^2(a^{*2}U_{11}h^2+b^{*2}U_{22}k^2+c^{*2}U_{33}l^2+2b^*c^*U_{23}kl+2a^*c^*U_{13}hl+2a^*b^*U_{12}hk)]$

Table A-2.2.5. Bond Distances in Compound (+)-2.21, Å

C1-O4	1.410(3)	C1-O1	1.412(3)	C1-C2	1.531(3)
C1-C6	1.555(3)	C2-C3	1.519(3)	C3-O5	1.433(3)
C3-C4	1.527(4)	C4-C5	1.516(4)	C5-O1	1.4521673)
C5-C24	1.532(5)	C6-N1	1.464(3)	C6-C7	1.521(4)
C7-S1	1.812(3)	C8-O2	1.213(3)	C8-N1	1.354(3)
C8-S1	1.785(3)	C9-N1	1.459(3)	C9-C10	1.509(3)
C10-C15	1.383(3)	C10-C11	1.387(4)	C11-C12	1.380(4)
C12-C13	1.394(4)	C13-C14	1.373(4)	C13-O3	1.374(3)
C14-C15	1.389(4)	C16-O3	1.424(4)	C17-O4	1.431(3)
C18-Si1	1.843(5)	C19-Si1	1.884(6)	C20-C21	1.511(5)
C20-C23	1.533(6)	C20-C22	1.538(5)	C20-Si1	1.860(3)
C24-C25	1.500(5)	C25-C26	1.521(5)	C26-C27	1.476(4)
C26-C29	1.573(5)	C27-C28	1.175(5)	O5-Si1	1.6252(19)

Table A-2.2.6. Bond Angles in Compound (+)-2.21, °

O4-C1-O1	111.90(19)	O4-C1-C2	105.0(2)	O1-C1-C2	111.1(2)
O4-C1-C6	111.37(19)	O1-C1-C6	103.92(19)	C2-C1-C6	113.70(19)
C3-C2-C1	111.15(19)	O5-C3-C2	107.18(19)	O5-C3-C4	110.0(2)
C2-C3-C4	109.7(2)	C5-C4-C3	111.4(2)	O1-C5-C4	110.2(2)
O1-C5-C24	106.2(2)	C4-C5-C24	111.9(3)	N1-C6-C7	107.20(19)
N1-C6-C1	111.07(19)	C7-C6-C1	114.22(19)	C6-C7-S1	107.07(17)
O2-C8-N1	126.3(2)	O2-C8-S1	123.00(19)	N1-C8-S1	110.74(18)
N1-C9-C10	112.3(2)	C15-C10-C11	117.8(2)	C15-C10-C9	120.4(2)
C11-C10-C9	121.8(2)	C12-C11-C10	121.6(2)	C11-C12-C13	119.6(3)
C14-C13-O3	125.0(3)	C14-C13-C12	119.7(2)	O3-C13-C12	115.2(3)
C13-C14-C15	119.9(2)	C10-C15-C14	121.5(3)	C21-C20-C23	108.2(4)
C21-C20-C22	109.1(3)	C23-C20-C22	110.6(4)	C21-C20-Si1	111.3(3)
C23-C20-Si1	107.8(2)	C22-C20-Si1	109.7(3)	C25-C24-C5	115.4(3)
C24-C25-C26	115.6(3)	C27-C26-C25	112.3(3)	C27-C26-C29	107.8(3)
C25-C26-C29	110.1(3)	C28-C27-C26	178.7(4)	C8-N1-C9	119.4(2)
C8-N1-C6	117.2(2)	C9-N1-C6	122.21(18)	C1-O1-C5	114.6(2)
C13-O3-C16	117.6(3)	C1-O4-C17	116.1(2)	C3-O5-Si1	126.97(17)
C8-S1-C7	92.09(12)	O5-Si1-C18	110.72(19)	O5-Si1-C20	106.06(13)
C18-Si1-C20	114.0(2)	O5-Si1-C19	107.8(2)	C18-Si1-C19	108.9(4)
C20-Si1-C19	109.1(2)				

References:

[vii]Bruker (2009) SAINT. Bruker AXS Inc., Madison, Wisconsin, USA.

[vii]Bruker (2009) SHELXTL. Bruker AXS Inc., Madison, Wisconsin, USA.

[vii]Sheldrick, G.M. (2007) SADABS. University of Gottingen, Germany.

[vii]Sheldrick, G.M. (2008) Acta Cryst. A64,112-122.

[vii]Sheldrick, G.M. (2008) Acta Cryst. A64,112-122.

[vii]$R1 = S||F_o| - |F_c|| / S |F_o|$

$wR2 = [Sw(F_o^2 - F_c^2)^2/Sw(F_o^2)^2]^{½}$

$GOF = [Sw(F_o^2 - F_c^2)^2/(n - p)]^{½}$

where n = the number of reflections and p = the number of parameters refined.

[vii]"ORTEP-II: A Fortran Thermal Ellipsoid Plot Program for Crystal Structure Illustrations". C.K. Johnson (1976) ORNL-5138.

BIBLIOGRAPHY

Allingham, J. S.; Klenchin, V. A.; Rayment, I. *Cell. Mol. Life Sci.* **2006**, 63, 2119-2134.

Amagata, T.; Johnson, T. A.; Cichewicz, R. H.; Tenney, K.; Mooberry, S. L.; Media, J.; Edelstein, M.; Valeriote, F. A.; Crews, P. *J. Med. Chem.* **2008**, 51, 7234-7242.

Ayscough, K. R.; Stryker, J.; Pokala, N.; Sanders, M.; Crews, P.; Drubin, D. G. *J. Cell Biol.* **1997**, 137, 399-416.

Berretta, G.; Coxon, G. D. *Tetrahedron Lett.* **2012***, 2,* 214-216.

Brown, C. A.; Ahuja, V. K. *J. Chem. Soc., Chem. Commun.*, **1973**, 553-554

Brown, H. C.; Hamaoka, T.; Ravindran, N. *J. Am. Chem. Soc.*, **1973**, *95*, 6456–6457

Brown, H. C.; Jadhav, P. K. *J. Am. Chem. Soc.* **1983***, 7,* 2092-2093.

Chatterjee, A. K.; Choi, T.; Sanders, D. P.; Grubbs, R. H. *J. Am. Chem. Soc*, **2003**, 125 (37), 11360–11370

Chen, K.; Semple, J.; Joullie, M. *J. Org. Chem.* **1985***, 21,* 3997-4005.

Coue, M.; Brenner, S. L.; Spector, I.; Korn, *FEBS Lett.* **1987**, 213, 316-318.

Evans, P. A.; Grisin, A.; Lawler, M. J. *J. Am. Chem. Soc.* **2012**, 134, 2856-2859.

Frantz, D.; Fassler, R.; Carreira, E. *J. Am. Chem. Soc.* **2000***, 8,* 1806-1807.

Fürstner, A.; Kirk, D.; Fenster, M. D. B.; Aissa, C.; De Souza, D.; Muller, O. *Proc. Natl. Acad. Sci. U. S. A.* **2005**, 102, 8103-8108.

Fürstner, A.; Kirk, D.; Fenster, M. B.; Aissa, C.; De Souza, D.; Nevado, C.; Tuttle, T.; Thiel, W.; Mueller, O. *Chem. Eur. J.***2007**, 13, 135-149.

Fürstner, A.; Nagano, T.; Mueller, C.; Seidel, G.; Mueller, O. *Chem. Eur. J.* **2007**, 13, 1452-1462.

Fürstner, A.; Turet, L. *Angew. Chem. Int. Ed.* **2005**, 44, 3462-3466.

Gomtsyan, A. *Org. Lett.* **2000**, 2, 11-13.

Gouiffes, D.; Moreau, S.; Helbecque, N.; Bernier, J. L.; Henichart, J. P.; Barbin, Y.; Laurent, D.; Verbist, J. F. *Tetrahedron,* **1988,** *44* (2), 451-*9*.

Huber, F.; Schnauss, J.; Roenicke, S.; Rauch, P.; Mueller, K.; Fuetterer, C.; Kaes, J. *Adv. Phys.* **2013**, 62, 1-112.

Huerta, F. F.; Minidisa, A. B. E.; Bäckvall, J. *Chem. Soc. Rev.,* **2001**, 30, 321-331

Kashman, Y.; Groweiss, A.; Shueli, U.; *Tetrahedron Lett.* **1980**, *21*, 3629-3633.

Kingsbury, J. S.; Harrity, J. P. A.; Bonitatebus, P. J.; Hoveyda, A. H. *J. Am. Chem. Soc.* **1999***, 4,* 791-799.

Klenchin, V. A.; King, R.; Tanaka, J.; Marriott, G.; and Rayment, I. *Chem. Biol*. **2005**, *12*, 287–291.

Lindlar, H. *Helv. Chim. Acta* **1952**, 35, 446-456.

Li, D. R.; Murugan, A.; Falck, J. R. *J. Am. Chem. Soc.* **2008**, 130, 46-8.

Littlefield, R.; Almenar-Queralt, A.; Fowler, V. M. *Nat. Cell Biol.* **2001**, 3, 544-551.

Lodish, H.; Berk, A.; Zipursky, S. L. Section 18.1, The Actin Cytoskeleton. In *Molecular Cell Biology ;* W. H. Freeman, Ed.; 2000; Vol. 4th edition., pp http://www.ncbi.nlm.nih.gov/books/NBK21493/.

Marshall, J.; Yanik, M. *J. Org. Chem.* **2001***, 4,* 1373-1379

Mitsunobu, O. *Synthesis* **1981***, 1,* 1-28.

Morrison, H.; Rodriguez, O. J. *Photochem.* 1974, 3, 471–474.

Morton, W. M.; Ayscough, K. R.; McLaughlin, P. J. *Nat. Cell Biol.* **2000**, 2, 376-378.

Nahm, S.; Weinreb, S. M. *Tetrahedron Lett.* **1981***, 39,* 3815-3818.

Neeman, I.; Fishelson, L.; Kashman, Y. *Mar. Biol.* **1975**, 30, 293

Newman, D.; Cragg, G. *J. Nat. Prod.* **2004**, 67, 1216-1238.

Ramharter, J.; Mulzer, J. *Org. Lett.* **2009***, 11,* 1151-1153.

Reetz, M. T. *Acc. Chem. Res.* **1993**, 26, 462-468.

Reetz, M. T. *Angew. Chem. Int. Ed.* **1984**, 23, 556-569.

Reguero, M.; Olivucci, M.; Bernardi, F.; Robb, M. A. *J. Am. Chem. Soc.* **1994**, 116, 2103-2114.

Sanger, J. W. *Proc. Natl. Acad. Sci. U. S. A.* **1974**, 71, 3621-3625.

Sasse, F. H.; Steinmetz, G.; Höfle, H. Reichenbach, *J. Antibiot.* **1993**, *46*, 741

Schmidt, B. *J. Org. Chem.* **2004**, 69, 7672-7687

Seki, M.; Hatsuda, M.; Mori, Y.; Yoshida, S.; Yamada, S.; Shimizu, T. *Chem. Eur. J.* **2004***, 23,* 6102-6110.

Sim, H.; Feng, X.; Yun, J. *Chem. Eur. J.* **2009**, 15, 1939-1943.

Smith, A. B.; Noda, I.; Remiszewski, S. W.; Liverton, N. J.; Zibuck, R. *J. Org. Chem.* **1990**, 55, 3977-3979.

Snider, B.; Zhongping S. *J. Am. Chem. Soc.* **1992**, 114, 1790-1800

Spector, I.; Shochet, N.; Kashman, Y.; Groweiss, A. *Science* **1983***, 4584,* 493-495.

Osborn, J. A.; Jardine, F. H.; Young, J. F.; Wilkinson, G. *J. Chem. Soc. A* **1966**, 1711-1732.

Parikh, J.; Doering, W. *J. Am. Chem. Soc.* **1967***, 89,* 5505-5507.

Valeriote, F.; Grieshaber Charles, K.; Media, J.; Pietraszkewicz, H.; Hoffmann, J.; Pan, M.; McLaughlin, S. *J. Exp. Ther. Oncol.* **2002**, 2, 228–236.

Voorhees, V.; Adams, R. *J. Am. Chem. Soc.*, **1922**, *44* (6), 1397–1405

Wang, J. S.; Sanger, J. M.; Sanger, J. W. *Cell Motil. Cytoskeleton* **2005**, 62, 35-47.

White, J. D.; Kawasaki, M. *J. Am. Chem. Soc.* **1990**, 112, 4991-4993.

White, J. D.; Kawasaki, M. *J. Org. Chem*. **1992**, 57, 5292-5300.

Williams, R. M.; Kwast, E. *Tetrahedron Lett.* **1989**, *30*, 451

Wittig, G.; Haag, W. *Chemische Berichte-Recueil* **1955**, 88, 1654-1666.

Wuts, P. G. M. and Greene, T. W. *Greene's Protective Groups in Organic Synthesis*, 4th ed.; Wiley: Hoboken, NJ, **2007**

Yu, S.; Pan, X.; Ma, D. *Chem. Eur. J.* **2006***, 25,* 6572-6584

Zibuck, R.; Liverton, N. J.; Smith, A. B. *J. Am. Chem. Soc.* **1986**, 108 (9), 2451–2453.

Zibuck, R.; Liverton, N. J.; Smith, A. B. *J. Am. Chem. Soc.* **1992**, 114, 2995-3001.

ABOUT THE AUTHOR

Brett Williams was born in 1986 in Smethport, PA to Dan Williams and Becky McKeirnan. The first few years of his life were spent in a humble trailer on top of Bush hill amongst his dear McKeirnan family. From 1990-1997, Brett and his mother toured the states of Pennsylvania and New York moving to a new town or city each year, but in the summer of 1997 they came full circle and moved to an Angus cattle farm in Port Allegany, PA, which was only one hill away from their McKeirnan family members.

Upon moving to the farm, Brett quickly learned the value of hard work, where the requirement for such was always plentiful. He simultaneously acquired a distaste for the mindless labor that was also bountiful. At Port Allegany High School, Brett was fascinated by both music and science classes. Throughout his schooling, he learned to play several instruments and developed an interest in the physical sciences that has guided him through his ensuing endeavors.

In 2004, Brett enrolled at Duquesne University in Pittsburgh, PA with the intention of becoming a pharmacist. However, after taking organic chemistry I and II *via* two four week sessions at the University of Pittsburgh the summer of his freshman year, he quickly changed his major to chemistry and transferred to Pitt. At the University of Pittsburgh, Brett joined the research group of Professor Craig Wilcox and after working briefly on Wilcox's "precipiton" project he was given the opportunity to study the effect of additives on the rate and E/Z selectivity of the Wittig olefination.

During the summer of 2007, Brett was fortunate to work as an intern in Bristol-Myers Squibb's process chemistry department, where he met several organic chemists who were previous graduate students and postdoctoral researchers from the Amos B. Smith, III lab at the

University of Pennsylvania. The internship at BMS had convinced Brett that a career as an organic chemist was without a doubt what he wanted to pursue.

After completing his B.S. degree in chemistry at the University of Pittsburgh in the spring of 2008, Brett moved to Philadelphia, PA, to attend graduate school at the University of Pennsylvania. He spent his post-graduation summer working for Professor Amos B. Smith, III and getting accustomed to life in the inner city of Philadelphia. After officially joining the Smith group, Brett worked on a myriad of projects throughout his first year, but starting his second year he was able to focus exclusively on the total synthesis of (+)-18-*epi*-latrunculol A, a natural latrunculin A congener. After completion of the total synthesis of (+)-18-*epi*-latrunculol A, Brett took full advantage of the intellectual freedom Professor Smith had (unofficially) granted him by investigating novel methods to accomplish the cyclization of *δ*–hydroxy enones under mild conditions. Focusing on reaction development was an extremely gratifying endeavor and resulted in a photochemical isomerization/cyclization sequence that is currently being developed further through collaboration with first year graduate student, Bo Li.

In October 2013, Brett will begin a postdoctoral fellowship with Professor F. Dean Toste at the University of California, Berkeley. Along with his enthusiasm to reside in the Bay Area, Brett is very excited to focus purely on reaction development and to study the wonders of organometallic chemistry.